Optimization of Wind-Solar Energy Systems using Low Wind Speed Turbines to Improve Rural Electrification

A thesis submitted for the degree of Doctor of Philosophy
at the University of Strathclyde

by

Umarin Sangpanich

Supervisor: Professor K. L. Lo

Power Systems Research Group
Department of Electronic and Electrical Engineering
University of Strathclyde
Glasgow, United Kingdom

January 2013

DECLARATION OF AUTHOR'S RIGHTS

This thesis is the result of the author's original research. It has been composed by the author and has not been previously submitted for examination which has led to the award of a degree.

Signed: Date:

To my parents Wason and Daranee Sangpanich

ACKNOWLEDGEMENTS

I would like to express my very great appreciation to my supervisor, Professor K. L. Lo, the head of the Power Systems Research Group (PSRG), the University of Strathclyde in Glasgow, for his supervision and valuable guidance during the planning and development of this research work. His willingness to give his time so generously has been very much appreciated.

I would specifically want to acknowledge the scholarship support from the Faculty of Engineering at Sri Racha, Kasetsart University and the Energy Policy and Planning Office (EPPO) in Thailand.

I would like to thank the following government agencies and state enterprises in Thailand:

- The Electricity Generating Authority Thailand (EGAT) for wind speed data
- Sinlapakorn University for solar radiation data
- The Thai Meteorological Department for temperature data
- The Provincial Electricity Authority (PEA) for distribution system information

I would like to offer my special thanks to Joyce and David Maxwell for devoting their time and assistance in proofreading this thesis with regard to English grammar, and for their encouragement throughout my study.

I am particularly grateful for the suggestions and encouragement given by Aj. Chaya Jivacate and Asst. Professor Khuen Intharasuwan.

I wish to thank my parents, sisters, brother and friends for their constant support and encouragement during this research period.

TABLE OF CONTENTS

ABBREVIATIONS

AC OPF	AC Optimization of Power Flow
ACS	Ant Colony Search
AI	Artificial Intelligence
AM	Air Mass
ANN	Artificial Neural Networks
BFOA	Bacterial Foraging Optimization Algorithm
BIPV	Building Integrated Photovoltaics
BNN	Biological Neural Networks
BOS	Balance of System
COE	Cost of Energy
CRF	Capital Recovery Factor
DBSC	Decentralized Battery Storage Control
DFIG	Doubly-Fed Induction Generator
DOD	Depth of Discharge
DSG	Diesel Generator
EA	Evolutionary Algorithms
EHS	Electricity Home System
EHV	Extra High Voltage
EP	Evolutionary Programming
ES	Evolutionary Strategies
FCR	Fixed Charge Rate
GA	Genetic Algorithm
GenOpt	Generic Optimization
GP	Genetic Programming
HAWT	Horizontal Axis Wind Turbines
HOGA	Hybrid Optimisation by Genetic Algorithms
HOMER	Hybrid Optimization Model for Electric Renewables
HV/MV	High Voltage/Medium Voltage
HWST	High Wind Speed Turbine
ICC	Initial Capital Cost
IRR	Internal Rate of Return
LAC	Levelized Annual Cost
LBP	Loss of probability of Battery power supply at Peak demand
LCM	Least Common Multiple
LCOE	Levelized Cost of Energy
LCS	Learning Classifier Systems
LF	Levelized Factor
LFC	Levelized Fixed Cost
LPSP	Loss of Power Supply Probability

LRC	Levelized Replacement Cost
LWST	Low Wind Speed Turbine
MOEA	Multi-Objective Evolutionary Algorithm
MOOPs	Multi-Objective Optimization Problems
NGAS-II	Non-dominated Sorting Genetic Algorithm
NPV	Net Present Value
NREL	National Renewable Energy Laboratory
O&M	Operation and Maintenance
OLTC	On-Load Tap-Changer
PBP	Payback Period
PEA	Provincial Electricity Authority
PI	Profitability Index
PMDC	Permanent Magnet DC
PMG	Permanent Magnet Generator
PMSG	Permanent Magnet Synchronous Generator
PPI	Producer Price Index
PSO	Particle Swarm Optimization
PT	Potential Transformer
PV	Photovoltaic
RE	Rural Electrification
RETs	Renewable energy technologies
ROI	Return on Investment
SA	Simulated Annealing
SAIDI	Standard Average Interruption Duration Index
SAIFI	Standard Average Interruption Frequency Index
SCIG	Squirrel Cage Induction Generator
SG	Synchronous generator
SHS	Solar Home System
SOC	State of Charge
SOMES	Simulation and Optimization Model for Renewable Energy Systems
SPEA	Strength Pareto Evolutionary Algorithm
SPEA2	Strength Pareto Evolutionary Algorithm 2
STATCOM	Static Compensator
STC	Standard Test Conditions
SVC	Static VAR Compensator
SW	South-West
TOU	Time of Use
TPV	Thermo-photovoltaic
VAWT	Vertical Axis Wind Turbines
WHS	Wind Home System
WOE	Waste of Energy
WT	Wind Turbine
X/R	Ratio of Inductance (X) over Resistance (R)

List of Figures

List of Tables

ABSTRACT

Electricity is significant in improving the quality of life for people in rural and remote areas in developing countries. There are two main options for Rural Electrification (RE), namely grid extension and stand-alone systems. The governments and developers face the challenges of their limitations, namely technical, economic and environmental effects of each RE choice. This thesis intends to improve RE by focusing on renewable energy technologies, namely Wind Turbine (WT) and Photovoltaic (PV) systems. They have been developed and applied to RE because they are simple and environmentally friendly. They can be installed as separate units and they are sustainable alternative energy solutions.

Installation, cost and performance are crucial issues of WT and PV applications, and are based on the terrain and climate where the renewable are installed. The efficiency of WTs and PV modules has increased, while their cost has declined continuously. However, a PV system still has installation costs around two times more expensive per watt than WTs. Most WTs using current technology can be financially worthwhile for high wind speed areas, having wind speeds greater than 6.4 m/s at 10 m hub height, but most rural areas have wind speeds of less than 6 m/s at the same height. Therefore, Low Wind Speed Turbines (LWSTs) have evolved, by increasing rotor diameter and while maintaining similar generator capacity. This is to reduce Levelized Cost of Energy (LCOE) for WTs in low wind speed areas.

This thesis proposes simple cost models, namely the Sum-component cost model and the Total-cost model in order to calculate the LCOE of LWSTs. In addition, novel aspects of this thesis are that the optimization processes of stand-alone hybrid WT-PV systems and hybrid WT-PV systems using batteries at peak demand in remote area power systems provide simple, fast and flexible methods, by applying Multi-objective Evolutionary Algorithm (MOEA). The MOEA can analyze complex objective problems and provide an accurate multi-objective method. Results from relevant case studies show that the cost models and the optimization processes proposed are novel and are valuable tools for analysis and design, including the approaches for improving the system reliability and for estimating the Initial Capital Cost (ICC) of WTs having different rated wind speeds. The proposed algorithms are generic and can be utilized for other energy planning problems.

CHAPTER 1

1. INTRODUCTION

1.1 Thesis background

1.1.1 Rural electrification

The majority of people in rural and remote areas in developing countries are farmers and poor, have a low quality of life and lack educational opportunities, for example, Thailand. Electricity is the key to improve the quality of life for rural people, in both the social and economic infrastructures, in rural and remote areas. For example, electric light can increase extra income such as making crafts at night to sell and improve education. In addition to television for entertainment, they can obtain news and other information to acquire knowledge. Electricity allows people to do more in the evenings. Water pumping is an aid to agriculture and can give people a safe and satisfactory water supply. Communication tools are provided for the public and government officials or volunteers working in the area. These help to facilitate work in schools and health services, and they contribute to sustainable community development.

For rural development, both public and private sectors have worked together to increase an ongoing Rural Electrification (RE). Several key policies that can be achieved in many countries are summarized in [1], [2]. The government, for instance, has set up an organization that is responsible for RE and has provided financial support. Subsidies can be in many forms such as grants for the difference between actual electricity price and the price that people can afford, funding for some parts of initial investment cost of a project, reduction of tax paid on imported components and long term loan guarantees. Thai government has also accelerated RE, described in detail in Section 1.1.4. However, many people who live in rural and remote areas still lack electricity supply. From the International Energy Agency (IEA) survey in 2008 [1], it is shown that there is a power shortage to approximately 1.5 billion people or 22% of the population in the world, in which 85% of them live

in rural areas. Moreover, the IEA foresees that it is possible that 1.3 billion people who live in South Asia and Africa will still lack electricity by 2030 if the current policies cannot be improved. The policies may need to be revised because the RE development seems harder to do than ever before. Households are more widely scattered and terrain, such as distant mountains and islands are more difficult to access, causing higher electricity prices. Furthermore, there are businesses in the countryside and therefore the RE policies cannot aim only at poor rural households, but also at a mix of farms and industries, leading to the need for applications of various technologies. Hence, the technology applications are based on energy requirements, resources and target groups and therefore this represents a greater challenge for the development of RE.

Choosing the right technology is proposed as one of the significant solutions for RE development challenges. There are two main choices for the RE, namely, grid extension and stand-alone systems. The main technical, economic and environmental effects of each RE have been extensively investigated. For example, the report of Sandgren *et al.* [3], presented in 2009, provides a summary of types of technology solutions, both grid extension and stand-alone systems, with distinct advantages and limitations including guidelines for planning. The reports of the World Bank and the Alliance for Rural Electrification (ARE) [4], [5], published in 2008 and 2011 respectively, provide reviews of factors affecting the choices and discuss the different technology options for stand-alone systems.

The main distinct advantages and limitations of RE types identified in the literatures are concluded in Table 1.1. The decision on whether to select between them should depend on specific circumstances of the rural area. Grid extension becomes more difficult and expensive for investment, maintenance and operation for terrain which is hard to access. At present, rural areas without electricity seem to be farther away from the existing grid and basic infrastructure. The investment cost in developing countries will be 10,000 to 30,000 US$/km [3]. The cost of energy can be up to 0.7 US$/kWh, seven times the usual cost (about 0.1 US$/kWh) in an urban area [6].

Table 1.1 Summary of categories which should be taken into consideration for RE [3], [4], [5], [6], [7]

Particular	Grid extension	Stand-alone systems	
		Decentralized systems	Centralized systems
System types	Medium voltage transmission lines and low voltage distribution grid systems (1Ø and 3Ø)	Small stand-alone system, electricity home system (SHS, WHS, Pico-hydro, battery)	Village electrification system or mini-grid system (diesel, RETs, hybrid systems)
Number of users	One or more of the village	Individual users or usages: single households, public utilities, business units	A village (from 5 to 100 households relying on the demand)
Power capacity	Above 200 kW [3]	20 W to 10 kW [3]	5-500 kW [5], 10-1,000 kW [3]
Cost of energy	0.1- 0.7 US$/kWh [6]	SHS: 0.4-0.6 US$/kWh [5] WHS: 0.15-0.25 US$/kWh [5]	0.25-1 US$/kWh [5]
Appropriate areas	Areas with medium to high population density and not too far from the national grid, though not in the forest reserves	Areas with low population density and far from the national grid	Areas with medium to high population density and far from the national grid, islands and areas combined with diesel mini-grid systems
System design	- Technical, economic, social, satisfactory and environmental surveys for design of electrical wiring to the load area. - Decision from the number of connections per distance, design	A survey of potential energy sources, appliance usage and usage behavior for designing the sizing of power capacity and battery storage to meet load demand, with evaluation of technical, economics, social, satisfaction and environment	Issues of potential energy sources, technical, finance, social, satisfaction, environment and organization need to be examined for designing the proper sizing of generating capacity and energy storage to meet load demand.
Operation and maintenance	- Operation cost will rise due to energy losses and high or peak demand. - Maintenance cost is based on terrain and may increase in mountains and areas difficult to access.	- Maintenance simple but difficult access, increase cost and inefficient. - SHS requires less maintenance of WHS.	Need to have a technician and a staff at a station, for simplicity and ease of administration.
Role of users	Loss of agricultural land in some parts	- Small system: training in how to use a system and to manage electricity demand of the users themselves - Larger system: need for training in O&M	A staff and a technician can be local people who need training to use and manage the system, including demand side management.

Energy Sector Management Assistance Programme (ESMAP) reported in 2000 [7] that there are several ways to decrease the cost of grid extension such as using higher voltage, better quality poles to cut life-cycle costs, and standard materials and designs. Suitable size and location of transformer are important for installation, namely, small transformers for small load centres close to Medium Voltage (MV) lines. The life-cycle costs of transformers should be estimated instead of only the initial capital cost. In addition, a three-phase line has higher efficiency transmitting power than a single-phase line; the single-phase line should increase use, especially for domestic appliances because it is cheaper than the three-phase line. However,

three-phase appliances are commonly cheaper than single-phase appliances and motor rating of above 10 kW needs to be three-phase motors normally used in farms, hospitals and industries [3]. Consequently, user types, including densities of some load types, in the present and future, are necessary for design and selection of line configurations.

Survey of number of potential connections is significant for grid extension because some households may not want to connect and some users, such as industries, have high demands. It is not possible to be practicable for lower than two connections per km, but it is probable to be a practicable option compared to off-grid systems for greater than 30 connections per km. Distance is averaged from the rural centres to the grid centre. Besides the grid extension can be decided from distance to existing grid and existing basic infrastructures. [3]

Crucial issues of the grid extension for RE [5], [7], [8] are low load demands and poor profiles (low load capacity factors) in the beginning of a project and it may not be a worthwhile investment. After that new users will gradually increase over time. As a result, grid-connected systems will have reduced security and quality of power when they have many new users, especially at peak time, affecting user confidence. To solve this problem, other generation systems will be used for supporting the peak load demand. It is possible to apply energy storage systems, which will be reviewed in Chapter 2.

Another alternative for RE is stand-alone systems which can be classified into two forms, namely, decentralized and centralized systems compared in Table 1.1 and detailed in depth in Chapter 2. A Diesel Generator (DSG) is often used for both a small stand-alone system and in a village electrification system because of low initial investment and ease of installation and use. However, oil price has risen over the past 12 months by 31.6%, over the past 5 years by 61.8% and over the past 10 by 327.1% [9]. The increase in oil price is possibly because of leaked oil in the Gulf of Mexico in 2010, and it has also impacted on the environment. Moreover, petroleum retail price will add transportation fees considering the difficulty of transportation and distances from an oil refinery. For example, in Thailand from [10], the highest transportation fee is 2.32 Baht/litre or 4.73 pence/litre (exchange rate 49 Baht per Pound [11]) at Amphour Wiang Haeng, Chaing Mai province. In addition to

increasing oil price, it is necessary to be aware of both air and noise pollution, especially CO_2 emissions as a result of global warming. Consequently, it is a challenge to develop a sustainable RE, in the prices that people are willing to pay and with minimal environmental impact.

Renewable energy technologies (RETs) are the keys to producing clean energy futures and being sustainable alternative energy solutions. For many decades, they have been developed and applied to be alternatives for the RE such as water pumping, centralized battery stations, telecommunications, Electricity Home Systems (EHS) and village electrification systems or mini-grid systems. Their potential is not based only on technologies but depends on terrain and climate because they rely on natural sources such as solar, wind, water, wave and geothermal.

This thesis studies the solar and wind energy technologies for the RE, with reasons for their advantages and for RET's limitations. For example, a small hydro system can produce low cost energy but those areas need to have a high water capacity factor. In fact, the dry season when water flow is inadequate to produce the electricity to meet load demand may be more than two or three months in dry areas. In addition, it needs good installation and maintenance which have high investment cost. For another alternative, wave energy is interesting for islands but the potential of wave energy sources is relative to wind flow [12]. However, with current technology, many islands, such as Thailand [13], will not have high potential for wave energy.

For solar energy, Photovoltaic (PV) modules have been developed and used widely for RE because of simple and environmentally friendly installation. PV module prices have declined continuously, and will be reviewed in Section 1.1.2.1. Range of Cost of Energy (COE) of a Solar Home System (SHS) in Table 1.1 is an example for comparison with the range of a Wind Home System (WHS). Their COE were reported for Africa in 2010 [5] and Thailand [14]. SHS is a more expensive COE than WHS due to varying solar radiation (particularly cloudy days in rainy seasons) and having electricity demand in the evening in most households. As a result, batteries may directly depend on energy demand and it may increase costs of the system. In contrast, wind energy can have a potential both during the day and at

night, especially a high potential in rainy seasons. Development of Wind Turbines (WTs) has progressed rapidly leading to low price per watt for WTs, especially large WTs. Installation, cost and performance WTs will be presented in Section 1.1.2.2. The potential of wind and solar energy in Thailand will be described in Section 1.1.4.1.

Consequently, it could be more efficient to combine a WT with a PV system to form a hybrid system to decrease quantity of batteries needed. However, the hybrid wind-solar-storage system will be appropriated for the system that is larger than an electricity home system, i.e. a mini-grid hybrid system. It is a challenge to design the proper mini-grid (also known as micro-grid, with a capacity of 5-500 kW [5] or 10-1,000 kW [3]) hybrid system with full potential for both technologies and economizing on project budgets. Many approaches have been proposed to optimize sizing of hybrid stand-alone systems, small to medium sizing systems, discussed in Chapter 3. A new method to design the proper sizing of equipment by applying battery management in an optimization method to avoid the system failing is proposed in this thesis and illustrated in Chapter 5.

From the issue mentioned above, increasing electricity demand affects the security and power quality of the systems, this thesis proposes the approach to optimize the sizing of WTs, PV modules and batteries for reserving the peak load demand by a power system still stable. The minimum Levelized Cost of Energy (LCOE) and the minimum Loss of probability of Battery power supply at Peak demand (LBP) as well as the minimum Waste of Energy (WOE) will be objectives of the sizing system optimization in this thesis. The approach and case studies will be demonstrated in Chapter 6. Furthermore, economic and technical feasibilities of both the mini-grid systems when isolating and connecting with a national grid system which are the keys to design policies and projects to reflect actual cost of energy over the life of the projects for sustainability of the RE are assessed.

1.1.2 Installation, cost and performance trends of solar and wind generation

1.1.2.1 Photovoltaic modules

Photovoltaic modules are uncomplicated for installation and maintenance. Hence, they have not been only applied for RE but have also been applied for use in many areas such as building architecture, electricity for machines and lighting lamps in streets, to decrease fuel consumption, which helps lead to CO_2 emission reduction. Considering only PV grid-connected systems installed in the world, there has been an increase every year from 16.6 GW at the end of 2010 to 27.7 GW in 2011 [15]. It motivates the competitive market from large capacity requirements decreasing manufacturing costs and retail prices of PV modules and systems including electronics and safety system devices as well as installing devices such as cables and panel support frames. It leads to development of innovative PV technologies which have higher performance but lower costs.

The Solarbuzz [16] surveys the prices from thousands of retailers in the USA, Europe, China and other Asian countries and of exact price changes, not related to currency exchange rate variations. Furthermore, the prices surveyed for market requirements of above 125 MW, do not include sales taxes. The retail prices have sharply declined since 2009 and the highest price ratio of 2011 of 7.6:1 was in September 2011. The retail prices per watt peak of PV in the United States and Europe have reduced to about one half of that in the decade, earlier shown in Figure 1.1. From 313 price points or 28% of the survey in January 2012, PV module prices are as low as 2.00 US$/W (1.54 €/W), which is more than the amount of the price points in December 2011 (281 price points or 25% of the survey). In addition, the European Photovoltaic Industry Association (EPIA) and Greenpeace International report [17] summarised that the price of PV modules has declined by 22% of every doubling of additive PV installed (in MW). The price range of PV systems in the mature markets reduced from about 5 €/Wp in 2007 to 2.5-3.5 €/Wp in 2010. Due to the decrease of PV modules, the electricity cost of PV systems in Southern Europe in 2007 averaged 0.3-0.6 €/kWh and declined to 0.14-0.20 €/kWh in 2010, by nearly 50-70%. The module prices are expected to reduce to 0.7-0.93 €/W by 2030 and 0.56 €/W by 2050 so the PV systems will have a very low cost for electricity at that time.

Over the last three decades of PV development and until now, there have been three generations of PV technologies [17] and they will be described in detail in Chapter 2. The basic Crystalline Silicon (c-Si) is the first technology and forms the majority (approximately 80%) of the market today with cell efficiency of 14-22% and module efficiency of 12-19% and is expected to have 23% efficiency by 2020, at cheaper prices. Greater efficient modules will diminish costs for Balance of System (BOS) equipment, installation and land. PV modules are guaranteed commonly for 25 years, which is the minimum PV module lifetime today. After 20-25 years, however, assurance is given that the module performance will be around 80% of the initial output power. Their target is a lifetime of 40 years by 2020. Nevertheless, most modules used for longer than 25 years ago are still generating power. The Solarbuzz survey [16] concludes that a mono-crystalline silicon module and a multi-crystalline silicon solar module have the cheapest retail price of 1.28 US$/W or 0.99 €/W and 1.14 US$/W or 0.88 €/W from an Asian dealer and a US dealer respectively.

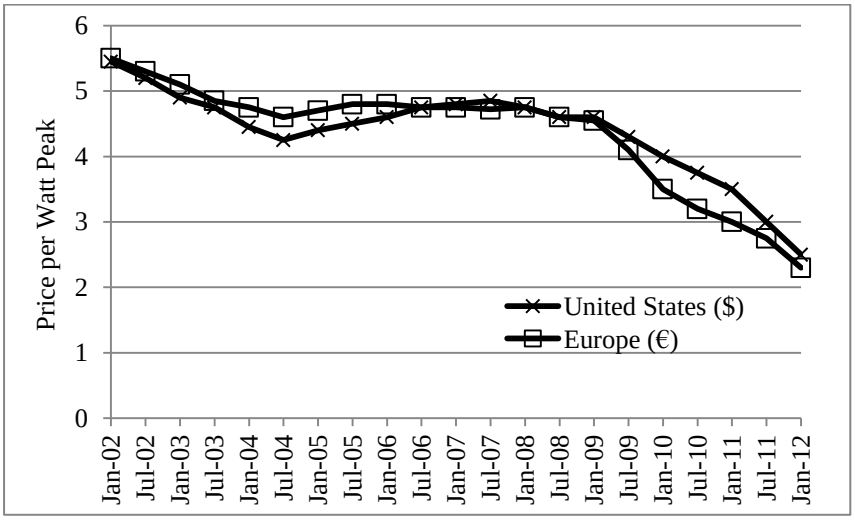

Figure 1.1 Retail PV module price index of the NPD Solarbuzz [16]

The crystalline silicon modules are normally applied for stand-alone and grid-connected systems. Reduction of investment cost of a PV system depends on the maturity of the market, type of PV and BOS equipment (such as an inverter) technologies, applications and system sizes. Consequently, this thesis illustrates the case studies by evaluating economic feasibility for stand-alone PV systems and PV

systems that can support grid-connected at peak demand in each range price of PV modules.

1.1.2.2 Wind turbines

Wind turbines (WTs) are a clean technology and can produce electricity without fossil fuels. Hence, most countries that have high wind speeds have installed WTs and at the end of 2011 in the entire world there was a totally installed WT capacity of nearly 239 GW, as reported recently by the World Wind Energy Association (WWEA) [18]. This is approximately 3% of the global electricity demand. WWEA [19] foresees that WT capacity in the world will be 600 GW by 2015 and 1,500 GW by 2020. They also suggest that governments have to consider and set policies which more strongly promote renewable energy, especially wind turbines, because these are still working after the earthquake and tsunami in Japan in 2011, whilst nuclear energy is in calamity. This has impacted on the people and the environment.

Some developing countries have improved on policies for development of power generation systems in both urban and rural areas leading to greater stability and reliability. WWEA presented in [19] that, for example, Romania had the top growth rates by adding 40 times of WT capacity in 2010. In Africa, new policies plan to support wind farms on a small scale and in combination with other sources, especially for RE to serve hundreds of millions of Africans in areas without electricity. Moreover, the Global Wind Energy Council (GWEC) concluded in [20] that the target of the Indian government was an increase of 78.7 GW WT capacity between 2007 and 2012. India has the third largest new WT in the world, installed in 2011, with about 2.7 GW, so now the total output is around 15.77 GW [19]. In Thailand, the government has planned to install WT capacity of 800 MW from 2008 to 2022. However, the main problems of WT installation in developing countries arise from unclear policies and shortage of financial support as a result of weak performance in market structures. In addition, it is difficult to find high wind potential locations in developing countries.

Archer and Jacobson [21] evaluated global wind speeds in 2000 from measuring wind speed stations distributed across the world. They found that there are only

approximately 13% of all reports that show annual average wind speeds at 80-m hub height of above 6.9 m/s (class 3 or higher) such as close to coasts in Alaska and Northern Europe. The classes of wind power density and speed, set by the Energy Information Administration (EIA) of the U.S. government, are shown in Table 1.2 [22]. Generally, the measured mean wind speed is 6.64 m/s (class 6) and 3.28 m/s (class 1) at 10 m above the ocean and land, respectively. Calculating wind speeds at 80 m in height above the ocean and land they are 8.60 m/s (class 6) and 4.54 m/s (class 1), respectively. Most of WTs in current technology have the rated wind speeds of more than 11 m/s from a figure shown in [23]. Although they can be used in class 6 sites because their cut-in wind speed range is 2-4 m/s, it is not easy to find class 6 sites located in rural areas. Furthermore, there will be the same problems as grid extension, that is, difficult terrain for electrical wiring and loss through long transmission lines, bringing about higher COE. Consequently, Low Wind Speed Turbines (LWSTs) have been developed to reduce COE for wind turbines in low wind speed areas.

Table 1.2 Classes of wind power density at heights of 10 m and 50 m above ground [22]

Wind power class	**10 m**		**50 m**	
	Wind power density (W/m^2)	**Speed* (m/s)**	**Wind power density (W/m^2)**	**Speed* (m/s)**
1	0-100	0.0-4.4	0-200	0.0-5.6
2	100-150	4.4-5.1	200-300	5.6-6.4
3	150-200	5.1-5.6	300-400	6.4-7.0
4	200-250	5.6-6.0	400-500	7.0-7.5
5	250-300	6.0-6.4	500-600	7.5-8.0
6	300-400	6.4-7.0	600-800	8.0-8.8
7	400-1,000	7.0-9.4	800-2,000	8.8-11.9

Remark: *Mean wind speed is based on Rayleigh speed distribution of equivalent mean wind power density. Wind speed is for standard sea-level conditions. To maintain the same power density, speed increases 3%/1000 m (5%/5000 ft) elevation.

However, in order to catch more wind energy in low wind speed areas where may have wind speeds of lower than class 4, for example, wind turbines should be designed with larger rotor blades and taller towers than in high wind speed areas. In addition, other parts of wind turbines will be improved to meet the increasing size of a rotor diameter and the maintaining capacity of a generator. The improvement in some parts will increase costs of WTs and at the same time the others can reduce the costs. There are many factors that make the costs change and it is complicated to predict the costs because of technological advances. As a result, this thesis develops cost models and demonstrates simple procedures to forecast the cost and they can be

used for evaluation of economic feasibility of LWSTs at different rated wind speeds. More details about LWST improvement, WT cost models and a case study will be illustrated in Chapter 4.

Generally, small WTs are appropriate for RE due to low load demand in rural and remote areas. Range of small WT sizes is identified by a rated power output from various publications such as below 10 kW [24], lower than 50 kW [5] and less than 100 kW [25]. For a well site in the U.S., American Wind Energy Association (AWEA) reported in 2009 [26] that costs of WT installation are assessed to be 3-6 US$/W and COE of 0.15-0.20 US$/kWh. Efficiencies of WT components have been improved such as blades from about 32% to 45%, alternators from 65-80% to 90-92% and current inverters of over 90%.

WT sizing is a key factor of WT costs because it seems that the larger sizes the cheaper capital cost per watt and the lower (Operation and Maintenance) O&M costs per kWh generated. Hence, many developers focus on large WT sizes. From IEA report, now the largest WT size is 7.5 MW and is expected to be 20 MW by 2020 [27]. Jos Beurskens of the Energy Research Centre Netherlands, who was a leader of the upwind project, said "Making a 20 MW WT is not just upscaling today's 5 MW machines. Nevertheless, we have already identified the necessary innovations in terms of design, materials and way the turbine is operated" [28]. Hearps and McConnell [29] reviewed that the current investment costs for large WTs are approximately 1,725 US$/kW and the costs are possible to decrease to 1,420 US$/kW by 2030. They are lower than the costs in the GWEC report, in which the current investment costs are about 1,890 US$/kW and are foreseen to be 1,590 US$/kW by 2030. Bolinger and Wiser [30] reported for WT price trends in the U.S. that WT costs had the lowest range of around 750 US$/kW between 2000 and 2002. However, due to WT development for low wind speed areas, the costs have increased to 900-1,400 US$/kW for 2010-2011.

Large WTs may not be suitable to use for stand-alone systems in rural areas because of low load demand and poor capacity load factor but they have been applied for grid connection. However, this thesis evaluates economic feasibility for large LWSTs and current WTs both being used for hybrid stand-alone systems by assuming high load

demand and reserving peak demand for a grid-connected system described in Chapter 5 and 6, respectively.

1.1.3 Optimization for renewable energy systems

Various optimization techniques have been proposed, namely, graphical construction techniques, probabilistic approach, iterative technique, artificial intelligence methods and multi-objective design, for both optimum sizing of stand-alone hybrid wind-solar generation systems [31], [32] and optimizing battery storage in distributed generation systems using renewable energy sources [33]. Multi-objective optimization design is considered because, although it may take time to obtain solutions, it can give good results in complex problems or non-linear problems, in the case of variation of both power generation and load demand. Moreover, it can optimize two or more conflict objectives such as the minimum cost, the highest system reliability and the lowest pollution emissions.

Multi-objective optimization has been developed to solve problems for two or more conflict objectives since the late 1950s [34]. In 1985, the first Multi-Objective Evolutionary Algorithm (MOEA) was developed and it has become a popular approach for multi-objective optimization, by using the basic principles of biological evolution. After that, many researchers have proposed many types of MOEAs and applied them for several multi-objective problems such as engineering and science fields. The Strength Pareto Evolutionary Algorithm 2 (SPEA2), proposed by Zitzler *et al.* in 2001, is a current MOEA that is the most advanced and gives the best performance for real-world problems, approved in [35]. It has become a standard approach for solving multi-objective problems. Many researchers have applied it for optimizing sizing of renewable generation systems for grid and off-grid systems. For example, the Hybrid Optimization Genetic Algorithm (HOGA) software has been developed by the Electric Engineering Department at the University of Zaragoza in Spain [36]. Moreover, the doctoral thesis of Alarcn-Rodrguez [37] presented in 2009, proposes a multi-objective planning framework for analyzing the integration of distributed energy resources. Consequently, this thesis utilizes the SPEA2 for optimizing sizing of both off-grid and grid hybrid renewable generation systems. The

concepts and development of MOEA and the SPEA2 are described and their applications for hybrid renewable systems are reviewed in Chapter 3.

Even though, many methods for optimizing the sizing of hybrid renewable systems have been proposed [31]-[33], all optimization methods have not included a battery management method, dividing batteries into groups or strings, can be called a Decentralized Battery Storage Control (DBSC) method. However, the DBSC method was tested and analyzed and it was found that it has a better performance for charging batteries of WT battery charging stations than a single battery storage control method and it can reduce cost per charged battery; although, it has more expensive initial investment cost than another [38]. Additionally, it can improve storage lifetime and decrease maintenance cost of battery storage systems from results of simulation in [39], [40]. This thesis develops a new method for designing the proper sizing of components of a hybrid renewable generation system by applying the DBSC method in the optimization procedure. The further advantages of the new method are expected to be that the optimum sizing of system components can be decreased, leading to reductions of investment costs, WOE and LCOE and an increase in the system reliability. The new method and results, as well as evaluation for economic feasibility of the renewable generation systems, are illustrated in Chapter 5.

1.1.4 Rural electrification in Thailand

At present, Thailand still has some rural or remote areas without electricity supply, in spite of government policy actively promoting RE. The national plan for Thailand has accelerated RE since 1972, through the responsibility of the Provincial Electricity Authority (PEA), because only 10% of provincial areas in Thailand had an electricity supply at that time [41]. In addition, the King of Thailand's projects and the Royal projects have aimed to improve the quality of life for people in rural areas, through collaboration of the Royal Thai government, foreign governments, universities, public and private agencies and volunteers. Also, wherever the projects have been placed, the electricity has been accessed [42], [43]. As a result, Thailand's RE development has improved, which can be seen from the IEA survey [44] in 2008,

but there still remains 0.7% of people in Thailand, or 0.4 million people, who live in rural areas without an electricity supply. Although, it seems to be only a small percentage of the population, they live in rural areas where terrains are very difficult to access, such as islands and mountains. Also, environment impacts are significant, in that grid extension or diesel generation should not be used, which are discussed in Section 1.1.1. Therefore, a stand-alone renewable energy system will be more suitable to apply to the remaining rural areas.

Furthermore, even where grid-connected systems were extended to rural areas, the overall quality of electricity service in provincial areas should be improved. In 2006, the Standard Average Interruption Frequency Index (SAIFI) and the Standard Average Interruption Duration Index (SAIDI) of Thailand, excluding Bangkok, were studied and it was found that there were approximately 12 interruptions per year and about 500 minutes per year, respectively. Moreover, the South has had weak grid systems, from data in 2007, which show the highest frequent power outage in Thailand of 52 times per year, each period averaging one hour. Grid systems of Northeastern Thailand should also be developed because, although power outages were 20 times per year, the duration of each time had an average of four hours [45]. Consequently, integration of distributed generation systems, in order to improve quality of grid systems, has been investigated, especially using renewable energy systems, namely, PV and WT systems, which will be studied specifically in this thesis.

1.1.4.1 Potential of wind and solar energy in Thailand

The speed and direction of wind depends on two monsoons that are the North-East (NE) monsoon in November to April and the South-West (SW) monsoon in May to October, presented in Figure 1.2. This figure shows fifty-five wind-monitoring stations installed by the Department of Alternative Energy Development and Efficiency (DADE), starting the measurement in 1997 [46], which the Thai government and private sectors have used to explore the wind sources vital for investment of wind site installation. In 2001, the World Bank explored and estimated the total wind energy potential of Thailand as 92.6% and 7.2% of the total land area

has wind speeds lower than 6 m/s and 6-7 m/s at 65 m height respectively. Only 0.2% of total land area has 7-8 m/s [47].

In 2001, wind data of 134 wind-monitoring stations was calculated from computer programs and by Fellow Engineers Consultants Co., Ltd., and was supported by the DADE, as shown in Figure 1.2. This wind map shows the annual mean wind speed, including calm, varying from 3 m/s up to 9 m/s at 50 m height. The high wind potential, especially from November to April, is above 5 m/s at 50 m height [48]. Furthermore, there are a few areas where the high wind potential is above 6.4 m/s at 50 m height, at the east coast and in the high mountains of the south and in the chain of mountains in the west [48], [49]. However, the wind data of some stations was collected every three hours and so their accuracy may not be sufficient to select wind sites.

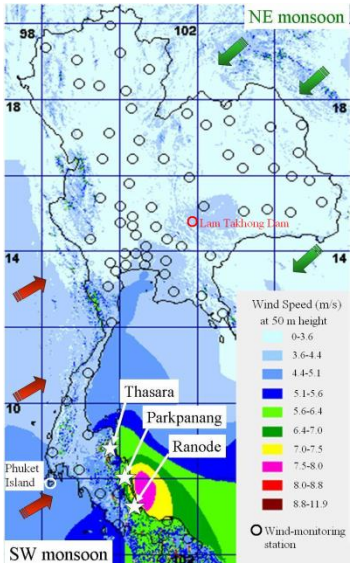

Figure 1.2 Speed and direction of wind, including calm and wind-monitoring stations in Thailand, sources: [46], [48], [49]

In 2006, the wind energy potential of southern Thailand was assessed from 18 wind-monitoring stations and the wind data was thoroughly measured by Taksin University, Songkranarin University and Walailuk University and supported by the National Research Council of Thailand (NRCT). The mean wind speeds, k-shape and c-scale parameters of the Weibull distribution were determined by the WAsP 9.0 program. It was found that the highest potential is at three stations; namely, Thasara, Parkpanang and Ranode, with mean wind speeds of above 5.5 m/s at 50 m height

[50]. Thus, it may be stated that Thailand could be identified to be a low wind speed area. Economic feasibility of wind farms in these three station areas was evaluated in [51].

Although the wind energy potential in Thailand may be low, the annual average solar energy in Thailand is quite high, at approximately 4.5-4.7 kWh/m^2 per day and the sunshine duration is approximately 6-8 sunshine-hours per day [52]. About 14.3% of the Thailand area has the highest annual average solar energy of approximately 5.28-5.56 kWh/m^2 per day. Also, wind energy has high potential in a rainy season, contrasting with solar energy, which has low potential in a rainy season, because of cloud cover. Consequently, it could be more efficient to combine a WT with a PV system as a hybrid system.

At Lam Takhong Dam, Nakhon Ratchasima province in Thailand, as shown in Figure 1.2, seemingly has the potential for both wind and solar energy from [53] and [54], respectively. Hence, this thesis uses this location for a case study. Hourly wind speed and hourly solar radiation data collected in 2006 are employed in this research. The hourly wind speed data was measured at 45 m of hub height (height above sea level approximately 661 m). An annual mean wind speed of approximately 5.71 m/s at 45 m of hub height can be classified to be class 2 of wind resource site. The annual average solar energy was approximately 4.92 kWh/m^2 per day and the sunshine duration was approximately 8 sunshine-hours per day. More details of the area are described in Chapter 5.

1.1.4.2 PV and WT installations in Thailand

The Ministry of Energy (MOEN) of Thailand has promoted and supported the RETs both for RE and distributed generation systems through the Renewable Energy Development Plan (REDP), with the target to decrease the use of fossil fuels, which impact the environment and to increase renewable generation from 6.4% in 2008 to 20% by 2022 [20]. Installations of PV and WT systems are expected to be at least 500 MW and 800 MW, respectively, by 2022. In this regard, the Thai government has encouraged investors by, namely, tax incentives, support of partial investment funds, energy soft loan, technical supports and an adder or feed-in premium [55]. An

adder is a subsidy, for renewable energy development, from the government, by which the government will purchase electricity from investors, with adder rates announced in the renewable energy policy stated in June 2010. Adder rates rely on the type of RETs and power capacities of systems. An adder rate of a PV system was decreased from 8 Baht/kWh (or 16.33 pence/kWh) to 6.5 Baht/kWh (or 13.27 pence/kWh). A WT system has two adder rates, if installed capacity is less than or equal to 50 kW, an adder rate is 4.5 Baht/kWh (or 9.18 pence/kWh) and the adder rate is 3.5 Baht/kWh (or 7.14 pence/kWh) for installed capacity of above 50 kW. Moreover, to stimulate investment in three Southern provinces, Pattani, Yala and Narathiwat, an extra adder of 1.5 Baht/kWh (or 3.06 pence/kWh) for two kind systems will be added. The time duration of adders is 10 years. This thesis applies the adder policy for evaluating economic feasibility of PV and WT systems.

However, there are many lessons learnt from PV and WT systems installed, which the Thai government, developers and investors should consider, namely, technical, economic and environment issues as mentioned in Section 1.1.1. Problems and barriers of PV and WT systems installed in Thailand are discussed in Chapter 2. Accordingly, in order to be more clear for a RE plan in Thailand, this thesis analyzes and evaluates PV and WT applications of both grid and off-grid systems in Thailand.

1.2 Thesis objectives and methodology

The aim of this research is to develop models and methodology for investigating the proper alternatives for rural electrification with particular emphasis on applications of wind and solar energy technology by:

1. Optimizing the sizing of WTs, PV modules and batteries and evaluating the economic feasibility for:
   1.1 Hybrid stand-alone systems with battery management
   1.2 Hybrid stand-alone systems using LWSTs.
   1.3 Hybrid wind-solar systems using batteries for peak demand in remote area power systems.
2. Evaluating the economic feasibility of LWST technology.
3. Examining the proper alternatives for RE in Thailand.

In order to achieve the aim of this thesis, the research approach involves several key steps:

1. Explore in detail the problems of electrical utilities and applications of renewable energy generation to serve people in rural areas.
2. Study multi-objective optimization to choose an optimal algorithm for examining the proper alternatives for RE.
3. Review the state of the art of wind power technology for low wind speed areas, with particular focus on installation, cost and performance.
4. Develop cost models for economical evaluation of WTs that have different rated wind speeds.
5. Develop the processes of optimization for:
   - Hybrid stand-alone systems with battery management for RE in low wind speed areas.
   - Hybrid stand-alone systems using LWSTs for rural electrification in low wind speed areas.
   - Hybrid wind-solar systems using batteries for peak demand in remote area power systems.
6. Evaluate the economic feasibilities of the hybrid systems, with case studies in Thailand.

1.3 Contributions to knowledge

The main original contributions of this thesis are discussed fully in Chapter 7, and are summarized below:

1. Cost models of LWST to predict initial capital cost of LWSTs are proposed, which developers can use to approximate LWST costs for various rated wind speeds or rotor diameters and then they can evaluate cost of energy and economic feasibility of WTs.
2. A new method is proposed that combines the evolutionary multi-objective optimization and the battery management to find optimal sizing of WTs, PV modules and batteries for the hybrid stand-alone systems. There are four types of the hybrid systems, namely, WT-Battery systems, PV-Battery systems, WT-PV-Battery systems and WT-PV-Battery systems with DSGs. The method can provide valuable

information for the proper alternative energy systems in rural and remote areas where wind and solar energy systems will be installed.

3. A new method is developed that integrates the evolutionary multi-objective optimization and AC optimal power flow for estimating optimal sizing of WTs, PV modules and batteries of the hybrid systems applying LWSTs and using batteries at peak demand in a remote area power system.

4. The proper alternative for RE in Thailand is analyzed. It highlights WT and PV systems; especially LWST applications in Thailand where areas are identified as low wind speed areas. Developers and investors can use it for considering and planning both the technical design and the economical assessment for investment in RE.

1.4 Thesis structure

This thesis is organized in seven chapters and reflects on the methodological steps and the contributions of this work. Chapter 1 provides an introduction to the whole thesis. It discusses the background and motivation of this research. Furthermore, it presents the research objectives, the research methodology and contributions to knowledge of this thesis.

Chapter 2 reviews applications of renewable energy generation for RE. It presents the concepts and models as well as types of PV, WT, battery and DSG systems. Specifically, the technologies of PV and WT systems are overviewed. The configurations and concepts of stand-alone hybrid renewable energy systems and improvement in remote area power systems with renewable energy systems and energy storage systems will be reviewed. The concept of battery storage system and management will be proposed as background for optimizing hybrid system design in Chapter 5. Moreover, the principle of evaluation of economic feasibility for renewable energy systems is given in the conclusion.

Chapter 3 presents a critical review of the state of the art of optimal sizing techniques for stand-alone hybrid renewable energy systems and hybrid renewable energy systems by using batteries at peak demand in remote area power systems. It also describes the principles and developments of MOEA and SPEA2 including their applications for optimization of the hybrid systems.

Chapter 4 has three sections. Initially, characteristics of wind generation are described to define low and high wind speeds. Next, an LWST is identified. Also, advantages and disadvantages of increased rotor diameter and generator capacity for LWSTs are discussed. Finally, cost models of WTs will be proposed, and an example will be provided for assessment of economic feasibility of WTs that have different rated wind speeds.

In Chapter 5, the procedure of optimization for stand-alone hybrid renewable energy systems using SPEA2 is illustrated. Operational processes of battery management for the hybrid stand-alone systems are proposed, with four kinds of systems, namely, WT-Battery systems, PV-Battery systems, WT-PV-Battery systems and WT-PV-Battery systems with DSGs. This thesis will highlight system reliability and the cost of energy, including evaluation of economic feasibility of systems and environmental assessment (CO_2 emissions). Two main case studies will be illustrated, i.e. mini-grid hybrid systems with a peak load of 30 kW and large hybrid stand-alone systems with a peak load of 1 MW. The first case study results are for analyzing advantages and disadvantages of battery management and DSG support in both technical and economic terms. The second case study evaluates the economic feasibility of low and high wind speed turbines.

Chapter 6 proposes processes for the optimization of hybrid renewable energy systems, using batteries at peak demand in a remote area power system. Operational procedures of the hybrid systems are proposed for three types of systems, namely, WT-Battery systems, PV-Battery systems and WT-PV-Battery systems. There are four relevant issues discussed. First, three simulation systems, which have different positions of simulated hybrid renewable energy systems installed in a remote area power system, are illustrated. Second, impacts of the hybrid systems on the power system are investigated. Third, the design methods of switched capacitor size are proposed and demonstrated. Finally, the evaluation of the economic feasibility of the hybrid systems is detailed for low and high wind speed turbines. Moreover, it presents the economic evaluation when initial capital cost of WTs, PV modules and batteries is varied.

Chapter 7 will summarise the thesis and discuss the contributions of this work. Future work for the development of this research is proposed.

1.5 Associated publications

1. **U. Sangpanich**, G. A. Ault, and K. L. Lo, "Economic feasibility of wind farm using low wind speed turbine," in Universities Power Engineering Conference (UPEC), 2009 Proceedings of the 44th International, 2009, pp. 1-5.
2. **U. Sangpanich**, K. L. Lo, "Design and Evaluation for Economic Feasibility of Wind Turbine and Photovoltaic Systems in Thailand," in Thai Students Academic Conference in Europe 2012: Contribution to Thailand, The Royal Thai Embassy, The Hague and The Thai Students Association in the Netherlands, 2012, pp. 10-11. (Paper Awards)
3. K. L. Lo, **U. Sangpanich** and O. Anaya-Lara, "A novel optimization algorithm of hybrid wind-solar systems using decentralized battery management for rural electrification" (Journal paper under preparation)
4. K. L. Lo, **U. Sangpanich** and O. Anaya-Lara-, "A simplified cost model for economic evaluation of low wind speed turbines of different rotor diameters" (Journal paper under preparation)
5. K. L. Lo, **U. Sangpanich** and O. Anaya-Lara, "Techno-economical optimization of a hybrid wind-solar system incorporating batteries for application in a remote area" (Journal paper under preparation)

CHAPTER 2

2. RENEWABLE ENERGY SYSTEMS IN RURAL AREAS

2.1 Introduction

Renewable energy technologies (RETs) have been rapidly developed and widely used for Rural Electrification (RE) because of the dramatic increase in oil price and awareness of environmental issues. In addition, grid extension is frequently very expensive and impracticable in isolated rural areas. Most grid systems in remote rural areas also become weak due to continued increasing energy demand and this is especially at peak load demand. Reliable and stable access to electricity including energy security is significant for the sustainable RE development. Solar and wind energy can thus be alternative energy. This is for the reason that they are not only sustainable but that they also produce electricity without chemical and radioactive emissions. However, PV and WT systems have unstable power output and investment costs that may still be relatively expensive but this will mainly depend on locations and technologies.

Consequently, this thesis uses lessons learnt from PV and WT system applications in the past for guidance in the selection and development of PV and WT systems for the RE. Many PV and WT systems applied in Thailand are overviewed and the important issues of the applications are remarked. This chapter hence presents models of PV, WT, battery and DSG systems applied in the thesis. Specifically, the technologies of PV and WT systems are overviewed. The chapter further reviews the configurations and concepts of stand-alone hybrid renewable energy systems and improvement in remote area power systems with renewable energy systems and energy storage systems. Besides, the concept of battery management is proposed as background for optimizing hybrid system design in Chapter 5. Finally, the principle

of evaluation of economic feasibility for renewable energy systems is given in the conclusion.

2.1.1 Lessons learnt from using PV and WT systems in Thailand

Thailand is a good example for RE development from 10% [56] of provincial areas to currently 99.3% [57] of population having electricity over the last four decades. Even though, it remains a small percentage of the population without electricity, the government continues to maintain the development of electrification for all citizens in the country according to the constitution of 1997. The constitution stated that the government must provide utilities, including electricity to all citizens equally in terms of quality and price. However, the remaining areas without electricity are very difficult terrains to access, such as islands and mountains. Furthermore, the government recognizes the importance of environment issues. Therefore, RETs have been developed and applied to reduce fossil fuel consumption and to avoid environment impacts. PV and WT technologies can be considered to be clean RETs. However, there are many remarkable lessons learnt from PV and WT applications in Thailand as follows:

Photovoltaic (PV) systems: The total PV power capacity in Thailand was about 108 MW [58], [59], in the proportion of PV systems installed to be stand-alone systems of approximately 30% and grid-connected systems of about 70% [59], in February 2012. It has been set a target of 2,000 MW by 2021 [60]. PV modules have been applied in Thailand since the 1970's for mobile telecommunication equipment of the military and mobile rural medical volunteers under the Royal Patronage of the Princess Mother. In the 1980's, PV stand-alone systems were used widely for school radio and television programmes, water pumping, centralized battery charging and telecommunication. Output energy of many systems cannot meet load demands because of undersized and system underperformed. For PV centralized battery charging stations, users do not understand correctly how to manage battery charging leading to shorter lifespan of batteries and so the PV stations have been abandoned. In addition, four village PV stand-alone systems of each approximately 40 kWp were installed by PEA and supported from Japan. They had been used as a stand-alone

system for about 10 years and now they are connected with grid systems because of higher demand and grid extension of PEA. [61]

In the 1990's, installation of PV systems had been reduced because of world economic crisis. Otherwise, in the 2000's, there were many PV projects of the government. For example, in 2004 and 2005, the government promoted renewable energy to RE by a Solar Home System (SHS) project to 203,000 households. The SHS has power capacity of 120 W AC, which has high COE that is about 31.15 Baht/kWh or 63.57 pence/kWh [14]. Many SHSs have failed from problems [14], [62] i.e. technical problems such as quality of equipment (especially a battery), lower system performance than expectation due to PV modules installed in shady locations. They have not been properly maintained and correctly used, that is, overload from increase of user demand. When a charge controller is broken, users will connect directly PV modules and batteries, and hence batteries will deteriorate quickly.

The first large PV farm [63], power capacity of 500 kWp, in Thailand was installed in Mae Hong Son province in 2004 to support 22 kV line with a very long distance of approximately 200 km. Geography it is difficult for construction of a 115 kV overhead power line, which is not also allowed for passing through forest conservation areas. PV modules of the system have efficiency of 12% from manufacturing specification but their efficiency reduces to about 9% for 4 month per year because of forest fire smoke. Therefore, the annual average COE of the PV system is approximately 13.35 Baht/kWh or 27.24 pence/kWh. It is more expensive than the annual average COE of 2-3 Baht/kWh or 4-6 pence/kWh for hydropower plants installed and of about 9 Baht/kWh or 18.37 pence/kWh for DSG plants. In 2007, hydropower plants and DSG plants had the total power capacity of 9.14 MW and 7.4 MW, respectively. However, they have been insufficient for increasing load demand. Hence, a part of the SHS project mentioned above was placed in this province. In 2009, a pilot PV plant of 1 MWp using solar tracking with water weighted system at Sirindhorn dam, Ubon Rachathani province was installed and connected with a distribution line of PEA. The plant has very high investment and O&M costs including insurance and then it will not be worthwhile for investment [64]. On the other hand, the PV plant will be useful for study to improve on PV applications.

In addition to the example projects of the public sectors as mentioned above, there have been many PV grid-connected systems installed by private sectors with incentive financial support schemes of the government, namely, grid-connected rooftop PV systems and PV power plants. For instance, 8.7 MW and 7.5 MW PV plants were installed in 2011 and 2012, respectively [58].

Wind turbines (WTs): Thailand's wind energy potential is approximately 1,600 MW and there are fairly good wind potential with an average wind speed of 6.4 m/s at 50 m hub height, especially at the east coast and in the high mountains of the south and in the chain of mountains in the west [65], [48]. In Thailand, wind energy technology has been utilized, namely, a water pumping system, rice field irrigation, a salt farm and electricity generation. The currently total installed WT capacity is 7.28 MW and a target has been set for total wind power capacity of 1,200 MW by 2021 [60]. However, different areas in Thailand will have distinct time period of the high wind potential, i.e., from November to April for North and Northeast and from May to October for Southwest. As a result, most wind turbines installed will be combined with other energy sources such as PV systems and generators or connected with a grid system.

For example, a pilot hybrid wind-solar-storage system at Promthep Cape, Phukhet province [66] illustrated in Figure 1.1 had been installed by the Electricity Generation Authority of Thailand (EGAT) between 1983 and 1992 with 1.125 kW, 18.5 kW (only this one was connected to a grid system of PEA in 1988), 2 kW, 0.85 kW and two 10 kW. Now, 0.85 kW and two 10 kW still operate to charge batteries and feed electricity to a grid system, respectively. A 150 kW WTwith cut-in and rated wind speeds of 4 m/s and 13 m/s, respectively, was installed and connected with a distribution line of PEA in 1996. This system can operate acceptably well, but the cost of generation without subsidy is approximately 24.8 ¢/kWh at a monthly wind speed of 4.0 m/s to 6.1 m/s and its capacity factor of 15% [67].

At present, the largest wind grid-connected system project [64] was installed by EGAT at Lam Takhong Dam, Nakhon Ratchasima province in 2009 shown in Figure 1.1. It consists of two 1.25 MW wind turbines connected with distribution line of PEA. This area has a mean wind speed of approximately 6 m/s at 50 m height. It was expected that the COE without subsidy should be about 12 ¢/kWh. Other wind

turbines installed, especially in rural areas have small sizes; for instance, a hybrid mini-grid system at Ko Jig Island on the eastern coast of Thailand has been operated since 2004 with a 7.5 kWp PV array, a 65 kVA DSG and a 252 kWh battery storage system. Two 5 kW wind turbines were added in December 2006. Suwannakum *et al.* [68] assessed the annual average performance ratio of approximately 70% and the specific COE of 0.259 €/kWh.

The COE of WT systems may be high and are not worthwhile because the capacity factor is quite low. This is likely because the rated and cut-in wind speeds of this WT system are 12-13 m/s and 3-4 m/s respectively, which are quite high wind speeds and may not be effective in low wind speed areas. Alternatively, the wind resource assessment may not be practical and/or adequate to select a wind site because it might be evaluated from only the annual mean wind speed. Furthermore, both difficulty and costly of transportation are crucial barriers for import WTs from overseas. The WTs installed are often broken, especially rotors and bearings, are procurement of spare parts from overseas usually of delays [66]. Consequently, in order to promote WTs to be sustainable energy, the Ministry of Energy, the Ministry of Education and state enterprises such as EGAT and PEA agreed to co-operate to develop suitable WTs for the weather of Thailand or countries, which locate in tropics and have low wind speeds.

The most crucial issues for using PV and WT applications for RE can be concluded as follows:

1. For home energy systems, technicians and users have insufficient knowledge and incorrect understanding, and so life time of the systems will decrease leading to a downturn in many projects.
2. Increase of load demand and difficult maintenance of home energy systems, which can be solved by using centralized energy systems, namely, mini-grid systems, which are larger systems.
3. Large systems can make conflicts among people from, namely land use and noise pollution. Wind farms will make noise for residents so most of the wind farms will be installed away from urban. To solve the problem of land use, the large systems may have to be found away from the residential areas.

4. Stand-alone systems installed are undersized and underperformed. This is a crucial technical issue requiring effective approaches for planning and evaluating the systems for a specific site.

2.2 Photovoltaic generator

A Photovoltaic (PV) generator operates by converting solar radiations or photons directly into electricity using semiconductor properties. A PV cell or a solar cell is a fundamental unit of the PV generator. PV cells are connected to form a PV module to obtain the suitable power levels for applications and they are covered by glass or plastic to prevent them being damaged from environment during operation. The PV module can be applied alone or connected in an electrical circuit with same performance modules to assemble a PV array. This section will discuss models of a PV system and main environmental impacts to predict the performance of a PV module under different operating conditions for the PV system design. Moreover, the current PV technologies will be described in this section.

2.2.1 Reviews of Photovoltaic models

The performance of a PV module is the key to design of PV systems both stand-alone and grid-connected systems to assess the effectiveness of the systems. It bases on technologies, production processes and operating conditions. Under real operation conditions, the PV performance will be different from PV module specifications of manufacturers tested under Standard Test Conditions (STC). STC from IEC 60904-3 is defined at 1,000 W/m^2, 25°C cell temperature, with a reference solar spectral irradiance called Air Mass 1.5 (AM1.5). Hence, mathematical models of a PV system have been developed and used in the renewable energy system design for evaluating system reliability, LCOE and economic feasibility of the PV system. However, to estimate PV power output, firstly, global and diffuse solar radiation data should be calculated to be the global radiation on an inclined surface according to a technique in [69].

A PV cell can be represented by equivalent electrical circuits. The general equivalent circuit of a PV cell consists of a photocurrent source (I_{ph}), one diode and series and shunt resistances, illustrated in Figure 2.1(a) [69]. Series resistance (R_s) is the internal resistance of each cell and the resistance of connection between the metallic contacts and semiconductor. Shunt resistance (R_{sh}) occurs from leakage across the p-n junction of the cell. Three important parameters are short-circuit current, open-circuit voltage and a fill factor to characterize performance of a PV cell. A fill factor is the ratio of the maximum output power and the product of short-circuit current and open-circuit voltage, which is a measure the actual I-V characteristic. If the fill factor is above 0.7, it means that the cell is good [70]. They are utilized for estimating output power of a PV system by considering a temperature effect.

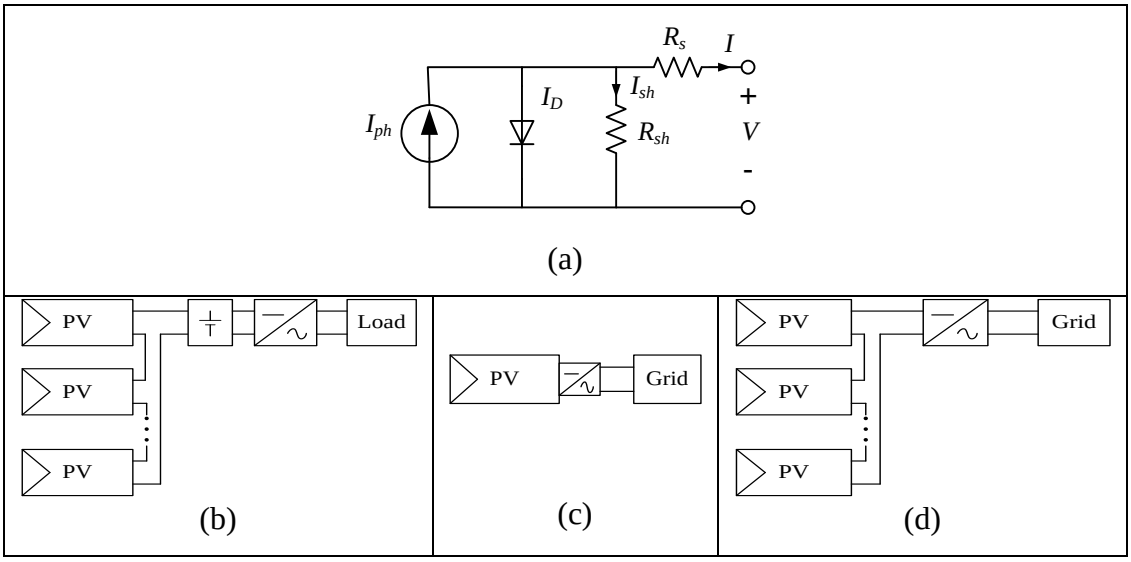

Figure 2.1 (a) Equivalent circuit of a PV cell (b) stand-alone PV system (c) AC PV module (d) Grid-connected PV system

PV cells are connected and assembled together forming a PV module or panel. The module produces direct current electricity that can be stored in an energy storage system for stand-alone systems, shown in Figure 2.1(b), or fed into a grid system, illustrated in Figure 2.1(c) and (d). A stand-alone PV system can be designed and used, such as decentralized systems for individual users or usages with a capacity of below 10 kW and centralized systems for a village (from 5 to 100 households) with a capacity of above 10 kW [3]. The range of grid-connected PV system sizes can be identified by a rated power output of inverter [71]. For example, small sizes, such as

an AC PV module generally have a power rating of 50-400 Wp. Medium sizes of distribution generation system having a capacity of 2-4 kWp or large sizes of central generation system having PV modules connected as a large array with a capacity of above 10 kWp.

The effects of the solar radiation and the cell temperature can be illustrated as the I-V characteristic in Figure 2.2. The higher solar radiation, the higher both current and voltage and so the more output power of the cell. In contrast, increasing temperature of a PV cell can increase slightly the short-circuit current but it decreases significantly the open-circuit voltage leading to reduction of cell efficiency. The output power of a cell made from silicon reduces by 0.4-0.5% per ^{o}C [69]. Many PV mathematical models have been analyzed from the equivalent circuit by considering the environmental effect. [72], [73] and [74] are examples applying the principle to develop the mathematical models for optimizing of the number of PV modules for stand-alone systems by using the Genetic Algorithms (GAs) and they are expected to obtain a solution closer to the exactness. Nonetheless, the models may be complicated because some parameters have to be investigated from special experiments.

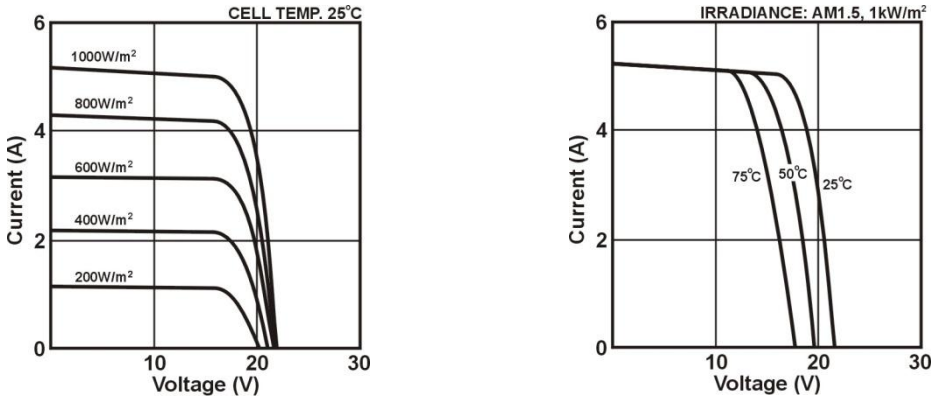

(a) (b)

Figure 2.2 Typical I-V characteristic and power curves of a crystalline silicon module (a) at various irradiations but constant temperature [69] (b) at different temperatures but constant irradiation [75]

Hence, the simple PV model was proposed by estimating from the production of the global radiation on an inclined surface, a PV array area and PV system efficiency shown in Equation 2.1. It has been applied with different purposes by ignoring the

temperature effect. For example, Hocaoglu *et al.* [76] and Askari *et al.* [77] desired to focus the processes to find optimual sizing of system components for stand-alone hybrid systems. Senjyu *et al.* [78] and Suryoatmojo *et al.* [79] utilized it in the procedures of optimum sizing methods using multi-objective methods. It is also easily used for assessment of technologies; for example, Nelson *et al.* [80] assessed fuel cell and battery technologies using in stand-alone hybrid WT-PV systems.

The simple PV model as follows:

$$P_{pv} = \eta_{pv,sys} \cdot H_{\beta} \cdot A_{pv} \cdot N_{pv} \tag{2.1}$$

where H_{β} is the global radiation on an inclined surface (kW/m^2), A_{pv} is the area of a PV module (m^2), N_{pv} is the number of PV modules and $\eta_{pv,sys}$ is the PV system efficiency. Nevertheless, in order to consider the temperature effect, the PV system efficiency of this equation developed by Evans *et al.* [81] has been applied for the optimum sizing design of a PV system such as in [82], [83], [84]. This thesis uses this equation including the temperature effect.

2.2.2 Photovoltaic technologies [69], [17], [85]

Photovoltaic technology was started from discovering the photovoltaic effect of Becquerel in 1839. In 1883, the first PV cell was built by C. Fritts who coated a thin layer of Au to form the junction of Se semiconductor. The modern junction semiconductor of PV cells was patented by R. Ohl in 1946. In 1954, D. Chapin et al. who worked at Bell laboratories improved the modern PV cell using silicon p-n junction, which had an efficiency of approximately 5%.

At present, PV technologies can be divided into three generations, i.e., first is crystalline silicon (c-Si), second is thin film and third is concentrator PVs including organics and other technologies. The current commercial PV module efficiency is based on technologies as shown in Table 2.1. Crystalline silicon modules are the majority of market today, about 80%. Two main types are mono-crystalline (mc-Si) and poly-crystalline (pc-Si) forms. Their efficiencies have been improving since 1954 until now they have a range of 14-22%. Typical module power ranges from

120 to 300 Wp. They have been applied mostly in both stand-alone and grid-connected systems.

Table 2.1 Current commercial PV module efficiency [17]

Technology	Crystalline Silicon		Thin Film				Concentrator PV
	Mono	Poly	a-Si	a-Si/µc-Si	CdTe	CIGS&CIS	III-V multi-junction
Cell efficiency	16-22%	14-18%	4-8%	7-9%	10-11%	7-12%	30-38%
Module efficiency	13-19%	11-15%					~25%
Area needed per kW (for modules)	~7m^2	~8m^2	~15m^2	~12m^2	~10m^2	~10m^2	-

Thin film modules are built by spray coating very thin layers of PV semiconductor materials to decrease costs of products but the efficiency is reduced to a range of approximately 2-12% depending on types. Four types of the current commercial thin films are amorphous Silicon (a-Si), multi-junction thin Silicon film (a-Si/µc-Si), Cadmium Telluride (CdTe) and Copper, Indium, Gallium, (di)Selenide/(di)Sulphide and Copper, Indium, (di)Selenide/(di)Sulphide (CIGS and CIS). Presently, CdTe modules are the most cost-effective thin film technology, with the efficiency of up to 11%. CIGS and CIS technology has the highest efficiencies of thin film technologies, which can reach to 20% in the laboratory but the process is more complicated than others leading to higher production costs. Nominal power modules are in the range of 60 Wp to 300 Wp. Although, thin film modules are cheaper than c-Si modules, they have lower efficiencies bringing to need larger areas for installation and higher costs for mounting. Moreover, because they have a flexible structure, they may be more appropriate for construction of a building. Consequently, they are being developed for the Building Integrated Photovoltaics (BIPV) such as installation onto roofs of buildings and window glazing by using semitransparent PV cells.

For the third generation, Concentrator PV (CPV) uses lenses to focus direct irradiation on to very small amounts of very efficient cells, which are silicon or III-V compounds that are normally Gallium Arsenide (GaA). They are suitable for applying in very sunny areas and need to have a tracking system. However, both the very high efficient cells and the tracking system that can achieve to follow the sun are very expensive, which need to evaluate economic feasibility. For Organic PV (OPV), current cell efficiencies are approximately 4-6% and 5 MW of cells were manufactured in 2009. A target has been set to above 1 GW for production by 2012.

The current commercial efficiencies of hybrid Dye-Sensitised Solar Cells (DSSC) are lower than 4%. Nonetheless, DSSC were produced of about 30 MW in 2009 and they have been planned to produce 200 MW by 2012. Production costs of both OPV and DSSC are reducing and they may achieve to 0.5 €/W by 2020. Other third generation technologies have recently emerged, such as spherical CIS, Thin-Film polycrystalline silicon PV cells, Thermo-photovoltaic (TPV) low band-gap cells that can be applied in Combined Heat and Power (CHP) systems.

2.3 Wind turbines

This section presents mathematical models and main components of WTs for two main types, namely, Vertical Axis Wind Turbines (VAWT) and Horizontal Axis Wind Turbines (HAWT). Current technologies as well as the advantages and disadvantages of each type are also discussed. Furthermore, the main parameters of WTs affecting the performance are studied, so that they will be the basis of improvement on low wind speed turbines (LWSTs), which will be described in Chapter 4.

2.3.1 Models of wind turbines [75], [86]

At the design stage, output power of WT can be divided to two stages, namely, partial load and full load stages as shown in Figure 2.3. Firstly, a WT operates from a cut-in wind speed (normally 2-4 m/s) to rated wind speed (commonly 10-13 m/s). In this range, power output is varied by two major parameters, which are the swept area of rotor blades and the cube of the wind speed. The power output at *t* time can be calculated from Equation 2.2. In the full load stage, the captured power must be limited to a rated power of a WT generator at a rated wind speed of WT and the WT will shutdown at a cut-in wind speed (generally 25 m/s).

$$P_{wt}(t) = 0.5 \cdot\cdot \rho_a \cdot C_p \cdot A \cdot U^3(t) \tag{2.2}$$

where U is the wind speed (m/s), A is the cross-sectional area through which the wind passes (m^2) and ρ_a is an air density, which is 1.225 kg/m^3 at 15 ^oC and 1 ATM .

$C_p(\lambda,\beta)$ is the power coefficient or rotor efficiency, which is another important parameter that expresses how much aerodynamic power is captured by the rotor.

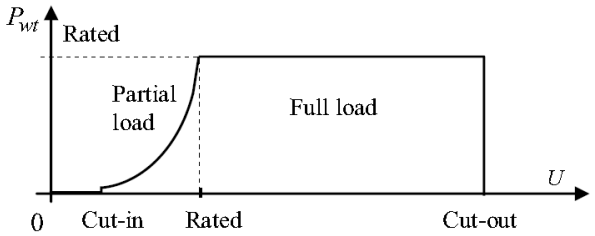

Figure 2.3 The power curve of a wind turbine [75]

The power coefficient is not a constant value and is related to tip speed ratio λ and pitch angle β, and depending on the design as shown in Figure 2.4. The maximum power coefficient in theory is 59.3% and it is called the Betz efficiency or Betz's law. For ideal efficiency, it will be reduced when blades spin slowly and be increased if blades spin quickly. However, although, the Darrieus rotor, which is a type of VAWTs, spins much faster than two- and three-blade rotors of HAWTs, the Darrieus rotor has a maximum efficiency of about 35%, which is much lower than that of HAWTs, with a range of roughly 40-50%. The tip speed ratio, a function that presents rotor efficiency, can be defined as:

$$\lambda = \frac{\omega R}{U} \tag{2.3}$$

where ω is the frequency of rotation and R is the rotor blade radius (m).

The pitch angle, the angle at which the rotor blade surface touches the wind, directly affects the power coefficient illustrated in Figure 2.4(b). As the pitch setting angle is slightly adjusted, the power output of WT will change dramatically. Hence, the pitch angle controller is important in regulating the power output. At a 90^o pitch angle, it is normally applied to stop operating. This can decrease the rotor idling speed and the system will be fully closed down by the parking brake. Nonetheless, the pitch control, which can maintain high reliability, will increase the cost of a WT system.

Solidity, defined as the ratio of total blade area and the swept area, is another parameter affecting performance, illustrated in Figure 2.4(c). Low rotor solidity, of which the lowest is one blade, has a relatively low maximum power coefficient because of high drag losses. Higher rotor solidity means more material is required

for rotor blades and hence higher weights, lower operational speeds and higher costs. Moreover, higher solidity turbines produce higher starting torque and their power coefficient can change rapidly, with a slight tip speed ratio, changing at a range closing to a peak of a performance curve. Nonetheless, too high solidity has a comparatively low maximum power coefficient. Alternatively, a WT with a high number of rotor blades, each of small solidity value, could give a high performance WT. Nevertheless, this does not only increase production costs but small blades will have weak and easily bendable structures. [86], [87]

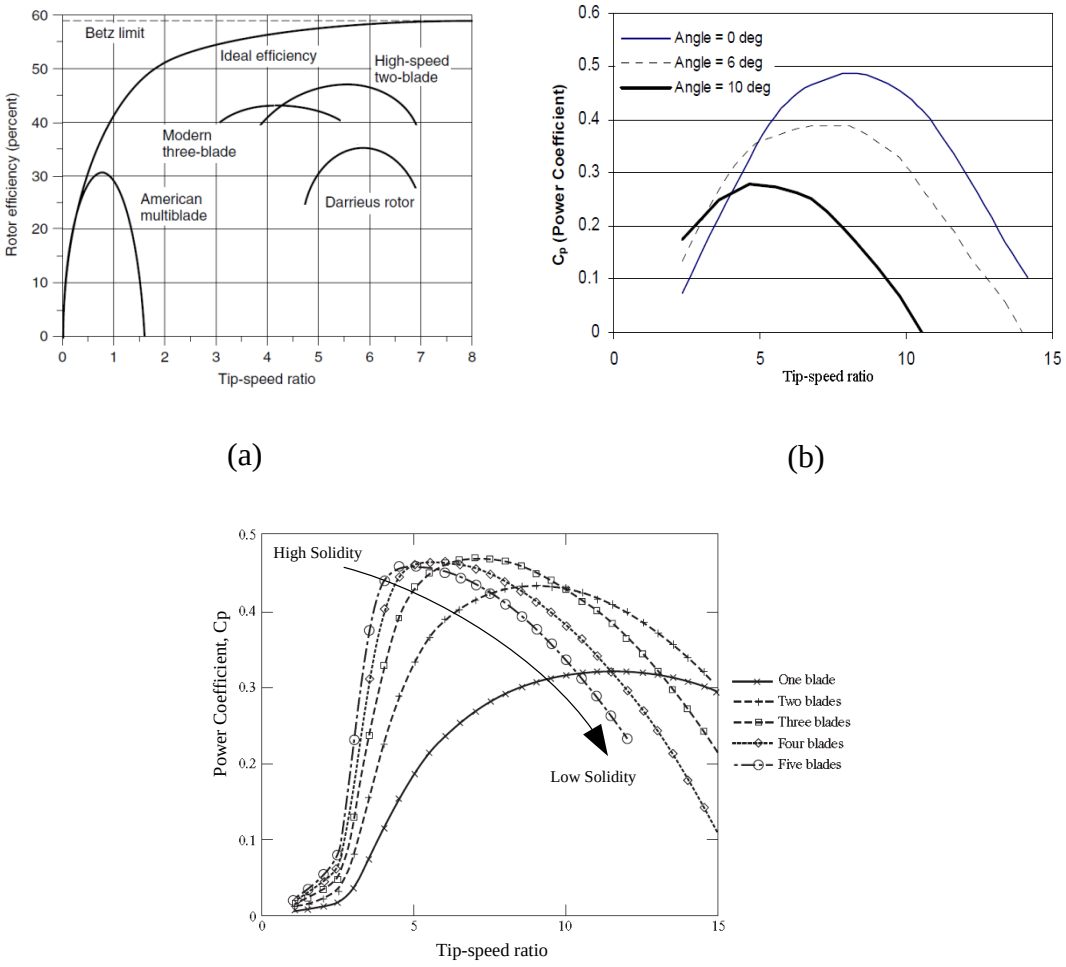

Figure 2.4 Power coefficient or rotor efficiency (C_p) versus tip-speed ratio for (a) various rotor models [75] (b) different pitch angles of HAWTs [88] (c) diverse solidities of HAWTs [86]

The high solidity is generally applied for a directly driven water pump and a micro WT used for battery charging. As a result of producing a high starting torque of high rotor solidity, a small power output can be generated at very low wind speeds. This is a suitable amount for charging batteries nearly constantly, until the batteries are fully charged. It can also provide almost continuous water pumping for a whole year. One-bladed turbines have the lowest solidity (less than 4%) that has minimum energy loss from drag forces, but it has instability and poor aerodynamic performance. A two-bladed turbine has solidity of approximately 4% and a three-bladed turbine has solidity of between 4% and 10% [87]. A three-bladed turbine has optimum solidity and so it is the currently most popular model. However, two blades may be considered as a satisfactory alternative because they have a wider performance curve and that may lead to a larger energy capture. Additionally, they will have lower production costs due to less material used for rotor blades and lower weights. [86], [87]

The variation of wind speeds, dependent on height and surfaces of the ground, can be represented by two mathematical models [75]. One is a logarithmic law proved from a theoretical foundation of aerodynamics. It is usually used in terms of a reference wind speed U_0, at reference height H_0, which is generally applied in Europe, as follows:

$$U = U_0 \left[\frac{\ln(\frac{H}{z})}{\ln(\frac{H_0}{z})} \right] \tag{2.4}$$

where H is the height above the ground level and z is the ground surface roughness length.

Another model, commonly applied in the United States, is simplified from a power law which has been obtained from providing a logical fit to the data:

$$U = U_0 \left[\frac{H}{H_0} \right]^{\alpha} \tag{.5}$$

where α is the friction coefficient based on the ground surface roughness. Normally, for open terrain, the friction coefficient can be estimated roughly as the “one-seventh” (1/7) rule-of-thumb.

To plan and design a WT system in each site, a capacity factor is a measure of the wind availability. The annual capacity factor is calculated from the WT energy produced in a whole year divided by the production of the rated power of a WT system and the number of hours in a year. The annual energy production of a WT system is defined by:

$$E_{WT} = T\bar{P}_{WT} \tag{2.6}$$

where *T* is a time period (h) and $\bar{P}_{WT}$ is the average power from the WT defined by [89]:

$$\bar{P}_{WT} = (\eta - l_s - l_a)A_v \int_0^{\infty} P(U)f(U)dU \tag{2.7}$$

where *P(U)* is the power output from a WT system at wind speed, *U*. η is the conversion efficiency, l_s is the soiling losses, l_a is the array losses, A_v is the WT availability and *f(U)* is the probability density function as follows:

$$f(U) = \frac{dF(U)}{U} \tag{2.8}$$

where *F(U)* is the cumulative distribution function. An equation of Weibull distribution [86] is a probability density function:

$$f(U) = \frac{k}{c}\left(\frac{U}{c}\right)^{k-1} exp\left[-\left(\frac{U}{c}\right)^{k}\right] \tag{2.9}$$

where *k* is the shape parameter and *c* is the scale parameter.

Wind power density is a quantitative measure of wind energy available at sites. It depends on wind velocity and air density, which are based on a hub height above ground. Alternatively, it can be calculated from the ratio of the average annual power available and the swept area of a turbine.

2.3.2 Technologies of wind turbines

In wind energy technologies there are several issues, namely, wind resource assessment, site selection, aerodynamic analysis, WT design, performance and

reliability improvement of WTs and grid connection, reviewed in [90], [91]. This section summarizes current types and components of WTs depending on size and applications.

2.3.2.1 Types of wind turbines

Wind turbines can be classified into two types based on the axis of the rotation of turbine blades. A Horizontal Axis Wind Turbine (HAWT) is the most widespread turbine configuration. Another is a Vertical Axis Wind Turbine (VAWT) that can operate well in low wind speed levels and makes less noise than a HAWT. However, VAWTs have disadvantages, making HAWTs more suitable for development and installation until now. This section describes the advantages and disadvantages, as well as the basic principles of VAWT and HAWT technologies.

1) Vertical axis wind turbine [75]**,** [92]**,** [93]

VAWTs have two main types, namely, drag- and lift-driven turbines, illustrated in Figure 2.5. Drag based turbines, such as an anemometer and the Savonius model, have high solidity and high torque but a low power coefficient, which is lower than 15%. Lift based VAWT, such as the Darrieus model, developed by G. M. Darrieus in the 1920s, consists of low solidity machines applying symmetrical aerodynamic airfoils. In theory, the maximum power coefficient of the lift based VAWT is 59.26%. Hence, the Darrieus turbine is only one of the VAWT types that can compete in a market today. Power output of the Darrieus VAWT can be calculated from Equation 2.2. The swept area of a Darrieus rotor will be estimated as about two-thirds the production of the maximum rotor width and height as shown in Figure 2.5 (a). The advantages and disadvantages of the VAWT are summarized as follows:

Advantages

- Simplicity of structure and independent of the wind direction
- No yaw control system required to turn rotor facing into the wind and hence no losses because of yaw control and thus a decrease in cost and failure factor
- Low level of noise, which is appropriate for installation on top of a building in a residential area

- Location of the generator and controller on the ground so VAWTs have easier maintenance and lower maintenance costs than HAWTs and the system on the ground will reduce loading of tower and construction.

Disadvantages

- The blades are near the ground where winds are slower and there is higher turbulence [92], [93]. Therefore, VAWTs will generate low power output because power in the wind varies on the cube of velocity. More turbulent winds increase stress on VAWT. The turbulence intensity relies on the ground surface roughness and decreases with increasing height [86].
- VAWTs have slightly more expensive drivetrain parts than HAWTs.
- The Darrieus model is difficult to start by itself in low wind speeds because of very little starting torque. However, the Savonius model, which is easier to start, can be applied as a machine starter to the Darrieus model, but this will raise the installation and maintenance costs.
- Larger sizes of VAWTs have higher material costs per square meter of surface covered, than the costs of HAWTs having the same power capacity. The Darrieus model needs guy wires for structural shaft support and larger sizes require more space and have a higher cost of guy wire structures, especially increasing installation costs of offshore structures.
- At high wind speeds, controlling output power to protect the generator of the Darrieus VAWT is more difficult than using pitch-controlled blades of a HAWT.

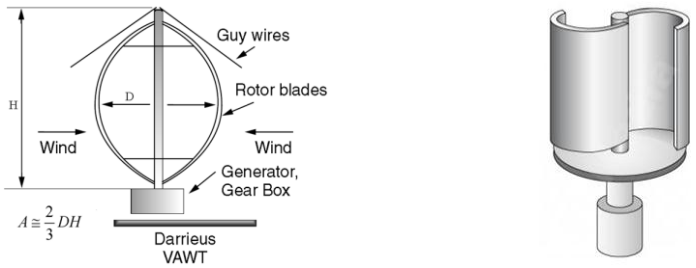

(a) (b)

Figure 2.5 Vertical axis wind turbines: (a) Darrieus turbine (b) Savonius turbine

2) Horizontal axis wind turbine [75]**,** [86]**,** [92]

The majority of WTs in the market today is the horizontal axis type. Two main models of HAWT are upwind and downwind models, presented in Figure 2.6. An upwind turbine has the rotor blades facing the wind while a downwind turbine has blades on the back of the nacelle and faces away from the wind. They have distinct advantages and disadvantages. The advantage of a downwind turbine is that it has no requirement for the yaw, because it can physically adjust itself precisely to wind direction. Unfortunately, the disadvantage is the wind shadowing effects of the tower. The wind shadowing effects diminish wind over a short period, while a blade passes the tower leading to bending in the blade. The bend will reduce the blade performance, causing higher noise levels as well as lower power output than it is designed for. Conversely, although an upwind turbine needs a yaw control system which increases complication, weight and cost, it can work more smoothly and generate more power output. Therefore, the upwind type is the most popular among modern WTs.

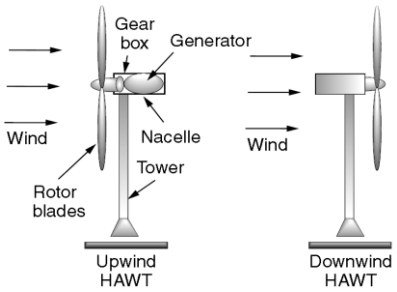

(a) (b)

Figure 2.6 Horizontal axis wind turbines: (a) upwind model (b) downwind model [75]

Owing to the many positive points of HAWTs, they have been developed rapidly leading to the largest WT size of 7.5 MW at present. Most WTs in the market today are three-blade HAWTs, but the development of two-blade HAWTs has grown because they tend to be cheaper than three-blade turbines. However, both HAWTs have many critical issues that need to be improved. The advantages and disadvantages of HAWTs can be concluded as follows:

Advantages

- HAWTs can start operating by themselves (Self starting) at low wind speeds.
- Pitch control can be applied to regulate power output and to shutdown the WT when necessary.
- Now, because of mass production, HAWTs have been developed, which give higher performance and lower cost than VAWTs

Disadvantages

- Noise and tower interference that are caused by the tower shadowing effect
- Increase of complex structure, weight and costs due to a yaw mechanism and a stall control
- Structural strength is required for the weight of a generator and controller located on top of a tower.
- Maintenance is more difficult because a nacelle is on the top of a tower.

2.3.2.2 Components of wind turbines

The main components of a typical WT are rotor blades, a mechanical drive train including rotor hub and nacelle, an electrical system and a tower, illustrated in Figure 2.7. WTs have been developed from small size, with an average commercial WT size of 50 kW, with a 15m rotor diameter in 1980, until now, the largest WT is 7.5 MW with a rotor diameter of 150 m. Developers attempt to improve the larger WT size for a cost-effective project, because it seems to be the larger size which has the lower installation cost per watt leading to lower LCOE. Sizing of WTs can be classified as small, medium and large WTs and they have different technologies used in each subsystem. The configuration and cost of the three sizing ranges of modern HAWTs are shown in Table 2.2, in which the sizes and technologies affect prices of WTs and installation costs.

Small WTs are used in both stand-alone systems installed in places such as individual homes, boats, water pumping and centralized station and a grid-connected system. The range of small WT sizes is identified by a rated power output from various publications such as below 10 kW [25], [95], lower than 50 kW [5] and less than 100 kW [26], [96]. Nonetheless, most small WTs have a power output range of 1 kW to 10 kW. Figure 2.7 shows a three-blade HAWT, the design of most small

WTs, as a fixed-pitch and variable-speed turbine, a passive yaw, a direct drive (no gearbox) and a Permanent Magnet Generator (PMG).

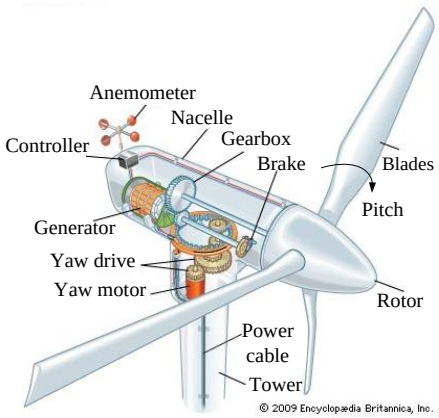

Figure 2.7 Main components of a Horizontal Axis Wind Turbine (HAWT) [94]

Table 2.2 Small, medium and large WT configurations and costs [5], [25], [26], [90], [91], [95], [96], [97], [98], [99], [100], [101], [102]

WT size	Configuration	Generator	Installation cost* (US$/kW)	LCOE** (US$/kWh)
Small (<10 kW)	2 or 3 blades, fixed pitch, passive yaw	Direct-drive, PMG	4,000-8,000	0.12-0.30
Medium (10–1,000 kW)	2 or 3 blades, passive or active blade pitch and yaw	Direct-drive or geared, PMSG or induction generator, 1 phase (<35 kW) or 3 phase power	3,000-6,000	0.09-0.20
Large (>1 MW)	2 or 3 blades, active blade pitch and yaw	Gearbox, synchronous or induction generator or PMSG, 3 phase AC	≅ 3,000	0.07-0.11

Remarks: *, ** costs in 2009 [95]

Medium WTs have a range of sizes, between small and large WTs, and so, at the small range end, they will have the same applications and technologies as small WTs. At the larger range end, they will be connected to a grid system, the same as large WTs. Their technology has been improved to have higher efficiency and larger size. Consequently, there are not many new medium WTs in the active markets because most medium WTs are refurbished [95].

The technologies of the main WT components are as follows:

1) Blade technology [90]**,** [91]

The optimal number of blades is an important issue for WT ability, to capture energy from the wind, described in Section 2.3.1. Most current small WTs are three-bladed HAWTs, but VAWTs and two, four or more blades of HAWTs are also applied for

micro-scale systems, of less than 1 kW. Blades of small WTs are commonly at a fixed pitch angle and need a wide and high twist angle at the root for starting well. Blades of larger WTs are designed by specially considering vibration to avoid fatigue failure under unsteady wind circumstances. The shape of modern large blades is improved by making them thicker, increasing the lift-to-drag ratio by around 20%, when the power coefficient is about 0.5. General construction material is fibreglass, with durable polyester and foam to decrease buckling danger.

Blades of small WTs can be made from such as wood, steel and aluminium and are handmade. Wood such as timbers, solid planks and veneers are strong, cheap, flexible and light weight, but steel is heavy and expensive. Aluminium is light weight, easy to work with but expensive and subject to metal fatigue. For modern WTs, fibreglass is used because of its lightweight, strong, inexpensive and good fatigue characteristics, especially for blades of large WTs. Newer construction materials such as wood epoxy and carbon fibre and newer manufacturing processes have been investigated for producing larger blades at no cost increment and giving increasing strength, reliability and performance.

2) Control system technology

Small WTs are generally designed as fixed-pitch turbines and variable-speed turbines, which are simple, effectively controlled and easy to maintain, due to decrease of power electronic prices. However, if variable-speed control is used, there is an added cost because of the larger size of direct drive generators and power electronics converters, or slip rings on wound rotor induction generators [97]. Nonetheless, WTs that have a power capacity of above 1 MW need to use variable-speed generators [98]. Therefore, the proper design has to be investigated to be economical in capturing more energy. Variable-speed control turbines can increase energy generation by 20% to 30%, compared with fixed-speed control turbines [103]. Nevertheless, the selection depends on locations that have different factors such as wind potential, system reliability required, maintenance, cost and profit from energy generation. Moreover, they can control the active and reactive powers separately in automatic generation control operation and so they reduce power oscillation and improve reactive power injection [104].

Larger WTs will have variable pitch control, using a pitch actuator, to adjust the pitch angle of WTs. A pitch actuator can control the power captured from the wind power and the control can limit the rotor rpm at high wind speeds. Variable pitch control can achieve the maximum electrical power output by two methods, investigated by Muljadi and Butterfield [88]. One is to control the aerodynamic power captured by the blades depending on the pitch rate, the control algorithm and the shape of the power coefficient curve based on pitch angle. Another is to control power output of the generator, by increasing the load relying on the voltage and current rating of the generator and power converter. The current limit of generator is associated with the torque limit, while the voltage limit relates to the generator frequency or speed limit.

Most small WTs commonly use a passive yaw, which is the component responsible to keep WT blades in the wind with the maximum power extracted and to secure a WT from high wind speeds. It can be provided by various mechanisms. Small WTs using a tilting tail hinge and an offset pivot axis have much better performance, simpler structure and maintenance. They are more robust and more cost-effective than small WTs with other passive yaw mechanisms [105]. Nevertheless, an active yaw for small WTs has been investigated; for recently example, Wu and Wang [106] designed an active yaw mechanism for small WTs that have a capacity of above 5 kW.

For an active yaw, direction of wind is controlled by hydraulic or electric motors, which are mostly used for larger WTs, especially large WTs in MW sizes, due to the safety. The design concept is that a yaw control system must not react too quickly to wind turbulence, because the yaw mechanism will move continuously, which would decrease its lifetime. Another issue is twisted cables, when the nacelle of WT turns more than four times; an algorithm and a sensor counting of turnings should be provided to turn the nacelle in the opposite direction to prevent cables from being twisted due to yaw movement in the acute-angular direction. [99]

3) Gearbox technology

A gearbox is an optional component of WTs to increase blade rotation speeds that are more appropriate to drive a generator. It can make the WT system more complex

and lead to higher production costs. Furthermore, the WT system has a drive train requiring frequent maintenance. Bradley [100] discussed the international WT gearbox standard and development. The current WT gearbox standard uses for design and specification for WT power capacities of above 40 kW [100]. Musial *et al.* [107] and Ragheb *et al.* [108] describe the gearbox problems and improvements in gearbox reliability and lifetime, because most gearboxes generally fail within an operation period of 5 years and would need replacement.

However, small WTs do not need to use a gearbox. The direct drive concept allows the rotor to be directly connected to a generator without a gearbox. This reduces the complication of the system, leading to a decrease in production and maintenance costs. The power output of a rotating electrical machine can be estimated by [86]

$$P = KD^2Ln \tag{2.10}$$

where D is the rotor diameter, L is the length of a generator, n is the rotational speed and K is a constant. Hence, when the rotational speed is diminished, the length of a generator or the rotor diameter needs to expand. Increase of the diameter is more cost-effective in order to raise the power output by the square greater than linearly.

4) Generator technology

Most small WTs use Permanent Magnet Generators (PMGs), which are commonly direct drive. Direct-drive PMGs are simple, robust and high efficient technology because of recent development in high efficiency of permanent magnet materials, especially NdFeB (Neodymium-Iron-Boron) [109]. Although, material price may increase for high efficiency of the permanent magnet, recently NdFeB magnet price becomes cheaper at 10 €/kg [101]. A PMG can be improved from either a DC generator or an AC generator that designs the independent external DC supply for the field winding, called the exciter, by replacing permanent magnets leading to lower costs. It can also give fast response to changes in wind speeds due to the constant strong stator field. The drawback is cogging torque caused by the geometry of the PMG reducing the efficiency, investigated in [110], [111], [112]. The cogging torque affects self-start capability and generates noise and mechanical vibration.

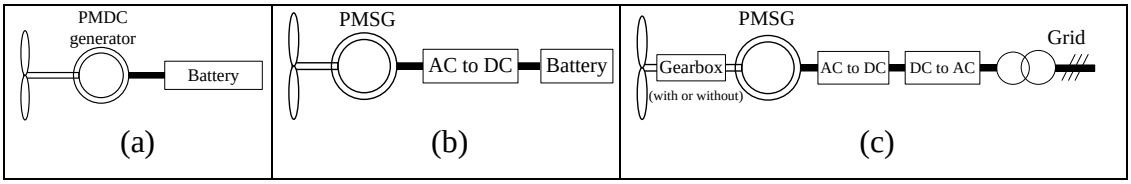

Figure 2.8 Schemes of PMG systems (a) PMDC generator connected directly to battery (b) PMSG connected with a rectifier to charge battery (c) PMSG with a full scale converter

PMGs have been developed and applied for small WTs to charge batteries, shown in Figure 2.8 (a), (b) and (c). A Permanent Magnet DC (PMDC) generator can directly charge batteries. A Permanent Magnet Synchronous Generator (PMSG) needs to have a rectifier to convert three-phase AC to DC. In order to connect with a grid system, PMGs require a full scale converter, 100% of nominal power. Hence, they were started using only for small and medium WTs but PMSGs are now applied also for large WTs due to decreasing cost of permanent magnets and power electronic devices. High pole count PMSGs are recommended in [101] for low speed gearless WTs and they can be applied for a WT power capacity range of 2-5 MW, by using variable-speed control and pitch controlled WT.

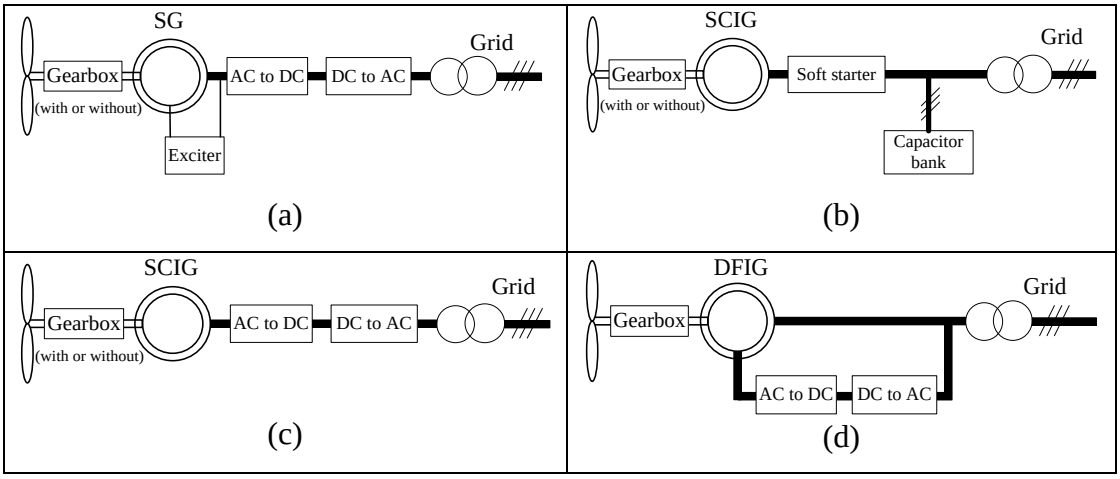

Figure 2.9 Schemes of (a) a SG system (b) a SCIG system with a capacitor bank and a soft starter (c) a SCIG system with a full scale converter (d) a DFIG system

Larger WTs that are between the end of medium size and the large size typically have two main generator types, namely, synchronous and asynchronous induction generators. There have been various techniques developed in each type to increase cost effectiveness of wind energy generation and to reduce drawbacks of the WT

system. Characteristics, designs and positive and negative points of each generator type for using in WTs were reviewed and discussed in [97], [98], [101], [102] and they can be concluded as follows:

Synchronous generators (SGs) operate at a fixed speed related to the constant supply frequency, presented in Figure 2.9 (a). In order to use in WTs, they will have power electronic frequency converters. They also need to have the exciter and thus slip rings and brushes are required for the flow of DC from the exciter to the rotor. This needs well maintenance for replacing brushes and cleaning up slip rings. Furthermore, WTs using SGs need to have a gearbox to adjust speeds from blades to the speeds required of a generator [75]. On the other hand, gearless WT systems can be applied for direct-drive SGs that have low-speed high-torque and they need to have variable-speed control and full-scale power electronic converters for the grid connection. However, the size, weight and cost of these direct-drive generators increase for higher power levels and lower rotor speeds.

Most of WTs in the world apply asynchronous induction generators greater than SGs because induction generators do not need the exciter, brushes and slip rings. They can form the required magnetic field in the stator instead of the rotor. As a result, they reduce complexity, cost down to one-tenth of the SG, maintenance requirement and stresses of the mechanical components of WTs during gusty wind situations. Furthermore, they can be used rather than AC generators for variable-speed operation. They can be connected parallel with a grid system; even though, the amount of power generated varies with wind speeds. The key advantage is that this generator decreases the ‘short circuit risk’ of the power plant. On the other hand, they have the main drawback that is reactive power consumption. Two types that can succeed in using for WTs are Squirrel Cage Induction Generator (SCIG) and Doubly-Fed Induction Generator (DFIG). [91], [113], [114]

WTs using SCIGs are commonly referred to as a fixed speed turbine but they can drive at two different constant speeds by changing the number of pole pairs of the stator winding. The disadvantage is that SCIGs consume reactive power and this is undesirable, particularly in case of large WTs and weak grids. As a result, capacitor banks are required to compensate reactive power to make a power factor close to one, illustrated in Figure 2.9 (b). However, SCIGs can operate in variable speed

mode at all wind speeds by using a full scale converter, about 120% of rated generator power, instead of the capacitor bank and soft-starter, shown in Figure 2.9 (c). Moreover, output frequency of the converter does not need to be the same as the grid frequency. Nevertheless, a full scale converter is costly. [102], [113]

DFIG has the basic operation principle and the stator construction as same as SCIG. However, the rotor is provided with a three-phase winding and it has a power electronic converter for control over the active and reactive power transfer between the rotor and the grid system, illustrated in Figure 2.9 (d). The power electronic converter could have a rate of around 30% of full scale, reducing its size and cost. The selection of the rated power of the rotor converter is decided from costs and speed range desired. A variable-speed control system with a multi-stage gearbox is provided to reduce fluctuations in the active power output and perform reactive power compensation. The advantage of DFIG is that the rotor currents of the converter can be adjusted to control the stator active and reactive power independently. In addition, reactive power can be regulated by the grid-side converter and independently from generator operation, leading to performance of voltage support to the grid system. On the other hand, it has the disadvantages; for example, it may have harmonic from the power electronic converter [114]. Owing to using a gearbox, high maintenance is required and other drawbacks are mentioned in the part of gearbox technology. [102], [113]

In the future, trends of WT generators will be direct drive and grid connected generators. The gear boxes or the full scale power electronic converters may be eliminated, which increases reliability and efficiency of the overall system due to no loss in the gearbox and the converters. However, there are the key challenges that are large size and heavy weight of the direct drive generators. [97]

5) A tower of wind turbines [115]

The higher the smoother wind flow and the higher wind speed and so WTs can produce more electrical energy, mentioned in Section 2.3.1. Nevertheless, higher towers have to be stronger structure because of gravity, rotation, vibration and wind thrust loads leading to increasing costs. Furthermore, the structure must be able to be durable to environmental impacts such as corrosion from sea water, with lifetime of

20-30 years. Consequently, the selection of height tower is a trade-off between costs and energy production. Generally, costs of a structural tower are approximately 20% of total initial capital costs of WT.

Towers of small WTs must be above 10 m to avoid wind turbulence near the ground and most of them are preferably higher than 15 m [5]. Small WTs usually use towers having guy wires for structural shaft support on three or four sides. They will have lower cost than freestanding towers and less of tower shadow effect due to lower tower diameters but they need more space to anchor the guy wires. Their structure can be wooden poles, lattice truss towers, rods and angle iron.

Towers of large WTs, higher than 50 m, are commonly made from tubular steel, lattice truss and concrete. Most modern large WTs use tubular cylindrical pole towers, which are produced separately in 20-30 m of each section. Tower base is larger than the top due to increase of their strength and economical use of materials. A conical pole tower will require an extra cost of $15,000 for every 10 m, if the tower height is above 50 m.

Lattice truss towers are cheaper than conical pole towers because their structure uses less steel with about half the material using for freely standing conical pole towers. Moreover, the wind can flow through their structure with lower flow resistance than tubular towers and less of tower shadow effect. However, one drawback is that their structure may have a lower visual and artistic attraction than conical towers and so they may not be popular to utilize, particularly in large WTs.

2.4 Improvement on rural electrification with renewable energy systems

This section discusses the system concepts and configurations of stand-alone hybrid renewable energy systems. The modelling of power reliability for finding the optimum sizing of renewable energy systems is presented. Improvement in remote area power systems with renewable energy systems and energy storage systems is reviewed. The modelling of battery storage systems and the concept of battery management are provided as background for optimizing hybrid system design. The

models of a DSG for estimating power generation, fuel cost and CO_2 emission are presented.

2.4.1 Stand-alone hybrid renewable energy systems

The design for the appropriate hybrid stand-alone system is a trade-off between the project cost and the quality of services for users. The system design can consider a hybrid stand-alone system to be three subsystems [116], namely, the production, distribution and user subsystems. The production subsystem consists of the generation (RETs and generator set fuel sources), storage (batteries), converter (inverters and bi-directional converters) and control (energy management control systems) components. All components are connected through the bus bar for distributing the produced electricity to the users via the mini-grid.

The availability of resources is the key to determining the capacity of the hybrid system, which needs to exactly match with local demand. Over-sizing of the capacity can lead to excessive costs and electricity production that is not utilized. On the other hand, under-sizing capacity results in insufficient power leading to displeasure of end-users, an increase of stress on the components and a decrease of their lifetime. Several techniques to calculate the optimum sizing of the stand-alone hybrid system minimizing costs are described and discussed in depth in Chapter 3.

The power reliability of a stand-alone hybrid renewable energy system is a key to finding the optimum sizing of the system due to the uncertainty of wind speed and solar radiation characteristics. The power reliability model generally uses the Loss of Power Supply Probability (LPSP) model. The LPSP is the probability showing that the power supply can have adequate power for load demand. It has two existing methods for designing a stand-alone hybrid PV-WT system. The first method applies probabilistic techniques to combine the fluctuating nature of resources and loads, without considering data in time-series. The second method is the concept of the Chronological method, which is a time series simulation method, based on the energy balance of the overall system. LPSP can indicate that the system has sufficient power for load demand during a period considered. [31]

In order to obtain more precise results for the effect of battery energy accumulation, this thesis uses the Chronological method, with a resolution of one hour each time

series throughout the year. The model can be applied for the power system that consists of WTs, PVs and batteries with/without DSGs supporting. For the systems with DSGs supporting, DSGs will operate when output power from WTs, PVs and batteries is not sufficient. However, operation of DSGs will be restricted to a specified minimum and the rated power output of the generator and the amount of CO_2 emission, described in Section 2.4.4. The LPSP from time 0 to T can be modified to be:

$$LPSP = \begin{cases} \frac{\sum_{t=0}^{T} Time\left(P_{ex}(t)>P_{DSG,r}(t), P_{ex}(t)<P_{DSG,min}(t)\right)}{T}, diesel\ generator \\ \frac{\sum_{t=0}^{T} Time(P_{ex}(t)>0)}{T}, no\ diesel\ generator \end{cases} \quad (2.11)$$

where $P_{DSG,r}$ is the rated power of DSGs, $P_{DSG,min}$ is the specified minimum power of DSGs and $P_{ex}(t)$ is the load power exceeding the power available at time t. That is:

$$P_{ex}(t) = P_L(t) - P_{av}(t) \quad (2.12)$$

where $P_{av}(t)$ is the power available at time t from power sources, referred from [73]. It can be described by:

$$P_{av}(t) = P_{wt}(t) + [P_{pv}(t) * \eta_{c,pv}] + [C \cdot V_b \cdot min\left[I_{b,max} = \frac{SOC_{min} \cdot Ah_r}{\Delta t}, \frac{Ah_r \cdot (SOC(t) - SOC_{min})}{\Delta t}\right]] * \eta_{c,batt} \quad (2.13)$$

where C is a constant that is 0 for battery charging process and 1 for battery discharging process. $\eta_{c,pv}$, $\eta_{c,batt}$ are the converter efficiency for converting DC to AC, of PV and batteries, respectively. Batteries will be charged by output of WTs converting to DC and DC output of PV array for the hybrid system in Figure 2.10(a). This system has a main converter for inverting power of both PV array and batteries. In case of the system in Figure 2.10(b), power charging to batteries has to convert from AC to DC for the hybrid system. Charge and discharge of batteries are reliant on the instructions of the charge controller. When an LPSP is 0, the load will be satisfied at all times. Otherwise, if an LPSP is 1, the load will never be satisfied.

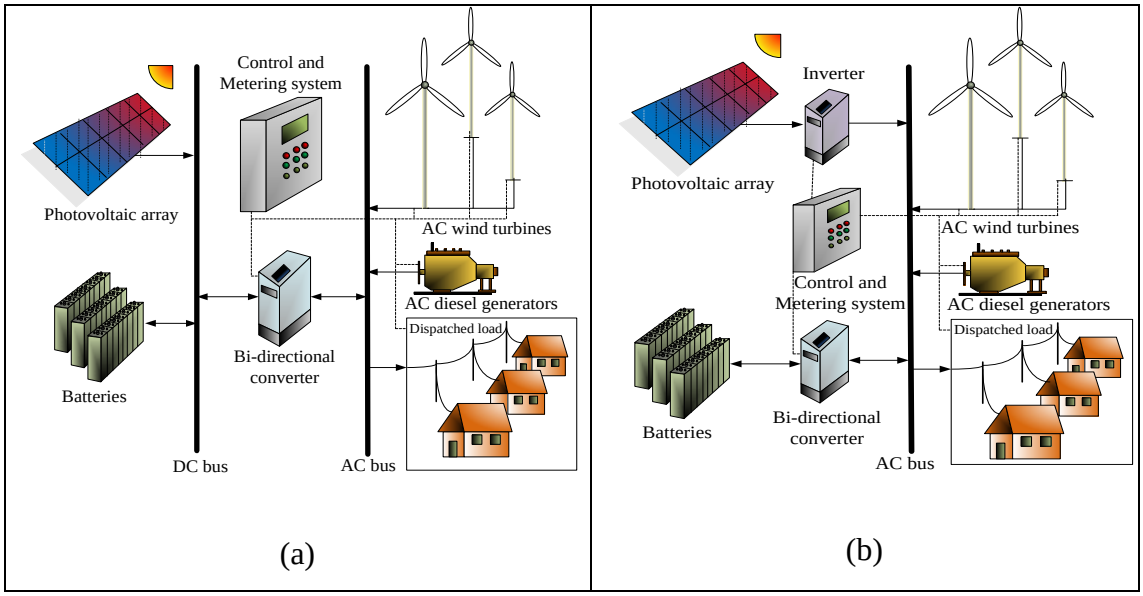

Figure 2.10 Schematic of hybrid mini-grid systems coupled at (a) DC/AC bus bar (b) AC bus bar

The distribution subsystem can be designed by DC and/or AC buses as the main connection point. The differences of the system concepts and configurations between the DC/AC- and AC-coupled hybrid mini-grid systems are shown in Table 2.3. The typical stand-alone hybrid systems consist of a DC bus for battery systems and an AC bus for the DSG and distribution to load, illustrated in Figure 2.10(a). The renewable energy systems such as PV and WT systems can be connected to either the AC or DC bus based on the system size and arrangement. Alternatively, the modular AC-coupled hybrid systems, as shown in Figure 2.10(b), tend to be used in larger hybrid systems with greater advantages, such as more flexibility, greater ability to expand and better cost effectiveness when compared with DC/AC coupled hybrid systems. One drawback of AC-coupled hybrid systems is the loss of three power conversion cycles, from inverting DC to AC of DC sources, AC to DC for battery charging and DC to AC for battery discharging. Both systems can supply more than one house or other single point systems, which have a range of energy demand from 2-3 kWh per day to levels of MWh per day. Nevertheless, larger systems commonly are composed of more and larger equipment and so they will have lower power costs due to an economy of scale. [116], [117], [118]

Table 2.3 Summary of DC/AC- and AC-coupled hybrid mini-grid system configurations [116], [117], [118]

Particular	DC/AC bus bar	AC bus bar
Power capacity	0.5-5 kW, DC voltage is 12, 24, 48 or 60 V [118]	3-100 kW [118]
System concepts	To provide AC power from DC sources and to charge batteries from both AC and DC sources	Each DC source is converted to AC power for supporting load and charging batteries. DC power from batteries discharging is converted again to AC power to smooth power fluctuation.
Distinctive points	Battery can be charged directly from DC sources, reducing losses from converting AC to DC.	- The system is more flexible and expandable. - In low and medium voltage levels, AC lines have better efficiency and lower losses than DC lines. - The system has more cost effective.

The user subsystem consists of all the equipment on the end-user side of the system, such as meters, internal wiring, grounding and appliances. The appliance type and electricity demand of users, who are willing to be connected, are significant factors in designing the system with the correct power generation capacity. In case of villages, the mini-grid system will support domestic, commercial, public and industrial loads. Furthermore, the demand of consumers is based on activities in each season and the location of the rural community.

2.4.2 Improvement in remote area power systems with hybrid renewable energy systems

Grid-connected systems in remote areas have long feeders and usually operate at a medium voltage level, which are generally designed for small loads. When the grid systems have many new users, they will be weaker grid systems due to the decrease of security and quality of power of grid-connected systems, especially at peak demand. Connection of distributed generations that have both positive and negative influences on the weak grids depends on capacity, location in a grid system and technology of components. The properly distributed generations can improve system losses, voltage regulation, power quality and reliability and can be more cost-effective than other technical options, such as capacitor banks [119], [120], [121].

Nonetheless, when the distributed generations that are renewable energy systems, such as PV and WT systems, connect to the weak grid systems for supporting loads, they lead to higher disturbances on the distribution network and can cause several crucial issues, namely, power losses, system security, stability, power quality and

reliability [122], [123]. The doctoral thesis of Fuangfoo [122] presented in 2006, studies the impact of multiple distributed generations on a real distribution network in remote areas in Thailand. He investigates both issues of steady state, namely, voltage regulation, system losses, power quality and reliability, and dynamic stability performance. Limpananwadi and Tayati [123] found that locally distributed generations can strongly affect reliability, system losses and voltage regulation in a remote distribution network in the North of Thailand.

In order to reduce the disturbances on the distribution network, energy storage systems have been developed in both technical operations and financial benefits. The role of energy storage systems, the current storage technologies and modeling and simulation tools is concluded in [124], [125], [126], [127]. Mohd *et al.* [125] also suggest that the standard of planning tools and models needs to be investigated thoroughly for development of the energy storage system. The best appropriate energy storage technologies of four application types for supporting WT generation are recommended in [127]; i.e., primary frequency control should use flywheels and batteries, spinning reserve and intra-day wind unsteadiness improvement should apply batteries and flow batteries, and long term wind unsteadiness improvement should use compressed air energy storage and pumped hydroelectric storage.

There have been many static and dynamic models and simulations for energy storage system applications for compensating the fluctuations of PV and WT power generation and reducing cost of the reserve power capacities leading to more reliable grid system operation [128], [129], [130], [131], [132], [133]. Lund and Paatero [128] used DESIGEN simulation tools designed at Helsinki University of Technology to study the voltage fluctuation in different parts of the distribution network having a large WT with different sizes of a storage energy system. Nyamdash *et al.* [130] demonstrate different sizes of energy storage systems combining with WT systems and found that the sizing of energy storage systems is the key to reducing CO_2 emission of thermal plants in the power system, depending on wind levels of each site. Nevertheless, the results show that the current types of energy storage systems are not yet a worthwhile investment. Pinson *et al.* [131] proposes the dynamic sizing of energy storage systems to assess the necessary reserves for securing the system operation because of variation of WT power

generation. Bludszuweit *et al.* [132] used both MATLAB/Simulink and the optimization tool HOMER to demonstrate battery sizing supporting a hybrid PV-WT system placed in the weak grid system. However, the weak system is assumed to be a stand-alone system. Both software give dissimilar results due to different battery models used but both software shows that adding PV modules in a WT-Battery system can reduce the battery capacity.

It can therefore be seen that it is more efficient to combine WT and PV systems with the energy storage system to improve the performance of the weak grid system. Nonetheless, the optimum sizing of each system must be investigated by considering both technical terms and economic analysis. As a result, this thesis modifies the models and method for designing the optimum sizing of PV, WT and energy storage systems of the stand-alone hybrid systems to the optimum sizing of hybrid PV-WT system using batteries at peak demand for the weak grid power system by minimizing the LCOE and waste of energy (WOE) and considering the issues, namely, power losses, voltage regulation and system reliability as well as economic feasibility. The details of models and method are described and the case study is illustrated in Chapter 6.

2.4.3 Battery-management systems

Uncertainty of renewable energy systems, such as PV and WT systems, and limitation of battery power charging and discharging are crucial issues for designing and managing battery storage systems of the hybrid systems. Therefore, division of batteries into groups or strings, which can be called to be the Decentralized Battery Storage Control (DBSC) method, can give better performance, longer lifetime storage and lower maintenance cost of battery storage systems than a single charge controller [39], [40], [38]. The single charge controller groups all batteries into parallel strings shown in Figure 2.11 (a). The drawback is that the batteries in the same string must have the same capacity and initial State of Charge (SOC) [38]. On the other hand, if a battery has a higher initial SOC, it would be charged faster and have gassing while other batteries in the string are still undercharged. This leads to the reduction of battery lifetime. Moreover, battery charging is limited by the minimum and maximum charging power, but power that charges batteries varies, depending on the power remaining from feeding load demand. Hence, the energy

produced will be wasted and the wasted energy will increase in larger battery energy storage systems.

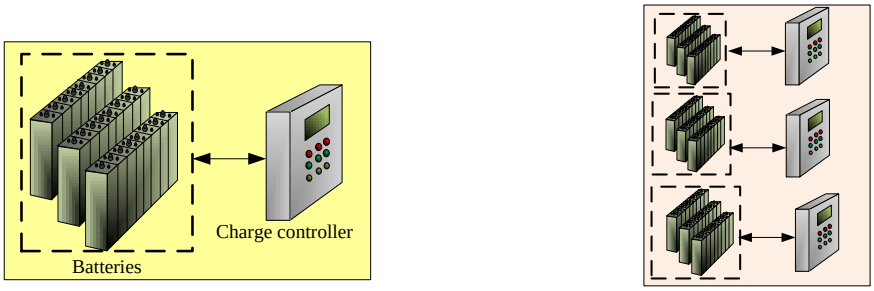

(a) (b)

Figure 2.11 Two battery charging concepts: (a) single charge controller (b) multi-charge controllers

To solve the issues above, an individual battery charge controller is a good option but larger systems will be more expensive. Consequently, this thesis proposes the DBSC method with multi-charge controllers, of which each group has different sizes, presented in Figure 2.11 (b). The aims of the DBSC method are to prolong the battery lifetime and to minimize lost of power supply, cost of energy and wasted electrical energy. Additionally, the system should be practical and economical for operation. The results of case studies to demonstrate this method are described in Chapter 5.

2.4.4 Diesel generator model

A Diesel Generator (DSG) will be connected to load demand through the AC bus. It will operate when the output power from renewable energy systems and energy storage systems is insufficient for load demand. However, it is recommended by manufacturers of the DSGs that DSGs should operate between a specified minimum and the rated power output of the generator [79], [134]. The typical specified minimum recommended power output of DSG ranges from 25% to 50% of rated [135]. The fuel cost can be determined for a year as follows [134]:

$$FC = C_f \sum_{t=1}^{8760}(0.08415P_{DSG,r} + 0.246P_{DSG}(t)) \quad (2.14)$$

where C_f is the fuel cost (£/litre), $P_{DSG}(t)$ is the actual power generated by DSG at time t, and $P_{DSG,r}$ is the rated power of DSGs. Energy in kWh produced by DSGs will emit CO_2 of 0.699 kg [134].

2.5 Evaluation of economic feasibility for renewable energy systems

Levelized Cost of Energy (LCOE) is widely applied to measure electric power generating costs, which can be utilized for comparing generation costs fairly, from different energy sources [29]. LCOE is a measure of a comprehensive evaluation of energy cost over a lifetime of a system with inflation rate. The LCOE in £/kWh for a system is composed of Levelized Fixed Cost (LFC), Levelized Annual Cost (LAC) and Levelized Replacement Cost (LRC) as follows:

$$LCOE = \frac{LFC+LAC+LRC}{E_{use}} \tag{2.15}$$

where E_{use} is the useful energy production (kWh/year), LFC is the annualized capital cost of a system consisting of component cost and installation cost multiplied by Fixed Charge Rate (FCR). FCR is a Capital Recovery Factor (CRF) adding in other costs, namely, costs occurring when a system is unable to operate, a reduction in value of a system, Return on Investment (ROI), insurance and taxes. It is based on system ownership and current capital costs, ranging between 10% and 18% per year. [75]

LAC referred from [74] is all future costs, namely, Operation and Maintenance (O&M) cost and fuel cost, considering the present value and the impacts of inflation, called the Levelized Factor (LF). The LAC is applied to change the increasing annual O&M and fuel costs into a sequence of the same annual amounts. For LRC applied as in [73], it is the levelized value of all the replacement costs of each component happening within the project lifetime.

A technique of project evaluation used to assess the economic feasibility of the hybrid systems is a Net Present Value (NPV), an Internal Rate of Return (IRR), a Payback Period (PBP) and a Profitability Index (PI) calculated following methods in [75], [136]. It measures the productivity of capital investment and the flows of costs

and returns over the life time of the systems. The profitability criteria for decision making are shown in Table 2.4.

Table 2.4 The profitability criteria of decision for the project investment

Investment	NPV	Payback period	IRR	PI
Worthiness	> 0	< life time	> discount rate	> 0
No worthiness	< 0	> life time	< discount rate	< 0
Indifferent case	= 0	= life time	= discount rate	= 0

2.6 Summary

Examples and lessons learnt for PV and WT system applications in Thailand are discussed. It can be seen that the decentralized systems, micro stand-alone systems for individual houses, were not successful for RE. However, the centralized stand-alone systems or mini-grid systems may be more suitable, depending on the system design. The models of PV, WT, battery and DSG systems are presented. The technologies of PV and WT systems are overviewed. The technologies of WT components adopted for small, medium and large WTs are discussed. The configurations and concepts of stand-alone hybrid renewable energy systems and improvement in remote area power systems with renewable energy systems and energy storage systems are reviewed. The concept of battery management is proposed as background for optimizing hybrid system design. Finally, the principle of evaluation of economic feasibility for renewable energy systems is concluded.

CHAPTER 3

3. OPTIMIZATION FOR RENEWABLE ENERGY SYSTEMS

3.1 Introduction

Due to the uncertainty of wind speed and solar radiation characteristics, the optimal sizing of hybrid renewable energy systems is a complex optimization problem. Therefore, several researchers have made an effort to develop techniques for the optimal sizing of hybrid renewable energy systems. This chapter presents a comprehensive and critical literature review of techniques for finding the optimal sizes of hybrid renewable energy systems. Moreover, the merits and demerits of software widely known and used for seeking the optimal sizes of hybrid renewable energy systems or simulating the hybrid system are discussed. This chapter also provides an overview of mathematical optimization, the concepts of convex and non-convex optimization, and the fundamentals of single- and multi-objective optimization. Brief descriptions of Genetic Algorithm (GA) and Multi-Objective Evolutionary Algorithm (MOEA) are presented. The advantages and disadvantages of several MOEA techniques are discussed and summarized. Finally, the Strength Pareto Evolutionary Algorithm 2 (SPEA2), which is applied in this thesis, is described in detail.

3.2 Optimization techniques for hybrid PV-WT systems

There have been several optimization techniques developed for seeking the optimal sizes of hybrid renewable energy systems. Luna-Rubio *et al.*, 2012 [137] present a brief overview of the current status of optimization methodologies for both stand-alone and grid-connected hybrid renewable energy systems. Banos *et al.*, 2011 [32] overviewed single- and multi-objective optimization techniques of renewable energy

systems, namely, wind power, solar energy, hydropower, bioenergy, geothermal energy and hybrid energy systems. Nema *et al.*, 2009 [138] reviewed the current and future state of art design, operation and control requirements of stand-alone hybrid PV-WT systems with backup systems such as a diesel generator, a battery system or a grid-assisted mode system. Furthermore, reviews of current simulation and optimization techniques and software, including simulation modeling, for stand-alone hybrid PV-WT-diesel systems with energy storage in batteries or hydrogen have been presented by Bernal-Agustin and Dufo-Lopez, 2009 [139] and for stand-alone hybrid PV-WT-battery systems proposed by Zhou *et al.*, 2010 [31].

In order to obtain real optimal solutions for real optimization problems, such as design of optimal sizing of the hybrid renewable energy system, having fluctuating resources such as solar and wind energy, the formulation of the problem requires a good compromise between the accuracy of the optimization approach and the detail of the model of hybrid system in both meteorological data and mathematical models. The mathematical models of hybrid system components are described in Chapter 2. Many optimization techniques have been developed for the hybrid PV-WT system and stated in the literature, such as graphical formalism technique, worst-case scenario technique, probabilistic approach, iterative technique and multi-objective optimization technique.

3.2.1 Graphical formalism technique: The graphical formalism technique for finding the optimum size of PV and WT systems, by using supply-demand criteria lines to minimize cost, was proposed by Markvart in 1996 [140]. Borowy *et al.*, 1996 [141] presented a methodology to optimize the sizing of PV modules and batteries by fixing WT capacity in a hybrid WT-PV-Battery system by using 30 years of recorded data. The minimum cost will be at the point of tangency of the linear cost assumed and the curve from the relationship between the number of PV modules and the number of batteries. Based on the method of Borowy, the accuracy was improved by using practical mathematical models of PV, WT and battery characteristics, presented by Ai *et al.*, 2003 [142].

A disadvantage of the graphical technique is that it can search the optimum of only two parameters, either PV and battery or PV and WT.

3.2.2 Worst-case scenario technique: Protogeropoulos *et al.*, 1997 [143] developed the sizing and techno-economical optimization for the hybrid solar-wind-storage system by using the load fraction and considering the worst-load and the worst-renewable month in a year. Habib *et al.*, 1999 [82] proposed the optimization procedure based on calculating the optimal percentage of power produced by PV modules and WTs at a constant load. The techniques are created by using the worst case of a year to design the systems. With monthly average data used, they may not give appropriate and precise results because of the fluctuating nature of resources and loads. Moreover, the worst case technique will be too costly, suggested by Celik, 2003 [144] and Luna-Rubio *et al.*, 2012 [137].

3.2.3 Probabilistic approach: In 1992, Bakirtzis [145] compared the probabilistic approach between independent time series and Markovian time series and found that the serial correlation of surplus generation should be used for evaluating system reliability. A general numerical probabilistic model of an autonomous system consisting of several WTs (wind farm), many PV modules (PV park) and battery storage was presented by Karaki *et al.* in 1999 [146]. Conti *et al.*, 2000 [147] developed a probabilistic model to calculate the long-term performance of a hybrid wind-solar system in terms of the monthly average data and used a Fuzzy logic based multi-objective optimization process. An analytical model of hybrid wind-solar systems using a probabilistic approach based on the convolution technique to evaluate long-term performance for both stand-alone and grid-connected applications was proposed by Tina *et al.* in 2006 [148]. This analytical model has been applied for seeking the optimal sizing of a grid connected system with the Fuzzy logic based multi-objective optimization approach, presented by Terra *et al.* in 2006 [149].

Although the probabilistic approach is good to assess the long-term performance, it cannot be shown as the dynamic changing performance of the hybrid renewable energy system [31].

3.2.4 Iterative technique: Kellogg *et al.*, 1998 [150] proposed an iterative optimization procedure to find the optimal sizing of PV and WT stand-alone systems and a hybrid PV-WT system. Yang *et al.*, 2003 [151] and 2007 [152] have presented an iterative optimization method to find the optimal number of PV modules, WTs and batteries for hybrid PV-WT-battery systems by considering Loss of Power

Supply Probability (LPSP) and minimizing the system cost. Hocaoglu *et al.*, 2009 [76] utilized an iterative approach to search the minimum number of PV modules and WTs and the maximum number of batteries that could be. The optimum point is the minimum system cost that could be reached between a minimum battery capacity and the acquired maximum battery. Kaabeche *et al.*, 2011 [153] used an iterative procedure to follow the deficiency of power supply probability model and the levelised unit electricity cost model for searching the optimal sizing of a hybrid PV-WT-battery system.

Design of a hybrid renewable energy system, including control strategies and multi-criteria decision, is very complicated with non-linear functions. Hence, the iterative optimization technique will be time-consuming. Also, it sometimes cannot achieve the real solution because of a non-convex function, explained in Section 3.4.

3.2.5 Multi-objective optimization technique: Multi-objective optimization techniques have been used for complex multi-objective problems, such as the hybrid systems with nonlinear and non-convex objectives and constraints. They have been approved so that they can provide better results, compared with other techniques, both the design of stand-alone and grid-connected hybrid renewable systems [32], [31], [154], [155].

Fadaee and Radzi, 2012 [154] review the multi-objective optimization of stand-alone hybrid renewable energy systems by using Evolutionary Algorithms (EA). They found that the most popular techniques are GA and Particle Swarm Optimization (PSO). Xu *et al.*, 2005 [74] used GA with elitist strategy for an optimal number of WTs, PV modules and batteries and a fixed tilt angle of PV panels. The objective is the minimum total capital cost and is subject to the constraint of the LPSP. Shi *et al.*, 2007 [156] used the fast elitist Non-dominated Sorting Genetic Algorithm (NGAS-II) to minimize three objectives, the total system cost, the system autonomy level and the wasted energy rate. Capacity of WT, PV and battery are selected to be populations.

Yang *et al.*, 2008 [73] applied the basic GA to optimize the number of WTs, PV modules and batteries, slope angle of PV panels and tower height of WT by minimizing the total annual cost and LPSP. The proposed method has been used for

the design of a hybrid system generating power for a telecommunication relay station. The hybrid system was installed on a remote island along the South-East coast of China and the battery is in good working order, having had few instances of over discharge throughout the studied year from hourly measured field data, analyzed by Yang *et al.*, 2009 [157]. Suryoatmojo *et al.*, 2009 [79] applied Breeder Genetic Algorithm to minimize the total annual cost of hybrid system and to optimize the number of WTs, PV modules and batteries to support existing diesel generators for reducing CO_2 emission. Kaviani *et al.*, 2009 [72] applied a PSO algorithm to seek the optimal number of PV modules, WTs and batteries with the minimum cost.

The Strength Pareto Evolutionary Algorithm (SPEA) has been developed to be the SPEA2 version, becoming one of the most efficient that can give the best results, investigated by Zitzler [118], [158]. Bernal-Agustin *et al.*, 2005 [159] used the SPEA for optimizing the size of a stand-alone hybrid PV-WT-diesel-battery system by minimizing the total system cost and the CO_2 emission, for two different load profiles but without considering seasonal variation. Dufo-Lopez and Bernal-Agustin, 2008 [160] applied SPEA for the design of stand-alone hybrid PV-WT-diesel-hydrogen-battery systems by minimizing three objectives, namely, the total cost, CO_2 emission and unmet load. They also have developed the Hybrid Optimisation by Genetic Algorithms (HOGA) tool, of which the current version uses both the SPEA and SPEA2 [36]. Furthermore, the SPEA2 has been applied for development of a distributed energy resources planning tool, proposed by Alarcon-Rondriguez, 2009 [37].

In conclusion, the time-series simulation approach has been investigated that can provide real optimal solution and it is the most generally applied renewable energy system optimization procedure. Time-series meteorological station data is commonly used for feasibility study and design of the hybrid system, with normally a resolution of one hour time intervals. Even though the time-series simulation method requires considerable computational effort, the total computation time has been reduced thanks to the development of optimization techniques and current computer technology. Additionally, the multi-objective optimization techniques have been utilized more extensively to provide valuable information about the correlations

between the cost and system reliability, including the benefits and impacts of the hybrid system when connecting to the power system.

3.3 Optimization software for hybrid renewable energy systems

Two optimization programs are generally used for hybrid renewable energy systems, shown in Table 3.1. The Hybrid Optimization Model for Electric Renewables (HOMER) is the public domain software, developed by National Renewable Energy Laboratory (NREL) in the USA [161]. This program uses the enumeration technique, attempting to calculate all possible combinations of the hybrid system component sizes. This is a drawback, as users must consider the component sizes, which will not be the exact optimum sizing of the hybrid system component. The Kinetic Battery Model (KiBaM) is applied in the control strategy, proposed by Manwell and McGowan in 1993 [162]. This model is the basis of a chemical kinetics process, developed to model large lead-acid storage batteries.

Hybrid Optimization by Genetic Algorithms (HOGA) is a simulation and optimization program developed by the Electric Engineering Department of the University of Zaragoza in Spain. Installing and running applications of the program are described in [36]. System modelling and procedure of the current version are illustrated in [163]. Two GA techniques are applied: The SPEA is used for the main algorithm to seek for possible component configurations of the hybrid system to minimize the total system costs. The SPEA2 is utilized for the secondary one to search for the appropriate control strategy for each of the configurations, discovered by the main algorithm. The new control strategy has been improved by two options of estimation of battery life time and two options of different mathematic models for battery operation [164].

The selection of the use of the SPEA and SPEA2 of the HOGA is a good choice because it can optimize either single- or multi-objective optimization problem. Furthermore, this method can search the optimum sizing of component configurations, different from the HOMER program in which the user must fill the sizes to be considered. Nevertheless, the HOGA program has not prepared for battery group management that its benefits are described in Section 2.4.3 and

demonstrated in Chapter 5. Both the HOMER and HOGA programs can be downloaded and used free of charge. They also provide economic assessment and pollution emissions for the hybrid renewable energy system connected to the grid system but they do not optimize power flow of the hybrid system. Consequently, they do not check that the hybrid system will affect power quality, system security and reliability of the grid system.

Table 3.1 Comparisons between HOMER and HOGA programs [36], [161], [162], [163], [164]

Particular	HOMER	HOGA
Optimization techniques	Enumeration technique	SPEA and SPEA2 techniques
System components	PV generator, batteries, wind turbines, hydraulic turbines, AC generators, fuel cells, electrolyzers, hydrogen tanks, AC-DC bidirectional converters and boilers	PV generator, batteries, wind turbines, hydraulic turbine, AC generator, fuel cells, electrolyzer, hydrogen tank, rectifier and inverter
Control strategies	The KiBaM model	The Ah Model or the KiBaM Model
Information requirement	Resources (component types, sizes to consider, costs, efficiency, longevity), economic constraints, sensitivity variables and control methods	Resources (component types, costs, efficiency, longevity), financial data, genetic algorithm parameters and control methods or data
Loads	AC, DC, and/or hydrogen loads, as well as thermal loads	AC, DC, and/or hydrogen loads
Results	NPC, the amount of emissions and energy	NPC, the amount of emissions, unmet load
Merits	Providing graphical simulation results easily to understand.	- Two options between single and multi-objective - Providing graphical simulation results easily to understand.
Demerits	- Computation times may increase very much relying on the number of variables used. - A user must fill sizes of each component to consider as it seeks for the optimal system. - A user must choose the type of battery, which cannot optimize between different types of battery.	The accuracy and speed to receive results of this software depends on the setting of configuration parameters of the GA method.

Beside two optimization software tools, the Generic Optimization (GenOpt) [165] program applies the linear simplex optimization method. This software can calculate economic optimization of the hybrid system by using HYDROGEMS. HYDROGEMS [166], developed by the Institute for Energy Technology (IFE) in Norway, is a series of libraries consisting of PV modules, WTs, diesel generators, polymeric and alkaline fuel cells, electrolysers, hydrogen tanks, lead-acid batteries, and DC/AC converters. The libraries are also used by Transient Energy System Simulation (TRNSYS) software and are free for TRNSYS users. TRNSYS [167] is energy system simulation software, developed in 1975 by the University of

Wisconsin and the University of Colorado in the USA. It was initially developed to simulate thermal systems but now it can simulate a hybrid system. It can provide good graphics with great detail and precision; however, it is not free of charge.

Other simulation software tools, such as HYBRID2, INSEL, RAPSIM and SOMES, are obtainable just for evaluating performance and designing of the hybrid systems but not for searching the optimum size of the hybrid system. Most of them are not free of charge but HYBRID2, developed by the Renewable Energy Research Laboratory (RERL) of the University of Massachusetts, can be downloaded and used free of charge. The HYBRID2 [168] can give a very precise solution of simulation by defining time intervals from 10 minutes to 1 hour. The hybrid systems may be composed of multiple WTs of different types, PV generators, multiple diesel generators, battery storage, four types of power conversion devices and three types of electrical loads.

Integrated Simulation Environment Language (INSEL) [169] is a simulation program of renewable energy systems, created at the University of Oldenburg. It is flexible to create the system models and configurations but it is not free of charge. Remote Area Power Supply Simulator (RAPSIM) [170] is basically a simulation program for hybrid PV-WT-Diesel-Battery systems, developed at the University of Murdoch in Perth, Australia. It calculates the total costs throughout the lifespan and the user can modify the components to analyse the effect on the total cost. It is not free of charge. Simulation and Optimization Model for Renewable Energy Systems (SOMES) [171] has been developed at Utrecht University in the Netherlands. This software can simulate the performance of renewable energy systems, which can consist of PV arrays, WTs, a motor generator, a grid, battery storage and many types of converters. It is not free of charge.

3.4 Key concepts of optimization

This section provides an overview of mathematical optimization, the concepts of convex and non-convex optimization, and the fundamental of single- and multi-objective optimization. Brief descriptions of GA and MOEA are presented. Finally, the SPEA2, which is applied in this thesis, is described in detail.

3.4.1 Optimization problem [172], [173]

A mathematical optimization problem can be generally stated as the following:

$$\min F(x) = \min(f_1(x), f_2(x), \dots, f_m(x)) \tag{3.1a}$$

$$\text{Subject to} \quad g_j(x) \geq 0, \ \ j = 1, 2, \dots, J \tag{3.1b}$$

$$h_k(x) = 0, \ \ k = 1, 2, \dots, K \tag{3.1c}$$

$$x_i^{(L)} \leq x_i \leq x_i^{(U)}, i = 1, 2, \dots, n \tag{3.1d}$$

F(x) is a vector of *m* multi-objective functions, $f_i(x)$, which *m* is equal to one for a single-objective problem. Each objective function can be either minimized or maximized. Equation 3.1a shows all objectives as minimization. To solve a minimization problem into a maximization one, the objective function is multiplied by -1, min (-$f_i(x)$), from the duality principle in the context of optimization. A solution $x = (x_1, x_2, \dots, x_n)$ is the decision vector consisting of the set of *n* decision variables. The decision value that can be continuous, discrete or integer in nature is limited within a lower $x_i^{(L)}$ and an upper $x_i^{(U)}$ bound. These bounds are called a "decision variable space" or "search space".

The terms $g_j(x)$ and $h_k(x)$ are inequality and equality constraint functions, respectively. They can be linear or nonlinear functions. If all objective and constraint functions are linear, the optimization problem is called a linear programming problem. Nevertheless, if any of the objective or constraint functions are nonlinear, the optimization problem is called a nonlinear programming problem. Furthermore, if problems do not have constraints, they are mentioned as unconstrained optimization problems. A solution *x* will be called a *feasible solution* for any solution *x* that satisfies all constraints and variable bounds. Conversely, if a solution *x* does not satisfy all of both constraints and variable bounds; it is known as an *infeasible solution*.

The mapping *F(x)* establishes the decision vector from the decision space to the objective space in which a feasible solution is identified. The three spaces and a mapping between them are illustrated in Figure 3.1. The figure shows a multi-

objective optimization problem having three decision variables (x_1, x_2, x_3) and three objective functions ($f(x_1)$, $f(x_2)$, $f(x_3)$).

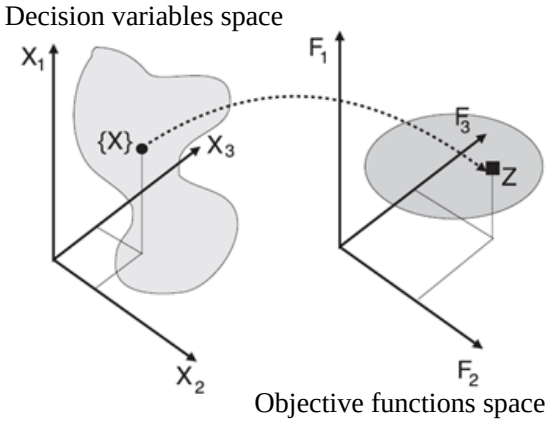

Figure 3.1 Representation of the decision space and the objective space of multi-objective optimization problem [173]

3.4.2 Convex and non-convex optimization [37], [172], [173]

The difficulty in solving optimization problems can be identified from convexity. A set C is convex if for any two vectors, $f_1(x)$ and $f_2(x)$, in C and all the line between $f_1(x)$ and $f_2(x)$ is also within C, illustrated in Figure 3.2. It can see that convex objective functions have a single optimal point that is the global optima. Otherwise, non-convex objective functions have some parts of the line between both vectors that is out of C and then they have more than one optimal solution. These solutions are called local optima. However, a non-convex function has only a single global optimal solution. Therefore, any discontinuous set, such as discrete variables, and any nonlinear equality constraint are non-convex. Moreover, integer or mixed integer optimization problems then have a non-convex feasible region. Nonetheless, nonlinear objective functions can be either convex or non-convex as shown in the figure. For a convex multi-objective optimization problem, all objective functions are convex and the feasible region is convex; alternatively, all inequality constraints are non-convex and equality constraints are linear.

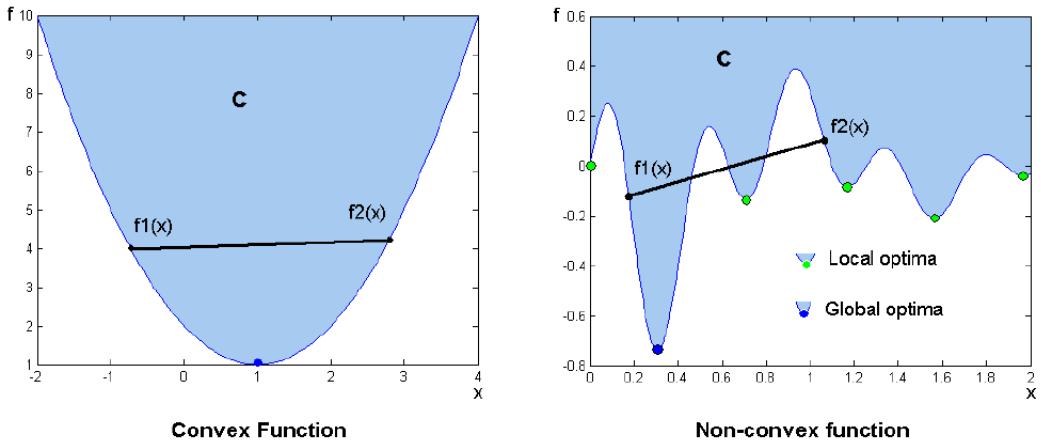

Figure 3.2 Non-convex and convex objective functions [37]

3.4.3 Single-objective optimization

A single-objective optimization problem has only one goal. Even though some problems may have many local optimal solutions, they have the goal of finding the global optimum solution. Several optimization techniques have been developed to achieve the goal. They can be classified, namely mathematical, Artificial Intelligence (AI) and heuristic techniques to solve the single-objective optimization problem. The mathematical methods or numerical methods are based on gradient search or neighborhood search (or called local search) techniques, designed for solving specific types of problems [174]. The main groups of mathematical optimization methods can be classified as follows [175]:

- *Analytical methods* are the classical optimization techniques using differential calculus to solve the continuous and differentiable twice objective function and constraints in a real continuous decision variables set. These techniques are a basis for developing most of mathematical methods.
- *Linear programming* solves the problems in case of objective function and constraints that are linear. The decision variables set is real continuous.
- *Integer programming* studies the case in which the objective function and constraints can be either linear or nonlinear but some or all decision variables take on integer values.

- *Quadratic programming* is for a quadratic objective function. Constraints are specified using only linear equalities and inequalities within a real continuous decision variables set.
- *Nonlinear programming* is designed to solve the objective function or constraints or both that is nonlinear in a real continuous decision variables set.
- *Dynamic programming* studies in the case of the objective function that can split into sub-problems. Variables are constrained to take on discrete values.
- *Combinatorial programming* studies the general case for linear or nonlinear objective function and constraints in which the set of feasible solutions is discrete or can be decreased to a discrete one.

With a proper mathematical method, the convex problems can be solved to obtain a precise optimal solution in a short time, even when the problems have numerous variables involved. On the other hand, non-convex (nonlinear, discrete and combinatorial) problems will be very difficult and will consume much computation time to be solved by mathematical methods, even with a few variables [172]. Additionally, the optimal solution, reached from the mathematical methods, is the global optima. However, both AI and heuristic optimization techniques are generally acceptable in solving the non-convex problems by providing near-optimal solutions. A heuristic technique of learning uses reasoning and past experience to solve problems and find an optimal solution. Many researchers define AI as the intelligence of machines which perceives and proceeds actions, based on human's thought characteristics [31]. Because humans has logic from experiences; therefore, some authors prefer to group AI and heuristic techniques. Moreover, most modern heuristic optimization techniques are based on biological systems. The AI and heuristic optimization techniques can be mainly grouped by nature as follows [174], [176]:

- *Evolutionary Algorithm (EA)* is the basic of genetics and evolution, imitating the evolutionary process of species that sexually reproduce.
- *Simulated Annealing (SA)* is based on the thermodynamics of the metal annealing process.
- *Tabu Search (TS)* applies human memory structure in optimization to avoid repeating using the same solution more than one time.

- *Ant Colony Search (ACS)* mimics ant's behaviour where ants seek ways for food and find the way back to their nest.
- *Neural networks* are based on the brain functions, defined to be two types, namely Biological Neural Networks (BNN) and Artificial Neural Networks (ANN). The BNN is created from real biological neurons, functionally related in a nervous system. The ANN is the modern neural network techniques, imitating characteristics of biological neurons.
- *Fuzzy programming* imitates human linguistic classification and reasoning function, using probabilistic logic.
- *Particle Swarm Optimization (PSO) algorithm* was developed from simulating social behaviour, imitating the movement of living beings such as a bird flock and fish shoal.
- *Bacterial Foraging Optimization Algorithm (BFOA)* is based on how bacterial matter searches for nutrients, involving the movement and communication of bacteria.

3.4.4 Multi-objective optimization [173]

Most real-world optimization problems involve multi-objectives by nature, normally with conflicting objectives, such as the decision between cost and quality. Each objective matches a different optimal solution. Consequently, the Multi-Objective Optimization Problems (MOOPs) have more than one optimum solution. The problems can be solved by either "ideal" multi-objective optimization techniques or preference-based techniques. The processes of both techniques are illustrated in Figure 3.3. In order to make a decision for only one solution required, the higher-level preference information is needed in both types of techniques. A difference between the two is the sequence of decision making and optimization. The "ideal" multi-objective optimization searches the group of trade-off optimum solutions, with all equally significant objectives.

Alternatively, a preference-based technique, shown in Figure 3.3(b), estimates the relative importance of each objective from higher-level preference information to provide a single-objective problem and then finds one optimal solution via a single-objective optimization technique. However, to quantify subjective preference values,

sufficient qualitative information and skill to be used in the analysis are required because the preference values are very sensitive to the relative preference objective applied in forming the single-objective function. A variation in the relative preference objective will also give a different optimal solution.

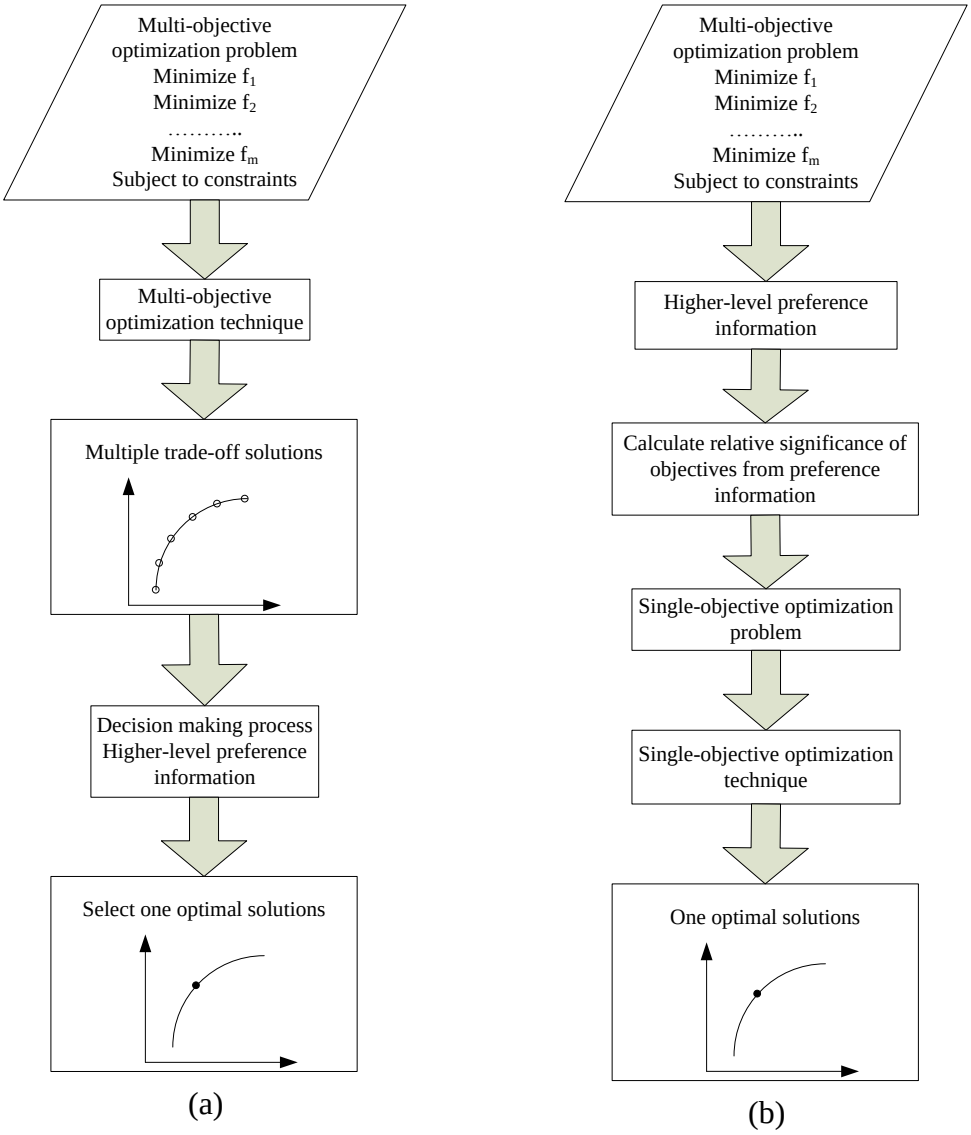

Figure 3.3 Multi-objective optimization processes (a) an "ideal" technique (b) a preference-based technique [173]

Unlike the ideal multi-objective optimization, various possible trade-off solutions are provided, which allow more informed choices and may lead to the analysis of relationships between objectives. Furthermore, the ideal approach is "more methodical, more practical and less subjective" [173]. These are keys in designing

the hybrid renewable energy systems, requiring a more precise representation than is possible in the scope of each objective. Moreover, in order to study the hybrid systems in different circumstances and designs, for example, Low Wind Speed Turbine (LWST) application and battery management application in stand-alone hybrid WT-PV systems are demonstrated in Chapter 5. In addition, hybrid WT-PV-battery system designed to reserve the peak load demand is illustrated in Chapter 6. The minimum LCOE and the maximum system reliability as well as the minimum WOE are objectives of the sizing system optimization in this thesis.

3.4.5 Dominance and Pareto-optimality [173]

Most multi-objective optimization algorithms are created from the idea of "domination", comparing any two solutions and selecting the better one. It is said that a solution $x^{(1)}$ dominates another solution $x^{(2)}$, when $x^{(1)}$ is no worse than $x^{(2)}$ in all objectives and $x^{(1)}$ is better than $x^{(2)}$ in at least one objective. In this case, $x^{(2)}$ is said to be dominated by $x^{(1)}$ or $x^{(1)}$ is said to be non-dominated by $x^{(2)}$. This concept of dominance is known as "weak dominance", which is the most commonly used. Consequently, "dominance" used in this thesis refers to "weak dominance".

An example of domination in a two-objective minimization problem is illustrated in Figure 3.4. The dominance relation shows that solution $x^{(1)}$ dominates solutions $x^{(3)}$ and $x^{(4)}$; solution $x^{(3)}$ dominates solution $x^{(4)}$ and solution $x^{(2)}$ dominates solution $x^{(4)}$ and $x^{(5)}$. Solutions $x^{(1)}$ and $x^{(2)}$ do not have any solution that dominates them; therefore, they are non-dominated and called the *Pareto-optimal* solutions. Furthermore, these solutions form the *non-dominated set* of the given set of five solutions. For the non-dominated set of the entire search space *S*, it is called the *Pareto-optimal set*. Like global and local optimal solutions in the case of single-optimization, the *globally and locally Pareto-optimal sets* of multi-objective optimization are presented in Figure 3.4. In this example, solutions 1 and 2 are members of the globally Pareto-optimal set or called *Pareto-optimal front* and solutions 5 is a member of the locally Pareto-optimal set.

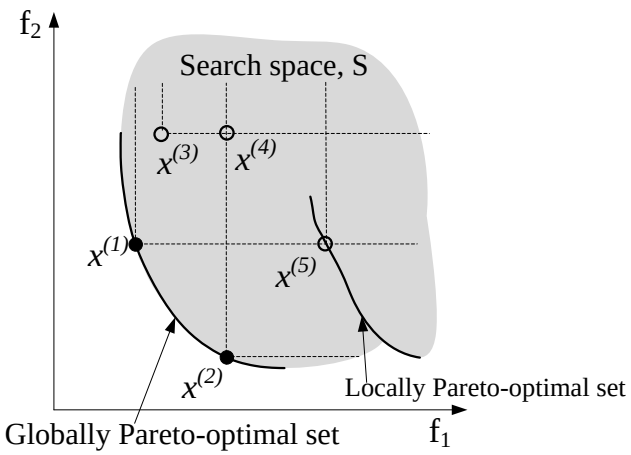

Figure 3.4 Pareto-optimal solutions

3.4.6 Multi-objective optimization techniques

Multi-objective optimization techniques can be classified into two groups, namely classical methods and heuristic methods. The classical multi-objective optimization methods have been used for the past four decades. They are developed from single-objective optimization approaches, by utilizing a preference-based technique, shown in Figure 3.3. Furthermore, the concepts, advantages and disadvantages of the classical methods are summarized in Table 3.2. Most of these methods can solve the non-convex multi-objective problems, excepting the weighted sum methods. However, all methods need some problem knowledge, such as appropriate weights or upper bound vector (ε) or goal values. In addition, if users need to obtain multiple Pareto-optimal solutions, they have to run many simulations because a single run of a classical method can find only one Pareto-optimal solution.

The heuristic methods, for solving single-objective problems presented in Section 3.4.3, are modified to be the multi-objective heuristic optimization. They have been developed to eliminate the limitations and drawbacks of the classical methods. The multi-objective heuristic optimization techniques can find multiple Pareto-optimal solutions, in one simulation run, of both convex and non-convex problems. The EA, a type of the heuristic methods, works with several solutions at any given time. They are described in detail in the next section.

Table 3.2 Concepts, advantages and disadvantages of classical methods [173], [177]

Methods	Concepts	Advantages	Disadvantages
Weighted-sum	Change the multi-objective problem to a single-objective problem by converting the multi-objective function into a weighted-sum of the objectives.	- Simple and easy to use - Suitable for problems having a convex Pareto-optimal front	- Very difficult for optimization problems mixing maximization and minimization types, and nonlinear MOOP - Different weight vectors may not lead to different Pareto-optimal solutions. - It cannot find all solutions for a non-convex Pareto-optimal front.
ε-constraint	Reformulate the MOOP by keeping an objective and expressing others as inequality constraints	It can be used for problems having either convex or non-convex objective space.	- Need the same amount of information as the weight-sum methods and need more if the problem having various objectives. - Require a large number of iterations for several objectives to search various solutions belonging to the Pareto-optimal front.
Weighted metric (weighted Tchebycheff problem)	Instead of using a weighted-sum of the objectives, other ways of combining multi-objectives such as weighted distance metrics.	The weighted Tchebycheff metric guarantees searching all Pareto-optimal solutions when the ideal solution is a utopian objective vector.	- It needs knowledge of the minimum and maximum function values of every objective to normalize the objective functions. - It is necessary to optimize all objectives individually to obtain the ideal solutions.
Rotated weighted metric	It is a weighted metric method but using rotation matrices, around the ideal point of weighted distance metric.	Different Pareto-optimal solutions can be received by varying the angle and the weight vector.	- It is difficult because it has to fix many parameters. - Not guaranteeing that a Pareto-optimal solution can be found in every problem.
Benson's	Similar to the weighted metric technique but taking the reference solution randomly from the feasible region.	- Avoid scaling problems by normalizing individual differences before the summation. - Obtain different Pareto-optimal solutions by changing the weight vector before summation. - Non-convex multi-objective problems can be solved if selecting the proper reference solution.	- Require several additional constraints. - Difficulties for gradient-based methods to solve the non-differentiable objective function.
Value function	A mathematical value function, relating all objectives, is provided by users and must be valid for the entire feasible search space.	- Simple and ideal for sufficient value function information - Suitable for multi-attribute decision analysis problems with a discrete set of feasible solutions	- Solutions depend on the selected value function. - Users need to create a value function that can be commonly used over the entire search space; otherwise, it is in danger of applying an over-simplified value function.

3.4.7 Evolutionary algorithms

Evolutionary Algorithms (EA), population-based meta-heuristic optimization algorithms, imitate the principles of natural evolution to form processes of search and optimization. There are five major groups of EA, namely, Genetic Algorithms

(GA), Evolutionary Strategies (ES), Evolutionary Programming (EP), Learning Classifier Systems (LCS) and Genetic Programming (GP). Even though they were individually developed, they have the same common basic concepts of procedural structure using evolutionary mechanisms like selection, crossover, mutation and survival of the fittest to filter a group of solution candidates. [178]

Presently, GA is the most popular known type of EA [179]. Most applications of heuristic approaches to hybrid renewable energy systems are based on GA from several researches, reviewed in Section 3.2.5. This is because GA is a very good technique to solve complicated nonlinear problems. GA was developed for single-objective optimization problems and has been modified for multi-objective optimization problems. MOEA, based on the GA structure, are very good at dealing with multi-objective problems that are combinatorial nonlinear. Therefore, this section describes the principles of GA, including merits and demerits. Furthermore, the development history and concepts of MOEA are introduced and discussed.

3.4.7.1 Genetic Algorithms

A Genetic Algorithm (GA), developed by John Holland in 1975, is a stochastic optimization method, inspired by both natural selection and natural genetics. The concepts of GA involve a *population of strings*, called *chromosomes* or the *genotype of the genome*, encoding candidate solutions to an optimization problem, one gene in the chromosome representing each decision variable. Chromosome encoding is shown in Figure 3.5. Variable sets in the decision space or candidate solutions are called *individuals, creatures* or *phenotypes*. Solutions or string chromosomes are represented in binary, as strings of 0 and 1 but there can be other encodings, such as vectors of integer numbers or vectors of real numbers. To solve real-world optimization problems using GA, the selection of suitable encoding methods is a key issue, discussed in [37], [179]. Binary encoding was widely used in the past, but now many researchers confirm that it cannot be used in several real-world problems. The real number encoding has the best performance for function optimizations and constrained optimizations [179]. The integer number encoding is appropriate for combinatorial optimization problems [179]. The encoding process evolves chromosomes into better solutions, which are new chromosomes or called *offspring*,

with three basic genetic operators, namely selection, crossover and mutation. A successive iteration process is called a *generation*.

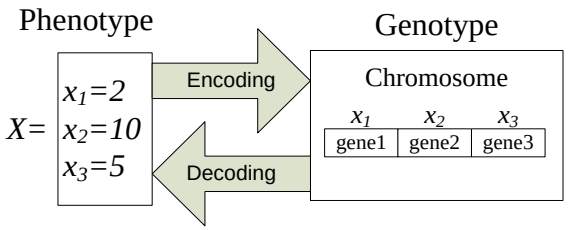

Figure 3.5 Encoding and decoding of chromosome

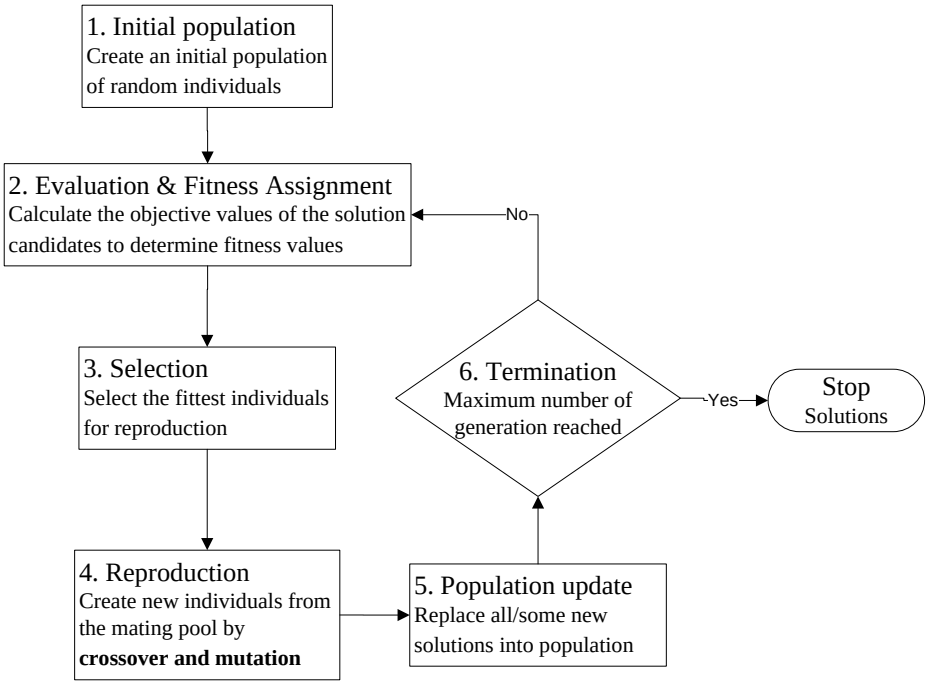

Figure 3.6 Basic sequences of GA

The basic structure of GA is presented in Figure 3.6. Only the objective function information and probabilistic transition rules are used in GA for genetic operations. The number of steps may be different, depending on the author's explanation but the process is the same. The main processes from the figure can be explained as follows:

1. Initial population: The first population of solutions is created in individuals, by two ways, namely, the heuristic initialization and random initialization [179]. The heuristic initialization can improve the speed of GA to get solutions in some cases but it may be difficult to search global optimal solutions due to reducing the solution

space leading to the lack of variety in the population. The most common method is the random individual creation that should be in the decision space to perform better search efficiency [173], [179].

Furthermore, the suitable size of population, normally between 30 and 100, is important to achieve an efficient GA [174]. If the problem is more difficult, the population size should be larger [173]; however, the speed to converge will be slower [174]. On the other hand, too small a size will not have diversity in the population causing GA to converge to local optima.

In conclusion, both the search space and the search speed are key factors in achieving the optimal solution for GA process.

2. Evaluation and fitness assignment: Both steps can be considered as a single step. First, the decision variables (x) are necessary to decode from the chromosome. Then, each population is evaluated with the objective functions and constraints. Objective values are used to calculate fitness values to each phenotype, relying on the dominance relationships and the problem constraints. A range of fitness values may be between 0 and 1 to normalize the objective function for uniformity among many problem domains [179].

3. Selection: Several selection methods have been developed and generally used, namely, roulette wheel selection, ($\mu+\lambda$)-selection, tournament selection, truncation selection, elitist selection, ranking and scaling mechanisms, and sharing selection [179]. It has been confirmed that the tournament selection has better or comparable convergence and calculating features if compared to other reproduction operators [173]. The concepts of tournament selection are two solutions, of which the better solution is chosen and placed in the mating pool, illustrated in Figure 3.7. A mating pool is created and applied in the crossover to generate new solutions. The merit is that it is easy to adjust selection pressure by changing the tournament size [179]. The larger tournament size, the smaller the chance of weak individuals being selected.

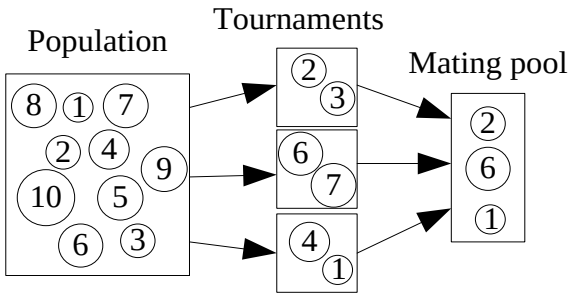

Figure 3.7 Tournament selection

4. Crossover: Crossover is the major operator of GA [179]. It provides the better two chromosomes, called *offspring*, by interchanging genes between two good chromosomes, called *parents*. This means not all parents in the mating pool are combined. The performance of the crossover operator affects the performance of GA on computation time and accuracy solutions. The crossover probability [179] is used to control the expected number of chromosomes to apply in the crossover operation. The higher the crossover probability, the better the solutions obtained. However, if the value of this probability is too high, it will take a lot of computation time. This probability is generally between 0.6 and 1 [180] or another range that may be better is between 0.65 and 0.85, as suggested by some researchers [174].

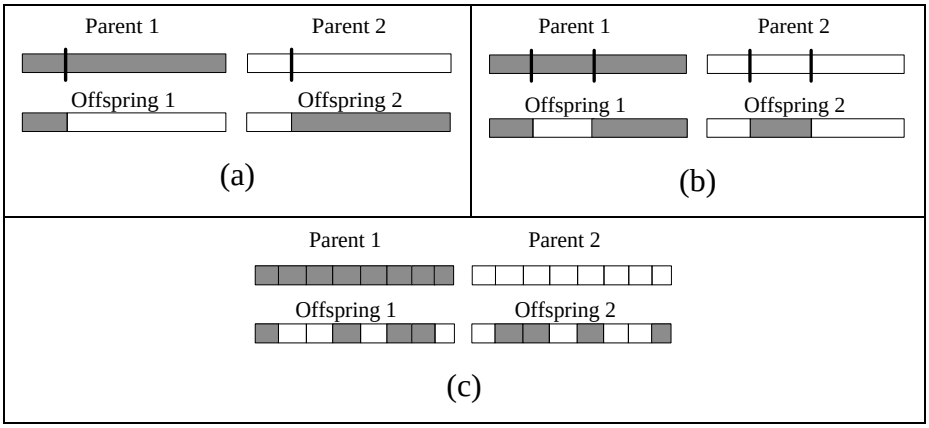

Figure 3.8 Conventional crossover operators: (a) one-cut point, (b) two-cut point and (c) multi-cut point or uniform

Many crossover operators have been proposed for real number encoding and they can be classified into four techniques [179]. First, conventional crossover operators can be used in the case of binary or integer or real representation. Two groups of the conventional operators are simple crossovers (namely, one-cut point, two-cut point

and multi-cut point or uniform), shown in Figure 3.8, and random crossovers (namely, flat crossover and blend crossover). Second, arithmetical operators are formed by using the theory of linear combination of vectors from the convex area. Third, direction-based operators are constructed by applying the estimated gradient direction to genetic operators. Finally, stochastic operators use random numbers with some distribution for modifying parents to obtain offspring.

5. Mutation: Mutation is another significant operator in providing a search element to GA. The offspring from the crossover operator is modified again in this operator for two reasons. First, the mutation operator gives the different genes that were not explored in the decision space for the initial population [173], [179]. This operator also restores the genes that were deleted from the population in the selection process [179]. The mutation probability is the proportion of the total number of genes in the population. The optimal mutation probability is important in controlling the modification of new genes, discussed in [37], [179]. For too low a mutation rate, various genes that may be practical are never investigated. For too high a mutation rate there will be much random disturbance amongst genes, leading to the offspring starting to lose the similarity to the parents. This means that the ability of algorithm to learn from the history of the search will be reduced.

Figure 3.9 Mutation operators: (a) a bit-swapping operation (b) random mutation

Several mutation operators have been developed for a binary encoding, real numbers encoding and integer encoding. The mutation operation for a binary encoding is a bit-swapping operation. For real number encoding, the mutation operators are such as random mutation, dynamic mutation (or non-uniform mutation), and directional mutation. Examples of a bit-swapping operation and random mutation are shown in Figure 3.9. Furthermore, many mutation operators for integer encoding have been

proposed, such as, inversion mutation, insertion mutation and displacement mutation. [179]

6. Population update: Two processes of the population update are replacement and elitism processes. To replace the new offspring created in the population, the old population may be replaced, either all or some members, to prove which one is better [180]. Elitism is very important for GA to obtain the global optimal solutions. The concept of elitism is "survival of the fittest" [178]. This means that a good solution discovered will never be lost during crossover or mutation process unless a better solution is found.

The elitism concept is applied in MOEA and found that MOEA based on elitism has better performance than the non-elitist approaches [173]. The SPEA2, utilized in this thesis and expressed in Section 3.4.8, is an elitist method.

Advantages and disadvantages of Genetic Algorithms

The main advantages and disadvantages of GA, identified in the literature, are summarized in Table 3.3. Even though the GA has been accepted, with a potential to solve several complicated nonlinear optimization problems, it has two main drawbacks, namely, no guarantee of finding the global optimal solution and requiring a large computational time. It would be better to solve linear and convex optimization problems with other methods, such as mathematical methods. Hence, a good understanding of the problem to be solved is important in selecting a sufficient solution method. Computational time may be one of the main criticisms of GA in the past. Nowadays, however, GA can solve difficult problems faster, thanks to the development of high performance computers, which have fast speed and large memories. Moreover, various parallel implementations of GA have been developed; therefore, GA can possibly be used in online optimization problems.

Table 3.3 Summary of GA advantages and disadvantages [37], [173], [179]

	Advantages	Disadvantages
1. Applications	**1. Very good for real-world optimization problems:** - Traditional optimization methods are difficult to solve, such as discrete, non-convex, nonlinear, non-differentiable functions. - Computing time is not crucial, such as system design or planning. - With or without constraints **2. Benefits due to separation of GA process and objective evaluation:** - Easy to interface with any type of objective functions and constraints, or simulation models, or local search optimization methods. - No need functions of GA objective evaluation.	- Unsuitable for real time or online optimization problems.
2. Adaptability	- Simple concepts and algorithm easy to be coded, without deep mathematical knowledge but powerful search methods. - Users can effortlessly improve the GA performance, such as by providing specific first population, crossover and mutation operators. - Supports multi-objective optimization - GA can be modified to be several powerful multi-objective optimization techniques.	Initial population values and crossover and mutation probability rates are the key factors for finding the global optimal solution, discussed in Section 3.4.7.1.
3. Robustness	GA is good for "noisy" environments, which is an uncertain objective evaluation, i.e. more efficient and more robust than other conventional heuristic methods.	- GA cannot achieve with deceptive functions, occurring when a bad chromosome is created by two good genes. This effect is known as *deception.*
4. Solutions	Give multiple optimal solutions in different conditions of decisions.	Convergence to local optimal solutions can happen when GA is not good implemented or the populations have many subjects.
5. Computational time	- Users can adjust computational time, basing on the number of populations and generations, relying on the difficulty of problems. - GA has parallel implementations, such as coarse-grained and fine-grained parallel GAs, leading to very short computational time.	- The more difficult the problem, the larger computational time is required due to need of more the number of population and generations. - GA does not guarantee searching a global optimal solution in a set time.

3.4.7.2 Multi-Objective Evolutionary Algorithms

The EAs have been developed to solve multi-objective problems, called Multi-Objective Evolutionary Algorithms (MOEA). Three main goals of MOEA are accuracy, diversity and spread. Various MOEA have been developed to achieve the goals. They can be classified, for example: Deb *et al.* [173] divide MOEA into non-elitist MOEA and elitist MOEA. The elitist MOEA uses an elite-preserving operator to update populations in the last step before carried on to the next generation, introduced in Section 3.4.7.1 (the GA population update). Additionally, Abraham *et al.* [181] sort MOEA into three types, namely, aggregating functions, population-based approaches and Pareto-based approaches. The aggregating functions are the

mathematical methods. The notions of these techniques are the combination of all the objectives into a single objective, overviewed in Section 3.4.6. The population-based approaches are the use of population of EA to vary the search, but not directly using the Pareto dominance concept in the selection procedure. The Pareto-based approaches apply the non-dominated sorting concept in GA. This concept was proposed by Goldberg in 1989 [173].

Several MOEA techniques have been proposed for nearly three decades and until now they are divided into two generations [37], [181], [182]. Most MOEA techniques have been modified from the concepts of GA. The concepts of representative MOEA techniques in the first generation are summarized in Table 3.4 Furthermore, their advantages and disadvantages are briefly described. The first MOEA is the Vector Evaluated Genetic Algorithm (VEGA), proposed by Schaffer in 1984 [173]. Most techniques in this generation are non-elitist MOEA. Most of them are simple modifications but they do not provide a well-converged and well-distributed set of non-dominated solutions.

Consequently, MOEA techniques in the second generation have been developed by using the concept of elitism. It was verified that the elitism is a process to guarantee the convergence of algorithms to the Pareto-optimal front [182]. The concepts, advantages and disadvantages of MOEA approaches in this generation are summarized in Table 3.5. It shows that the MOEA of this generation outperform the MOEA proposed in the first generation, in term of better spread, better diversity and faster convergence of Pareto-optimal solutions. The first one is the Strength Pareto Evolutionary Algorithm (SPEA), developed by Zitzler *et al.* in 1998 and it was improved to give a new version, SPEA2, presented in 2001. It has been investigated that SPEA2 outperforms a number of state-of-the-art algorithms in both test problems and real-world problems [37], [35]. Although, SPEA2 may not have fastest convergence in all test problems (compared with NSGA-II, C-NSGA-II, PAES and ε-MOEA), it provides a better diversity in the Pareto-optimal solutions, especially when the number of objectives is higher [35], [183]. Moreover, it shows that SPEA2 has an overall performance as good as ε-MOEA, as recently proposed by Deb *et al.* in 2011.

Table 3.4 Summary of MOEA concepts, advantages and disadvantages in the first generation [37], [173], [181], [182]

MOEA	Concepts	Advantages	Disadvantages
1. Vector Evaluated Genetic Algorithm (VEGA), 1984	- Population-based approaches - Non-elitist MOEA - Using the proportionate selection method, modified by dividing the mating pool into subpopulations, based on the number of objectives, for selecting parents from their individual performance.	- Applying a simple idea - Easy to use	- VEGA converges to the extreme of each individual objective. - A good solution of all objectives may not be the best in any of them.
2. Weight-Based Genetic Algorithm (WBGA), 1993	- Population-based approaches - Non-elitist MOEA - Keep varieties of the weight vectors among the population members and then combine together to compute the fitness of a solution.	- Not much modification to convert a basic GA to WBGA - Less complicated algorithm than other MOEA.	- Increasing complexity for a problem, having both minimization and maximization objectives. - Difficult to solve non-convex problems. - Difficult to choose a suitable set of weight vectors for a uniform spread of non-dominated solutions required.
3. Multi-Objective Genetic Algorithm (MOGA), 1993	- Pareto-based approaches - Non-elitist MOEA - Using the proportionate selection method - Modifying a fitness assignment scheme with ranking procedure.	- Simple fitness assignment scheme - Easy to apply to many optimization problems, such as combinatorial optimization problems. - Suitable for a spread of Pareto-optimal solutions required on the objective space.	Due to design of fitness assignment procedure, - MOGA may be sensitive to the shape of the Pareto-optimal front and to density of solutions in the search space. - MOGA may converge slowly or cannot find a good spread in the Pareto-optimal front.
4. Non-dominated Sorting Genetic Algorithm (NSGA), 1994	- Pareto-based approaches - Non-elitist MOEA - Using the proportionate selection method - Modifying a fitness assignment scheme with ranking and a sharing strategy, keeping diversity among solutions of each Pareto-optimal front.	- Improving the speed of convergence while it can find diverse solutions in the Pareto-optimal front.	- The performance is sensitive to the sharing parameter (or called niche radius).
5. Niched-Pareto Genetic Algorithm (NPGA), 1994	- Pareto-based approaches - Non-elitist MOEA - Using the binary tournament selection - Applying a dynamically updated niching strategy	- No explicit fitness assignment is required. - Probably suitable for problems having many objectives. - Using the tournament selection operator that outperforms other selection operators	- Niche radius has more effect on the algorithm than NSGA and so there are more requirements for using a suitable niche radius value.
6. Classical MOEA, such as random weighted GA, 1995	- Applying classical methods and GA - Aggregating functions - Non-elitist MOEA	Suitable for linear and convex optimization problems.	- They may not be good to solve nonlinear or non-convex problems. - Other drawbacks are dependent on types of classical methods, described in Table 3.2.

Table 3.5 Summary of MOEA advantages and disadvantages in the second generation [35], [37], [182], [183]

MOEA	Concepts	Advantages	Disadvantages
1. Strength Pareto Evolutionary Algorithm (SPEA), 1998	- Pareto-based approaches - Elitist MOEA, applying elitism to maintain Pareto-optimal solutions. - Modifying a fitness assignment that avoids using the niching mechanism.	- It guarantees that Pareto-optimal solutions will not be lost through crossover or mutation. - Increasing the speed of convergence towards the Pareto front because the elitism concept is added in the selection and crossover procedure.	- SPEA is sensitive to the external population size introduced. For a large size, it is difficult in converging to the Pareto-optimal front. For a small size, the elitism effect will be lost. - SPEA has the same problems caused by the design of the fitness assignment as the MOGA.
2. Pareto-Archived Evolutionary Strategy (PAES), 1999	- MOEA using an Evolutionary Strategy (ES) - Using a (1+1)-ES (two-membered ES) by comparing the offspring and the parent solution that locate in an elite population. - and local search strategy - Elitist MOEA	- Directly controlling on the diversity that can be reached in the non-dominated solutions. - The PAES should outperform other methods for problems having a search space with non-uniformly dense solutions due to equal-sized hypercube selected.	- Difficult to select the suitable values of an appropriate archive size and the depth parameter that directly control the spread of solutions. - Requiring the knowledge of minimum and maximum possible objective function values. - A serious disadvantage is smaller hypercube sizes than desired if the population members focus in a narrow region, either due to premature convergence or due to the nature of the problem.
3. Elitist Non-dominated Sorting Genetic Algorithm (NSGA-II), 2000	- Pareto-based approaches - Elitist MOEA using an elite-preservation strategy and an explicit diversity-preserving mechanism.	- No need niching parameters such as niche radius - A variety of non-dominated solutions, using the crowding comparison process. - The elitism mechanism eliminates an already found non-dominated solution.	- A loss of convergence property due to the crowded comparison is applied to limit the population size.
4. Strength Pareto Evolutionary Algorithm 2 (SPEA2), 2001	- Pareto-based approaches - Elitist MOEA - Incorporating a fine-grained fitness assignment strategy. - Applying the nearest neighbour density estimation technique. - Using an enhanced archive truncation method	- SPEA2 outperforms the SPEA on all problems. - SPEA2 gives a better spread of points, especially if the number of objectives increases.	- Take more computing time for the clustering process and the truncation operator.

3.4.8 Strength Pareto Evolutionary Algorithm 2

Strength Pareto Evolutionary Algorithm 2 (SPEA2) is an elitist MOEA and is based on the basic GA structure, described in Section 3.4.7.1. SPEA2 is the second version of SPEA. The similar and different concepts of SPEA compared with other MOEA can be described briefly as follows [184]:

The same concepts as other MOEA are

- the storage of the non-dominated solutions in an extended Pareto set (or called external archive) that is a secondary elite population.
- the use of the Pareto dominance concept to assign scalar fitness values to individuals
- the use of the clustering approach to decrease the number of non-dominated solutions kept by preserving the existing characteristics of the Pareto-optimal front.

SPEA has four points that make it different from other MOEA:

- Integrating the above three techniques, namely elitism, Pareto dominance and clustering approach in a single algorithm.
- The fitness of each individual is set from only the solutions kept in the external archive or irrelevant members of the population dominate each other.
- All solutions in the external archive are involved in the selection process.
- A novel niching approach is provided for achieving a well-distributed set of solutions without requiring distance parameters, such as the niche radius.

Collecting Pareto-optimal solutions in the external archive is a good process to guarantee that the solutions will not be lost through crossover or mutation. In addition, the combination of the elitism concept in the selection and crossover processes increases the speed of convergence towards the Pareto-optimal front. However, drawbacks of SPEA are that the algorithm is sensitive to the external population size introduced. For a large size, there is difficulty in converging to the Pareto-optimal front. For a small size, the elitism effect will be lost. Moreover, due to the design of the SPEA fitness assignment, the algorithm will be sensitive to the shape of the Pareto-optimal front and to the density of solutions in the search space.

SPEA will also converge slowly or cannot find a good diversity in the Pareto-optimal front.

Consequently, the SPEA2 was developed in response to criticism of the SPEA. The overall algorithm, consisting of six main steps, is as follows: [35]

Input: *N* is the population size, $\bar{N}$ is the archive size and *T* is the maximum number of generations.
Output: *A* is the Pareto-optimal set

1. Initialization: Generate randomly initial populations, P_0, limited by constraints and create the empty archive external, $\bar{P}_0$. Set the initial generation count *t* to zero.
2. Fitness assignment: Evaluate the population P_t. Compute fitness values of individuals in P_t and $\bar{P}_t$, described in detail in Section 3.4.7.1.
3. Environmental selection: Copy all non-dominated individuals in P_t and $\bar{P}_t$ to $\bar{P}_{t+1}$. If the size of $\bar{P}_{t+1}$ is more than $\bar{N}$, then decrease $\bar{P}_{t+1}$ via the truncation operator. On the other hand, if the size of $\bar{P}_{t+1}$ is lower than $\bar{N}$, then fill $\bar{P}_{t+1}$ with dominated individuals in P_t and $\bar{P}_t$, explained in Section 3.4.7.2.
4. Termination: If *t* is greater than or equal to *T*, then the final solution is the non-dominated set, ($A= \bar{P}_{t+1}$). Stop.
5. Mating selection: Perform binary tournament selection with replacement on $\bar{P}_{t+1}$to fill the mating pool.
6. Variation: Create the new population (P_{t+1}) by using crossover and mutation operators to the mating pool. Increment generation counter ($t=t+1$) and go to step 2.

Steps 1, 5 and 6 are the same processes as GA. Step 4 is the termination of the algorithm, normally identified by the number of generations desired. Steps 2 and 3 are particularly modified for SPEA2. In Step 2, SPEA2 is improved by using a fine-grained fitness assignment strategy and incorporating a nearest neighbor density estimation technique. Furthermore, in Step 3, an enhanced archive truncation method is applied to guarantee the preservation of boundary solutions. The details of Steps 2 and 3 are described as follows:

3.4.8.1 Fitness assignment of SPEA2 [35]

The enhanced fine-grained fitness assignment for SPEA2 is proposed to avoid the situation where individuals dominated by the same Pareto members obtain the same fitness level and Pareto front solutions that dominate numerous solutions are assigned worse fitness levels. In this condition, the fitness of each individual is based on both the number of dominating and dominated solutions. Four main parameters have to be determined:

1. A strength value (S) is assigned to each individual in the archive $\bar{P}_t$ and the population *P*, matching the number of solutions it dominates. However, the strength of SPEA is a proportion of the number of current population members that an external solution dominates to the number of solutions in the population [184].

2. A raw fitness (R) is the sum of all the strengths of its dominators in both archive and population, while SPEA considers only archive members in this circumstance. If fitness is to be minimized, the raw fitness equals zero, representing a non-dominated individual. A high raw fitness of an individual means that this individual is dominated by several individuals. An example of fitness assignment schemes in SPEA and SPEA2 for a maximization problem with two objectives f_1 and f_2 are illustrated in Figure 3.10.

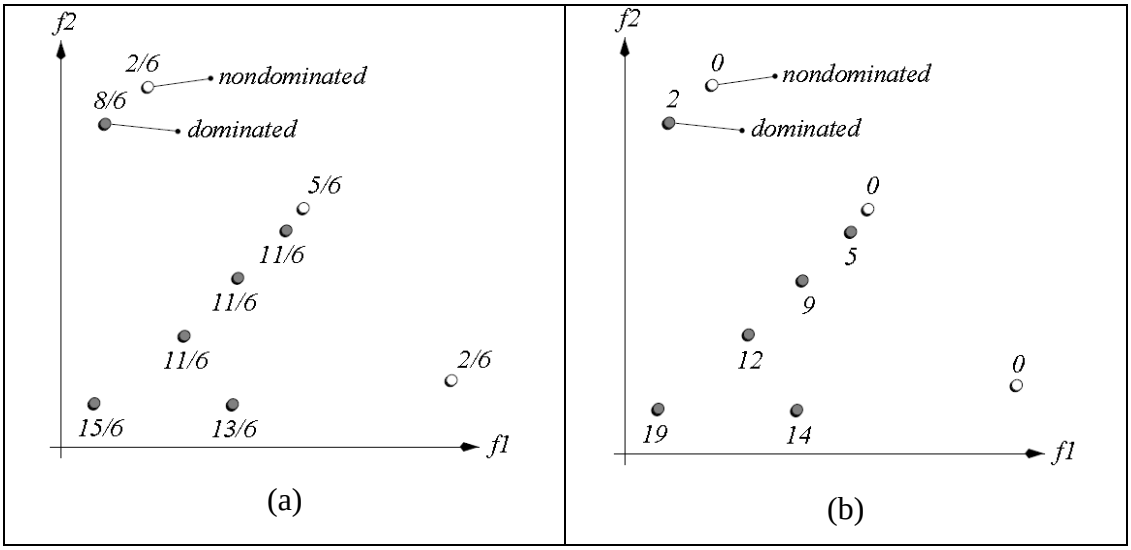

Figure 3.10 Fitness assignment schemes: (a) fitness values for a given population under the SPEA scheme (b) raw SPEA2 fitness values for the same population [35]

3. Density (D) is a parameter determined to discriminate between individuals that have the same raw fitness values. It may be the case that most of these individuals do not dominate each other, leading to worse fitness, even though, the raw fitness assignment gives a rank of niching mechanism based on the Pareto dominance concept. The density *D(i)* of an individual *i* is calculated by

$$D(i) = \frac{1}{\sigma_i^k + 2} \tag{3.2}$$

where $\sigma_i^k$is the distance to the k^{th} nearest neighbor. *k* is commonly defined to be the square root of the population size ($k = \sqrt{N + \bar{N}}$). Two is added in the denominator to make sure that its value is more than zero and that the density value is less than one.

4. The fitness value (F) is used to select the solutions that will be copied to the external archive. It is determined by the sum of the raw fitness and the density estimation.

3.4.8.2 Environmental selection of SPEA2 [35]

There are two issues in which SPEA2 differs from SPEA, in the archive update operation. Firstly, in SPEA2 the size of the external archive is constant over time. Secondly, the truncation method of SPEA2 provides a well spread of solutions stored in the external archive and prevents boundary solutions being lost. The first step in the environmental selection process is to copy all non-dominated solutions in both population and archive external sets to the archive of the next generation, according to three possible conditions:

1. If the non-dominated front ($\bar{P}_{t+1}$) fits in the archive ($|\bar{P}_{t+1}| = \bar{N}$), the environmental selection step ends.
2. If the non-dominated front ($\bar{P}_{t+1}$) is smaller than the archive ($|\bar{P}_{t+1}| < \bar{N}$), the best $\bar{N} - |\bar{P}_{t+1}|$ dominated individuals are copied to the new archive until the archive is full.
3. If the non-dominated front ($\bar{P}_{t+1}$) is larger than the archive ($|\bar{P}_{t+1}| > \bar{N}$), an archive truncation process is used to eliminate solutions iteratively until the size of

the non-dominated front is equal to the archive. At each iteration, the individual in $\bar{P}_{t+1}$ that has the nearest distance to another individual is selected for removal. If there are many individuals at the closest distance, the second smallest distance is used, and so on. It shows in Figure 3.11 the selection of the solutions to remove (on the left) and the order of the truncation method of three solutions removed.

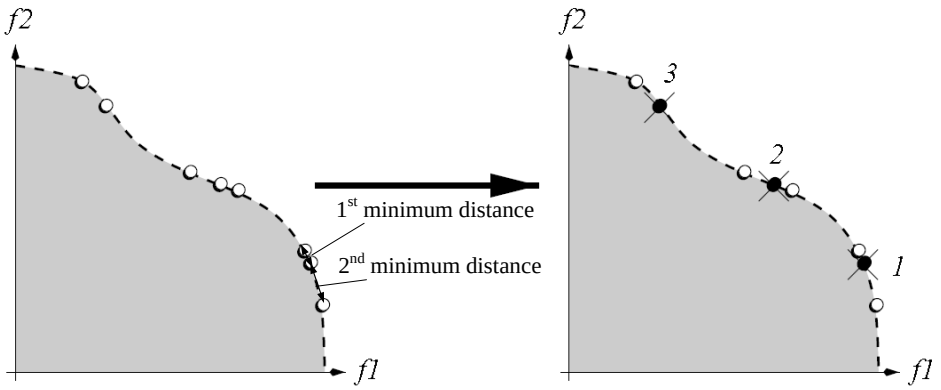

Figure 3.11 The archive truncation method used in SPEA2 [35]

3.5 Summary

In this chapter, a critical review of literature devoted to techniques and software for finding the optimal sizes of hybrid renewable energy systems is presented. The basic of mathematical optimization, the concepts of convex and non-convex optimization, and the fundamentals of single- and multi-objective optimization are described. Brief descriptions of GA and MOEA are introduced. The summary of concepts, advantages and disadvantages of several MOEA techniques are presented. Finally, the SPEA2 that outperforms most state-of-the-art optimization techniques is described in detail.

CHAPTER 4

4. COST MODELS OF LOW WIND SPEED TURBINE DESIGN

4.1 Introduction

Main WT components and major parameters of WTs affecting the performance were described as the basis of improvement of LWSTs. The improvement in some components will increase the cost of WTs while others can decrease the costs, explained in Section 4.4.3. There are many factors that make the costs change and it is difficult to forecast the costs because of technological advances. Therefore, there have been many attempts to develop cost models for forecasting the cost of WTs of various machine sizes and machine configurations. However, several cost models are out of date and many models that use specific WT configurations have limitations [185]. Furthermore, most of them need a deep knowledge of and information of WTs for calculation. Consequently, this thesis proposes the simplified cost models developed for estimating the cost of wind-generated electricity of LWSTs at different rotor diameters.

The chapter is structured as follows. Firstly, low and high wind speeds are characterized. Secondly, characteristics of LWST, including their development and improvement, are explained. Next, the development of WT design cost models is reviewed. The proposed cost models of this thesis are described. In a subsequent section, the detailed calculation of the cost models is explained and simple procedures are demonstrated to predict the cost. Finally, upwind 2-bladed and upwind 3-bladed turbines are used as case studies, discussing the results in terms of the Initial Capital Cost (ICC) and LCOE with other cost models.

4.2 Low and high wind speeds

The wind speed is a major characteristic of wind, directly affecting the amount of energy available for WT production. There are main factors of the wind speed variation (low or high wind speeds), namely, the differential pressure and temperature, rotation of the earth and topography [86]. These factors depend on the characteristics of the wind resource, as shown in Table 4.1 where a comparison is made between low and high wind speeds. The air flow is induced by the differential pressure and temperature. The higher the differential pressure, the higher the force on the air and the wind speed. The direction of the air flow is from higher to lower pressure. In the same way the thermal effect is the higher the differential temperature, the higher the force on the air and the wind speed. The air flow direction is from higher to lower temperature. Moreover, the rotation of the earth and the non-uniformity of the earth's surfaces alter the direction and the speed of the wind. For example, the tops of hills and mountains are windy due to altitude and also because the wind speed increases with height above ground. Beaches are local regions of increased wind speeds because of differential heating between land and sea.

Table 4.1 Comparison of the characteristics of the wind generation between low and high wind speeds

Particulars	Low wind speeds	High wind speeds
Air flow	- Lower differential pressure - Lower differential temperature	- Higher differential pressure - Higher differential temperature
Surface of wind resource location: - Types of terrain of wind resource	- More rough - Lands: cities, suburb, wooded countryside, forests, villages	- Less rough - Lands: the top of hills and mountains, flat grassy plains, flat desert - Sea, river
Height above ground	Lower level	Higher level
Season	Summer	Winter
Turbulence intensity: - Friction	- Higher - More obstacles in terrain	- Lower - Less obstacles in terrain

The classes of wind power density and speed are set by the Energy Information Administration (EIA) of the U.S. government, illustrated in Table 1.2 in Chapter 1. The table is useful to define the potential of wind speeds and evaluate the selection of the installed wind sites. Mean wind speeds and power densities [22] are extrapolated from the anemometer height level to 10 m and 50 m above ground by

use of a 1/7 power law, as shown in Equation 2.5 in Chapter 2. The power law is used to adjust the vertical distribution of wind speeds or the vertical wind profile. This thesis defines areas where the annual average wind speeds are lower than 6 m/s at 10 m hub height (class 4 or lower) as low wind speed areas.

4.3 Low wind speed turbines

For the LWST, at the design stage, a power output, calculated from Equation 2.2, is varied to track its minimum rated wind speed by the rotor diameter and other parameters similar to the High Wind Speed Turbines (HWSTs). WTs, with an increase in the generator rated power, deliver more energy in high wind speed areas, shown in Figure 4.1(a). For lower wind speeds, the rotor diameter should be expanded, by maintaining the generator rating, to increase the output power of a WT, illustrated in Figure 4.1(b). It shows that increasing the rotor diameter reduces the rated wind speed of a WT. A WT having lower rated wind speed can provide more output power. The rated wind speed can be used to identify the LWST and HWST, in the same way as using a power ratio. A power ratio is the rotor swept area in square meters divided by the rated generator size in kilowatts. The power ratio of LWST is above 4:1 [186], which is equivalent to rated wind speeds of lower than 10 m/s. Most WTs in current technology have rated wind speeds greater than or equal to 11 m/s and they are suitable for higher wind speeds.

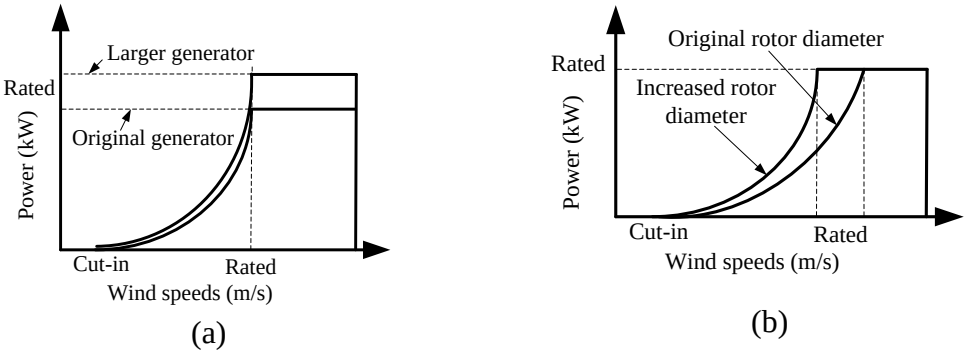

Figure 4.1 The power curves of WTs: (a) A larger generator increases the rated power (b) Increased rotor diameter decreases the rated wind speed.

Increasing the rotor diameter is a good strategy for low wind speed areas. However, there has to be an increase in size and strength of some other parts of the WT to

support heavier and longer rotors. On the other hand, this strategy will not increase the generator rating. It means that the generator capacity decreases when compared with HWSTs having the same rotor diameter. Increasing rotor diameter and decreasing generator capacity have advantages and disadvantages, summarized in Table 4.2. It shows that the choice for this strategy is a trade-off between costs and energy capture.

Table 4.2 Advantages and disadvantages of the increased rotor diameter and decreased generator capacity for low wind speed turbines [86], [186], [187]

	Advantages	**Disadvantages**
Increasing the rotor diameter		
1. Increased rotor diameter	Greater energy capture	- Increased rotor cost, weight and size - Increased foundation and transportation cost - Tower and foundation must be strong enough to support longer rotors. - Blades bend under loads and blade tips hit the tower. - Longer and heavier rotors are more difficult to transport. - Larger rotors capture more wind when extreme wind gusts occur, making them more vulnerable to damage.
2. Increased tower height	Greater energy capture	- Increased tower and foundation cost - Increased transportation cost
3. Operating at higher capacity in lower wind speeds	Greater generator efficiency	
4. Lower rated wind speed	Greater energy capture	
5. Increased rated torque		Increased drive train component size and weight
6. Increased extreme thrust		Increased weights of bearings, bedplate tower and foundation
7. Increased component size and cost		Increased O&M and replacement cost
Decreasing the generator capacity		
1. Smaller generator	Decreased generator weight and cost	
2. Operating at higher capacity in lower wind speeds	Greater generator efficiency	
3. Decreased tower head mass	Decreased foundation and tower costs	
4. Decreased power electronic system rating	Decreased power electronic system costs	
5. Lower rated wind speed		Lower energy capture

Several developers and manufacturers have been developing LWSTs for class 4 wind resource sites (5.6-6.0 m/s at 10 m hub height) for a decade. The latest LWST models have been launched since 2011, shown in Table 4.3. The first prototype of the G114-2 MW will be produced by 2013 [188]. Nowadays, therefore, the lowest

rated wind speed of WT in the market is 9.35 m/s. The G114-2 MW uses technology similar to the G97-2 MW turbine having the rotor diameter of 97 m (or a rated wind speed of 10.28 m/s at the design stage), introduced in 2010. Due to a 38% larger rotor diameter, it is expected to have 20% more energy output than G97-2 MW.

Table 4.3 The latest LWST models [188], [189], [190], [191], [192], [193], [194]

Manufacturers	LWST models	Rated power output (MW)	Rotor diameter (m)	Rated wind speed* (m/s)	Power ratio
Sinovel (China)	SL1500/89	1.5	89	9.89	4.15
Vestas (Denmark)	V100-1.8 MW	1.8	100	9.73	4.36
Siemens (Denmark, Germany)	SWT-2.3-113	2.3	113	9.73	4.36
Nordex (Germany)	N117-2.4 MW	2.4	117	9.64	4.48
Envision (China)	E93/15	1.5	93	9.61	4.53
Goldwind (China)	GW93/1500	1.5	93	9.61	4.53
GE (USA)	GE1.6-100	1.6	100	9.35	4.91
Gamesa (Spain)	G114-2 MW	2.0	114	9.23	5.10

Remark: * The rated wind speed of WT is calculated at the design stage.

The latest LWST models have been installed in medium-low wind speed areas. For example, GE expects that more than 1,500 of the GE1.6-100 will be placed by 2013 in the US, Canada, Brazil and Turkey [189]. The V100 1.8 MW turbine has been used in many projects, such as 77 turbines installed in the U.S. since mid-2012 [190], 28 turbines built in Mexico by 2013 [191], 27 turbines ordered by China in January 2012 [192].

All LWST models above are the three-bladed upwind HAWT model. New generation blades have a slender shape to minimize loads, despite a significant rotor-diameter increase in such models as the N117/2400 and the SWT-2.3-113. In spite of a very long rotor diameter, most rotor blades are still made in a single piece. However, Enercon and Gamesa now use segmented blades, making them easier to transport. Most modern rotor blades for LWSTs are made from carbon fibre. [187]

Direct-drive PMGs have been developed and used in large LWSTs to reduce ICC and O&M costs. For example, the GW93 1.5 MW turbine applies a permanent magnet generator, a full-power converter and a new ultra-low wind speed direct-drive version [192]. Siemens has developed direct drive with a permanent-magnet generator for the SWT-2.3-113 turbine [193]. Alternatively, some models, such as the GE1.6-100 turbine and the N117/2400 turbine, use DFIG with a fast speed gearbox [194].

4.4 Cost models of low wind speed turbine design

4.4.1 Wind turbine costs

The basis for all economic considerations concerning systems using wind energy is the manufacturing cost of the energy converters. This cost can be determined by using three key parameters that can be ordered in their importance: (1) rotor-swept area (2) rated generator power and (3) tower height. An overall approximate calculation of the specific manufacturing costs can only be based on "costs per square meter rotor-swept area". However, it is difficult to use this estimate for comparing the costs with other energy systems because the others are based on "costs per kilowatt". Consequently, the "investment cost per kilowatt-hour per year" is used for evaluating the investment profitability in an actual WT project with high accuracy and for comparing with the potential of other energy systems. [87]

Nevertheless, manufacturers of WTs will not produce every part of a WT by themselves [87]. Many manufacturers try to purchase as many components as possible from other vendors because they can take advantage of the price competition and the technical knowledge of the vendor industry. Moreover, the improvement of WT performance can modify a WT in some of its particular components. It is easy to know the cost of each WT component. Therefore, the cost division of a WT into main component costs or subsystem costs is a good way of developing a reliable tool for assessing the worthiness of investment in a WT project. It can also improve the accuracy of forecasts about the manufacturing costs of an improved WT.

Costs of a WT can be considered to be four main subsystems: (1) rotor blades, (2) a mechanical drive train including a rotor hub and a nacelle, (3) an electrical system and (4) a tower. The proportion of costs of WT components is quite similar; although, WTs have been designed with different technical concepts and sizes. The rotor blades have a cost share of approximately 16% to 34% of the total component cost. The cost fraction of the mechanical drive train, rotor hub and nacelle totals between 40% and 50% of the production costs. The share of the production costs of the electrical system ranges from 13% to 20%. For the tower, the cost fraction is about 12% to 20% of the total component cost. [87]

Another key factor of increasing manufacturing costs is WT weight. For example for LWSTs, the weight increases with increasing rotor diameter when WTs use the same material and technology. This is a challenge for designers to improve WTs by using light and strong but inexpensive materials to reduce the COE. The relationship between mass and rotor diameter is a power function, known as a mass model [87], [185]. From the mass-related specific cost function as a linear function, the specific manufacturing costs also increase with the rotor diameter in function of a power law, called a cost model [87]. However, mass is not considerable for electrical components and so in this case power is the better reference [87].

4.4.2 Development of wind turbine design cost models

There have been many efforts to develop a modern tool for estimating the COE of WTs. However, there are several factors, such as the rapid development of new WT technologies and the fluctuation of material costs, especially in main WT components. These factors impact on cost and performance of WTs. Therefore, various models developed are outdated and cannot predict the accurate COE. Furthermore, they are not a universally applicable estimating tool. For example, the specific manufacturing costs of a WT increases with the rotor diameter, calculating as follows [87]:

$$K_{wt,2} = K_{wt,1}\left(\frac{D_{r2}}{D_{r1}}\right)^{0.5\ to\ 0.6} \tag{4.1}$$

where $K_{wt,1}$ and $K_{wt,2}$ are the specific manufacturing costs ($US/m^2) of the first and second rotor diameters (D_{r1} and D_{r2}), respectively.

Recently, the National Renewable Energy Laboratory's (NREL) National Wind Technology Centre [185] has presented a tool for calculating the COE for onshore and offshore WTs. The tool has cost and mass models, based on rotor diameter, machine rating, tower height and other key turbine factors. They allow for roughly predicting the cost of WT components and subsystems for different sizes and configurations of components. They can be used for modelling the cost impacts of certain advanced technology which is studied under the Wind Partnerships for Advanced Component Technology (WindPACT) and LWST projects. However, their aim is not for forecasting the price of WTs due to unstable market factors. The

models are formed from fitting curves of industry and experimental data, including data from simulation programs to design WTs. Moreover, a mature design and a 50 MW wind farm installation, with mature component production are used to be representative of cost data. Nevertheless, these models also consider the impact on cost from variation in economic indicators such as the Gross Domestic Product (GDP) and Producer Price Index (PPI).

Additionally, Global Energy Concepts, LLC (GEC) [195] under a deal with the NREL has developed an operations and maintenance (O&M) cost model for commercial WT services. The target of this model is to support the LWST project. Data is from many WT projects, representing various WT types, WT ages and geographic areas, over the past decade. However, for larger than 1 MW WTs, the model is estimated by using extrapolated data.

These cost and mass models are useful for studying LWST projects. The models depend on quantifiable data and engineering decisions. Curve fitting is used to find the models of each main component in terms of power and linear functions. However, they are limited by many factors of data used, such as time duration, different area circumstances and different equipment qualities.

4.4.3 Proposed cost models of low wind speed turbine design

This thesis proposes a cost model to determine the ICC of LWST. The aims are to evaluate and compare the optimization between the technology of low and current wind speed turbines, by economic analysis. This cost model can be easily applied in the optimization methods for studying the LWST applications in either stand-alone or grid-connected hybrid renewable energy systems. The cost model considers three main parameters, namely rotor-swept area, rated generator power and tower height to estimate the investment cost per kilowatt-hour per year or the ICC of WT systems. It utilizes the concept of cost fractions in each WT component. The ICC (£/kW) of WT can be written as follows:

$$ICC_{wt} = \sum_{i=1}^{n}(f_{c,i} * C_{wt}) + C_{ins} \quad (4.2)$$

where f_c is the cost fraction of such as rotor blades, a mechanical drive train including a rotor hub and a nacelle, an electrical system and a tower. n is the number of subsystems, based on details of the cost data. The results will have more accuracy if the calculation has many subsystems. The total cost fraction is equal to 1. C_{wt} is the total component cost of WT (£/kW) and C_{ins} is the installation cost of WT (£/kW).

A formula using a power law for determining the increase in the specific manufacturing costs ($US/m^2) with rotor diameters, Equation 4.1, is discussed in [87]. A power of rotor diameter ratio ranges between 0.5 and 0.6 investigated in a theory. The results may differ from the current price because of the development of WT technology, different suppliers and cost issues. However, the power law may be used for prediction of LWST costs in question of the extra costs. As a result, the power law for calculating the new ICC of WT will be:

$$NIC_{wt} = ICC_{wt}\left(\frac{D_r}{D_{r0}}\right)^r \tag{4.3}$$

This model is called "Total-cost model" in this thesis. From Equation 4.2 the costs of each WT part are calculated and then the new ICC of WT can be:

$$NIC_{wt} = \sum_{i=1}^{n}\left(f_{c,i}\left(\frac{D_r}{D_{r0}}\right)^{r_i} * C_{wt}\right) + C_{ins}\left(\frac{D_r}{D_{r0}}\right)^{r_{ins}} \tag{4.4}$$

The installation cost is the ICC subtracted by the WT cost, so the new ICC of a WT is rewritten to be:

$$NIC_{wt} = \sum_{i=1}^{n}\left(f_{c,i}\left(\frac{D_r}{D_{r0}}\right)^{r_i} * C_{wt}\right) + (ICC_{wt} - C_{wt}) * \left(\frac{D_r}{D_{r0}}\right)^{r_{ins}} \tag{4.5}$$

where D_{r0} is the reference rotor diameter and r is the scaling exponent, calling "cost factor" in this thesis. r can be the cost factors of such as rotor blades, a mechanical drive train including a rotor hub and a nacelle, an electrical system, a tower. r_{ins} is the cost factor of installation. Each cost factor is based on the costs of WT components developed, namely, materials and designs of WTs to reduce weight, loads and costs and to increase speeds. For installation, site is a key cost, affecting transportation including access roads, civil works and labour. Therefore, the value of the cost factor r can be explained in three cases as follows:

Case 1: $r > 0$; means that costs of new WT components are higher because of more expensive cost of materials or increase of size, weight and loads. Alternatively, the higher costs for installation may be caused by the difficulty of transporting WTs to remote areas.

Case 2: $r = 0$; means that costs of new initial investment are not changed. If each WT part is considered, some parts may not need to be modified for the rotor diameter to be changed. Or with the new technology developed, the modification of the WT part can keep the costs constant.

Case 3: $r < 0$; means that costs of new WT components are cheaper. It is possible because of the development of new technology that may be discovered. For example, the new materials might make it cheaper, lighter or stronger.

In order to capture more energy in low wind speed areas, the rotor diameter has to be expanded. The LWST will be developed that affects size, weight and cost of WT components. For example, the size and weight of the drive train component will increase because rated torque is higher. Furthermore, weights of bearings, bedplate tower and foundation should be enlarged to support the extreme force. For LWSTs, the rated generator power is not changed and so the cost of the electrical system is assumed to be equal to the cost before it is improved. This means that the cost of the electrical system is only based on the rated power. The tower cost depends on the tower height; to seek the appropriate hub height. Consequently, the ICC (£) of LWST with the effect of changing rotor diameters can be modified to be:

$$ICC_{Lwst} = \sum_{i=1}^{n} \left(f_{c,i} \left(\frac{D_r}{D_{r0}} \right)^{r_i} * C_{wt} \right) + (ICC_{wt} - C_{wt}) * \left(\frac{D_r}{D_{r0}} \right)^{r_{ins}} + \frac{C_t H_t}{P_{wt,r}} \left(\frac{D_r}{D_{r0}} \right)^{r_t} \quad (4.6)$$

where $P_{wt,r}$ is the rated power of a WT (kW), C_t is the tower cost (£/m), r_t is the cost factor of the tower and H_t is the tower height (m). This model is called "Sum-component cost model" in this thesis.

4.5 Computation of LWST costs by using cost models

This section demonstrates how to calculate the ICC of a WT by using the Sum-component cost model and the Total-cost model. Two WT systems, namely upwind

2-bladed and upwind 3-bladed turbines mentioned from [196], are selected as case studies. Their results are compared with the results of NREL's cost model, referred from [185]. Furthermore, the total impact of these different models on total LCOE is determined in the case of grid-connected WT systems.

4.5.1 Methodology

This thesis proposes two simplified cost models, namely the Sum-component cost model and the Total-cost model, to predict the ICC of WTs having different rotor diameters. However, these cost models have key parameters that need to be determined. Each cost model has approaches for finding the parameters, as follows:

4.5.1.1 Sum-component cost model: The proposed cost model has two key parameters, namely cost fractions and cost factors. A forecast, for the ICC of LWST by using the Sum-component cost model (Equation 4.6), assumes that if WTs have the same design, technology, type and capacity and they are installed at the same location and time, they will have the same cost fractions and cost factors of each subsystem. The approach in using the Sum-component cost model has key steps as follows:

1. Prepare the cost data of two WTs that have different rotor blade diameters but other configurations are identical.
2. Provide the cost fractions of a WT that is set as the baseline, by estimating percentages of the component costs.
3. Determine each cost factor of Equation 4.6 from the component cost data of the two WTs.
4. Calculate the new ICC of WTs with other rotor diameters by using the cost fractions and the cost factors.

4.5.1.2 Total-cost model: A significant parameter of this cost model (Equation 4.3) is the cost factor. This cost factor is determined by using the ICC of two WTs having different rotor diameters. The assumption of WT system configurations for forecasting the ICC of a WT is the same as the Sum-component cost model.

4.5.2 Case studies

4.5.2.1 WT configurations

This thesis uses two WT models, namely upwind 2-bladed and upwind 3-bladed turbines from [196] which is the report of WindPACT turbine rotor design study. Both have a rated power of 1.5 MW and a hub height of 84 m. The baseline WT model has a rotor diameter of 70 m, with a rated wind speed of 11.54 m/s at the design stage. The two WT models were modified by a 12% increase in a rotor diameter of 78.4 m, with a rated wind speed of 10.7 m/s at the design stage. Specifications of WTs are the power coefficient of 0.5, the conversion efficiency of 95%, the soiling losses of 2%, the array losses of 5%, the availability of 95% and the air density of 1.225 kg/m^3. The expected annual operation and maintenance costs are set at 0.8 ¢/kWh (or 0.5 pence/kWh). The long-term replacement costs are set at $15/kW/year.

4.5.2.2 Results and discussions

Cost data of WT components of the two WT models referred from [196] are shown in Appendix A. Using the cost data, the cost fractions and cost factors of the Sum-component cost model in each WT is determined, the calculation example is described in Appendix E and the results are presented in Table 4.4. All subsystems are more expensive for larger rotor diameters, shown in terms of the cost factor, especially the cost of rotor blades that have cost factors of 2.58 for the upwind 2-bladed WT and 2.46 for the upwind 3-bladed WT . Costs of some components do not change and then their cost factors are equal to zero. Setting the Total-cost model is easier than the Sum-component cost model. The cost factors of the Total-cost model for upwind 2-bladed and upwind 3-bladed turbines are calculated to be 0.98 and 0.82, respectively.

Table 4.4 Cost fractions and cost factors of the Sum-component cost model for upwind 2-bladed and upwind 3-bladed turbines

Wind turbines	**Upwind 2-bladed**		**Upwind 3-bladed**	
Parameters	**Cost fraction**	**Cost factor**	**Cost fraction**	**Cost factor**
Initial capital cost of WTs	**100.00%**	**1.26**	**100.00%**	**1.02**
1. Rotor blades	**10.09%**	**2.58**	**14.94%**	**2.46**
2. Mechanical drive train including	**39.36%**	**1.53**	**38.38%**	**1.19**
Hub	8.58%	2.97	6.55%	1.99
Pitch mechanism and bearings	1.72%	3.04	2.95%	2.61
Low-speed shaft	2.02%	0.00	1.85%	0.00
Bearings	1.21%	0.00	1.11%	0.00
Gearbox	16.04%	0.90	14.21%	0.82
Mechanical brake, HS coupling, etc.	0.30%	0.00	0.28%	0.00
Yaw drive and bearing	0.61%	4.51	1.20%	2.87
Main frame	5.15%	2.00	6.27%	1.32
Hydraulic system	0.71%	0.00	0.65%	0.00
Nacelle cover	3.63%	0.00	3.32%	0.00
3. Electrical system	**27.14%**	**0.00**	**24.82%**	**0.00**
Generator	9.89%	0.00	9.04%	0.00
Variable-speed electronics	10.19%	0.00	9.32%	0.00
Electrical connections	6.05%	0.00	5.54%	0.00
control, safety system	1.01%	0.00	0.92%	0.00
4. Tower and foundation	**22.81%**	**1.54**	**21.86%**	**0.75**
Initial capital cost of WT systems	**100.00%**	**0.98**	**100.00%**	**0.82**
1. Initial capital cost of WTs	**74.40%**	**1.26**	**76.07%**	**1.02**
2. Balance of station	**25.60%**	**0.13**	**23.93%**	**0.13**
Transportation	3.83%	0.00	3.58%	0.00
Roads, civil works	5.93%	0.33	5.54%	0.33
Assembly and installation	3.83%	0.00	3.58%	0.00
Electrical interface/connections	9.53%	0.14	8.91%	0.14
Permits, Engineering	2.48%	0.00	2.32%	0.00

The Sum-component cost model and the Total-cost model can be used to calculate the ICC of WTs having different rotor diameters of upwind 2-bladed and upwind 3-bladed configurations, described in Table 4.5 and 4.6 respectively. This study uses the currency exchange rate in November 2011, of 0.6275 pounds per dollar [197]. The calculation example of the Sum-component cost model is illustrated in Section E.1 in Appendix E. The results are compared with the ICC, estimated from the NREL's cost model (described in Section 4.4.2), to check the accuracy of results of the two proposed cost models. Nonetheless, the ICC, calculated from the NREL's cost model, has small errors, the maximum of which is 2.24%, compared with the original ICC of two WT configurations for the upwind 3-bladed turbine with 78.4 m rotor diameters. The errors are possible because this cost model was established from fitting curves of industry and experimental data, including data from simulation programs to design WT. Due to the limitation of WT cost data, therefore, the ICC

estimated by the NREL's cost model is set to be the baseline for comparison in this thesis.

Table 4.5 The ICC of upwind 2-bladed turbines having different rotor diameters

Rotor diameter (m)	ICC of NREL's cost model (£/kW)	ICC of Sum-component cost model		ICC of Total-cost model		ICC of Sum-component cost model (4 subsystems)	
		(£/kW)	Δ%	(£/kW)	Δ%	(£/kW)	Δ%
121	1,090.77	1,114.05	-2.13%	1,022.10	6.30%	1,042.46	4.43%
102	843.18	853.34	-1.20%	805.86	4.43%	832.47	1.27%
78.4	616.73	622.92	-1.00%	622.67	-0.96%	622.89	-1.00%
70	555.27	557.22	-0.35%	557.22	-0.35%	557.22	-0.35%
66	529.19	528.94	0.05%	526.42	0.52%	527.92	0.24%
59	488.26	480.60	1.57%	467.98	4.15%	476.20	2.47%

Table 4.6 The ICC of upwind 3-bladed turbines having different rotor diameters

Rotor diameter (m)	ICC of NREL's cost model (£/kW)	ICC of Sum-component cost model		ICC of Total-cost model		ICC of Sum-component cost model (4 subsystems)	
		(£/kW)	Δ%	(£/kW)	Δ%	(£/kW)	Δ%
121	1,265.11	1,200.42	5.11%	990.35	21.72%	1,149.14	9.17%
102	951.56	922.26	3.08%	811.73	14.70%	905.74	4.82%
78.4	668.83	653.87	2.24%	654.18	2.19%	653.87	2.24%
70	593.25	596.13	-0.49%	596.13	-0.49%	596.13	-0.49%
66	561.42	570.55	-1.63%	568.43	-1.25%	569.99	-1.53%
59	511.79	525.60	-2.70%	515.13	-0.65%	523.08	-2.21%

The Total-cost model gives a higher different ICC from the baseline than the Sum-component cost model. In the case of upwind 2-bladed turbines, all cost models provide quite similar ICC results, with a maximum difference of 6.3% from the calculation of the Total-cost model. On the other hand, the ICC, computed by the proposed cost models, shows vast differences from the baseline in upwind 3-bladed turbines having the rotor diameter of 121 m. The different ICC solutions from the baseline are 5.11% and 21.72%, with estimates of the Sum-component cost model and the Total-cost model, respectively.

Discrepancies in solutions may arise because of the cost data of two WTs, the costs of assembly and installation, including some components, namely low-speed shaft and bearing, remain constant, while in the NREL's cost model these costs change with varying rotor diameters. A possible explanation for the costs remaining constant in two WT data might be that the rotor diameter increases only a small percentage of

12% (or 8.4 m) and this small increase does not affect the costs of a WT in some of its particular parts. Nevertheless, these costs should increase, especially in large rotor diameters. Moreover, the difference of mathematical models is the key factor. However, although, three cost models provide different ICC solutions; the trends of their solutions are identical, illustrated in Figure 4.2.

Additionally, the number of *n* subsystems, for calculating the cost factors in the case of the subsystems in relation to increasing rotor diameters, has an impact on the ICC of a WT, as shown clearly in the upwind 3-bladed turbine. Therefore, the evidence from this study suggests that a greater number of subsystems could provide a better result. It cannot state exactly how many errors occur in the proposed cost models because the NREL's cost models, the results of which were set to be the baseline in this study, were also established from fitting curves. Consequently, further research should be done to check the results of the proposed cost models with the actual costs estimated either by design simulation or from the actual installation, for WTs in several rotor diameters.

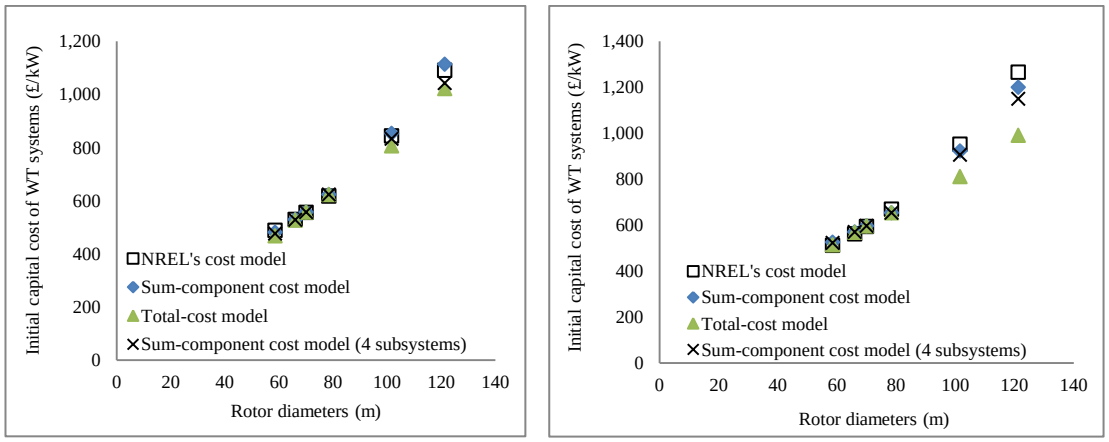

(a) (b)

Figure 4.2 The ICC of WT systems: (a) upwind 2-bladed and (b) upwind 3-bladed configurations

The ICC calculated by using specific manufacturing costs (£/m^2) in Equation 4.1 could not be applied in the case of LWST. Examples of this case are the two WT models above. The 70-m upwind 2-bladed turbine has a specific cost of about 161.59 £/m^2 whereas around 148.57 £/m^2 has to be paid for the turbine with a 78.4 m rotor

diameter. Similarly, the upwind 3-bladed turbine with a 70 m diameter has a specific cost of about 176.75 £/m^2, which is more expensive than the turbine with a 78.4 m diameter that has a specific cost of 158.19 £/m^2. If using Equation 4.1, the specific cost of WTs having larger diameters should increase. Otherwise, the power of this equation should be negative. The specific manufacturing costs of LWSTs may decrease because the rated power output does not change and so the costs of electrical systems in LWSTs do not rise with the increase of rotor diameters.

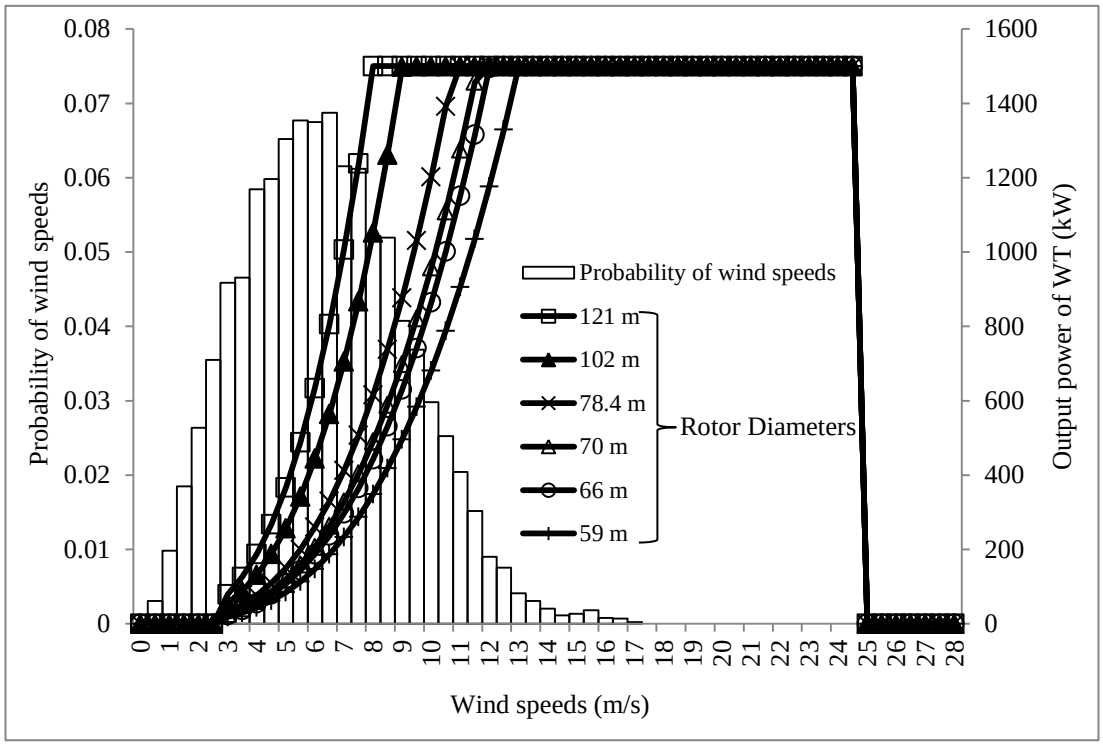

Figure 4.3 Output powers of WTs versus distribution probability of wind speeds at 84 m hub heights

One of the goals of this study is to determine the impact of increased rotor diameters in LWSTs on LCOE. In this study, the net annual energy productions were estimated at the design stage by using Equation 2.2 and they were assumed to be identical in both WT models. Moreover, cut-in and cut-out wind speeds were assumed to be 3 m/s and 25 m/s respectively. Nakhon Ratchasima province in Thailand was chosen to be a case study. It has a mean wind speed of approximately 6 m/s at 50 m hub height (class 2) [53]. The interest rate of 7.71% and the inflation rate of 2.89%, from Bank of Thailand in November 2011 [198], were used for calculating the LCOE.

Project lifetime of all case studies is 25 years. The output power curves and distribution probability of wind speeds at 84 m hub heights are illustrated in Figure 4.3.

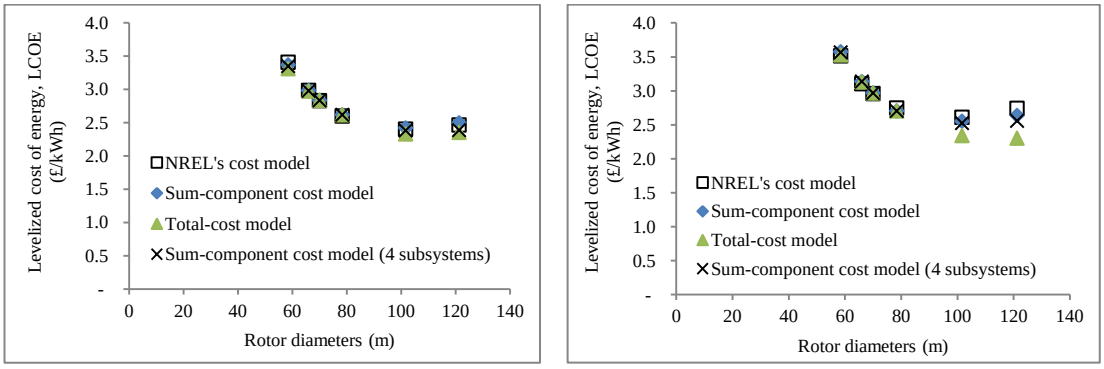

(a) (b)

Figure 4.4 LCOE of WT systems: (a) upwind 2-bladed and (b) upwind 3-bladed configurations

The ICC in Table 4.5 and 4.6 were used to calculate LCOE. The graphs in Figure 4.4 show that all models can provide similar trends of LCOE. In this case, LCOE will decrease if the rotor diameters increase up to 102 m diameter, after that LCOE will increase. Differences in results may increase for larger rotor diameters. The results show that LCOE of upwind 2-bladed and upwind 3-bladed turbines with 121 m diameter have a range of 2.35-2.50 pence/kWh and 2.30-2.74 pence/kWh, respectively. However, there are small differences (less than 4%) between the Sum-component cost model and the NREL's cost model. Consequently, the Sum-component cost model, which is a simplified cost model, may be applied to estimate the ICC for determining the LCOE of WT systems for any WT configuration.

4.6 Summary

The characteristics of the wind resource affect the wind speed variation (low or high wind speeds). Most areas on the earth have low wind speeds. As a result, LWSTs have been developed by increasing rotor diameter and maintaining the generator rating, to increase the output power of a WT in a period of low wind speeds. The prediction of WT costs is difficult because the improvement on LWSTs increases

investment but technological advances will reduce operation cost. Therefore, the cost models have been developed for predicting the cost of WTs at different machine sizes and machine configurations. Conversely, several cost models are outdated and many models have limitations of use in specific WT configurations. In addition, most of them need deep knowledge and information of WT for calculation.

The two simplified cost models, namely the Sum-component cost model and the Total-cost model, are proposed in this thesis for estimating the cost of wind-generated electricity of LWSTs at different rated wind speeds. The Sum-component cost model is modified from the Total-cost model by adding the cost fraction for more detailed calculation. The results show that the Sum-component cost model can provide smaller different solutions from the NREL's cost model than from the Total-cost model. However, the NREL's cost model are formed from fitting curves of industry and experiment data, as well as data from simulation programs to design WTs that need more data than the Sum-component cost model. Furthermore, more detailed breakdown of costs could provide a better result. The results show that there is a clear trend of increasing ICC when the rotor diameters are larger. However, LCOE will decrease if the rotor diameters increase up to a certain size, after that LCOE will increase.

In future investigations it might be possible to compare the results of the proposed cost models with the actual installation costs or the costs calculated by WT design programs, in various rotor diameters.

CHAPTER 5

5. OPTIMIZATION FOR STAND-ALONE HYBRID WIND-SOLAR SYSTEMS

5.1 Introduction

Three algorithms, namely the operation processes of stand-alone hybrid systems using battery management, diesel generator support or WTs at different rated wind speeds are developed and proposed in this chapter to deal with the issues as discussed in Chapter 1 and 2. The chapter explains important assumptions and decisions on which the operation is based. This study selects Lam Takhong Dam, Nakhon Ratchasima province in Thailand where these technologies have been applied, because this location has the potential for both wind and solar energy from [53], [54], respectively. Consequently, this location will be used for evaluating economic feasibility of these stand-alone hybrid wind-solar systems of Thailand.

This chapter is arranged as follows: Firstly, the development of SPEA2 operators for the optimization of stand-alone hybrid wind-solar systems and the selection of SPEA2 parameters are described. The models to estimate the possible maximum number of WTs are proposed in this chapter to set the optimal boundaries of the decision search for performing good search efficiency. Next, the detailed processes and calculations of operation of stand-alone hybrid wind-solar systems are explained, especially the battery charging and discharging processes. Additionally, the three algorithms of the operation processes of stand-alone hybrid wind-solar systems using battery management, DSG support or WTs at different rated wind speeds are illustrated in this chapter. Finally, two case studies to examine the issues above are demonstrated and discussed.

5.2 SPEA2 applied to the optimization of stand-alone hybrid systems

This section explains the application of the SPEA2 algorithm for the optimization problem of a stand-alone hybrid renewable energy system, provided in the MATLAB command line. The optimization procedure is illustrated in Figure 5.1. Decision variables and SPEA2 parameters are defined and the main process is provided as follows:

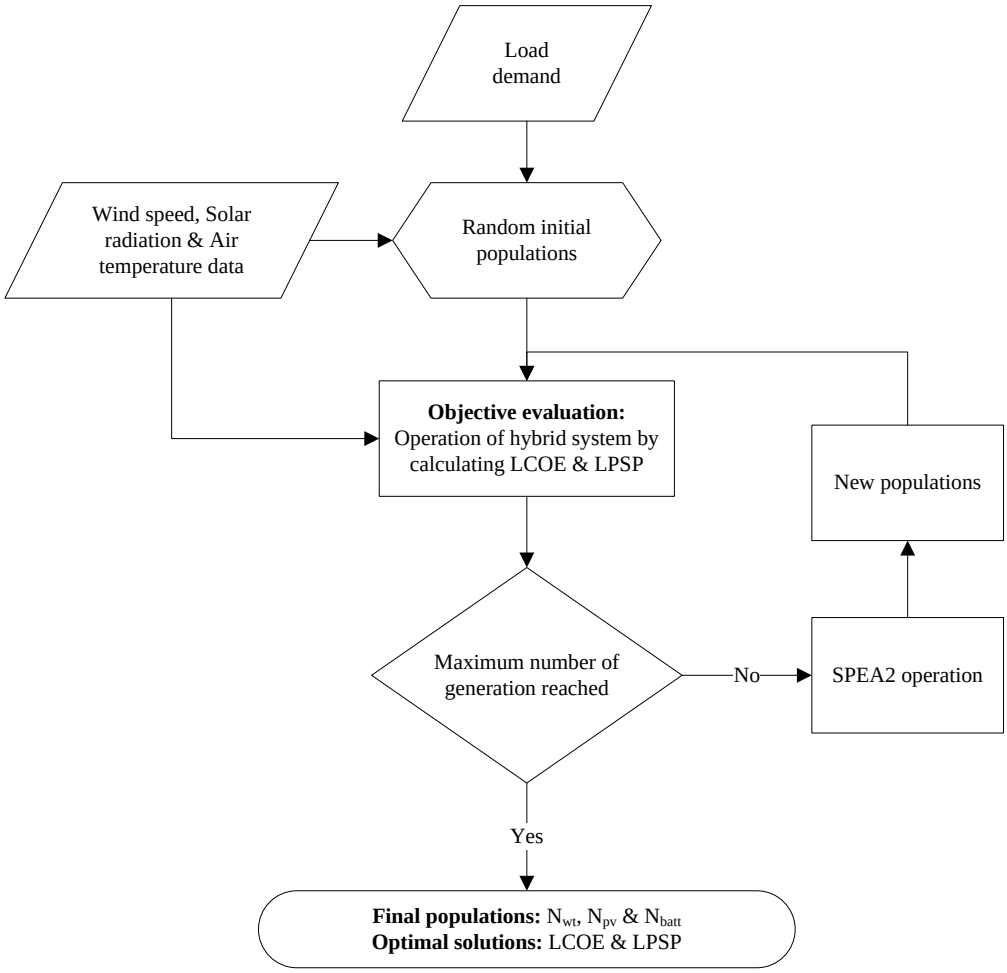

Figure 5.1 The optimization procedure for stand-alone hybrid systems by using SPEA2

5.2.1 Decision variables and Initial populations

This chapter studies four kinds of hybrid stand-alone systems, namely, WT-Battery systems, PV-Battery systems, WT-PV-Battery systems and WT-PV-Battery systems

with diesel generators. Decision variables of these systems are the optimal number of battery modules and the optimal number of WTs and/or PV modules, based on energy resources studied. The decision search space of each variable is set to be integers, which are greater than or equal to zero. Units of each energy resource system are encoded as genes in the chromosome. The chromosome is represented by a vector with a number of elements equal to the number of energy resource systems. Specifications, estimated costs and lifetimes of the hybrid system components are described in Appendix A and B.

In this study, the initial population of solutions was created in individuals by the random initialization method. It has been suggested that the random individual creation should be in the decision space to perform better search efficiency [173], [179]. Moreover, if optimal boundaries of the decision search space are set, some good solutions can be found in the first generation and these are good starters for searching in next generations [199]. Consequently, the decision search space of the first population can be set by the initial assumption of system configurations to be the inequality constraints as follows:

$$0 \leq N_{wt} \leq N_{wt,max} \tag{5.1}$$

$$0 \leq N_{pv} \leq N_{pv,max} \tag{5.2}$$

$$N_{b,min} \leq N_b \leq N_{b,max} \tag{5.3}$$

where N_{wt} is the number of WTs, $N_{wt,max}$ is the maximum number of WTs, N_{pv} is the number of PV modules, $N_{pv,max}$ is the maximum number of PV modules and N_b is the number of batteries. $N_{b,min}$ and $N_{b,max}$ are the minimum and maximum number of batteries, respectively. The models to estimate the possible maximum number of WTs are proposed in this thesis. The number of WTs for hybrid systems depends on key parameters, namely wind speeds, characteristics of WTs and load demand. Their maximum number could be calculated from an integer of a ratio of their power generated in the worst month and rated power of a WT.

$$N_{wt,max} = int\left[\frac{P_{worst,w}}{P_{wt,r}}\right] \quad (5.4)$$

where $P_{wt,r}$ is the rated power of a WT. $P_{worst,w}$ is the power of WTs that should be designed as following in the worst month.

$$P_{worst,w} = \frac{\bar{E}_{L,daily}}{\eta_{Batt}(1-d_{wm})\cdot h_{worst,w}} \quad (5.5)$$

where $\bar{E}_{L,daily}$ is the average daily load (kWh/day), d_{wm} is the percentage of degradation in performance for the average effect of friction considered as 0.1 and η_{Batt} is the battery efficiency. The hours of wind speeds when WTs can generate full power in the worst month can be calculated by applying the power law from Equation 2.2.

$$h_{worst,w} = \frac{24\cdot\sum_{i=1}^{n} U_{worst}^3}{U_{rated}^3} \quad (5.6)$$

where n is the number of hours, that is, hourly wind speed data input in this study. The sum of the cube of wind speeds in the worst month will equal a minimum of the sum of cube wind speeds in a year.

$$\sum_{i=1}^{n} U_{worst}^3 = min[\sum_{i=1}^{n} U_i^3] \quad (5.7)$$

The sum of the cube of wind speeds can be calculated by:

$$\sum_{i=1}^{n} U_i^3 = \int_{U_{c,in}}^{U_r} U_i^3 \cdot p\left(U_{c,in} \le U_i \le U_r\right)dU + \int_{U_r}^{U_{c,out}} U_r^3 \cdot p\left(U_r \le U_i < U_{c,out}\right)dU \quad (5.8)$$

where $p(U)$ is the probability density and U_i is the wind speeds at time i. $U_{c,in}$, U_r and $U_{c,out}$ are the cut-in, rated and cut-out wind speeds (m/s) of a WT, respectively.

The minimum number of WTs and PVs was set to zero. The possible maximum sizing of PV was determined by the methodology in [69]. The possible battery sizing models for finding the maximum and minimum number were referred from [83]. They are described in Appendix C.

5.2.2 Objective evaluation

The stand-alone hybrid systems were designed by an AC bus as the main connection point, as shown in Figure 2.10(b) and described in Section 2.4.1. The design for the suitable hybrid stand-alone system is a trade-off between the project cost and the quality of services for users. LCOE and LPSP are set to be objectives of this optimization problem. Both parameters were described in Chapter 2. The LCOE is usually used to measure the power generating cost of a project that has different power generation plants [29], [5], [17]. The power reliability is a key of the quality of services for users, especially a stand-alone hybrid renewable energy system because of the uncertainty of wind speed and solar radiation characteristics. Several researchers use LPSP to measure the system reliability [33], [31], [137]. The operation concepts of a stand-alone hybrid system for finding LPSP and the annual useful energy production for calculating LCOE are fully described in Section 5.3.

5.2.3 Reproduction

Reproduction is the process that creates new individuals from the mating pool by crossover and mutation. Many crossover operators have been developed for real number encoding. This study applies the uniform crossover technique, performing better than one-cut point and two-cut point crossover [199]. A crossover probability is commonly used between 0.6 and 1 [180]. Some researchers suggest that it should be between 0.65 and 0.85 [174] or between 0.4 and 0.9 for uniform crossover [200]. This work uses the crossover probability of 0.8.

The mutation operator provides the different genes which were not explored in the decision space and restores the genes that were deleted from the population in the selection process [173], [179]. A suitable mutation probability is a key to modifying new genes. Many researchers use a mutation probability of 0.001 [200]. Alternatively, a mutation probability is generally estimated by $1/L$ or about $1/(NL^{0.5})$, where L is the length of an individual population member and N is the population size [200]. A mutation probability of 0.006 is used for the SPEA2 binary test problems [35]. Alarcon-Rondriguez [37] used a mutation probability of $1/n$ in his doctoral thesis, where n is the number of decision variables for real-coded GAs. Some researchers suggest using a mutation probability of 0.001 and 0.01 for large

populations (100) and small populations (30), respectively. This study uses a mutation probability of 0.001.

5.2.4 Population and archive sizes

The appropriate size of population is normally between 30 and 100 [201]. Nonetheless, it depends on the difficulty of the problem, as discussed in Section 3.4.7. The LPSP, an objective, is calculated from the operation process of a stand-alone hybrid system that has several conditions, as described in the next section. This makes the optimization problem quite difficult to solve. This study had investigated the proper population size for this problem. It was found that the population sizes of 100 and 150 can provide the solutions that are similar. Therefore, this study uses 150 populations to obtain more accurate solutions.

The archive size is another key parameter to solve an optimization problem by using SPEA2. A large archive size or too many non-dominated solutions may decrease selection pressure because most solutions will have a same fitness, leading to a slowing down of the search, as mentioned in [158]. Ziztler *et al.* [35] set an archive size as same as the population size (i.e. between 250 and 400) in every test problems. Alarcon-Rondriguez [37] used population sizes between 100 and 400 and set the archive sizes between 25% and 75% of the population size. This study uses the archive size of 70 that is approximately 47% of the population size.

5.3 Operation of stand-alone hybrid wind-solar systems

Power reliability is important for designing a stand-alone hybrid renewable energy system using wind and solar energy technologies. The LPSP with the concept of the Chronological method is commonly used to check that the power supply has sufficient power for the load demand, during a period considered, applied in such as [77], [73] and [151]. This thesis applies the LPSP, with Equation 2.11 for the system consisting of WTs, PVs and batteries with/without the support of diesel generators. The effect of battery energy accumulation with a resolution of one hour each time series for a whole year is considered to achieve more accurate results. Therefore,

three main factors of the operation process have to be considered, namely, load power, output power of a power source, and State of Charge (SOC) of the battery.

The overall algorithm of a stand-alone hybrid system operation, illustrated in Figure 5.2, involves six main steps as follows:

Input: P_s is the output power from WT and/or PV systems and P_L is the load demand.
Output: LPSP is the loss of power supply probability, E_{use} is the annual useful energy production and E_w is the annual waste energy from renewable energy sources.

1. **Initialization:** Set the initial SOC to be 1.
2. **Battery processes:** In the case of the battery charging process, P_s will be stored in batteries whenever it exceeds P_L. Otherwise, for battery discharging process, the power from batteries will be required if P_s is not enough to supply P_L. The details will be described in Section 5.3.1.
3. **Exceeding load power:** Calculate the load power exceeding the power available by using Equation 2.12.
4. **System reliability:** Compute the LPSP by using Equation 2.11.
5. **Annual useful energy production:** Useful power is the power consumed by load and charged into batteries. E_{use} is calculated by summing the useful power in every hour for a whole year.
6. **Annual waste energy:** Waste power is P_s exceeding the load demand and battery charging power. E_w is estimated by summing the waste power in every hour for a whole year.

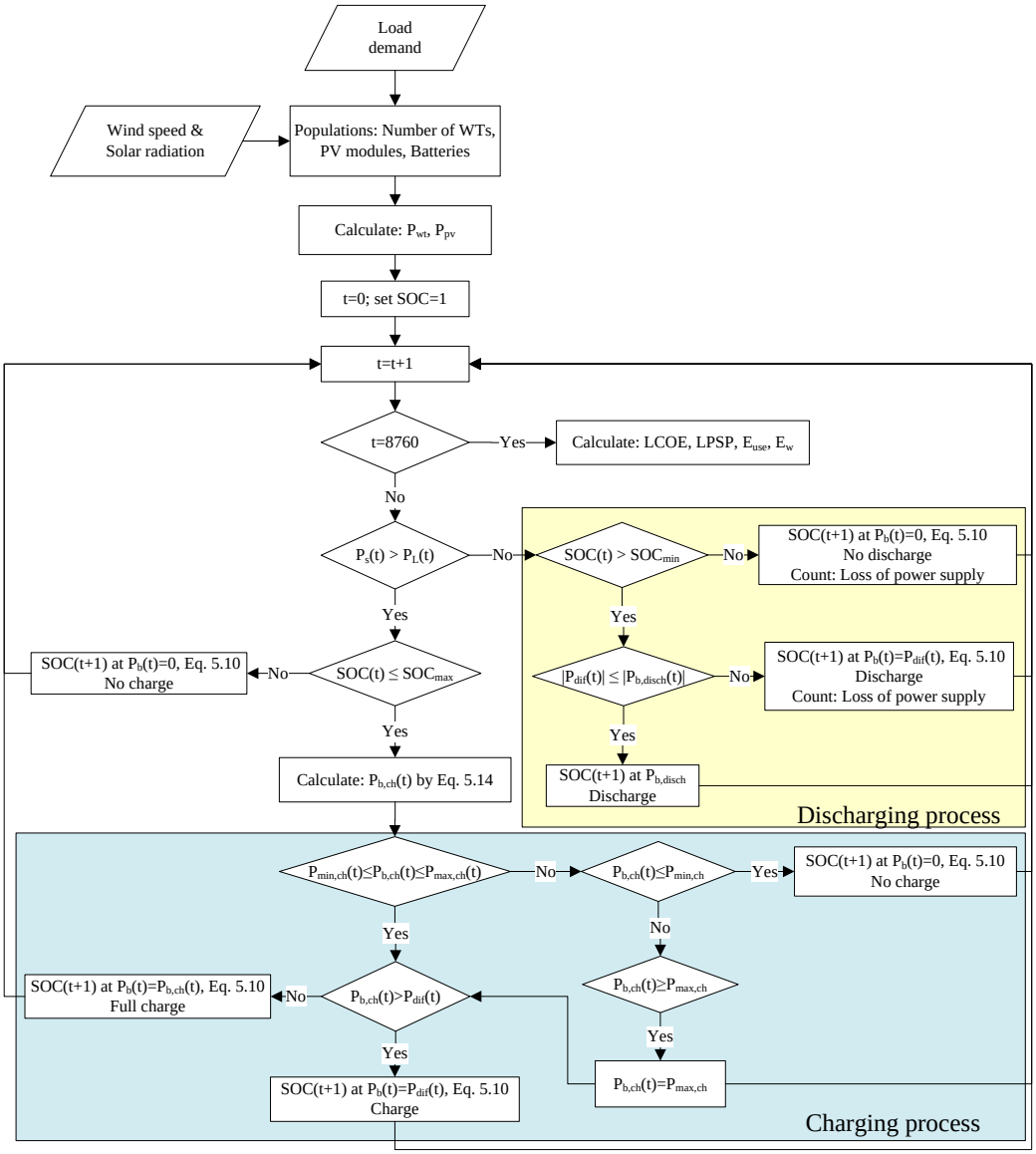

Figure 5.2 The operation process of a stand-alone hybrid WT-PV-Battery system

5.3.1 Battery charging and discharging processes

The state of charge (SOC) is a measure of the amount of energy in a battery, shown as a percentage of the energy stored in a fully charged battery. It is generally applied as a decision parameter to control overcharge and discharge batteries [33], [31], [137]. Battery charging and discharging processes must be limited within the range of the minimum and maximum SOC. The charge controller will stop the charging process if SOC reaches the maximum value, commonly set to be 100%, as for example used in [79], [156], [74]. Consequently, this study sets the maximum SOC equal to 100%. The minimum SOC can be determined by the maximum Depth of Discharge (DOD), as follows.

$$SOC_{min} = 1 - DOD_{max} \tag{5.9}$$

Most battery manufacturers suggest that the DOD of a battery should be no more than 50% for deep cycle, to prolong battery life [202]. However, some types of battery used in a PV system can discharge as high as 80% of the DOD [202]. Therefore, the maximum DOD values that are commonly used vary from 50% to 80% for the design of a hybrid renewable energy system, such as 50% [156], 60% [159], 70% [77] and 80% [73], [72]. This study uses 50% of the DOD as the basic study. Additionally, this study compares the effect of two maximum DOD values that are 50% and 75% on the results of design in term of LCOE and LPSP.

The SOC at any hour depends on the previous SOC. In this study, the first hour of the SOC was considered to be 100%. The SOC at time $t+\Delta t$ can be calculated by [73]:

$$SOC(t+\Delta t) = SOC(t) \cdot \left(1 - \frac{\sigma_{dish} \cdot \Delta t}{24}\right) + \frac{\eta_b \cdot P_b(t) \cdot \Delta t}{Ah_r \cdot V_b} \tag{5.10}$$

where σ_{dish} is the self-discharge rate relying on the accumulated charge and the battery state of health (0.2% per day [73]). Ah_r is the rated battery capacity given by a manufacturer. V_b is the voltage of a battery system (V). Δt is the time duration in this study assumed to be 1 hour. In this study, battery voltage and temperature changing while batteries are working is not considered.

The battery efficiency η_b is measured in charging and discharging states. The charging efficiency is set to be the round-trip efficiency that is normally more than 60%, mainly based on type and quality of a battery. The discharging efficiency is related to discharge duration, based on the storage technology, application and cost. The efficiency will be lower for discharging a high rate in short periods of time; for example, some types of storage systems can discharge a nominal 1 MW in 3 hours with 80% efficiency or, in an emergency case 1.5 MW in 10 minutes with 65% efficiency. Discharging a small portion can prolong battery lifetime and be less harmful to the storage system than a deep discharge. [203]

However, for simplicity in the analysis, many researchers assume that the battery charging and discharging efficiencies are kept constant at, such as 85% [72], 90%

[159], and 100% [73], [76]; although, the battery charging and discharging rates vary. This study also uses the battery efficiencies of constant 100%.

The battery charging or discharging power at time *t*, $P_b(t)$, is determined from the battery charging and discharging processes, as presented in Figure 5.2. These processes are dependent on the difference in power at time *t* between power sources and load demand. It can be defined by:

$$P_{dif}(t) = P_s(t) - P_L(t) \tag{5.11}$$

where $P_s(t)$ is the power output from sources, namely WT and/or PV systems and $P_L(t)$ is the load power, at time *t*. If the difference in power is negative, batteries will discharge. However, the SOC at time *t* must be greater than the minimum SOC. Batteries will charge when the difference in power is positive. The amount of battery charging power (kW) can be calculated by:

$$P_{b,ch}(t) = \frac{(SOC_{max} - SOC(t)) \cdot Ah_{rated} \cdot V_b \cdot \eta_{ch}}{1000} \tag{5.12}$$

Nevertheless, the amount of battery charging power is based on the capacity of the power conditioning equipment and battery characteristics [202], [203], [204]. This study considers the limitation of power that a battery can charge. This amount must be greater than or equal to the minimum battery charging power (kW). It can be defined by:

$$P_{min,ch} = \frac{Ah_{rated} \cdot V_b}{1000 \cdot \eta_{ch} \cdot h_{max,ch}} \tag{5.13}$$

Furthermore, a battery can charge until it reaches the maximum battery charging power (kW).

$$P_{max,ch} = \frac{Ah_{rated} \cdot V_b}{1000 \cdot \eta_{ch} \cdot h_{min,ch}} \tag{5.14}$$

where Ah_{rated} is the rated ampere-hour of battery cell. $SOC(t)$ is the state of charge of battery at hour *t*. η_{ch} is the efficiency of battery charging. $h_{max,ch}$ and $h_{min,ch}$ are charging time that is 12 to 16 hours for a sealed lead acid battery, and it can be 36 to 48 hours for large stationary batteries [204].

For the discharging process shown in Figure 5.2, when the SOC is reduced to the minimum point, the charge controller will cut off the load. In this study, batteries will independently discharge by having only one constraint, which is the SOC at time *t+1* which must not be lower than the minimum SOC. Two cases for the loss of power supply are no battery discharging power or insufficient power output from batteries to supply load demand and they are used for calculating the LPSP in Equation 2.11. The battery discharging power can be determined by:

$$P_{b,disch}(t) = \frac{(SOC_{min} - SOC(t)) \cdot Ah_{rated} \cdot V_b \cdot \eta_{disch}}{1000} \quad (5.15)$$

where η_{disch} is the efficiency of battery discharging.

The concept above is the main operation process. Nonetheless, two main issues of stand-alone hybrid renewable energy systems are studied in this thesis. Firstly, the improvement on the system reliability by using battery management compared with diesel generator support is discussed in both technical and economic terms. Secondly, the economic feasibility of LWST and HWST applications in stand-alone systems is evaluated. Hence, the main operation process was improved to deal with these issues by developing three algorithms that are the operation processes of stand-alone hybrid systems using battery management, diesel generator support or WTs at different rated wind speeds.

5.3.2 Stand-alone hybrid wind-solar systems using battery management

The battery management system was discussed in Section 2.4.3. The Decentralized Battery Storage Control (DBSC) method is division of batteries into groups or strings, to provide better performance, longer lifetime storage and lower maintenance cost of battery storage systems than a single charge controller [39], [40], [38]. Designing the optimal sizing of system components of a stand-alone hybrid system by using the DBSC method with multi-charge controllers in the optimization process is proposed. This thesis studies two important factors of the design. They are the number of battery groups and the sizes of each group, related to system cost and an improvement of system reliability. The battery process is modified by adding the

procedure of the DBSC method, with the simplified method proposed in this study as follows:

Modification 1: The number of batteries

1. Set the number of battery groups and fractions of each group. The sum of the battery group fractions must be equal to 1. For example, the fractions of the three groups are 1/6, 1/3, 1/2.
2. Calculate the Least Common Multiple (LCM) of the fractions set. From the example above, the LCM is 6.
3. Determine the new chromosome of the number of batteries by multiplying the chromosome of the number of batteries by the LCM in every generation. The aim is to ensure that the numbers of batteries in each group are integers.
4. Compute the number of batteries in each group by multiplying the new chromosome by the fractions set in Step 1.

Modification 2: Battery charging process

With most battery types, such as lead-acid and lithium-ion batteries, it is suggested that they should fully and frequently recharge to maintain good performance [202], [203], [205]. The lead-acid battery is the cheapest and most popular amongst battery types for energy management applications in a stand-alone renewable energy system [33], [203]. This thesis uses lead-acid batteries in the case studies. Therefore, the battery charging process in this study is set so that the battery group that has the lowest SOC will charge first. However, if some or all battery groups have the same SOC level, smaller groups will charge before larger groups, so that battery groups can have full and most frequent charge. If larger battery groups charge before smaller groups, the power remaining from supplying load demand may not be adequate to charge any smaller group. The overall algorithm of this process can be described as follows:

1. Determine the minimum and maximum battery charging power of each battery group by using Equation 5.13 and 5.14.
2. Calculate the battery charging power at time *t*, $P_{b,ch}\ (t)$, by using Equation 5.12, for the lowest SOC. Alternatively, if some or all battery groups have the same SOC level that is lower than the maximum SOC, the $P_{b,ch}\ (t)$ of the smallest battery group

will be computed by using the same equation. The battery can charge when power sources exceed load demand and the $P_{b,ch}$ *(t)* must be within the minimum and maximum battery charging power range of its group.

3. Compute the battery charging power at time *t* by sorting in ascending order, if the power sources remain from the previous charge. This process stops when no power sources remain or all battery groups are charged.

Modification 3: Battery discharging process

It is suggested that most battery types should avoid frequent full discharges [203], [205]. A shallow discharge can maintain better performance than a deep discharge [203]. Consequently, the battery group, which has the highest SOC level, discharges first. Nonetheless, if they have the same SOC level, larger battery groups will discharge before smaller battery groups.

5.3.3 Stand-alone hybrid wind-solar systems using diesel generator support

The battery charging and discharging processes of a stand-alone hybrid WT-PV-Battery system, as presented in Figure 5.2, are modified to have the diesel generator (DSG) support. This study designs a stand-alone hybrid using diesel generator support, by applying a DSG model as described in Section 2.4.4. Manufacturers suggest that DSGs should operate within a range of a specific minimum and the rated power output of the generator [79], [134]. This range is used as the main condition for designing DSG operation in this study. Consequently, if the required power is not within the range, a DSG will not operate. The DSG operation is planned for two cases as follows:

1. DSGs will run for fully charging batteries so that reserve energy can supply the needed energy to balance supply and demand, illustrated in Figure 5.3. In addition, full and frequent charge is good for prolonging battery lifetime.
2. DSGs will operate when the output power from WT, PV and battery systems is insufficient for load demand. DSG operation is added in the battery discharging process, as shown in Figure 5.4.

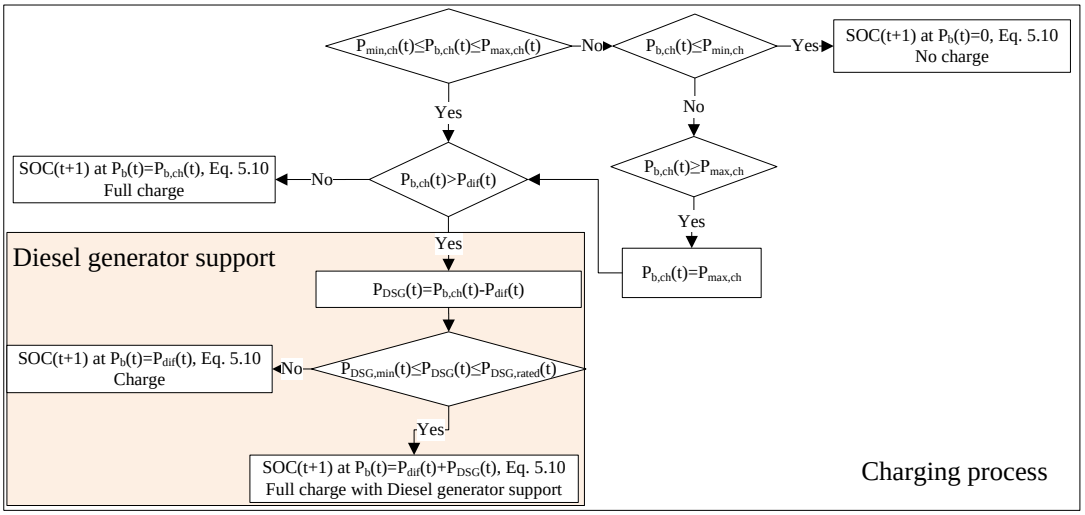

Figure5.3 Diesel generators supporting the battery charging process

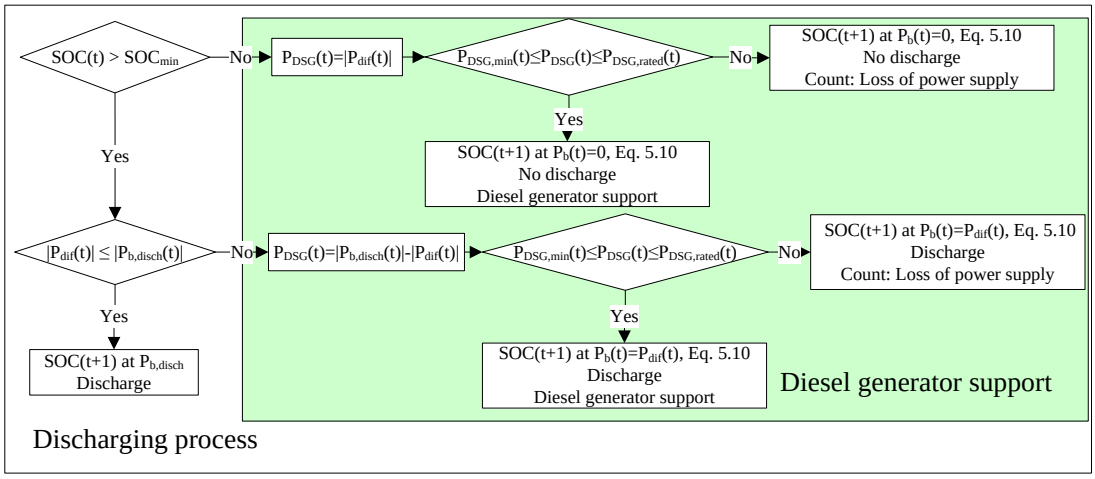

Figure 5.4 Diesel generators supporting load demand

5.3.4 Stand-alone hybrid systems using WTs at different rated wind speeds

The LWST is a WT improved to catch more wind energy in low wind speed areas by increasing the rotor diameter. An increase in the rotor diameter leads to a decrease in the rated wind speed and a WT having a lower rated wind speed can give more output power, as discussed in Chapter 4. The optimization problem for stand-alone hybrid systems using WTs at different rated wind speeds is studied for forecasting LCOE and evaluating the economic feasibility of LWSTs and HWSTs installed in low wind speed areas. Two steps are provided as follows:

1. Calculate output power of WTs at different rated wind speeds by using Equation 2.2 under the conditions explained in Section 4.3.
2. Estimate the ICC of WTs by using the cost models of WTs, proposed in Section 4.4.3.

5.4 Case studies

This section demonstrates case studies of two issues of stand-alone hybrid renewable energy systems. Firstly, advantages and disadvantages of battery management and DSG support to improve the system reliability are discussed in both technical and economic terms. Secondly, the economic feasibility of stand-alone systems using LWSTs and HWSTs is evaluated by using the Sum-component cost model, as proposed in Chapter 4.

Hourly wind speed and hourly solar radiation data at Lam Takhong Dam, Nakhon Ratchasima province in Thailand, collected in 2006 [53], [54], were used, as illustrated in Appendix D. Hourly temperature data was calculated from air ambient temperature data, collected every three hours in 2006, referred from [206]. This data was used for estimating the PV module efficiency relating to the cell temperature and then forecasting the hourly PV power output. The interest rate and the inflation rate are 7.7% and 2.9%, respectively, referred from Bank of Thailand in October, 2011 [198].

All optimization problems in this study used the SPEA2, run with 150 populations, 70 archives and 100 generations. Mutation and crossover probabilities were set to be 0.001 and 0.8 respectively. The simulation time is every hour of a whole year (8,760 hours). The total evaluation time of each case is approximately 20 minutes.

5.4.1 Case study I: Improvement on the stand-alone hybrid wind-solar system reliability by using battery management or diesel generator support

5.4.1.1 Load descriptions

The hybrid systems for rural electrification in Thailand were studied. Load profile from IEEE Reliability Test System [207] was applied to design the system reserved

for future load demand. The seasonal load profile was determined from the system peaking season in Thailand (the peak occurring in the 3rd week of April) [208]. The system load peak is assumed to be 30 kW and its profile is shown in Appendix E. The average daily load energy is 0.44 MWh/day and the total annual load energy is 161.37 MWh/year.

5.4.1.2 Configurations of system components

This study considers five types of stand-alone hybrid systems, namely stand-alone WT-Battery systems, stand-alone PV-Battery systems, stand-alone WT-PV-Battery systems, stand-alone WT-PV-DSG-Battery systems and a DSG. Specifications and costs of system components are described in detail in Appendix B. The configurations of main system components used in this case study can be summarized as follows:

1. Wind turbines: The size of a WT is 10 kW with the cut-in, rated and cut-out wind speeds of 3 m/s, 10 m/s and 16 m/s, respectively. A tower height is 12 m. The output power curves and distribution probability of wind speeds at 12 m hub heights are illustrated in Figure 5.5. From the wind data, a WT can produce electrical energy of 15.61 MWh/year. Its specifications and price is taken from [209]. The lifetime is assumed as 25 years in this study.

2. Photovoltaic modules: The mono-crystalline silicon 100 Wp modules, having an efficiency of 14.5%, are used in this thesis. The technical characteristics and costs of a PV module and an inverter are referred from [210], [211] and [212]. The manufacturer guarantees a lifetime of 25 years. From the solar radiation data [54] and the location, latitude 14^{o} 47' 58"N and longitude 101 33' 32.2"E, PV modules should be oriented facing the South with the optimum angle of 10^{o} to obtain the annual maximum output energy, calculated by using equations from [213].

3. Batteries: This study uses the sealed lead-acid 550 Ah battery, having the nominal voltage of 2 V. Specifications and prices are mentioned from [214]. In order to simplify, the charge and discharge efficiencies are assumed as constants of 100%. Bi-directional converter and charger costs are referred from [211] and [212].

4. Diesel generators: This study uses three DSGs that have rated power of 12.5 kVA, 25 kVA and 37.5 kVA (or 10 kW, 20 kW and 30 kW with a power factor of 0.8, respectively). DSGs have 25,000 operating hours and costs are shown in

Appendix B, taken from [116]. Diesel price of £0.607/litre or 29.76 Baht/litre in Thailand is referred from [215]. The price does not include transportation costs to remote areas. The estimation of fuel cost and CO_2 emission, presented in Section 2.4.4, was used.

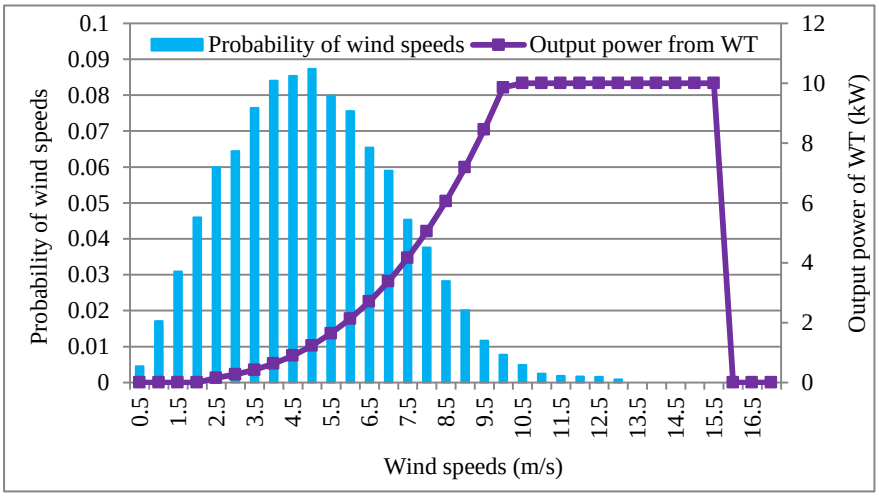

Figure 5.5 Output power of a 10 kW WT versus distribution probability of wind speeds at 12 m hub heights

5.4.1.3 Results and discussions

1. Battery management

The probability of this WT producing output power at the rated power (wind speeds of more than 10 m/s) is 2.12%, as shown in Figure 5.5. The probability, which the WT will not generate power due to wind speeds of lower than 2.5 m/s, is nearly 10%. In the worst case, the WT will delivery very low energy output or no energy output for a long period of approximately four days (26^{th} to 30^{th} November) while load demand is high, illustrated in Figure 5.6. Conversely, sometimes there will be high wind speeds but low load demand. Therefore, a storage system is required to meet load demand.

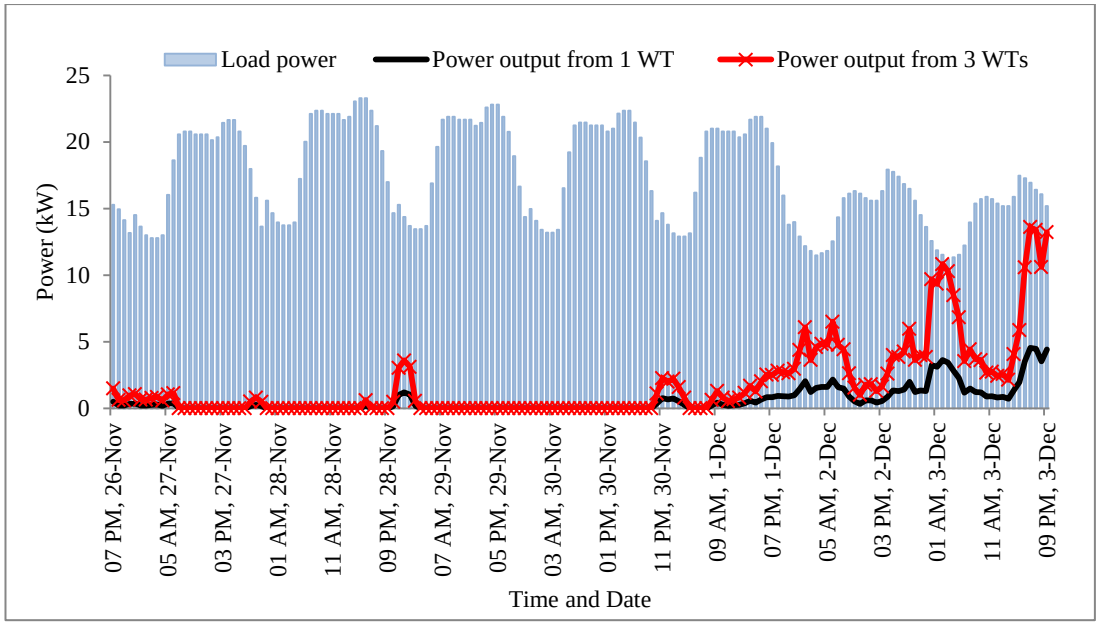

Figure 5.6 Output powers of one WT and three WTs versus load power on days with low wind speeds

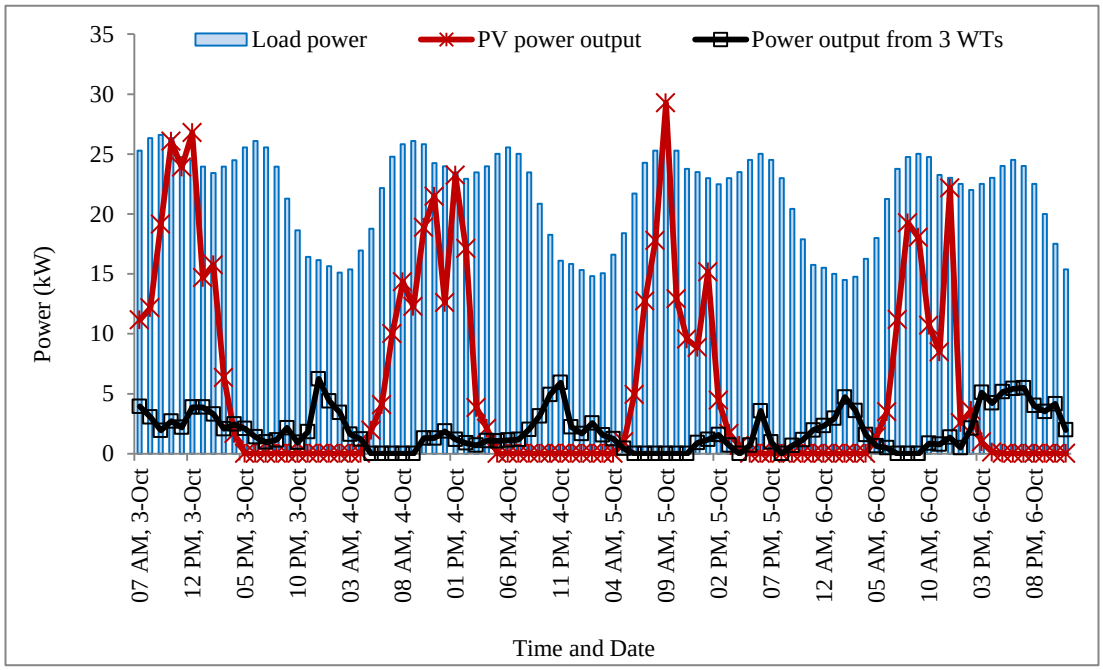

Figure 5.7 Output powers of 3 WTs and 30 PV modules versus load power cloudy days

A storage system is also necessary for stand-alone systems using PV technology, to store solar energy, especially for night time and cloudy days. There is a decrease in the daily solar energy and the sunshine duration occurring over several days continuously at the end of the rainy season, illustrated in Figure 5.7. It shows that 30

PV modules (30 kWp) are not sufficient for the load demand even during the day. Additionally, although, three WTs (30 kW rating) will be added, output energy of power supplies cannot meet the load demand.

Table 5.1 Comparisons between battery groups of stand-alone WT-Battery systems

Particular	**The number of battery groups**				
	1	**1**	**2**	**3**	**3**
Minimum state of charge, SOC_{min}	0.5	0.25	0.5	0.5	0.5 & 0.25
Battery lifetime (years)	15	15	15	15	15
Loss of power supply probability, LPSP	1.96%	1.87%	2.01%	0%	0%
Number Of WTs	89	50	43	43	40
Number of Batteries	672	960	1,344	4,176	2,880
Annual WT energy (MWh/year)	1,389.30	780.50	671.23	671.23	624.40
Annual total battery discharging energy (MWh/year)	25.16	31.57	33.82	36.46	37.74
Annual total useful energy (MWh/year)	178.15	188.24	225.69	312.29	273.87
Annual total waste energy (MWh/year)	1234	622.4	420.2	340.78	336.6
Total initial capital cost of system (k£)	2,398	1,237	1,456	2,282	1,830
Expected annual O&M (k£)	14.69	13.35	16.02	40.80	29.16
Levelized annual capital cost (£/kWh)	0.925	0.554	0.443	0.502	0.459
Levelized annual O&M cost (£/kWh)	0.110	0.094	0.094	0.174	0.142
Levelized replacement cost (£/kWh)	0.052	0.071	0.083	0.185	0.146
LCOE (£/kWh)	1.087	0.719	0.620	0.861	0.746

This section demonstrates and discusses two main issues of the settings of the battery management, namely the number of battery groups and the minimum SOC. A calculation example is presented in Section E.2.1 in Appendix E. One, two and three battery groups are examined and the two minimum SOC of 25% and 50% are compared, which results of stand-alone WT-Battery systems are shown in Table 5.1 and Figure 5.8. Moreover, results of stand-alone PV-Battery systems and stand-alone WT-PV-Battery systems are shown in Figure 5.9 and 5.10, respectively. In the case of the two battery groups, each group has the same size. The fractions of the three battery groups were set as 1/6, 1/3, 1/2.

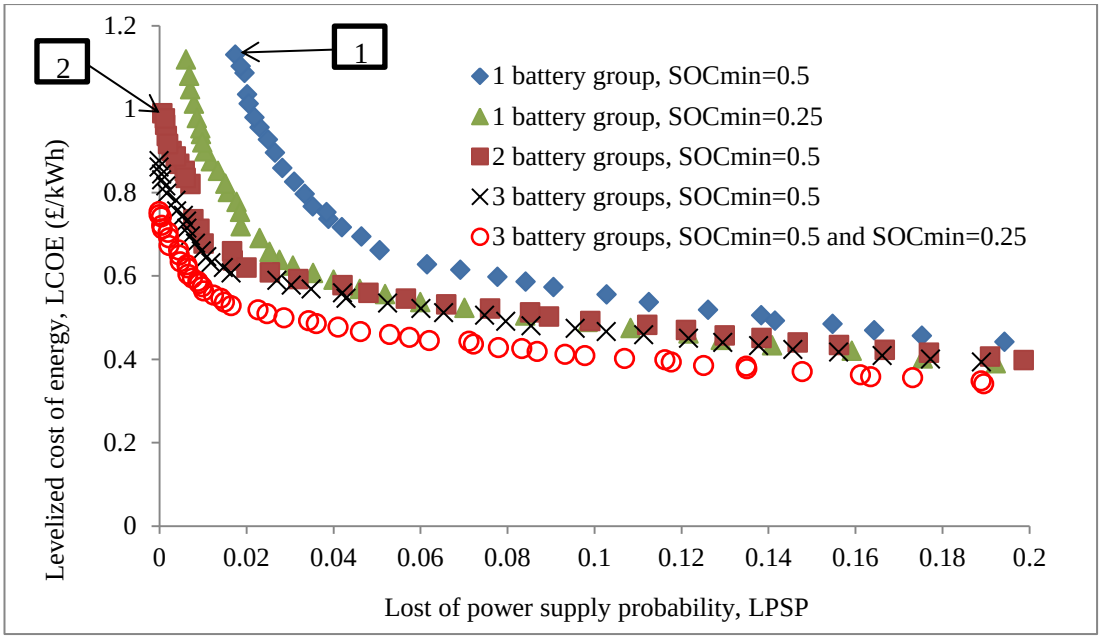

Figure 5.8 LPSP and LCOE of stand-alone WT-Battery systems

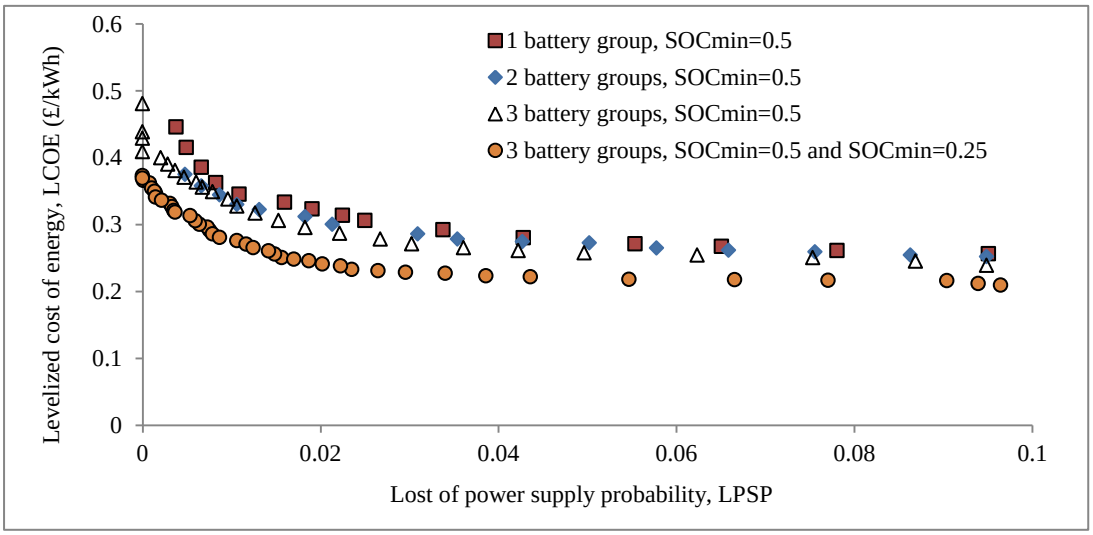

Figure 5.9 LPSP and LCOE of stand-alone PV-Battery systems

The DBSC method can improve the reliability of stand-alone WT-Battery systems, stand-alone PV-Battery systems and stand-alone WT-PV-Battery systems. The results show the stand-alone systems designed with the three battery groups will have higher reliability than the systems designed with one and two battery groups, when considering at the same LCOE levels. Moreover, the key point is that the three battery groups can provide the stand-alone WT-Battery systems and the stand-alone PV-Battery systems without loss of power supply throughout the year but the one

and two battery groups cannot meet the load demand. For example, the point 1 and point 2 illustrated in Figure 5.8, the one and two battery groups of stand-alone WT-Battery systems have the lowest LPSP of 1.75% and 0.13% with LCOE of £1.130/kWh and £0.977/kWh, respectively, for the minimum SOC of 50%. Furthermore, even though, the numbers of batteries increase for the systems using the battery management, the numbers of WTs and PV modules are decreased leading to lower LCOE, due to more expensive cost of WTs and PV modules.

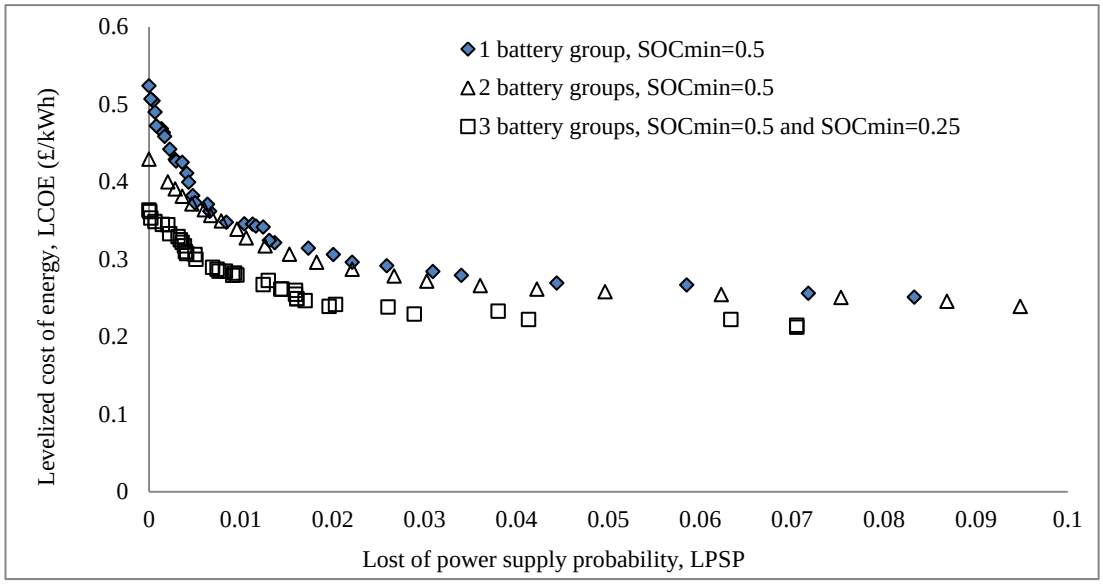

Figure 5.10 LPSP and LCOE of stand-alone hybrid WT-PV-Battery systems

The LCOE of three kinds of the stand-alone systems in this study can be decreased by using battery management. Using the three battery groups can give the cheapest LCOE, especially allowing for a minimum SOC of 25%. It seems that the lower the minimum SOC levels are set, the lower the LPSP and the cheaper the LCOE could be. However, although the minimum SOC allowable may be set at a low level as 25%, it should not be done frequently, as suggested by [203], [205].

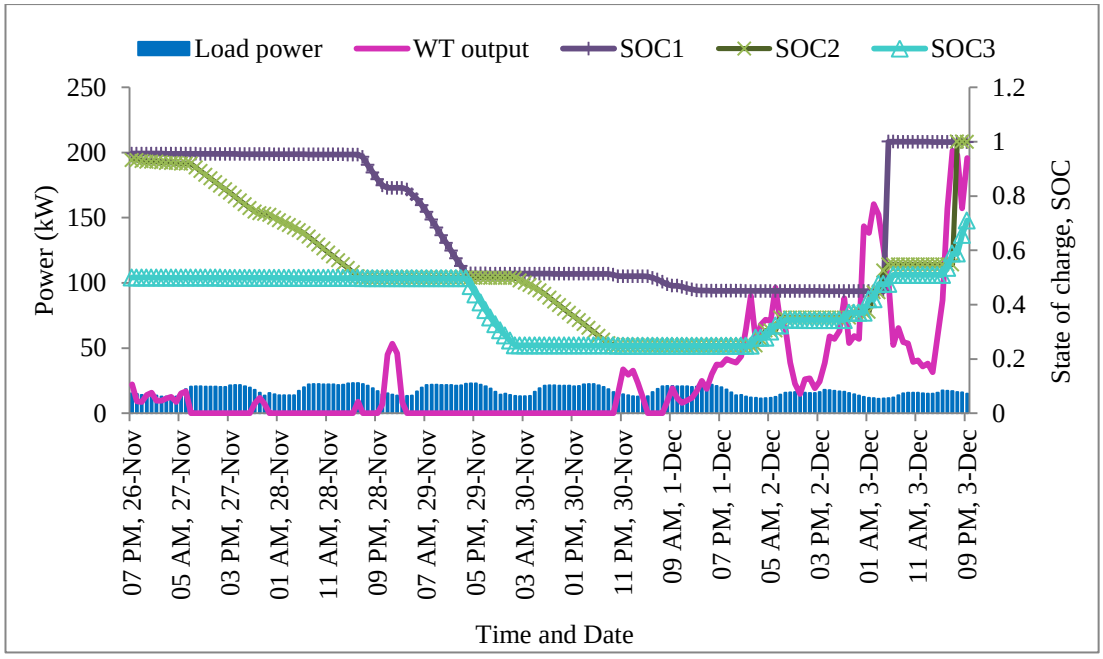

Figure 5.11 The SOC of the stand-alone WT-Battery system using three battery groups, setting the two minimum SOC levels

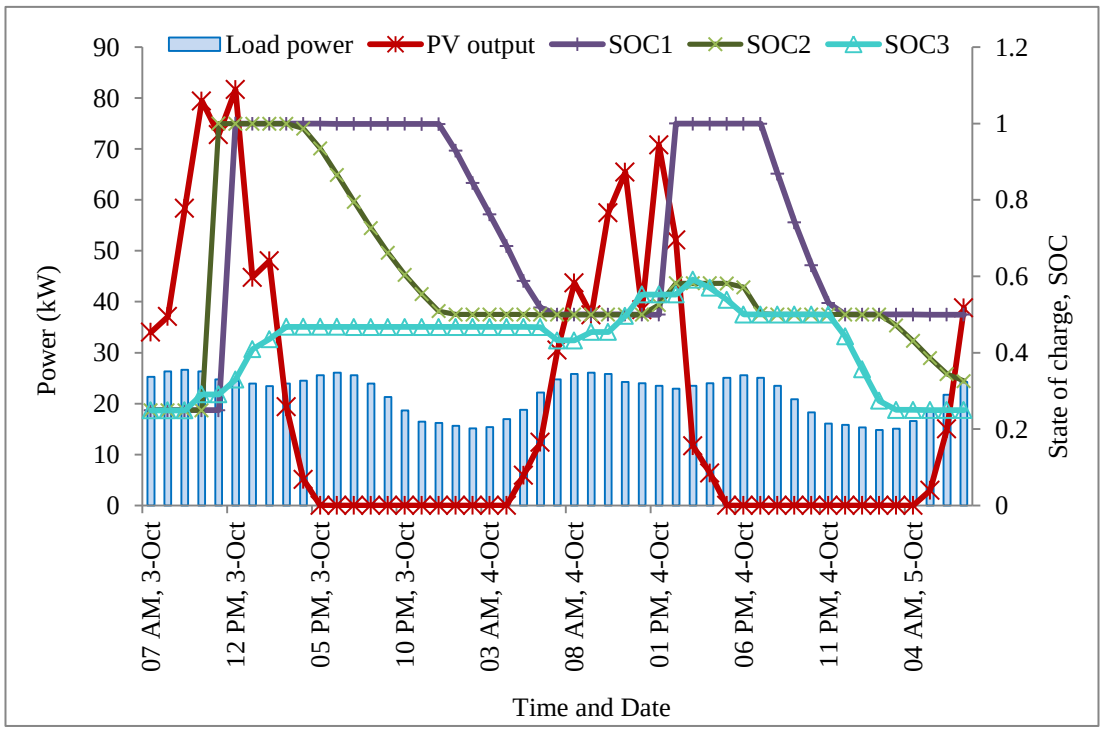

Figure 5.12 The SOC of the stand-alone PV-Battery system using three battery groups, setting the two minimum SOC levels

From the suggestion of most battery manufacturers [202], the DOD of a battery should not be greater than 50% for deep cycle, in order to prolong battery lifetime. As a result, this thesis proposes that the battery groups should set the minimum SOC at two levels, namely 50% and 25%. When all battery groups discharge up to the SOC of 50%, larger battery groups will discharge again until there is sufficient load demand or until their SOC of 25% is reached, as presented in Figure 5.11 and 5.12. The figures show that the systems using the three battery groups with the two minimum SOC set can supply load demand even in the worst case. These systems will have the lowest annual total waste energy because of the DSBC method and the technique for managing the SOC in battery charging and discharging processes, shown in more detail in Figure E.1 and E.2 in Appendix E. In addition, the optimal number of WTs, PV modules and batteries can be reduced while the system can provide high reliability without loss of power supply and the most important issue being the decrease of LCOE.

2. A comparison of stand-alone hybrid systems using battery management compared with diesel generator support

This section performs a critical analysis of stand-alone hybrid systems using battery management and DSG support. The stand-alone hybrid systems using the three battery groups with the two minimum SOC levels can give the best solutions of system reliability and LCOE, from the preliminary analysis in the previous section. Therefore, their results are compared with the results of a DSG and the stand-alone hybrid systems having DSG support in this section, as shown in Table 5.2 and Figure 5.13.

It is assumed that a DSG, rated power of 30 kW, is used for supporting load demand throughout the year. The minimum power output is set as 30% of the rated power. It can be seen from the results in Table 5.2 and the further result details in Table E.1 in Appendix E that this DSG can provide energy to support load demand with the lowest LCOE but it will emit CO_2 of 112.80 Ton/year. Its lifetime is expected to be about 3 years. However, DSGs have been used in rural areas which are farther away from the existing grid and/or difficult to access. The combination of the existing

DSG and the hybrid WT-PV-Battery system, to support the increasing load demand, to reduce the CO_2 emission and to prolong the DSG lifetime, has been studied. The stand-alone hybrid WT-PV-Battery systems, having a DSG of 10 kW or 20 kW power rating, are examined and their results are shown in Figure 5.13. The LCOE of the two systems may be twice as expensive as the single DSG mentioned above but the CO_2 emission can be reduced to about 87-95%. The CO_2 emissions of 6.02 Ton/year and 14.99 Ton/year are from systems having a DSG of 10 kW or 20 kW, respectively. If the DSG lifetime is 25,000 hours, a DSG will have the lifetime of about three years for continuous base load. Otherwise, for standby power only, it seems to have a longer lifetime, approximately 18 years.

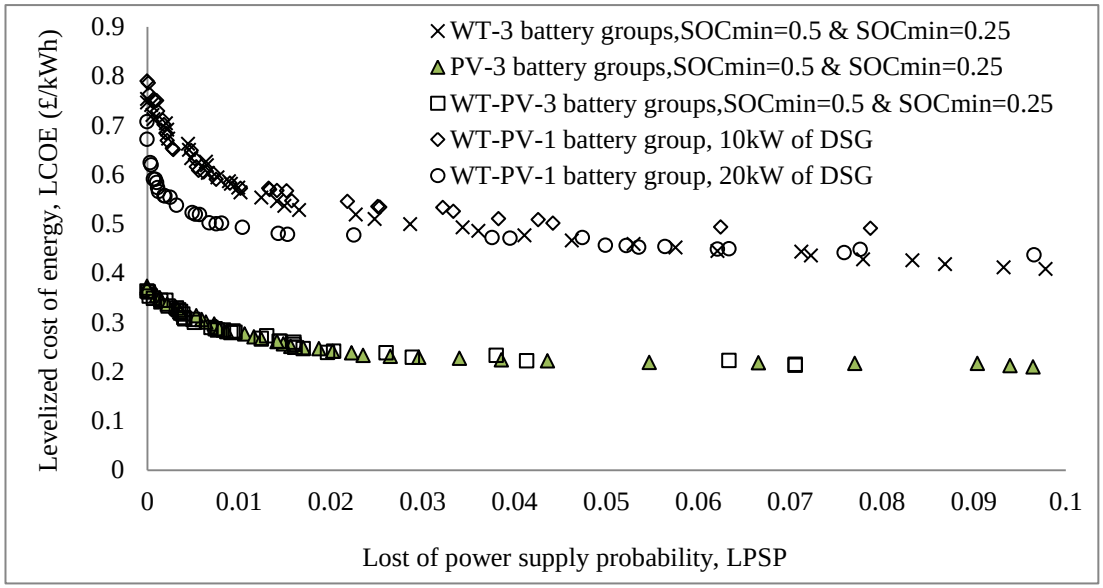

Figure 5.13 LPSP and LCOE of five stand-alone hybrid systems

For stand-alone PV-Battery systems and stand-alone WT-PV-Battery systems, using the three battery groups with the two minimum SOC levels, the results show the trend lines of the relationship between LPSP and LCOE are identical. It is possible because WTs added in the stand-alone PV-Battery systems can decrease the required number of batteries. WTs are expensive for initial investment while the decrease of the number of batteries can reduce O&M cost and replacement cost. These systems will have cheaper LCOE than the systems using DSG support. When considering the systems that can support load for a whole year without loss of power supply, their

LCOE will not be much more expensive than LCOE of the single DSG. Moreover, they are environmentally friendly and do not release CO_2.

Table 5.2 Comparisons of stand-alone hybrid systems between using battery management and DSG support

Particular	WT-Battery	WT-PV-Battery	WT-PV-DSG-Battery	PV-Battery	DSG only
Number of battery groups	3	3	1	3	-
Minimum state of charge, SOC_{min}	0.5 and 0.25*	0.5 and 0.25*	0.5	0.5 and 0.25*	-
Number of WTs	40	3	1	-	-
Number of PV modules	-	1,020	1,215	915	-
Number of Batteries	2,880	720	1,320	1,008	-
DSG capacity (kW)	-	-	20	-	30
Annual WT energy (MWh/year)	624.40	46.83	15.61	-	-
Annual PV energy (MWh/year)	-	197.07	234.74	176.78	-
Annual DSG energy (MWh/year)	-	-	21.45	-	161.37
Annual battery discharging energy (MWh/year)	37.74	59.38	74.72	87.22	-
Fuel consumption (litres/year)	-	-	7,709.90	-	61,811.51
Total initial capital cost of system (k£)	1,830	667.29	879.30	631	12.00
LCOE (£/kWh)	0.746	0.363	0.707	0.369	0.350
CO_2 (Ton/year)	-	-	14.99	-	112.80
Lifetime of a DSG (years)	-	-	18	-	3

3. Economic feasibility of stand-alone hybrid wind-solar systems

Changes in the price of WTs and PV modules depend on several factors, such as advances in technology and economies of scale. They affect the optimal capacity of each component of stand-alone hybrid wind-solar systems. The lower the price of either WTs or PV modules, the higher the capacity of such could be, while other capacities will reduce, leading to a decrease of LCOE. This section shows results of the optimal sizing of stand-alone hybrid wind-solar systems using the three battery groups with the two minimum SOC levels. Trend lines of the relationship between LCOE and price of WTs or PV modules of the systems are illustrated in Figure 5.14.

There is a clear trend of decreasing LCOE when reducing the WT price of stand-alone WT-Battery systems because the optimal number of batteries reduces while the optimal number of WTs is higher. The reduction of the number of batteries will lead to the decrease of O&M cost and replacement cost. WT price is cheaper than PV

module price but a stand-alone WT-Battery system will have the most expensive LCOE. Moreover, although WT price will be decreased to 25% of current WT price, the LCOE of this system still is more expensive than the LCOE of other systems, calculated using the current price.

This study uses the electricity price of 36 pence/kWh, considering the willingness and ability of Thai villagers to pay for electricity [68]. The new adder rates of 9.18 pence/kWh for a WT system of lower than 50 kW and of 13.27 pence/kWh for a PV system, announced in 2010 [55], were used for evaluating the economic feasibility of all systems in this study. The Thai government will subsidise these adder rates for 10 years. Nonetheless, this study assumes that the government will pay the adder rates for 25 years. It can be seen from the results in Table 5.3 and Figure 5.15 that these WT systems will not be worthwhile for investment. It is possible that this WT, having a small rotor diameter, is infrequent in generating the rated wind power, as discussed in previous sections. Increasing a tower height might not reduce LCOE because tower costs will rise. For stand-alone WT-PV-Battery systems, the LCOE will slightly decrease if WT price reduces, shown in Table 5.4. The reduction of the PV module price shows more impact on the decrease of LCOE of this system type.

This small WT may not be of much use for the stand-alone systems using PV modules, in supporting load demand. As can be seen from the results in Table 5.5 and 5.6 or trend lines in Figure 5.14, stand-alone PV-Battery systems and stand-alone WT-PV-Battery systems will give the same trend lines of relationship of LCOE and LPSP. In addition, it appears that stand-alone PV-Battery systems will be more worthwhile for investment when PV module price reduces to 25% of current PV module price, presented in Figure 5.15. However, for the current price of both WTs and PV modules, all stand-alone hybrid systems may not provide the profits in investment within project lifetime of 25 years. Some profits will be made when WT and PV module prices are lower than 75% of current prices for stand-alone PV-Battery systems and stand-alone WT-PV-Battery systems.

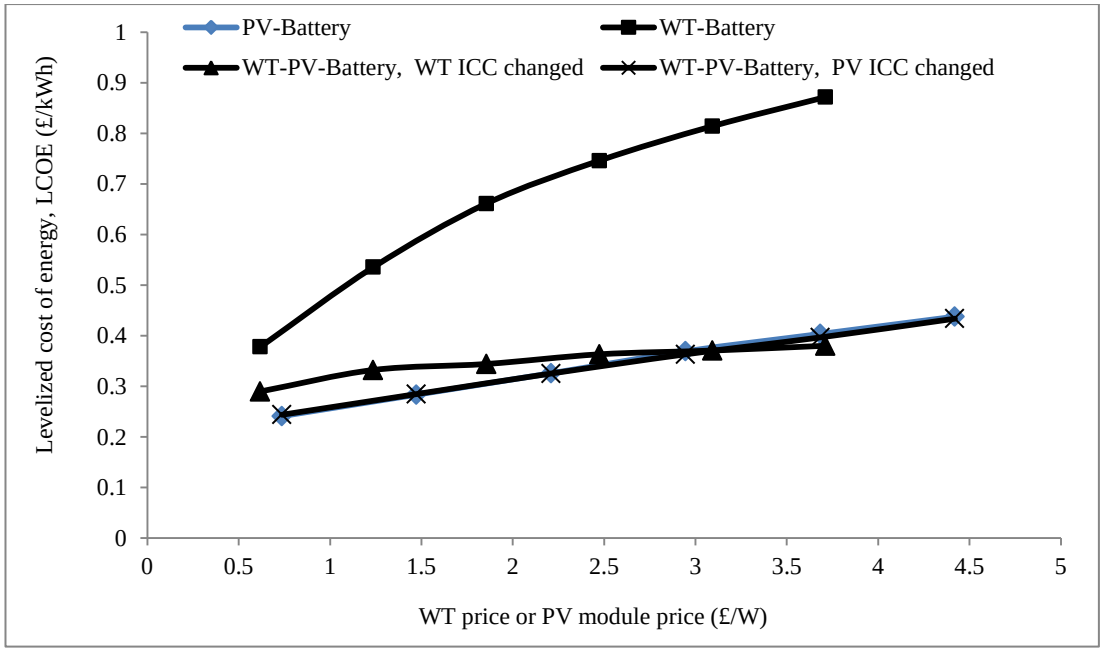

Figure 5.14 LCOE of stand-alone hybrid wind-solar systems in different WT prices and different PV module prices

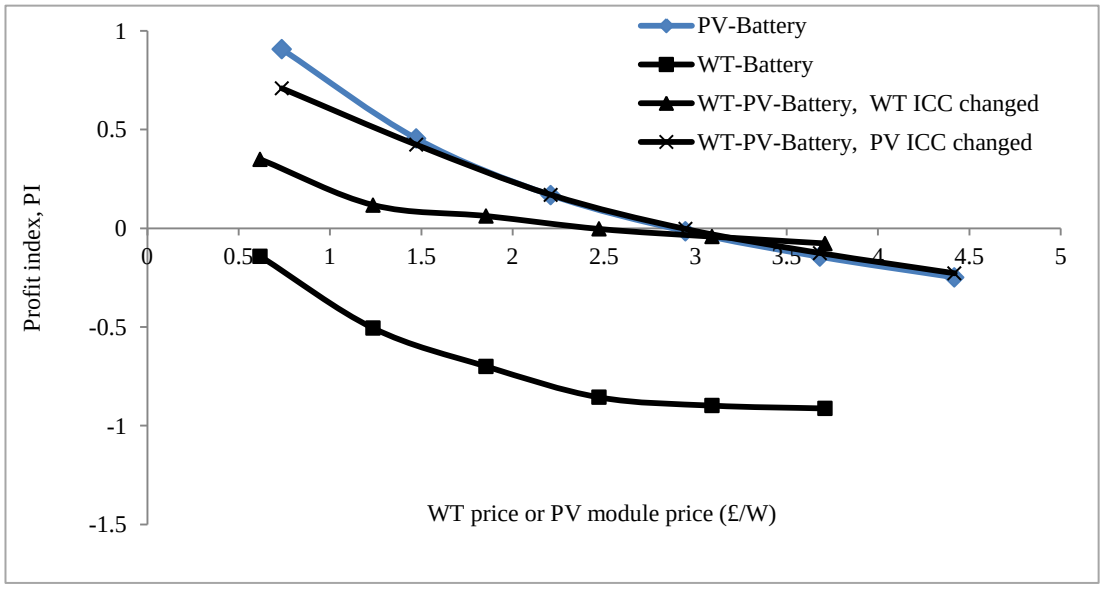

Figure 5.15 Profit indexes of stand-alone hybrid wind-solar systems in different WT prices and different PV module prices

Table 5.3 LCOE and economic feasibility of the stand-alone WT-Battery systems in different WT prices

% of current WT price	WT prices (£/W)	LCOE (£/kWh)	NPV (k£)	IRR	Payback (years)	Profit index
25%	0.62	0.3780	-1.06E+05	0.0542	>25	-0.1425
50%	1.24	0.5356	-6.09E+05	0.0018	>25	-0.5064
75%	1.86	0.6612	-1.07E+06	-0.0331	>25	-0.7000
100%	2.47	0.7460	-1.57E+06	-0.0899	>25	-0.8565
125%	3.09	0.8141	-1.80E+06	-0.1078	>25	-0.8983
150%	3.71	0.8716	-2.22E+06	-0.1136	>25	-0.9126

Table 5.4 LCOE and economic feasibility of stand-alone WT-PV-Battery systems in different WT prices

% of current WT price	WT prices (£/W)	LCOE (£/kWh)	NPV (k£)	IRR	Payback (years)	Profit index
25%	0.62	0.2899	1.88E+05	0.1103	12.51	0.3487
50%	1.24	0.3323	7.31E+04	0.0855	19.58	0.1174
75%	1.86	0.3442	4.04E+04	0.0792	21.75	0.0618
100%	2.47	0.3633	-2.37E+03	0.0716	>25	-0.0036
125%	3.09	0.3707	-2.95E+04	0.0669	>25	-0.0424
150%	3.71	0.3802	-5.54E+04	0.0628	>25	-0.0769

Table 5.5 LCOE and economic feasibility of the stand-alone PV-Battery systems in different PV module prices

% of current PV module price	PV module prices (£/W)	LCOE (£/kWh)	NPV (k£)	IRR	Payback (years)	Profit index
25%	0.74	0.2412	3.21E+05	0.1721	7.08	0.9066
50%	1.47	0.2835	2.08E+05	0.1238	10.23	0.4540
75%	2.21	0.3259	9.33E+04	0.0916	18.24	0.1671
100%	2.95	0.3693	-9.63E+03	0.0701	>25	-0.0153
125%	3.68	0.4035	-1.04E+05	0.0539	>25	-0.1447
150%	4.42	0.4377	-1.97E+05	0.0404	>25	-0.2490

Table 5.6 LCOE and economic feasibility of stand-alone WT-PV-Battery systems in different PV module prices

% of current PV module price	PV module prices (£/W)	LCOE (£/kWh)	NPV (k£)	IRR	Payback (years)	Profit index
25%	0.74	0.2438	2.99E+05	0.1484	8.63	0.7085
50%	1.47	0.2847	2.04E+05	0.1195	10.88	0.4226
75%	2.21	0.3253	9.77E+04	0.0916	18.07	0.1691
100%	2.95	0.3633	-2.37E+03	0.0716	>25	-0.0036
125%	3.68	0.3967	-9.44E+04	0.0567	>25	-0.1256
150%	4.42	0.4337	-1.91E+05	0.0437	>25	-0.2282

5.4.2 Case study II: Economic feasibility of stand-alone hybrid systems using LWSTs and HWSTs

The aims of this case study are to evaluate and compare the optimization between the low and current WT technologies by economic analysis and to investigate the feasibility of stand-alone WT-Battery system installation in low wind speed areas.

5.4.2.1 Load descriptions

Load profile from IEEE Reliability Test System [207] was applied as in the previous case study. However, the system load peak is assumed to be 1 MW for evaluating economic feasibility of stand-alone hybrid systems using a 1.5 MW WT and this load profile is shown in Appendix E. The average daily load energy is 14.74 MWh/day and the total annual load energy is 5.38 GWh/year.

5.4.2.2 Configurations of system components

This section does not only demonstrate comparisons between stand-alone WT-Battery systems using low and current WT technologies but these stand-alone WT-Battery systems are also compared with stand-alone PV-Battery systems in technical and economic terms. Specifications and costs of WTs and system components are described in detail in Appendix A and B, respectively. The configurations of major system components used in this study can be briefly described as follows:

1. Wind turbines: The 1.5 MW upwind 3-bladed turbines, used for analysing the proposed cost models in Chapter 4, are selected to be the case study. These WTs have five different rotor diameters, namely 121 m, 102 m, 78.4 m, 70 m and 59 m. At the design state, their rated wind speeds are 8 m/s, 9 m/s, 10.7 m/s, 11.54 m/s and 13 m/s, respectively. They have cut-in and cut-out wind speeds of 3 m/s and 25 m/s, respectively. The tower height is 84 m. The output power curves and distribution probability of wind speeds at 84 m hub heights are illustrated in Figure 4.3. Their costs are referred from Chapter 4. The lifetime is assumed as 25 years in this study.

2. Photovoltaic modules: The technical characteristics and costs of a PV module and an inverter used in this case study are assumed to be the same as case study I.

3. Batteries: This study uses the sealed lead-acid 1100 Ah battery, having the nominal voltage of 2 V. Specifications and prices are taken from [214]. The assumption is the same as in case study I. Bi-directional converter and charger costs are referred from [211] and [212].

5.4.2.3 Results and discussions

WT costs of stand-alone WT-Battery systems of different rated wind speeds were calculated by using the cost models, proposed in Chapter 4. These systems set three battery groups and the two minimum SOC levels of 50% and 25%. The example of calculation is described in Section E.2.2 in Appendix E. The optimal number of WTs and batteries were found and the relationship between LPSP and LCOE of these systems, illustrated in Figure 5.16. It seems that the lower the rated wind speeds, the cheaper the LCOE could be. However, the graph in Figure 5.17 shows that when the rotor diameters increase up to 121 m diameter or the rated wind speed of 8 m/s, LCOE tends to be more expensive. Large WTs, having rated wind speed of lower than or equal to 11.54 m/s at the design stage, will provide cheaper LCOE than stand-alone PV-Battery systems, using three battery groups and the two minimum SOC levels of 50% and 25%, as shown in Figure 5.16.

This case study also assumes the electricity price of 36 pence/kWh. The capacities of WT systems in this case study are more than 50 kW and so the adder rate of 7.14 pence/kWh was used in evaluating economic feasibility. The results are shown in Appendix E. The profitability graph shows that stand-alone systems using large LWSTs developed and installed in this low wind speed area will not be financially worthwhile, presented in Figure 5.18. Nonetheless, if the government can subsidise an adder rate of 16.33 pence/kWh, similar to the adder rate of a PV system that was used before the new renewable energy policy stated in 2010, then, using large LWSTs, having rated wind speeds of lower than or equal to 11.54 m/s, will be a worthwhile investment.

Furthermore, the profitability graph shows clearly that large LWSTs can possibly be more cost-effective than HWSTs, if their development can be achieved. However, in this case, large LWSTs, having a rated wind speed of 9 m/s, will give the most

profitable investment. The profits of large LWSTs, having rated wind speeds of lower than 9 m/s, tend to decrease.

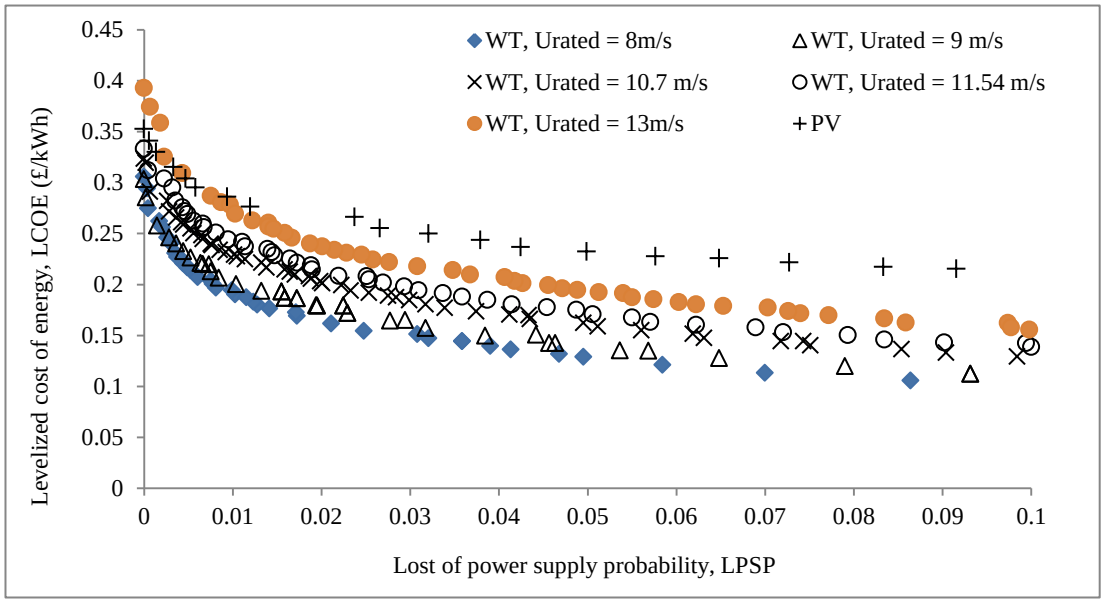

Figure 5.16 LPSP and LCOE of stand-alone systems using large WTs or PV modules

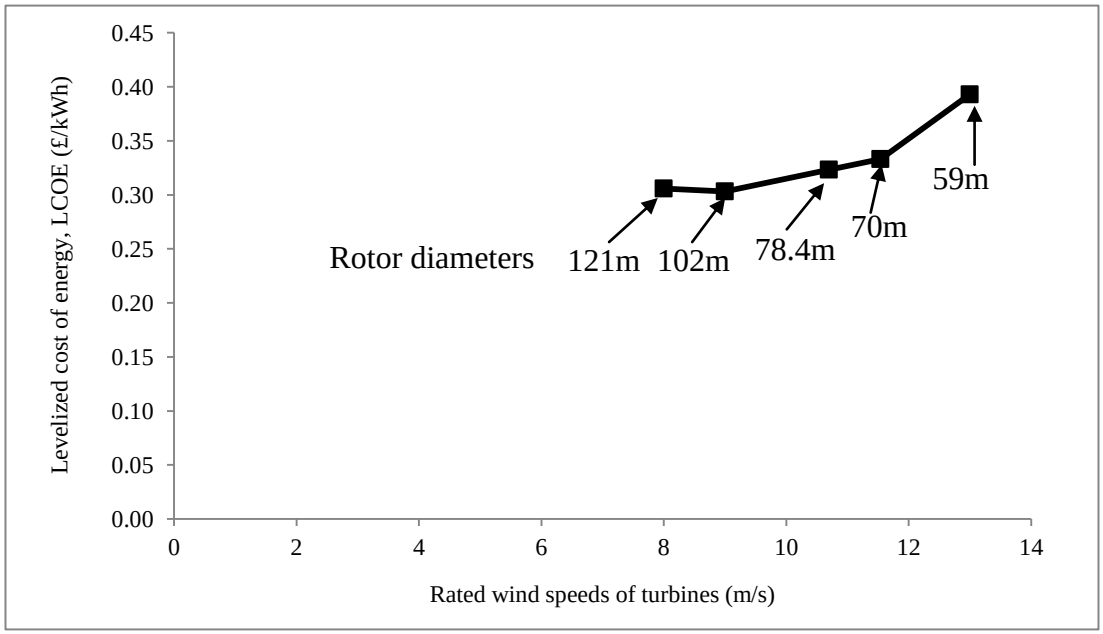

Figure 5.17 LCOE of stand-alone systems using large WTs having different rated wind speeds

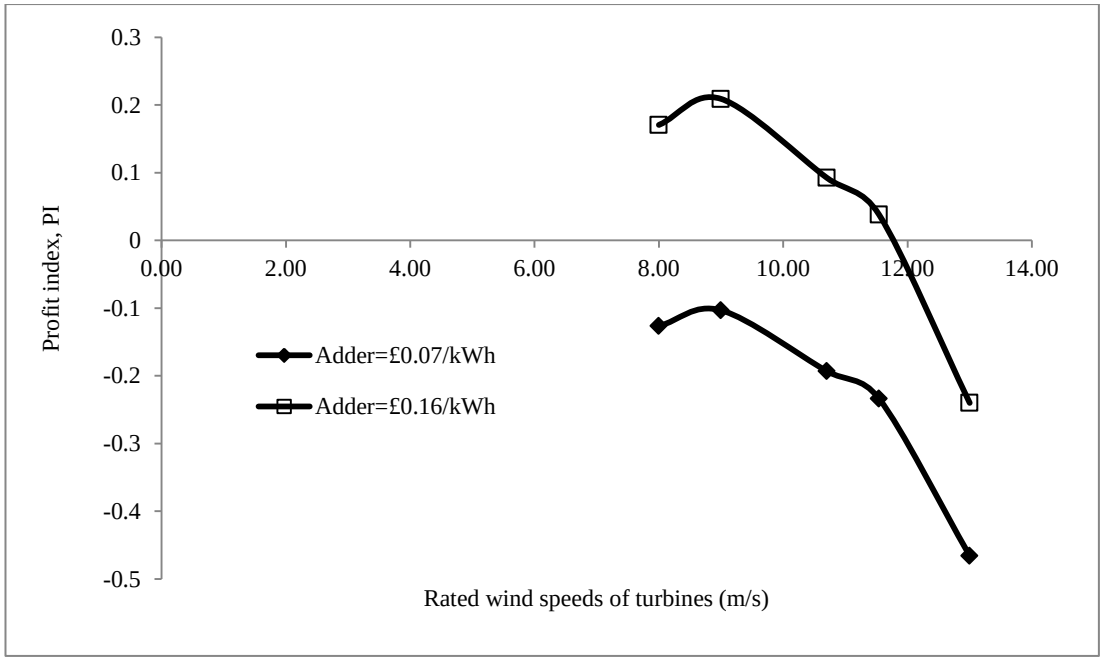

Figure 5.18 Profit indexes of stand-alone systems using large WTs having different rated wind speeds

5.5 Summary

This chapter presents the implementation of a multi-objective tool for the analysis of stand-alone hybrid wind-solar system installations. It applies the SPEA2 described in Chapter 3, the models of system components presented in Chapter 2 and the Sum-component cost model proposed in Chapter 4. The objectives are to examine two crucial issues, namely the improvement on the system reliability by using battery management compared with diesel generator support and the economic feasibility of LWST and HWST applications in stand-alone systems. Consequently, the main operation process of stand-alone hybrid wind-solar systems was proposed and modified to three algorithms, namely the operation processes of stand-alone hybrid systems using battery management, diesel generator support or WTs at different rated wind speeds.

The first issue, improvement on the system reliability by using battery management and DSG support, is examined in both technical and economic terms. For battery management, it is found that the DBSC method can improve the reliability of stand-

alone wind-solar systems and reduce the LCOE of the systems. Moreover, the lower the minimum SOC, the cheaper the LCOE could be but battery lifetime will decrease. Therefore, setting the minimum SOC into two levels, such as 50% and 25%, is proposed and demonstrated. The results show that the optimal capacity of the system can be decreased while LCOE and wasted electricity energy will be reduced and the system reliability will increase.

In this area, the stand-alone systems using PV modules can provide cheaper LCOE and more worthwhile financial installation than the systems using small WTs. Furthermore, the stand-alone systems having PV modules using battery management will have cheaper LCOE than the systems using DSG support. Nonetheless, the government may need to increase adder rates of both PV and WT systems or the price of system components might need to decrease to make the systems worthwhile for investment.

The second issue is the optimization between low and current WT technologies by economic analysis and the investigation of the feasibility of stand-alone WT-Battery system installation in low wind speed areas. Calculation of WT costs for different rated wind speeds uses the Sum-component cost model, proposed in Chapter 4. It appears that stand-alone systems using large LWSTs will have cheaper LCOE than the systems using PV modules. However, although using these large LWSTs in this area can reduce the LCOE, the systems need more subsidies from the government for worthwhile financial installation.

CHAPTER 6

6. OPTIMIZATION OF A HYBRID WIND-SOLAR SYSTEM USING BATTERIES FOR PEAK DEMAND IN A REMOTE AREA POWER SYSTEM

6.1 Introduction

This chapter proposes the optimization for a hybrid wind-solar system using batteries for peak demand in a remote area power system. A remote area power system in this chapter is a rural distribution system in remote areas. This hybrid system is called a grid-connected hybrid WT-PV-Battery system in this study. The voltage drop and rise problems are focused and solved by using the hybrid systems and switched capacitor banks. Simple methods to estimate the possible maximum power generation and the minimum size of switched capacitor banks at the end feeder are proposed. Furthermore, installation of this hybrid system in different locations is demonstrated.

This study applies the models of system components and the SPEA2, as presented in Chapter 2 and 3, respectively. It utilizes the Sum-component cost model, as proposed in Chapter 4, for estimating the ICC of WTs and evaluating the economic feasibility of the hybrid systems using LWSTs and HWSTs. Moreover, the process of the battery management, as proposed in Chapter 5, is applied for designing the optimal sizing of the hybrid WT-PV system using batteries for peak demand.

This chapter is structured as follows: Firstly, the definition and problems of a remote area power system are overviewed. Secondly, the concepts and technologies of voltage regulation and reactive supply are briefly described and, in more detail, for shunt capacitive compensation. Next, the application of SPEA2 and the AC

Optimization of Power Flow (AC OPF) for the optimization of a hybrid WT-PV system using batteries for peak demand in a remote area power system is explained. The model to calculate the possible maximum power generation is presented to designate the optimal boundaries of the decision search to provide a good search performance. The detailed procedures and computations of operation of the hybrid system are described. In addition, the design methods of switched capacitor size are proposed. Finally, case studies to inspect the issues above are demonstrated and discussed. This study sets the power system following the characteristics of a rural distribution system of the PEA in Thailand. The case studies use the same area as Chapter 5, namely Lam Takhong Dam, Nakhon Ratchasima province in Thailand. This location is an example for assessing the potential of technical system installation and for evaluating economic feasibility of the hybrid wind-solar system using batteries at peak demand in a remote area power system in Thailand.

6.2 Remote area power systems

This chapter studies remote area power systems, which are rural distribution systems in remote areas. Basically, distribution system designs have two main types, namely radial and meshed systems [216]. A typical radial system is shown in Figure 6.1(a). It is the simplest construction and it has the cheapest investment cost. Therefore, it is normally used for distribution systems in remote areas, although it has the lowest reliability. Remote area power systems have a long feeder and so the effect of line resistance (R) on voltage drop is high because its magnitude is commonly much more than the system reactive component (X). Remote area power systems generally have a X/R ratio of lower than 1, while urban power systems are usually higher than 1 [119]. The current flow (I) in the system can be defined in a function of the load complex apparent power (S_L) and the load voltage (V_2) as following:

$$I = \frac{S_L^*}{V_2^*} = \frac{P_L - jQ_L}{V_2^*} \tag{6.1}$$

where P_L is the load active power and Q_L is the load reactive power. The voltage drop on the feeder is calculated by:

$$|V_1 - V_2| = |I(R + jX)| = \left|\frac{(RP_L + XQ_L) - j(XP_L - RQ_L)}{V_2}\right| \quad (6.2)$$

The resistive voltage drop, *IR*, is in phase with load voltage and has a more significant effect on the load voltage than the reactive voltage drop, *IX*, illustrated in Figure 6.1(b). Consequently, the voltage angle (δ) between V_1 and V_2 is small and the voltage drop can be approximated by [217]:

$$\Delta V = |V_1 - V_2| \approx \frac{RP_L + XQ_L}{V_2} \quad (6.3)$$

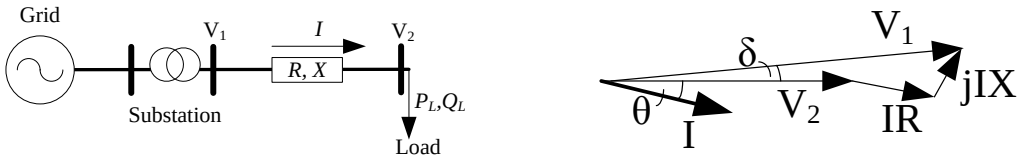

(a) (b)

Figure 6.1 A remote area power system: (a) one line diagram of a radial system and (b) phasor diagram

Remote area power systems will be weaker if load demand continues increasing due to many new users, especially at peak demand, as discussed in Chapter 1. Appropriate planning and designing distributed generation systems, which are renewable energy systems, such as WT and PV systems, are important. It has been found that an energy storage system is required for improving the performance of weak remote area power systems, as described in Chapter 2. This chapter proposes the algorithm of the optimization for a hybrid wind-solar system, using batteries for peak demand in a remote area power system by applying SPEA2, which will be explained in the next sections. Furthermore, the preliminary design of the suitable size and number of steps and stages of shunt capacitor banks, to regulate voltage levels, is presented.

6.3 Voltage regulation and reactive supply

WT and PV systems can cause many power system problems when they are connected to weak power systems, as discussed in Chapter 2. Voltage rise is a power quality problem that must be considered in power systems. On the other hand, voltage drop is a crucial issue of weak power systems, as discussed in Section 6.2. This section describes approaches for voltage regulation and reactive power supply.

6.3.1 Voltage regulation and reactive supply technologies

The common method is the use of transformer voltage taps or reactive power compensation. An On-Load Tap-Changer (OLTC) transformer is a transformer that can automatically control taps. It is mostly used in High Voltage/Medium Voltage (HV/MV) substation transformers [119]. Reactive power compensation devices are available as capacitive and/or inductive that can generate and absorb reactive power. Dynamic reactive power compensation devices, such as synchronous condensers, Static VAR Compensators (SVC) and Static Compensators (STATCOM) are good choices because they can rapidly respond to generate or absorb the reactive power. However, they are expensive capital costs of 30-35 $/kVAr for a synchronous condenser, 45-50 $/kVAr for SVC and 50-55 $/kVAr for STATCOM, mentioned in 2009 from [218] and 2011 from [219]. Therefore, they are normally applied in HV/MV substations.

Series and shunt capacitive compensations are methods of combating the problems of voltage drop and power loss in AC power systems [220], [221]. Series capacitive compensation operates directly on the series reactance of the line, to decrease the transfer reactance between supply point and the load. This approach reduces the voltage drop and increases power transfer. It usually is applied in Extra High Voltage (EHV) lines. It is limited to use in distribution systems because of the complicated protection needed for the capacitors and this makes investment costly. On the other hand, shunt capacitive compensation is mostly used in a receiving station, a distribution substation or along a feeder. It can give maximum benefit when employed right across the load. Presently, shunt capacitive compensation is usually

achieved through fixed and switched capacitor banks. Fixed capacitor banks are primarily used to generate low constant reactive power demand as a base [220]. Switched capacitor banks are used to match the compensation to the reactive demand changing throughout the day. The conventional capacitor banks have cheap capital costs of 8-10 $/kVAr (or 5.02-6.275 £/kVAr) and very low O&M costs, referred in 2009 from [218] and 2011 from [219]. Nonetheless, the use of switched capacitor banks must consider the sudden changes of switching capacitor steps making voltage transients on power systems. Capacitor banks can also increase existing harmonics under certain circumstances, even though they do not produce harmonics [222]. Harmonics occur from nonlinear loads, such as battery chargers, programmable controllers, computers and electronic ballasts. Harmonic resonant conditions must be avoided when using capacitor banks in the systems having nonlinear loads. Furthermore, adding capacitor banks in steps can cause over-voltage in remote area power systems, especially where renewable distributed generations is connected.

Another method that can help to supply reactive power in distribution systems, such as WT and PV systems, is the use of power converters of PV systems and some types of WTs [223], [224]. The reactive capability of converters is limited by internal voltage, temperature and current constraints. Furthermore, power system stability and reactive power availability are considered for possible reactive power supply. The availability of the maximum reactive power supply is dependent on the actual active power transfer and converter size. Converter cost is based on current rating and so if more reactive power is required, the converter size will be larger and the investment costs will be higher. Additional costs per kVAr of reactive power supply increase when the convertor size added is higher. For example, a 1 MW WT with converter cost of 150-300 €/MVA has the additional investment costs of 8-15 €/kVAr (or 6.832-12.81 £/kVAr) and annual cost of 0.6-1.2 €/kVAr for 0.1 MVAr, and the additional investment costs of 15-30 €/kVAr and annual cost of 1.2-2.4 €/kVAr for 0.2 MVAr, referred from [223] in 2008. The additional investment costs of converters are possibly more expensive than the capital costs of capacitor banks.

Although, distribution generations are used to supply the reactive power, they are not allowed to control voltage for distribution systems, as stated in IEEE 1547.

Generally, voltage in distribution systems is controlled at the distribution substation levels. Distribution generations commonly run with a fixed power factor or reactive power output with regard to the local system. A typical power factor requirement would be unity at the Point of Interconnection (POI). Consequently, WTs with a converter interface are frequently designed for operation from 90% to 110% of rated terminal voltage. For PV systems, inverters have a similar technological design to full-converter WTs and are designed to operate at unity power factor. In addition, for WTs without a converter, reactive power cannot be controlled. For example, induction-based WTs without converters absorb as much reactive power as other induction machines, in steady-state circumstances. Switched capacitor banks with many capacitor stages are typically utilized at the WT terminals to correct the power factor to unity. [224]

6.3.2 Shunt capacitive compensation

In this chapter the shunt multiple capacitor banks are selected for regulating voltage at load bus because they are possibly have the minimum investment cost and operating cost. If a shunt capacitor generating reactive power (Q_c) is installed in the load bus, illustrated in Figure 6.2(a), then the voltage drop on the feeder at time *t* can be decreased as following [217]:

$$\Delta V(t) \approx \frac{RP_L(t)+X(Q_L(t)-Q_c(t))}{V_2(t)} \tag{6.4}$$

where $P_L(t)$ is the load active power, $Q_L(t)$ is the load reactive power, $V_2(t)$ is the load voltage and $Q_c(t)$ is the shunt capacitor generating reactive power, at time *t*.

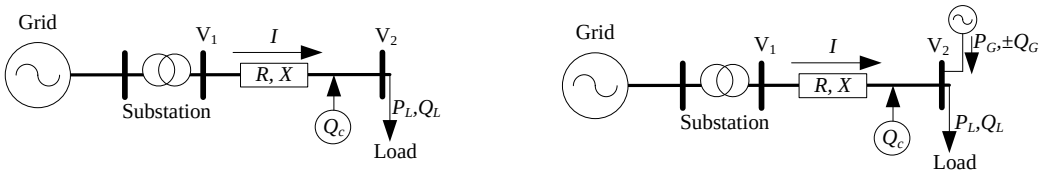

Figure 6.2 One line diagrams for a radial system having: (a) shunt compensation and (b) shunt compensation and distribution generation

6.3.2.1 Control methods [225]

Load demand changes during the day, so switched capacitor banks should be used for controlling voltage levels within limits and they can reduce more power losses. Switched capacitor banks can be automatically controlled by various parameters, namely time, temperature, voltage, current, reactive power and power factor. A time switch is the switching control, based on the time of day. This is the cheapest control but also the most vulnerable method, due to load fluctuation caused by such as weather and holidays. Voltage control is the most suitable way of using a capacitor to support and regulate voltage.

The power factor control is used for switching capacitor banks in this chapter. A power factor controller needs a current sensor (Current Transformer, CT) and a voltage sensor (Potential Transformer, PT). The current sensor should be installed on the source side (substation) of the capacitor bank to detect the power factor change when the bank switches. Moreover, the correct wiring for CT and PT is required to give accurate polarities to keep suitable phase angle relationship between current and voltage.

6.3.2.2 Switched capacitor step and stage considerations

The size and the number of switched capacitor steps and stages are significant in the design of voltage regulation and power factor correction equipment. They affect the smoothness of control and the cost of equipment and installation. Increasing the number of switched steps and stages and decreasing the size of each step and stage can reduce inrush current but the investment cost is more expensive. Two typical methods are (1) same-size switching step and (2) different-size switching steps. The same-size switching step method gives easier equipment design, installation, operation and maintenance than the different-size switching step method. Nonetheless, the different-size switching step method can decrease the number of stages possibly leading to the reduction of costs. [226], [227]

In this chapter, the switched capacitor bank is demonstrated under normal operating conditions. Issues of transients and harmonics are not described. In addition, the

technology of switched capacitor control is not discussed and not within the scope of this thesis.

6.3.3 Distributed generation impact on voltage

If a distributed generation system is located in the remote area power systems, as shown in Figure 6.2(b), the voltage drop on the feeder at time *t* can be reduced and the overvoltage may occur, as the following equation:

$$\Delta V(t) \approx \frac{R(P_L(t)-P_G(t))+X(Q_L(t)-(\pm Q_G(t))-Q_c(t))}{V_2(t)} \tag{6.5}$$

where $P_G(t)$ and $Q_G(t)$ are the active and reactive power of a distributed generation system at time *t*, respectively. Therefore, the control of capacitive compensation is more complicated for the distributed generation systems, such as WT and PV systems.

In addition, when the capacitor suitably compensates the reactive power demand and the distributed generation system deliveries the active power, the feeder current at time *t* ($I(t)$) will be reduced, leading to the reduction of power losses in the feeder at time *t* ($P_{loss}(t)$), as shown in the following equations:

$$I(t) = \frac{\sqrt{(P_L(t)-P_G(t))^2+(Q_L(t)-(\pm Q_G(t))-Q_c(t))^2}}{V_2(t)} \tag{6.6}$$

$$P_{loss}(t) = I^2(t)R \tag{6.7}$$

6.4 SPEA2 applied to the optimization for a hybrid wind-solar system using batteries for peak demand in a remote area power system

Improvement in remote area power systems with hybrid renewable energy systems was discussed in Chapter 2. The principle of SPEA2 was described Chapter 3 and the application of SPEA2 for optimization of stand-alone hybrid wind-solar systems

was illustrated in Chapter 5. This section explains the development of SPEA2 for finding the optimum sizing of a hybrid WT-PV system using batteries at peak demand for the weak power system, by modifying the models and method of the optimization for the stand-alone hybrid wind-solar systems, proposed in Chapter 5.

The optimization process of a hybrid WT-PV system using batteries at peak demand for a weak power system is presented in Figure 6.3. Decision variables of the system are the optimal number of WTs, PV modules and batteries. The decision search spaces and the initial populations use the same concepts and the settings as the optimization of stand-alone hybrid systems, as in Chapter 5. Specifications, estimated costs and lifetimes of the hybrid system components are described in Appendix A and B. The objectives of this optimization problem can be calculated by using the models of a stand-alone hybrid wind-solar system, explained in Chapter 2 and discussed in Chapter 5. However, the LPSP in this study is defined as Loss of probability of Battery power supply at Peak demand and called LBP. The objectives are the minimization of the LBP, LCOE and WOE, by considering the issues, namely, a generating capacity limit, power losses, voltage regulation and system reliability as well as economic feasibility. SPEA2 parameters, namely a crossover probability, a mutation probability, a population size and an archive size are defined by using the same concepts, as discussed in Chapter 5.

Both the populations and the objectives will be sent to the SPEA2 process to calculate new populations. This calculation process is repeated until the maximum generation numbers are reached. Finally, the optimal sizing of WT, PV and battery system will be selected from the minimum LBP, LCOE and WOE. The systems without loss of power supply are the first choices. Thereafter, the AC OPF is calculated by using MATPOWER version 4.05b. The MATPOWER is developed on MATLAB m-files by Zimmerman *et al.,* for calculating power flow and optimal power flow problems [228]. MATPOWER code is a good open source, suitable for researchers and educators to use and modify for studying power system problems. It is assumed that hybrid WT-PV-Battery systems generate free cost power in terms of operating and being emission free, in AC OPF computation. Their power output is treated as a negative load. The operation procedure of the hybrid system and the

preliminary sizing design of shunt capacitor banks for a load bus will be described in detail in next section.

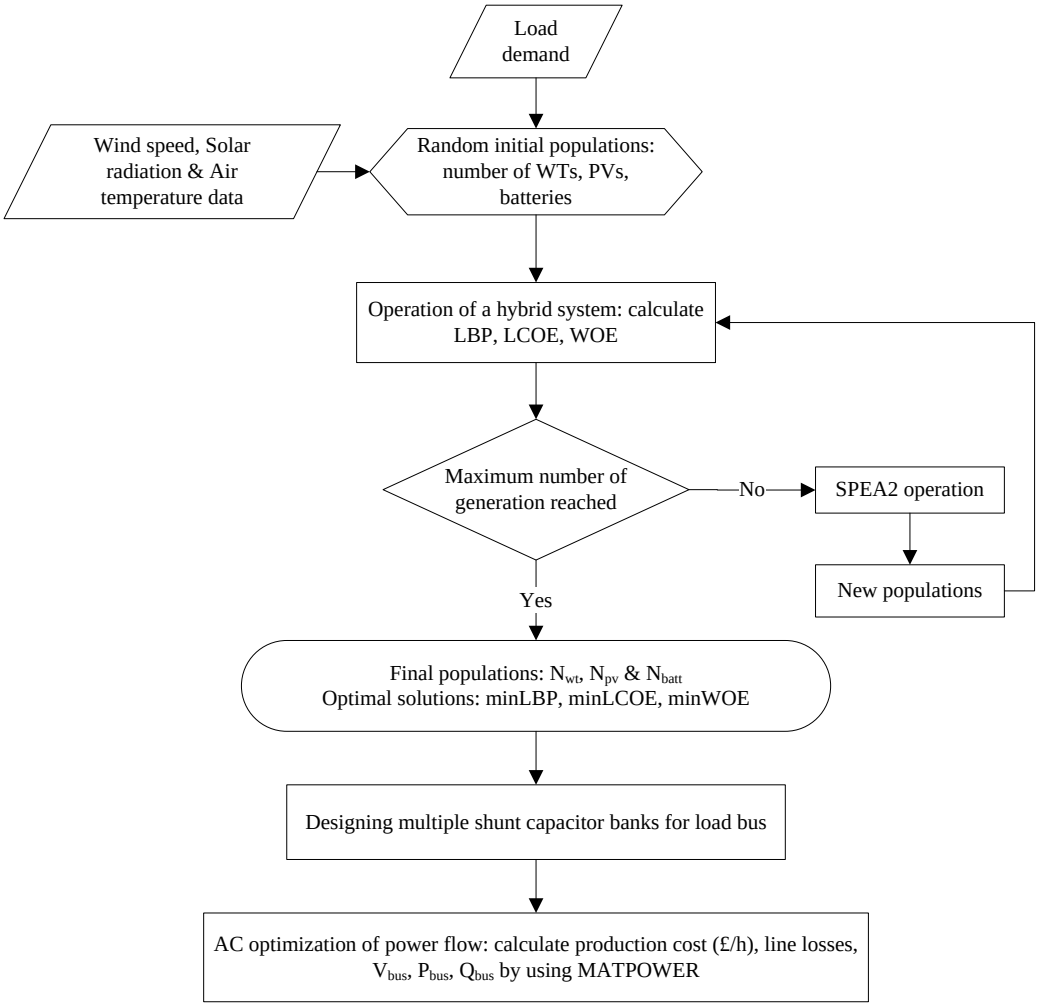

Figure 6.3 The optimization process of a hybrid wind-solar system using batteries for peak demand in a power system

6.5 Operation of a hybrid wind-solar system using batteries for peak demand in a remote area power system

The impact of connection of distributed generations, that are renewable energy systems, such as WT and PV systems, to remote area power systems, has been investigated by several researchers, as discussed in Chapter 2. This chapter intends to

improve the remote area power system by designing the optimum sizing of a hybrid wind-solar system using batteries and considering technical and economic terms. Three technical issues are examined, namely system reliability, power losses and voltage regulation. The analysis proposed is based on the evaluation of the impact of a hybrid wind-solar system using batteries at peak demand in power systems over the long-term. Consequently, the power system considers only steady-state impacts of distributed generation integration. The power system transient analysis of the impacts of distributed generations is beyond the scope of this work.

The power flow analysis is significant in determining the best operation of existing systems under the steady-state and normal operation of an interconnected power system. Power balance in the nodes and in the system is required, i.e. all active and reactive power injections are equal to active and reactive power withdrawn from a node as follows [229]:

$$\sum(P_{gi} + Q_{gi}) + \sum(P_{li} + Q_{li}) + \sum(P_{di} + Q_{di}) = 0 \qquad (6.8)$$

where P_i and Q_i are the active and reactive power injected to bus i, respectively. g, l and d represent generators, lines and loads connected to node i, respectively. This equation is a power balance equation and the set of power balance equations for all nodes is called the power flow equations. The power flow equations provide the magnitude and phase angle of the voltage at each bus and the active and reactive power flowing in each line.

Power flow analysis is used for planning and designing the future expansion of power systems. In this chapter it is applied for studying the integration of a hybrid wind-solar system, using batteries for improving the power system reliability during peak demand period. It has two formulas, namely DC and AC power flow equations, used in power flow and optimal power flow computations [230]. DC power flow equations are linear and calculate only active power flows by assuming power lines to be purely inductive and voltage nodes to be 1.0 per unit. They are fast to calculate and easy to apply in linear optimization formulas. Nonetheless, they are approximate methods that can provide thermal loading of lines but they cannot determine active line losses and voltage rise impacts. Conversely, AC power flow equations are

nonlinear and have to be solved by an iterative procedure and convergence occasionally cannot be achieved. However, an AC power flow formula can be used to analyse line losses, voltage rise and drop impacts and thermal loading of lines.

6.5.1 Constraints of distributed generation design

Constraints are important for designing an appropriate distributed generation system. The power flow equation is used as a key equality constraint that must be satisfied when considering the system in normal operation. Additionally, in practice, the network and equipment have technical limits. The technical limits are used to define the inequality constraints of the optimization. The technical constraints generally considered are a minimum and maximum node voltage variation, maximum thermal loading of equipment and maximum fault levels, including maximum sizes of distributed energy resource equipment [37]. Moreover, technical connection is restricted by constraints in operation conditions, such as fixed power factor.

This study focuses on a remote area power system that has weak radial networks, especially at peak demand. Fault levels are normally considered in large penetration of distributed generations in high and medium-voltage urban networks that are usually mesh systems [231]. Therefore, maximum fault levels are not calculated and not included as a constraint considered in this study. Voltage, thermal loading and distributed generation capacity limits are the main constraining factors in low-voltage and radial networks, especially in weak networks such as remote networks [231], [232]. The remote area power system has a low *X/R* ratio and power flows are mostly active, as mentioned in Section 6.2, and so the voltage drop can be managed by controlling the active power.

As a result, this chapter investigates the possibility of controlling the active power of hybrid WT-PV-Battery systems, to maintain the power system within operational constraints, namely voltage and thermal. It is assumed that combined heat and power units can be re-dispatched to supply network operation. Their production is heat load and so it must be enough for heat loads and cannot be curtailed. The technology and

implementation of the distributed generation control scheme is not discussed and not in the scope of this thesis.

The limits of distributed generation capacity on the feeder will be considered using two criteria, set to be the initial population and the decision search spaces. Firstly, the total capacity of the hybrid system designed in a feeder must be less than or equal to the allowable maximum distributed generation capacity limit. Secondly, the possible maximum total hybrid system generation should be investigated and used as a constraint, since a distributed generation system can cause a voltage rise problem in a power system. For simplicity, this study assumes that the grid-connected hybrid WT-PV-Battery system can correct a power factor to unity at the POI. This means that only active power is delivered from the hybrid system.

The possible maximum power generation can be calculated from the worst case. The worst case can occur during light load demand and both WT and PV systems simultaneously generating maximum power output. Two probable methods to find the possible maximum power generation are described as follows:

Method I: The possible maximum power generation can be calculated by using the AC OPF computation. The power generation is increased until voltage at the end bus is over the allowable maximum voltage. The possible maximum power generation may be higher than the line capacity limit. Therefore, the line capacity limit will be increased by higher than the actual limit because this constraint affects the computation and solution.

Method II: This thesis proposes a simplified method to determine the possible maximum generation by setting the worst case and applying the concept of distributed generation impact on voltage in Section 6.3.3. The worst case of the steady-state voltage rise is defined, namely expected maximum generation of the hybrid system and minimum demand. Therefore, from Figure 6.2(b), the possible maximum power generation ($P_{G,max}$) can be estimated by:

$$P_{G,max} = P_{L,min} - \left(\frac{\Delta V_{max} V_{2,max} - X Q_{L,min}}{R}\right) \quad (6.9)$$

where $V_{2,max}$ is the permitted maximum voltage at the end bus and ΔV_{max} is the permitted maximum voltage difference on the feeder (V). The permitted voltage variations are set, based on voltage levels and system standards. For example, the Electricity Safety, Quality and Continuity Regulations allow voltage variations of ±10% and ±6% of nominal voltage for system between 50 V and 1,000 V and for systems between 1,000 V and 132 kV, respectively [233]. For power systems in Thailand, the PEA permits voltage variations of ±5% of nominal voltage for system between 22 kV and 115 kV [234]. Consequently, the $V_{2,max}$ will be 23.1 kV and the ΔV_{max} will be 2.2 kV for the 22 kV system of the PEA.

In conclusion, technical limits of the power system in this study are expressed next:

$$V_{i,min} \leq V_i \leq V_{i,max} \tag{6.10a}$$

$$HBS_i \leq HBS_{i,max} \tag{6.10b}$$

$$S_k \leq S_{k,max} \tag{6.10c}$$

where V_i is the voltage at the i^{th} node, *HBS* is the total capacity of hybrid systems installed at that node and *S* is the apparent power flow at the k^{th} line (or equipment).

6.5.2 System operation processes

The proposed process is provided for finding the optimal sizing of WTs, PV modules and batteries of the hybrid system, designed for supplying a peak electricity demand period or for generating demand exceeding the line capacity limit. This hybrid system is also expected to reduce the production cost at peak demand in a remote area power system. For simplicity, this operation algorithm applies the concepts of the power balance as being the same as the operation process of a stand-alone hybrid system and the SPEA2 is used for seeking the optimal sizing of system components, as illustrated in Chapter 5. WT and PV systems provide power only when it is available. They are known as "must-take generators" or "must-run generators" [235], [236]. The algorithm of the hybrid system operation has six key steps as follows:

Input: P_s is the output power from WT and/or PV systems and $P_{L,p}$ is the load demand at peak demand periods.
Output: LBP is the loss of probability of battery power supply at peak demand, E_{use} is the annual useful energy production and E_w is the annual waste energy from renewable energy sources.

1. **Initialization:** Set the initial SOC to be 1.

2. **Battery processes:** Batteries will discharge when P_s is not enough to supply $P_{L,p}$. There are two sources for charging batteries: firstly, P_s that exceeds $P_{L,p}$ and secondly, power from other generator buses. Batteries are always fully charged to prepare power when they need to discharge. This system study sets three battery groups and the minimum and maximum SOC level of 50% and 100%, respectively.

3. **Exceeding load power:** Calculate the $P_{L,p}$ exceeding the power available by using Equation 2.12.

4. **System reliability:** Compute the LBP by using Equation 2.11, in the criteria of no diesel generator. This equation is applied because the battery discharging power deliveries to $P_{L,p}$ cannot help to supply load demand beyond 80% of peak demand at that time.

5. **Annual useful energy production:** Useful power is the P_s consumed by load of all buses and charged into batteries. Nonetheless, the P_s generating to other load buses must be less than the line capacity limit. E_{use} is calculated by summing the useful power in every hour for a whole year.

6. **Annual waste energy:** Waste power is P_s exceeding the load demand at the bus considered and battery charging power. E_w is estimated by summing the waste power in every hour for a whole year.

6.5.3 Design of switched capacitor size

This section proposes a procedure to find the size of switched capacitor banks for compensating capacitive power at the receiving end for the remote area power

system, connected with a distributed generation system, as illustrated in Figure 6.2(b). The overall algorithm for this design process, shown in Figure 6.4, has the following main steps:

1. Size of switched capacitor banks: The worst case is, when load is at its maximum power demand and yet, no active power generates from the hybrid system. The possible minimum size of switched capacitor banks can be determined from the expected minimum capacitive power compensation needed at the receiving end. Two approaches for finding this minimum capacitive power compensation are described as follows:

Method I: The expected minimum capacitive power compensation needed at the receiving end can be determined by using the AC OPF computation. The worst case is the maximum power demand. The capacitive power is treated as a negative reactive power load and is decreased until voltage at the end bus is lower than the allowable minimum voltage.

Method II: This thesis proposes a simplified approach to calculate the minimum capacitive power compensation needed at the receiving end, by applying the concepts of Section 6.3. The expected minimum capacitive power compensation can be estimated by:

$$Q_{c,min} = Q_{L,max} - \left(\frac{\Delta V_{max} V_{2,min} - R P_{L,max}}{X}\right) \tag{6.11}$$

where $V_{2,min}$ is the permitted minimum voltage at the end bus, for example, 22 kV minus 5% of the nominal voltage that is 20.9 kV.

2. The number and size of steps and stages: Divide the sizing of switched capacitor banks from the possible minimum reactive power, found in Step 1, into stages following an incremental format. The same-size switching step method is utilized, from the reasons as mentioned in Section 6.3.2.2. However, the cost is a significant factor also considered.

3. Power factor corrections: An algorithm for a process of reactive power compensation is designed under steady-state conditions. The aims are to evaluate the

overall operation of switched capacitor banks and to check that the size and the number of switched capacitor steps and stages designed are appropriate for the remote area power system, connected with a hybrid WT-PV-Battery system. Furthermore, voltage levels are checked hourly throughout the year to ensure they are within the permitted voltage variations. The AC OPF is computed by using the number and size of capacitor steps and stages at the load bus.

The concept of a static process is proposed in this section, by considering the effect of switched capacitor banks on the voltage and power factor in the remote area power system, with a resolution of one hour each time series for a whole year. A range of power factors are set as constraints. For example, power factors of load are required to correct within a range of 0.95 to 1 lagging. When load demand has the power factor at time *t* of lower than 0.95, the total amount of reactive power at time *t* that will be switched "ON" with each stage is based on the following condition:

$$\sum_{i=0}^{n} C_{sw,i}(t) \geq Q_L(t) - Q_{set}(t) \tag{6.12}$$

where $Q_L(t)$ is the reactive power at time *t* of load demand that has a power factor of lagging. $Q_{set}(t)$ is the limit of reactive power at time *t* at the load bus, defined as follows:

$$Q_{set}(t) = \sqrt{\left(\frac{P_L(t) - P_G(t)}{pf_{set}}\right)^2 - (P_L(t) - P_G(t))^2} \tag{6.13}$$

where $P_L(t)$ is the active power of load demand at time *t*, $P_G(t)$ is the active power output of a hybrid system at time *t* and pf_{set} is the minimum power factors set. However, if $P_G(t)$ is more than $P_L(t)$, all switched capacitor banks will be switched "OFF" ($\sum_{i=0}^{n} C_{sw,i}(t) = 0$).

4. Termination: Solution is achieved when the voltage levels of each bus are within the limits set. The power generation from power plants, the production cost, the power line losses and the CO_2 emissions are problems requiring solutions.

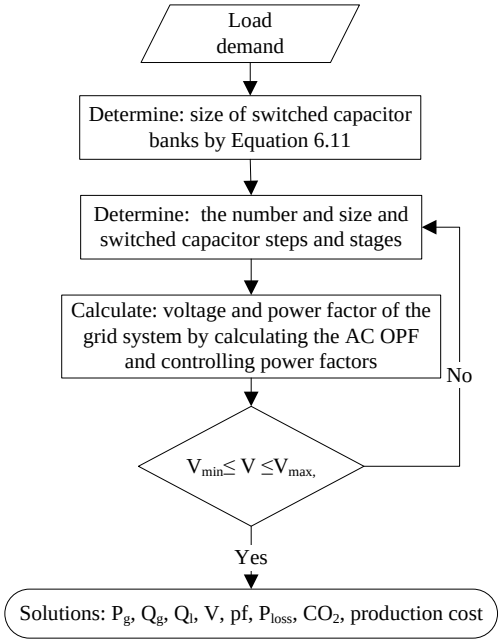

Figure 6.4 Design process of the number and size of switched capacitor steps and stages

6.6 Case studies

6.6.1 Site descriptions

The case studies used the distribution system characteristics in Thailand. A hybrid WT-PV-Battery system connected in a remote area power system, as illustrated in Figure 6.5, is used as a baseline and called “System A” in this chapter. The system data is described in Appendix D. The PEA of Thailand [234] sets the rules for applicants who want to connect distributed generations to PEA’s systems, by limitation of the total generating capacities of less than 8 MW for the 22-kV system. Additionally, a line capacity of 22 kV is limited at 8 MVA. The steady-state voltage of the 22 kV and 115 kV systems are be maintained within ±5% of the nominal voltage.

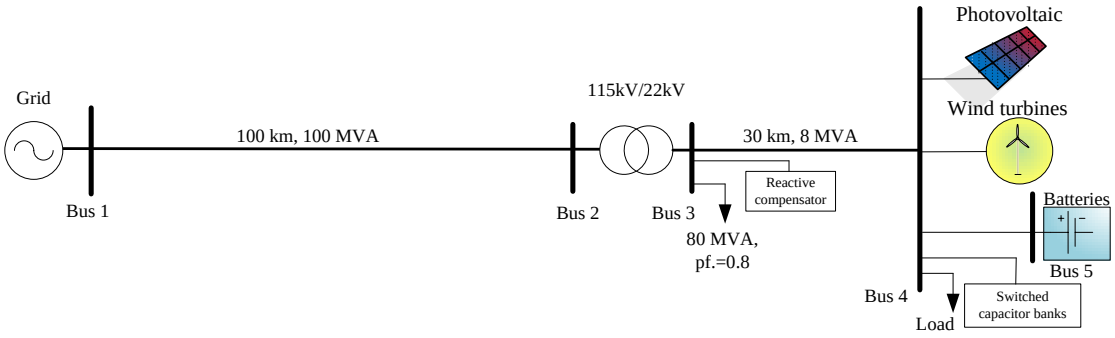

Figure 6.5 One line diagrams of a hybrid WT-PV-Battery system in a remote area power system

Hourly wind speed, hourly solar radiation and hourly temperature data at Lam Takhong Dam, Nakhon Ratchasima province in Thailand, collected in 2006 [53], [54], [206], are the same as used in Chapter 5. The interest rate and the inflation rate are 7.7% and 2.9%, respectively, mentioned from Bank of Thailand in October, 2011 [198].

6.6.2 Configurations of system components

This chapter considers three types of grid-connected wind-solar systems, namely WT-Battery systems, PV-Battery systems and WT-PV-Battery systems. The potentials of wind and solar energy technologies are compared in technical and economic terms. Furthermore, comparisons of WT-Battery systems and WT-PV-Battery systems between using low and current WT technologies are demonstrated with the 1.5 MW upwind 3-bladed turbines, used as an example in Chapter 4 and 5. The WT, having a rotor diameter of 70 m, is used as a baseline. This study uses the same specifications and costs of WTs, PV modules and batteries as Case study II in Chapter 5, as described in Section 5.4.2.2 and Appendix A and B. Initial capital costs of a bi-directional converter, system control and other components for grid-connected systems are also shown in Table B.3 in Appendix B. In addition, it is assumed that the grid generation system uses coal fuel, which generator data from IEEE 24-substation test systems is presented in Table D.2 in Appendix D.

6.6.3 Load descriptions

Grid extension in many remote areas becomes more difficult and expensive for investment, maintenance and operation because the areas are hard to access, while load demand in these areas is higher. Therefore, this study used load profile from IEEE Reliability Test System [207] to design the system reserved for future load demand. The seasonal load profile was defined from the system peaking season in Thailand, with the peak occurring in the 3rd week of April [208], established in Appendix E. The peak demand at bus 3 is supposed to be 80 MVA with the power factor of 0.8 (64 MW, 48 MVAr). The peak demand at bus 4 is assumed as 3.75 MVA with the power factor of 0.8 (3 MW, 2.25 MVAr). Batteries will supply load power of above 2.4 MW (80% of peak demand).

6.6.4 Results and discussions

All optimization problems in this study applied the SPEA2, operated with 150 populations, 70 archives and 100 generations. Mutation and crossover probabilities used 0.001 and 0.8 respectively. The simulation time is hourly throughout the year (8,760 hours). The evaluation time of each case, including the AC OPF computation, is approximately one hour.

6.6.4.1 Capacitive power compensation with switched capacitor banks

This study designs only the size of switched capacitor bank at the receiving end (bus 4). Due to the long feeder between bus 1 and 2, including heavy load assumed at low voltage side of the transformer (bus 3), bus 3 may be very sensitive while the worst case is happening. For simplicity in applying Method II in calculating the size of capacitor bank in Section 6.5.3, it is assumed that bus 3 is the start bus and voltage at bus 3 is equal to the permitted maximum voltage. Moreover, the allowable minimum voltage is assumed at bus 4. The voltage difference (ΔV) is assumed as 10% of the nominal voltage. Therefore, in the worst case the case study system requires the minimum capacitive power compensation of 1,307 kVAr at the receiving end, calculated by using Equation 6.11. This value is equal to the solution, estimated from

the AC OPF. This method assumes that automatic dynamic reactive compensations are located at bus 3 with the sizing range of ±100 MVAr.

For simplicity in dividing the sizing of switched capacitor banks and for avoiding the risk of the voltage drop, the 1,500 kVAr switched capacitor bank is used in this case study. There are 5 steps or possible switching outcomes with the step size of 300 kVAr. The switching sequence indicates the amount of kVAr that will be switched at each stage. It can be a 3-stage bank with 1:2:2 switching, described in Table 6.1, or a 5-stage bank with 1:1:1:1:1 switching. The higher the number of stages, the more expensive the capacity cost would be. This is because more components, such as switches, protection relays, capacitors, iron-core reactors for harmonic filter banks and fuses are needed [226]. Nonetheless, the impacts of inrush current, harmonic and switching frequency are beyond the scope of this study. Therefore, in all case studies, the multiple capacitor banks are switched by considering only an improving power factor of above 0.95, under normal operating conditions in hourly steps throughout the year, as described in Section 6.5.3. The minimum and maximum voltage results of each bus are shown in Table 6.2. It shows that the steady-state voltage of the system can be maintained within ±5% of the nominal voltage. The switched capacitor banks for MV systems that have the installation cost of 50 $/kVAr (31.38 £/kVAr) [227] and O&M cost of 1 $/kVAr (0.6275 £/kVAr) [237], were used for calculating LCOE of the hybrid systems. A lifetime is assumed as 10 years. Cost benefits of power factor correction are not described in this study.

Table 6.1 Possible switching outcomes of 3-stage capacitor banks

Step	Capacitive compensation (kVAr)	3-Stage		5-Stage	
		ON	OFF	ON	OFF
1	300	1	2,3	1	2,3,4,5
2	600	2	1,3	1,2	3,4,5
3	900	1,2	3	1,2,3	4,5
4	1,200	2,3	1	1,2,3,4	5
5	1,500	1,2,3	-	1,2,3,4,5	-

Table 6.2 The minimum and maximum voltage of the simulation system, using the switched capacitor banks at bus 4 but without a hybrid system

V_{bus1} (pu)		V_{bus3} (pu)		V_{bus4} (pu)	
Min	Max	Min	Max	Min	Max
1.05	1.05	1.0337	1.0461	0.950	1.05

6.6.4.2 Installation of distributed generation systems in different locations

In a general power system simulation, the distributed generation such as wind and solar systems will be placed on the load bus, as in System A, shown in Figure 6.5. However, practically, wind farms will make noise for residents, so most of the wind farms will be installed away from the residential areas. Additionally, the price of land in centre areas is higher than the areas located away from the centre. The large systems may have to be sited away from the residents. Consequently, the differences of the three simulation systems in this study are the distances between the distributed generation system and the load bus, illustrated in Figure 6.6. The system data are described in Appendix D.

System B: The distance at which the hybrid system is installed is 2 km from the load bus shown in Figure 6.6(a).

System C: The PV and battery system is set up at the load bus but the WTs are located 2 km from the load bus, presented in Figure 6.6(b).

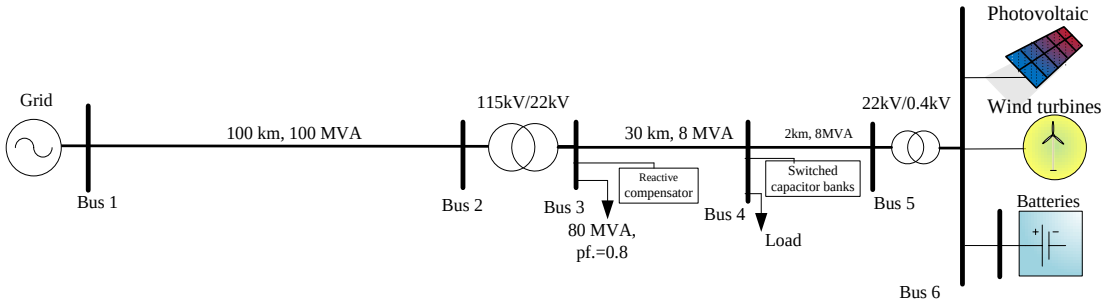

(a)

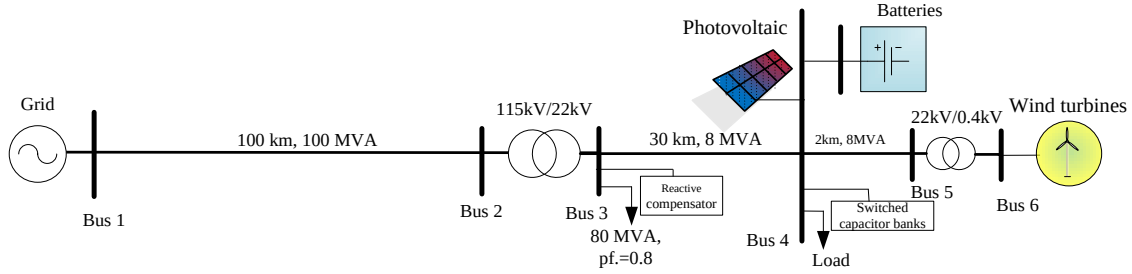

(b)

Figure 6.6 One line diagrams of: (a) System B and (b) System C

6.6.4.2.1 Maximum distributed generation capacity of the hybrid system

Renewable distributed generation systems, placed at the end bus of System B and C, will affect the voltage rise, while power systems have light load and high power generated from WT and/or PV systems. In these cases, to find the possible total maximum distributed generation, the worst case sets the allowable maximum voltage at the end bus (22 kV plus 5% of nominal voltage). For simplicity in applying Method II in Section 6.5.1, it is assumed that bus 3 is the start bus and voltage at bus 3 is equal to the permitted minimum voltage. In addition, the voltage difference (ΔV) is assumed as 10% of the nominal voltage.

From wind speed data, the probability of WTs having a rotor diameter of 70 m that can produce the maximum power output is about 3.07%. For a PV system, the probability of power output that is more than or equal to power module rating is around 0.91%. The probability of two power sources generating simultaneously the maximum power output is approximately 0.028%. However, from this data there is no circumstance where both WT and PV systems generating simultaneously will lead to the maximum power output occurring. Load power that is lower than or equal to 40% of peak demand has the probability of approximately 3.61%. The possible maximum power generations of System A, B and C are 6.28 MW, 5.58 MW and 5.58 MW, respectively. The probability of the voltage being more than the allowable maximum voltage is approximately 0.001%. The chances of this happening are very low. If this event occurs in practice, several choices can solve the voltage rise problem by, such as the disconnection of WT or PV system from a power system or the use of dump loads. In this study, the voltage drop and rise issues are investigated by calculating the AC OPF hourly throughout the year.

6.6.4.2.2Optimal solutions of three systems

Optimization results of three system simulations are illustrated in Figure 6.7. System A gives lower LCOE of the hybrid system than System B and C because WT, PV and battery systems are located at the load bus and so there are no power losses in the line of 2 km. Moreover, this case study found that WTs can provide less

expensive LCOE than PV systems and System A can have a greater number of WTs than System B and C. If many hybrid systems are designed with System A but in practice located on the power system in a structure of System B or C, the voltage rise may occur more frequently in the remote area power system than might be expected. Furthermore, the LCOE predicted will show more distinct differences and then the financial income will be less than expected.

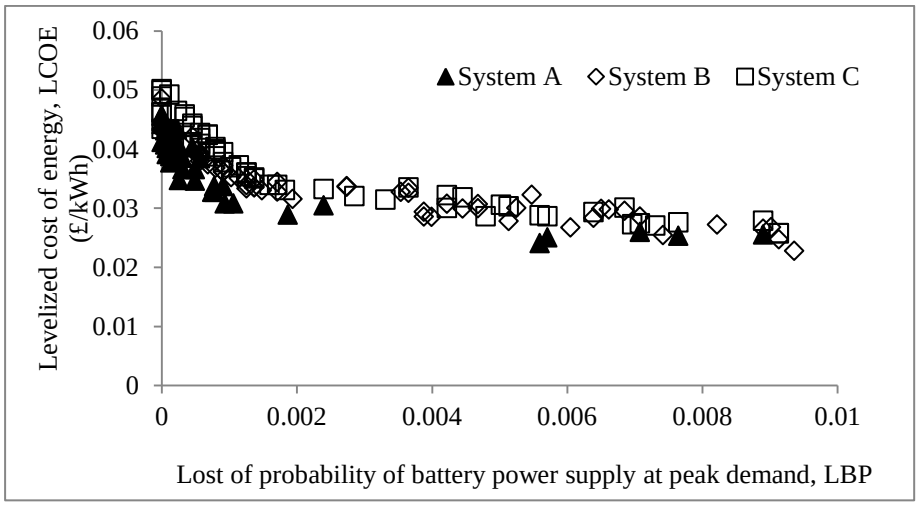

Figure 6.7 LBP and LCOE of three systems

Table 6.3 Optimal solutions of hybrid systems placed in System A, B and C

Particular	Simulation system		
	A	B	C
Number of WTs	4	3	3
Number of PV modules	1,200	2,400	2,400
Number of battery cells	5,700	5,700	5,700
WT capacity (MW)	6	4.5	4.5
PV capacity (MW)	0.12	0.24	0.24
Battery capacity (kAh)	125.40	125.40	125.40
Annual WT generating energy (MWh/year)	12,259	9,194	9,194
Annual PV generating energy (MWh/year)	208.66	417.32	417.32
Annual battery discharging energy (MWh/year)	155.44	157.20	157.00
Levelized Cost of Energy, LCOE (pence/kWh)	4.16	4.42	4.42

The optimal hybrid system, designed from the optimization process, can support every peak load that the power demand is higher than 80% of the peak demand (above 2.4 MW in this case study). Optimal solutions of hybrid systems, placed in

System A, B and C, are described in Table 6.3. The number of PV modules is increased for System B and C because the number of WTs needs to decrease due to the maximum power generation limitation, leading to more expensive LCOE. Comparisons of LCOE between WT and PV systems will be demonstrated in next section.

The energy profile on 11th April of System A, illustrated in Figure 6.8, is a good illustration of the supporting load of the hybrid system in the peak demand. The output energy of the hybrid system can match the peak load and the battery charging energy. The battery can have adequate energy to discharge to meet the peak load when the output energy of WT and PV systems is low but not enough to serve the peak load. Moreover, batteries will charge when the load demand is lower than 80% of peak demand. This means that the battery charging power required is higher than the allowable minimum battery charging power. When the output energy of WT and PV systems is in surplus after supplying load and charging batteries, the surplus energy will be delivered to support other load buses. In this figure, WT energy from 9 pm can supply load in bus 4 and also in battery charging. Additionally, WT energy remaining can be delivered to load in bus 3, which energy is shown as negative energy.

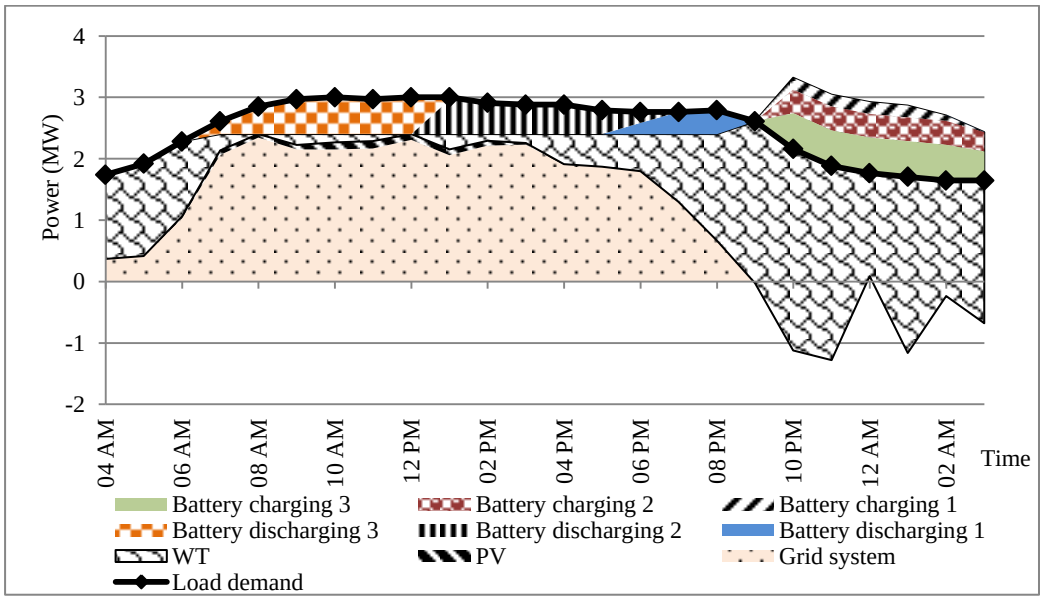

Figure 6.8 System A: Energy of WT, PV generating and battery discharging and charging on 11th April

6.6.4.2.3 AC OPF solutions

The optimal solutions of the hybrid system placed in System A, B and C can help the grid generation supply load in calculating the AC OPF, shown in Table 6.4. The larger size of the hybrid WT-PV system, able to be located in System A, can reduce electricity production, CO_2 emission and production cost of the coal power plant and line loss compared with System B and C. Moreover, Table 6.5 shows that the hybrid systems that have the proper sizing can improve voltage levels of the power system in each bus, when compared with the minimum and maximum voltage of the power system without the hybrid system (Table 6.2).

Table 6.4 Planning attributes of the three simulation systems with the hybrid system and the remote power system without a hybrid system

Particular	**Simulation system**			**No hybrid system**
	A	**B**	**C**	
Maximum thermal loading from bus 1 to bus 2 (%)	66.48%	69.97%	69.95%	70.19%
Maximum thermal loading from bus 3 to bus 4 (%)	61.19%	42.35%	42.30%	37.50%
Total energy generated from power system (MWh/year)	357,930	360,980	360,970	371,070
Annual CO_2 emission from coal power (ton CO_2/year)	349,150	352,125	352,106	361,968
Total energy line losses of a system (MWh/year)	9,985	10,022	10,019	10,679
Maximum electricity production cost (£/h)	1,297	1,309	1,308	1,312
Minimum electricity production cost (£/h)	474.86	495.85	494.84	543.38
Total electricity production cost (k£/year)	7,287	7,337	7,336	7,497

As the difference between System B and C mentioned, this difference does not greatly affect the power flow and voltage level of the power system in this case study because the PV and battery systems have very small capacity when compared with the WT system capacity. On the other hand, System A's results have distinct differences to the results of System B and C because System A has a larger size of hybrid system and does not have a 2 km line from the hybrid system to the load. This may increase noticeably if more hybrid systems are installed and longer distances between the residents and WT and PV systems are required. Therefore, the line design, namely type, size of conductors and structures is important in the increase or decrease of line characteristic impedance, affecting the design of proper hybrid

system size and the reduction of electricity production, CO_2 emission and production cost of the coal power plant and line loss.

Table 6.5 The minimum and maximum voltage of three system simulations

Simulation system	V_{bus1} (pu)		V_{bus3} (pu)		V_{bus4} (pu)		V_{bus5} (pu)	
	Min	**Max**	**Min**	**Max**	**Min**	**Max**	**Min**	**Max**
A	0.9650	1.05	0.9506	1.0392	0.9536	1.05	-	-
B	0.9856	1.05	0.9704	1.0417	0.9502	1.0439	0.9502	1.05
C	0.9856	1.05	0.9704	1.0417	0.9502	1.0439	0.9502	1.05

6.6.4.3 Economic feasibility of hybrid WT-PV systems using batteries at peak demand in a remote area power system

This study assumes the electricity price at which the PEA purchases electricity from a Very Small Power Producer (VSPP) with Time of Use (TOU) rate in Thailand in 2011 [238], described in Appendix D. The VSPP is "a private power producer that has installed capacity lower than 10 MW with PEA or MEA as a contracting partner" [55]. This study uses the new adder rates of 7.14 pence/kWh for a WT system of greater than 50 kW and of 13.27 pence/kWh for a PV system, which adder rates the Thai government will subsidise for 10 years, as announced in 2010 [55].

6.6.4.3.1 Changes in prices of WTs, PV modules and batteries

Hybrid WT-PV systems using batteries at peak demand in a remote area power system have cheaper LCOE than stand-alone hybrid WT-PV-Battery systems, if all WT energy can be used. As a result, in this design, all WT energy can be exhausted by load, leading to cheaper LCOE and higher PI of the system having WTs, illustrated in Figure 6.9 and 6.10. The Initial Capital Cost (ICC) is based on different prices of WTs and PV modules. Dash lines of 1 and 2 indicate the ICC of WTs in the WindPACT project [196] and the ICC of the current PV module prices [16], respectively. Results of economic feasibility are described in details in Appendix E. The results show that the optimal power capacity of grid-connected hybrid WT-PV-Battery systems consists of the WT power capacity being greater than the PV power capacity. Changes in the price of WTs will influence the LCOE of hybrid WT-PV systems, rather than changes in the price of PV modules. Furthermore, the WT ICC

of lower than 1.50 £/W, which is the investment costs in the U.S. [30], can create profit for the hybrid system having WTs. For the WT ICC of the WindPACT project, grid-connected hybrid WT-PV-Battery systems and WT-Battery systems will have payback periods of around 2 years and 2.5 years, respectively.

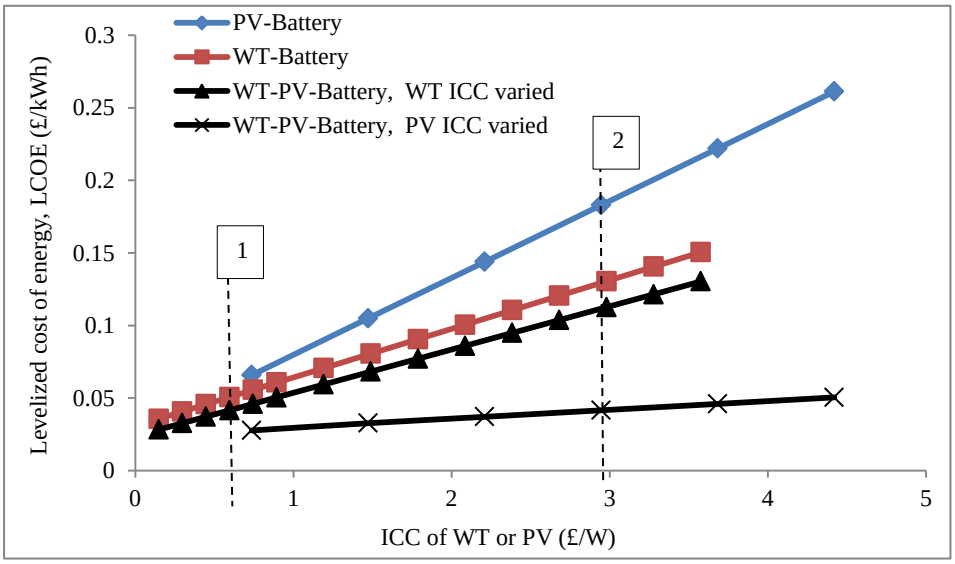

Figure 6.9 LCOE of hybrid systems using batteries for peak demand in remote area power systems at different ICC of WTs and PV modules

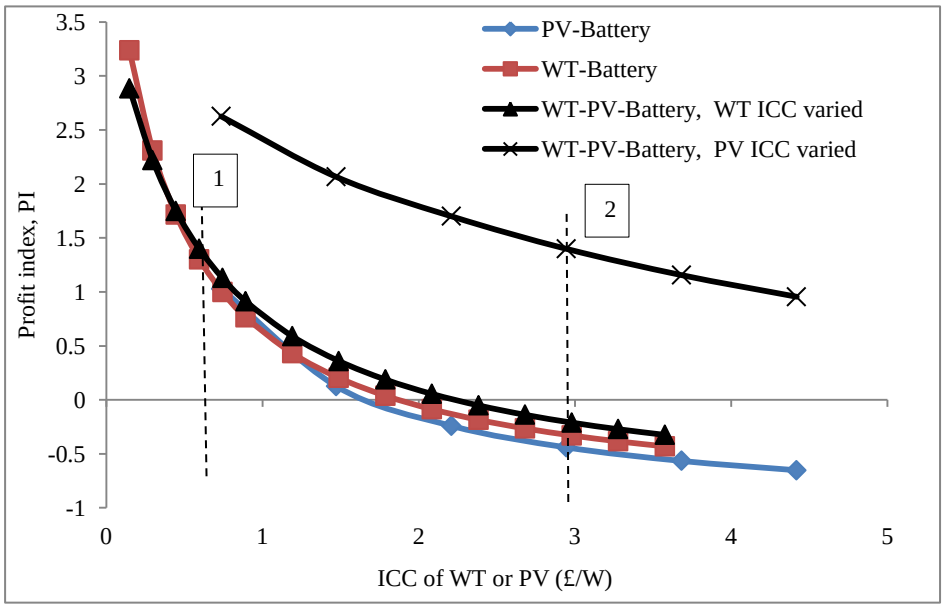

Figure 6.10 PI of hybrid systems using batteries for peak demand in remote area power systems at different ICC of WTs and PV modules

On the other hand, grid-connected PV-Battery systems will not be worthwhile for investment; although, the ICC of battery will decrease to 0.11 £/Ah (25% of ICC at the battery price referred from [214]) because the ICC of 2.95 £/W at the current PV module price is expensive. The ICC of PV systems should reduce to 1.50 £/W (or about 50% of ICC at the current PV module price) so that PV systems will provide some profits in investment with a payback of about 20 years. Decrease of battery price will show more impact on the reduction of LCOE and the increase of PI for grid-connected hybrid systems having WTs, presented in Figure 6.11.

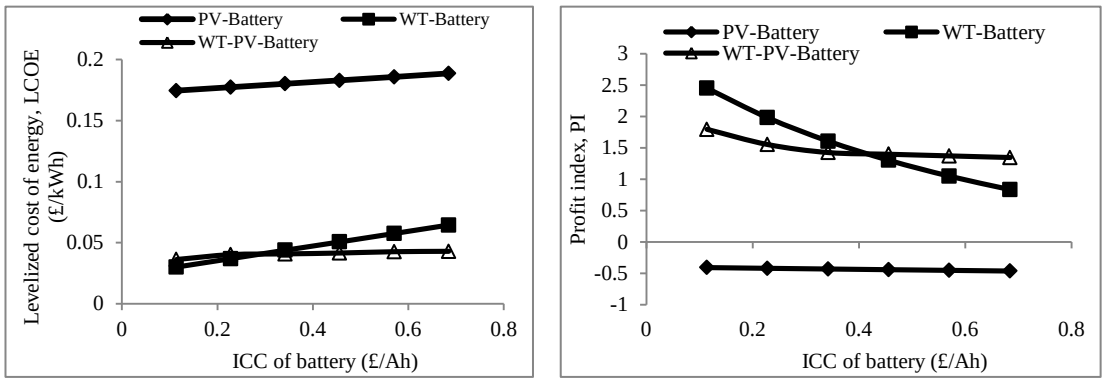

(a) (b)

Figure 6.11 (a) LCOE and (b) PI of hybrid systems using batteries for peak demand in remote area power systems at different battery ICC

6.6.4.3.2 Grid-connected LWST and HWST systems using batteries at peak demand

WT costs of WT systems, using batteries at peak demand in a remote area power system, of different rated wind speeds, were estimated by using the Sum-component cost model, proposed in Chapter 4. The optimal number of WTs and batteries were found and shown in the relationship between LBP and LCOE of these systems, as in Figure 6.12. It shows that the lower the rated wind speeds, the cheaper the LCOE could be. This is the same as in the case of stand-alone systems in Chapter 5, as shown by the comparison of their results in Figure 6.13. Grid-connected WT-Battery

systems will have less expensive LCOE than stand-alone WT-Battery systems. Grid-connected WT-Battery systems will be more financially worthwhile; even though the government will subsidise the adder rate of 7.14 pence/kWh for 10 years (25 years assumed in the stand-alone systems in Chapter 5).

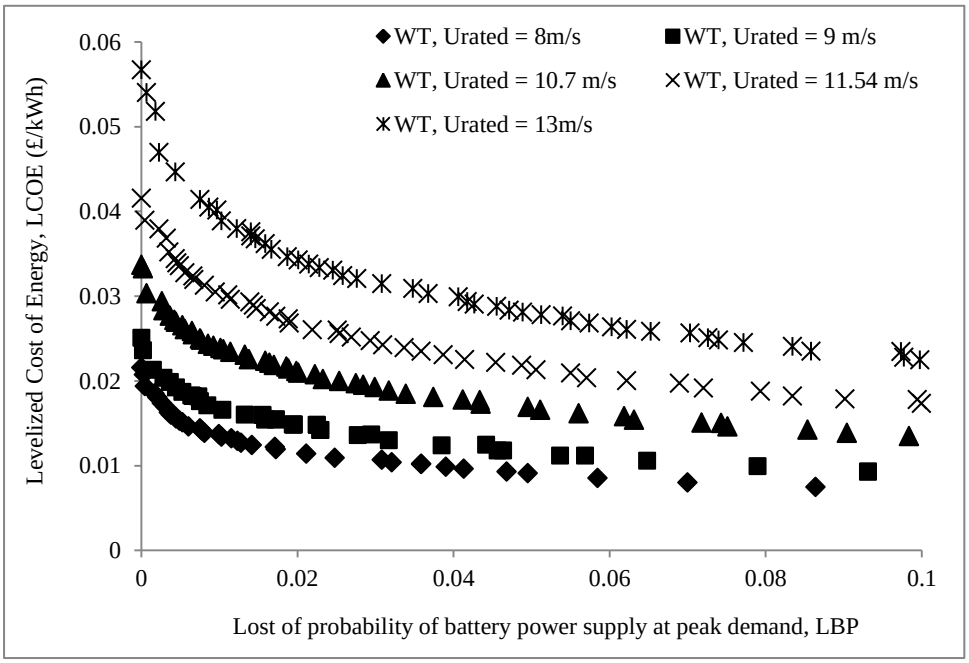

Figure 6.12 LBP and LCOE of grid-connected WT systems using batteries at peak demand, by WTs having different rated wind speeds

In Figure 6.13(b), the profitability graph shows that LWSTs can probably be more cost-effective than HWSTs, if LWSTs can be successfully developed. Additionally, it may take less than 2 years to obtain the profits from grid-connected WT-Battery systems using LWSTs, having rated wind speeds of below 10 m/s.

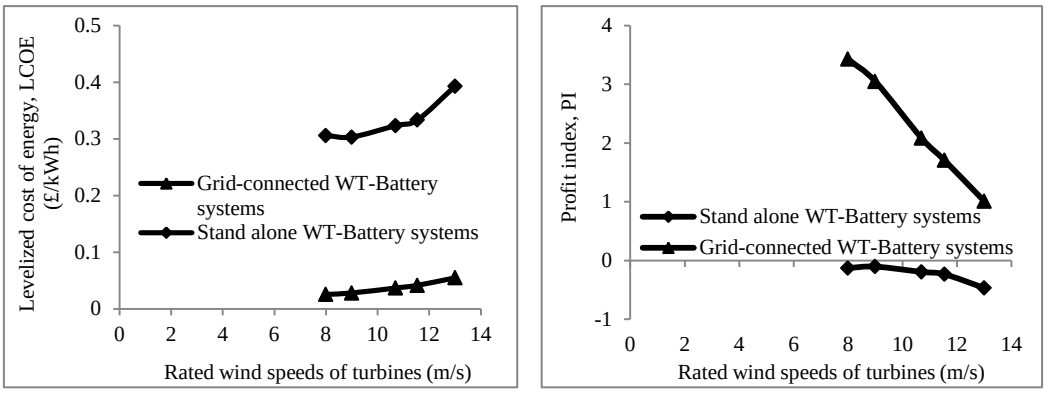

(a) (b)

Figure 6.13 (a) LCOE and (b) PI of grid-connected WT systems using batteries at peak demand, by WTs having different rated wind speeds

6.7 Summary

This chapter presents the implementation tool for the analysis of installations of a hybrid wind-solar system using batteries at peak demand in a remote area power system. It applies the models of system components and the SPEA2 described in Chapter 2 and 3, respectively. The Sum-component cost model proposed in Chapter 4 is utilized for estimating the ICC of WTs and evaluating the economic feasibility of the hybrid systems using LWSTs and HWSTs. In addition, the battery management process proposed in Chapter 5 is applied.

The objective of design for the optimal sizing of hybrid WT-PV system using batteries for peak demand in a remote area power system is to avoid the voltage rise and drop problems. These problems will occur for a long line at the end feeder during light and heavy load demand. Therefore, the concepts of voltage regulation and reactive supply are studied and applied for developing the models to calculate the possible maximum power generation and the minimum size of switched capacitor banks at the end feeder of a long line. Additionally, the installation of this hybrid system in different locations is demonstrated.

In the issue of the shunt capacitive compensation, the designed size of switched capacitor banks can improve the voltage levels within the allowable voltage limitation, demonstrated by calculating the AC OPF. The proposed concepts and model of the possible maximum power generation calculation can be applied for finding the maximum power generation of a hybrid system, connected with a remote area power system in different installation configurations. It is found that the nearer the location of renewable distributed generation systems or the lower the line resistance, the more the possible maximum generation could be. This will lead to a greater decrease in electricity production, CO_2 emission and production cost of the coal power plant and line loss of the power system. Consequently, the distance and the power wiring design, namely type, size of conductors and structures should be considered to increase the potential of the renewable energy resources because they affect the amount of line resistance.

The optimal solutions found from the SPEA2 application can improve the voltage levels of the power system and reduce electricity production, CO_2 emission and production cost of the coal power plant and line loss of the power system. The grid-connected hybrid system consisting of WTs can be worthwhile for investment. In addition, if LWSTs can be successfully developed, grid-connected WT systems using large LWSTs can be more profitable than using large HWSTs.

CHAPTER 7

7. CONCLUSIONS

7.1 Conclusions and contributions

Electricity is important in improving the quality of life for people in rural and remote areas in developing countries. There are two main options for Rural Electrification (RE), namely grid extension and stand-alone systems. From distinct benefits and limitations, as summarized in Section 1.1, this thesis aims to improve RE by focusing on renewable energy technology, namely WT and PV systems.

There are several crucial issues of WT and PV applications, namely installation, cost and performance, based on terrain and climate. For PV systems, although, the current PV module prices have decreased to about 2 US$/W (from 5.5 US$/W in the past decade) with increasing module efficiency of 12-19% [16], the Initial Capital Cost (ICC) of a PV system still has installation costs around two times more expensive per watt, than large WTs. However, most of WTs in current technology have rated wind speeds higher than 11 m/s [23] while most areas in the world have measured mean wind speeds of about 6.64 m/s and 3.28 m/s at 10 m in height above the ocean and land, respectively [181]. As a result, WTs, having rated wind speeds of below 11 m/s, have been developed for low wind speed areas and are called Low Wind Speed Turbines (LWSTs). LWST development can be done by increasing rotor diameter and maintaining generator capacity. This leads to changes in the ICC of WTs that will be different from the ICC of WTs in current technology.

7.1.1 The specification and development of the approaches for improving RE

There are two proposed approaches, namely the design of the appropriate centralized stand-alone hybrid WT-PV-Battery systems (mini-grid hybrid WT-PV-Battery

systems) and the improvement in reliability of remote area power systems, with a hybrid WT-PV system using batteries at peak demand. The design of these hybrid systems was based on the system reliability and LCOE. Furthermore, the economic feasibility of the systems using LWSTs and HWSTs was evaluated.

Novel aspects of this study are that the optimization processes of stand-alone and grid-connected hybrid WT-PV systems provide simple, fast and flexible methods for analysis and design, including the approaches for improving the system reliability and estimating the ICC of WTs having different rated wind speeds. Three main developments are proposed to deal with the issues above as follows:

1. **Cost models (Chapter 4):** In order to estimate the cost of wind-generated electricity of LWSTs, this thesis proposes two simple cost models, namely the Sum-component cost model and the Total-cost model. The Total-cost model can be calculated from a power of rotor diameter ratio or called a cost factor in this thesis. The Sum-component cost model is modified from the Total-cost model, by including the cost fraction for more detailed computation.

2. **Stand-alone hybrid WT-PV systems (Chapter 5):** The aims of this study are to investigate two important issues, namely the improvement on the system reliability by using battery management, compared with diesel generator support and the economic feasibility of stand-alone systems using WT (LWST and HWST) and/or PV systems. The optimal sizing of the main system components was calculated by using the Strength Pareto Evolutionary Algorithm 2 (SPEA2). This study also used the Decentralized Battery Storage Control (DBSC) method, which is division of batteries into groups for battery management. The Sum-component cost model, proposed in Chapter 4, was utilized for analyzing LWST and HWST applications. Furthermore, there are newly developed models and processes as follows:

2.1 The models to calculate the possible maximum number of WTs by using the worst month condition were developed. The maximum number of WTs is applied for setting the optimal boundaries of the decision search to perform good search efficiency.

2.2 The implementation of a multi-objective tool was developed for installation analysis of four stand-alone hybrid system types, namely WT-Battery systems, PV-Battery systems, WT-PV-Battery systems and WT-PV-Battery systems with diesel generators. Three algorithms of the operation processes of stand-alone hybrid wind-solar systems using battery management, diesel generator support or WTs at different rated wind speeds were proposed.

2.3 The simple processes of the battery management application in the optimization of hybrid WT-PV systems were proposed. It was found that this method can improve the reliability of stand-alone WT-PV systems and reduce the LCOE of the systems.

3. Hybrid WT-PV systems using batteries at peak demand in a remote area power system (Chapter 6): The objectives of this study are to improve existing grid systems in remote areas because of an increasing number of new users, and to evaluate the economic feasibility of hybrid WT-PV systems, using batteries at peak demand, in a rural distribution system in a remote area. The optimal sizing of the main system components was calculated by applying the SPEA2 and examined by using the AC OPF computation. The Sum-component cost model, proposed in Chapter 4, was used to evaluate the economic feasibility of LWST and HWST applications. The processes of the battery management proposed in Chapter 5 were modified and utilized for supplying load at peak demand.

For the system reliability, the design to find the optimal sizing of these hybrid systems considered and avoided the voltage rise and drop problems. These problems frequently happen in a long line at the end feeder during light and heavy load demand. Therefore, the simple processes to estimate the possible maximum power generation and the minimum size of switched capacitor banks at the end feeder of a long line were developed. The maximum power generation is determined by using the case of light load demand and both WT and PV systems, able to generate the maximum power output. It is utilized for setting the decision search to perform good search efficiency. The minimum size of switched capacitor banks is calculated in the case of maximum load demand. The switched capacitor banks are used for solving the voltage drop. Additionally, the algorithms of the hybrid system operation were

developed for investigating the effects of hybrid system installations in different locations in a remote power system.

7.1.2 The case studies

Lam Takhong Dam, Nakhon Ratchasima province in Thailand, was selected as a case study because it seemingly has the potential for both wind and solar energy. This location can be representative in assessing the potential of WT-PV applications in Thailand and other locations having similar climate, such as equatorial areas. This location can be classified as a low wind speed area because it has low annual mean wind speed of approximately 5.71 m/s at 45 m of hub height [53]. The case studies were considered for future load demand by using the load profile from the IEEE Reliability Test System and the seasonal load profile from the system peaking season in Thailand.

Even though the results from the case studies are related to the specific WT, PV and battery technologies and location analysed, some general conclusions can be identified. Furthermore, this is useful for planning in the development and improvement of WT-PV applications in the RE of Thailand or other locations having similar climate.

1. **Cost models (Chapter 4):** Upwind 2-bladed and upwind 3-bladed turbines of the WindPACT project were used as case studies. The Sum-component cost model could provide a better result than the Total-cost model, when comparing its results with the results of the NREL's cost model, due to a more detailed breakdown of costs. The results show that the larger the rotor diameters, the higher the ICC could be.

2. **Stand-alone hybrid WT-PV systems (Chapter 5):** There are two case studies. Firstly, improvement on the stand-alone hybrid WT-PV system reliability by using battery management or diesel generator support can be summarized as follows:

- The DBSC approach can improve the reliability of stand-alone WT-PV systems and decrease the LCOE of the systems.
- The lower the minimum SOC, the cheaper the LCOE could be but battery lifetime will reduce.

- If the minimum SOC can be set at two levels, such as 50% and 25%, the system can have the lower optimal capacity, while the system will have cheaper LCOE and lower wasted electricity energy and higher system reliability than the minimum SOC of 50%. In addition, this may prolong the battery lifetime, if compared with setting the minimum SOC of 25%.
- The stand-alone systems are suitable for PV applications because the systems using PV modules have cheaper LCOE and are therefore more profitable than using small WTs.
- The stand-alone system having PV modules using battery management can provide cheaper LCOE than the systems using DSG support.
- Although, this location has the potential for solar energy, the government should increase adder rates of PV systems or the price of system components may need to fall, to make the systems a worthwhile financial venture.

The second case study evaluated economic feasibility of stand-alone hybrid systems using large LWSTs and HWSTs. The conclusions of this study are as follows:

- Stand-alone system using large LWSTs will have cheaper LCOE than the systems using PV modules.
- Using these large LWSTs in this area can decrease the LCOE. However, the systems need more subsidies from the government for financially worthwhile installation.

3. **Hybrid WT-PV systems using batteries at peak demand in a remote area power system (Chapter 6):** The characteristics of a rural distribution system of the PEA in Thailand were used as case studies. The conclusions of this case study are:
- The designed size of switched capacitor banks can maintain the voltage levels within the permitted voltage limitation, demonstrated by calculating the AC OPF.
- The nearer the location of renewable distributed generation systems or the lower the line resistance, the more the possible maximum generation could be. This will be beneficial in greatly reducing electricity production, CO_2 emissions and production cost of the coal power plant and line loss of the power system.
- The distance and the power wiring design, namely type, size of conductors and structures, should be considered to increase the potential of the renewable energy

resources, because they affect the amount of line resistance and the possible maximum generation.

- The optimal sizing of the hybrid system can improve the voltage levels of the power system and reduce electricity production, CO_2 emissions and production cost of the coal power plant and line loss of the power system.
- The grid-connected hybrid system consisting of large WTs can be financially worthwhile installations.
- If LWST development can be achieved, grid-connected WT systems using large LWSTs can be more worthwhile for investment than using large HWSTs.

7.2 Suggestions for future work

Future work has been identified for the investigations, improvements and extensions of the implementation tools, developed for designing and analysing the stand-alone and grid-connected WT-PV-Battery systems in improving the RE in this thesis, as follows:

1. **Cost models:** The Sum-component cost model and the Total-cost model should be further investigated by comparing their results with the actual installation costs or the costs calculated by WT design programs, in various rotor diameters.

2. **Stand-alone hybrid WT-PV systems:** The proposed optimization algorithm of the stand-alone hybrid WT-PV-Battery systems with/without diesel generators can be improve and/or modified, while its concepts are still useful, as follows:

- Batteries can discharge power as much as load demands but the SOC at that time must not be lower than the minimum SOC, as designated in this thesis. However, the shallower the discharge, the less damaging the battery storage system could be [203]. Generally, batteries have a range of discharge, based on the suggestion of a manufacturer. Therefore, the battery discharging process will be more comprehensive, if discharge duration is considered for setting a range of the permitted discharging power.
- A different optimization algorithm of the battery management, considering the dynamic nature of the energy storage optimization, need to be developed.

- The optimization for the combination of stand-alone WT-PV systems with other renewable energy technologies and/or other energy storage technologies should be implemented based on resources and characteristics of each specific area.

3. **Hybrid WT-PV systems using batteries at peak demand in a remote area power system:** As the proposed concepts of the optimization algorithm of these grid-connected hybrid systems are still utilized, their optimization algorithm can be improved and/or modified in the battery management or the combination with other renewable energy and/or energy storage technologies, the same as the concepts mentioned above of the stand-alone systems. Furthermore, other investigations and developments on these systems are as follows:

- This study has been implemented to analyse only radial distribution systems and examined with only a series of two long feeders. In practice, there are many feeders connected as networks. As a result, the optimal solutions from this optimization algorithm need to be investigated in the rural distribution networks. However, several methods and tools can be used for analysing the impact of grid-connected renewable energy systems, as described in Chapter 2.
- The optimization algorithm for the renewable energy distribution systems using switched capacitor banks, considering the issues of transients and harmonics, should to be implemented.

APPENDIX A: Specifications and costs of wind turbines

Specifications for 1.5 MW Baseline WT Configurations

The NREL Statement of Work included the following specifications for the baseline configurations:

- Upwind
- Rotor diameter of 70 m
- Full-span variable-pitch control
- Rigid hub
- Blade flapwise natural frequency between 1.5 and 2.5 per revolution
- Blade edgewise natural frequency greater than 1.5 times flapwise natural frequency
- Rotor solidity between 2% and 5%
- Variable-speed operation with maximum power coefficient = 0.50
- Maximum tip speed <= 85 m/s
- Air density = 1.225 kg/m^3
- Turbine hub height = 1.3 times rotor diameter
- Annual mean wind speed at 10-m height = 5.8 m/s
- Rayleigh distribution of wind speed
- Vertical wind shear power exponent = 0.143
- Rated wind speed = 1.5 times annual average at hub height
- Cut-out wind speed = 3.5 times annual average at hub height
- Dynamically soft-soft tower (natural frequency between 0.5 and 0.75 per revolution)
- Yaw rate less than 1 degree per second

Table A.1 Costs of 1.5 MW upwind 2-bladed and upwind 3-bladed turbines

Wind turbines	Upwind 2-bladed		Upwind 3-bladed	
Parameters	**Baseline (k£)**	**Baseline diameter + 12% (k£)**	**Baseline (k£)**	**Baseline diameter + 12% (k£)**
A. Initial capital cost of WTs	**621.85**	**717.23**	**680.21**	**763.6675**
1. Rotor blades	**62.75**	**84.09**	**101.66**	**134.29**
2. Mechanical drive train including	**248.49**	**295.55**	**261.04**	**298.69**
Hub	53.34	74.67	44.55	55.85
Pitch mechanism and bearings	10.67	15.06	20.08	26.98
Low-speed shaft	12.55	12.55	12.55	12.55
Bearings	7.53	7.53	7.53	7.53
Gearbox	99.77	110.44	96.64	106.05
Mechanical brake, HS coupling, etc.	1.88	1.88	1.88	1.88
Yaw drive and bearing	3.77	6.28	8.16	11.30
Main frame	32.00	40.16	42.67	49.57
Hydraulic system	4.39	4.39	4.39	4.39
Nacelle cover	22.59	22.59	22.59	22.59
3. Electrical system	**168.80**	**168.80**	**168.80**	**168.80**
Generator	61.50	61.50	61.50	61.50
Variable-speed electronics	63.38	63.38	63.38	63.38
Electrical connections	37.65	37.65	37.65	37.65
control, safety system	6.28	6.28	6.28	6.28
4. Tower and foundation	**141.82**	**168.80**	**148.72**	**161.90**
B. Balance of station	**213.98**	**217.12**	**213.98**	**217.12**
Transportation	32.00	32.00	32.00	32.00
Roads, civil works	49.57	51.46	49.57	51.46
Assembly and installation	32.00	32.00	32.00	32.00
Electrical interface/connections	79.69	80.95	79.69	80.95
Permits, Engineering	20.71	20.71	20.71	20.71
Initial capital cost of WT systems	**835.83**	**934.35**	**894.19**	**980.78**

APPENDIX B: Specifications and costs of system components

B.1 Stand-alone hybrid systems

Table B.1 Specifications of system components

Components	Specifications
PV module	Mono-crystalline Silicon, Rated power = 100 W, V_{oc}= 21 V, I_{sc}= 6.13 A, V_{max}=17.6 V, I_{max}=5.68 A, Area=1.145x0.674 m^2, Efficiency= 14.5%
Wind turbine	10 kW, cut-in wind speeds of 3 m/s, rated wind speeds of 10 m/s and cut-out of wind speeds of 16 m/s
Batteries	Lead-acid battery, 550Ah, V_{rated}= 2V, Charge efficiency= 90%, Discharge efficiency=100%
Bi-directional converter	Efficiency=90%

Table B.2 Estimated costs and lifetime of system components

Components	Initial capital cost	Replacement cost	O&M cost	Lifetime
PV module including Tax - Installation cost and other components	£294.68 per module 20% of total PV system cost	£294.68 per module	0.5% of ICC	25 years
Wind turbine, 10 kW - Installation cost and other components	£17,320.3 per turbine 30% of total WT system cost	£17,320.3 per turbine	0.4% of ICC	25 years
Diesel generator	£400 per kW	£400 per kW	£0.1708/h	25,000 hrs
Battery, 550 Ah	£249.53 per cell	£249.53 per cell	3% of ICC	15 years
Bi-directional converter and system control	£451 per kW	£451 per kW	3% of ICC	15 years
Charge controller	£3.75 per Ampere	£3.75 per Ampere	3% of ICC	15 years

B.2 Hybrid wind-solar systems using batteries for peak demand in a remote area power system

Table B.3 Specifications of system components

Components	Specifications
PV module	Mono-crystalline Silicon, Rated power = 100 W, V_{oc}= 21 V, I_{sc}= 6.13 A, V_{max}=17.6 V, I_{max}=5.68 A, Area=1.145x0.674 m^2, Efficiency= 14.5%
Wind turbine	1.5 MW, described in Appendix A
Batteries	Lead-acid battery, 1,100 Ah, V_{rated}= 2V, Charge efficiency= 90%, Discharge efficiency=100%
Bi-directional converter	Efficiency=90%

Table B.4 Estimated costs and lifetime of system components

Components	Initial capital cost	Replacement cost	O&M cost	Lifetime
PV module including Tax - Installation cost and other components	£294.68 per module 20% of total PV system cost	£294.68 per module	0.5% of ICC	25 years
Wind turbine, 1.5 MW - Installation cost and other components	(Appendix A)	(Appendix A)	0.4% of ICC	25 years
Battery, 1,100 Ah	£502.06 per cell	£502.06 per cell	3% of ICC	15 years
Bi-directional converter and system control	£451 per kW	£451 per kW	3% of ICC	15 years
Charge controller	£3.75 per Ampere	£3.75 per Ampere	3% of ICC	15 years

APPENDIX C: The possible photovoltaic and battery sizing models

C.1 The maximum number of PV module model

PV array sizing is designed from bus voltage and a peak current rating of the array. The maximum number of PVs will be investigated from the maximum peak current rating of array.

$$N_{pv,max} = int\left[\frac{V_{Bus}}{V_{pv,r}}\right] \cdot int\left[\frac{I_{worst,pv}}{I_{pv,r}}\right] \quad \text{(C.1)}$$

where $V_{pv,r}$ and $I_{pv,r}$ are the rated voltage and rated current of a PV module respectively. V_{Bus} is the bus voltage specified from the sum of a full charging voltage of batteries and a blocking diode voltage of each PV module [69].

$I_{worst,pv}$ is the maximum peak current rating of array supplying a peak load current in the worst month when is the lowest solar energy [69]. It should also support the peak load current at the highest temperature by still normal operation because the PV power will decrease approximately 0.5% per ^{o}C.

$$I_{worst,pv} = \frac{1000 \cdot \bar{E}_{L,daily}}{\eta_{Batt} \cdot (1 - d_{pm}) \cdot V_{Bus} \cdot h_{worst,s}} \quad \text{(C.2)}$$

where d_{pm} is the percentage of degradation in performance for the average effect of dust accumulation (0.1) and $h_{worst,s}$ is the hours of full sun radiation on the inclined array in the worst period [69].

$$h_{worst,s} = \frac{\bar{S}_{min}}{In_{peak}} \quad \text{(C.3)}$$

where In_{peak} is the peak radiation intensity, 1,000 W/m^2 and S_{min} is the average daily solar radiation of the worst period in a year (Wh/m^2). The worst period is the period of storage reserve days.

C.2 The minimum and maximum numbers of batteries

A size of the battery storage system for renewable energy sources bases on a load demand, a number of days for storage reservation and factors such as maximum depth of discharge and temperature correction, rated battery capacity and battery life [83].

$$Ah_{sys,b} = \frac{1000 \cdot d_s \cdot \overline{E}_{L,daily}}{\eta_{b,t} \cdot DOD_{max} \cdot V_{Batt}} \quad \text{(C.4)}$$

where d_s is the battery autonomy or storage days and $\eta_{b,t}$ is the temperature correction factor.

In order to estimate the minimum battery system sizing, the daily load will be averaged in a whole year. On the other hand, the maximum battery system sizing will be calculated by the average daily load in the worst month when it has the highest load demand. The minimum and maximum numbers of batteries are:

$$N_{b,min} = int\left[\frac{Ah_{sys,b,min}}{Ah_{r,module}}\right] \quad \text{(C.5)}$$

$$N_{b,max} = int\left[\frac{Ah_{sys,b,max}}{Ah_{r,module}}\right] \quad \text{(C.6)}$$

where $Ah_{r,module}$ is the rated ampere-hour of battery module. $Ah_{sys,b,min}$ and $Ah_{sys,b,max}$ are the minimum and maximum ampere-hour of battery system respectively.

APPENDIX D: Site descriptions

D.1 Wind speed and solar radiation profiles

Lam Takhong Dam, Nakhon Ratchasima province in Thailand, latitude 14^{o} 47' 58"N and longitude 101 33' 32.2"E, seemingly has the potential of both wind and solar energy from [53], [54], where the hybrid system will be applied. Hourly wind speed and hourly solar radiation data collected in 2006 are employed in this research. The hourly wind speed data was measured at 45 m of hub height (height above sea level approximately 661 m) [53] , illustrated in Figure D.1. Wind speed distribution probability is shown in Figure D.2. An annual mean wind speed of approximately 5.71 m/s at 45 m of hub height can be classified to be class 2 wind resource site.

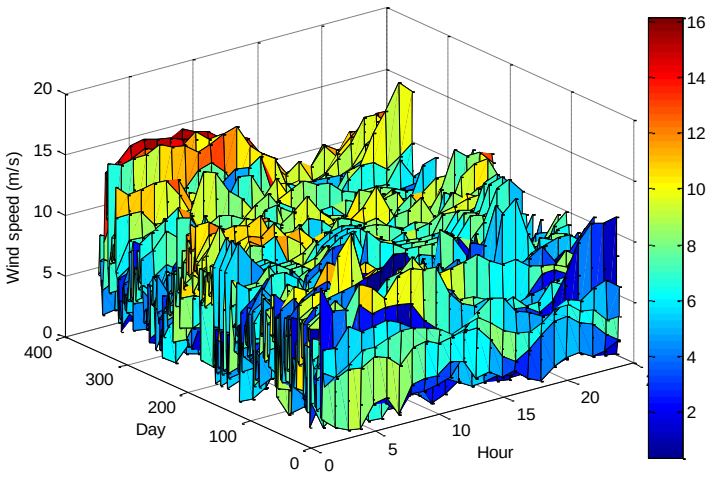

Figure D.1 The hourly wind speed data measured at 45 m of hub height

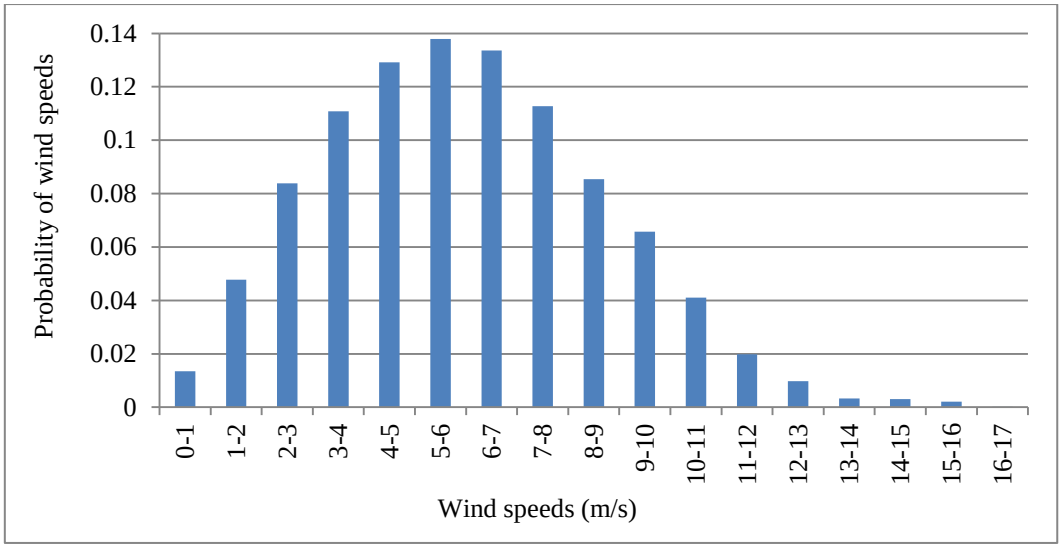

Figure D.2 Distribution probability of wind speeds in 2006 at 45 m of hub height

From the solar radiation data [54] and the location, PV modules should be oriented facing the south with the optimum angle of 10^{o} to obtain the yearly maximum output energy calculated by using equations from [213]. At this position, hourly solar radiation profiles in a year are shown in Figure D.3. The annual average solar energy was approximately 4.92 kWh/m^2 per day and the sunshine duration was approximately 8 sunshine-hours per day. Hourly temperature data assumed from air ambient temperature data averaged every three hours in 2006 by [206]. They were utilized for calculating the PV module efficiency relating to the cell temperature and then forecasting the hourly PV power output.

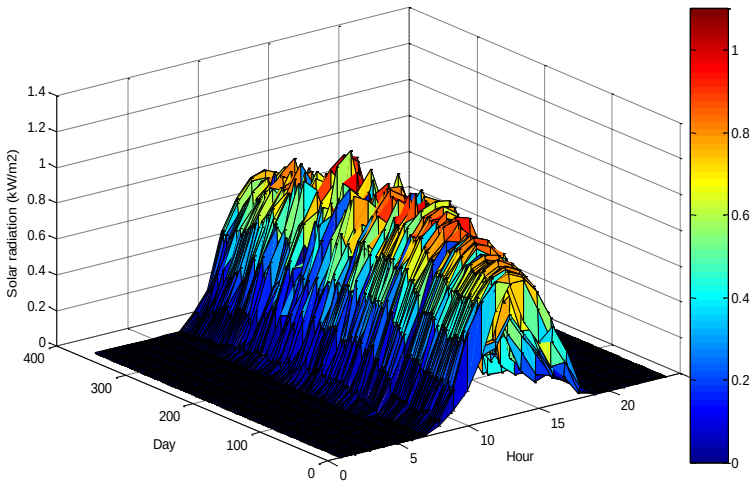

Figure D.3 Average hourly solar radiation in 2006 at 10^{o} of inclined plane facing the south

D2. System data

The grid hybrid WT-PV-Battery systems in Chapter 6 are calculated from [239] and listed in Table D.1. The three-phase megavoltampere base is identified as 100 MVA.

Table D.1 Data of the grid hybrid WT-PV-Battery systems

System	Sending end	Receiving end	R (pu)	X (pu)	B (pu)	Capacity (MVA)	Voltage (kV)	Length (km)
A	1	3	0.0650	0.3302	0.0427	100	115	100
	3	4	5.0950	2.1045	7.439E-04	8	22	30
B	1	3	0.0650	0.3302	0.0427	100	115	100
	3	4	5.0950	2.1045	7.439E-04	8	22	30
	4	6	0.3396	0.1403	5.321E-05	8	22	2
C	1	3	0.0650	0.3302	0.0427	100	115	100
	3	4	5.0950	2.1045	7.439E-04	8	22	30
	4	6	0.3396	0.1403	5.321E-05	8	22	2

Table D.2 Generator data of the grid hybrid WT-PV-Battery systems [207]

Fuel	Cost coefficient		
	a (£/h)	b (£/MWh)	c (£/MW/MWh)
Coal	197.4461	14.955	0.01315

Remark: 1$=£0.6275 in 2011, coal cost is 2.25 $/MMBTU in 2010 [240]

D.3 Time of Use

The PEA purchases electricity from a Very Small Power Producer (VSPP) for 11-33 kV systems in Thailand in 2011, with the Time of Use (TOU) rate shown in Table D.3. The peak and off peak periods and the monthly Fuel tariff (Ft) are identified in Table D.4 and D.5. [238]

Table D.3 Wholesale TOU rates

Peak (Baht/kWh)	Off peak (Baht/kWh)
2.9278	1.1154

Table D.4 Peak and off peak periods

Periods	Time	Days
Peak	09.00-22.00	Monday to Friday and the Royal Ploughing day
Off peak	22.00-09.00	Monday to Friday and the Royal Ploughing day
	00.00-24.00	Saturday, Sunday, the Labour day and normal public holidays, excluding the Royal Ploughing day and substitution days

Table D.5 The average monthly wholesale Fuel tariff in 2009

Month	1	2	3	4	5	6	7	8	9	10	11	12
Ft (Baht/kWh)	0.9098	0.9100	0.9101	0.9177	0.9177	0.9177	0.9177	0.9177	0.9206	0.9206	0.9206	0.9206

Appendix E: Calculation examples and results of Chapter 4, 5 and 6

E.1 Chapter 4

E.1.1 Cost fractions

From cost data of a 1.5 MW upwind 3-bladed turbine in Table A.1, the cost fraction of rotor blades is as follows:

$$Cost\ fraction\ of\ rotor\ blades = \frac{Cost\ of\ rotor\ blades}{ICC\ of\ WT}$$

$$Cost\ fraction\ of\ rotor\ blades = \frac{101.66}{680.21} * 100\% = 14.94\%$$

E.1.2 Cost factors

From cost data of a 1.5 MW upwind 3-bladed turbine in Table A.1 and Equation 4.3, the cost factor of rotor blades is as follows:

$$New\ cost\ of\ rotor\ blades = Cost\ of\ rotor\ blades\left(\frac{D_r}{D_{r0}}\right)^r$$

$$134.29 = 101.66\left(\frac{78.4}{70}\right)^r$$

$$\therefore Cost\ factor\ of\ rotor\ blades, r = \frac{ln1.321}{ln1.12} = 2.46$$

E.1.3 Initial Capital Cost of a LWST

The ICC of LWST due to changing rotor diameters, described in Section 4.4.3, can be calculated by using Equation 4.6.

$$ICC_{Lwst} = \sum_{i=1}^{n}\left(f_{c,i}\left(\frac{D_r}{D_{r0}}\right)^{r_i} * C_{wt}\right) + (ICC_{wt} - C_{wt}) * \left(\frac{D_r}{D_{r0}}\right)^{r_{ins}} + \frac{C_t H_t}{P_{wt,r}}\left(\frac{D_r}{D_{r0}}\right)^{r_t}$$

The cost fractions and cost factors were computed and presented in Table 4.4. An upwind 3-bladed WT having a rotor diameter of 70 m used to be a baseline was designed at a rated power of 1.5 MW and a hub height of 84 m. It has the ICC of 596.13 £/kW, the total WT component cost of 453.47 £/kW and the tower cost of 1,688 £/m. The ICC of WT having a rotor diameter of 121 m can be calculated by using the Sum-component cost model (4 subsystems) as follows:

$$ICC_{Lwst} = 453.47\left(0.10\left(\frac{121}{70}\right)^{2.58} + 0.39\left(\frac{121}{70}\right)^{1.53} + 0.27\left(\frac{121}{70}\right)^{0}\right) + (596.13 - 453.47) * \left(\frac{121}{70}\right)^{0.13} + \frac{1688 * 84}{1{,}500}\left(\frac{121}{70}\right)^{1.54}$$

$$\therefore ICC_{Lwst} = 1{,}149.14 \text{ £/kW}$$

E.2 Chapter 5

E.2.1 Case study I: Stand-alone hybrid wind-solar systems using battery management

The optimization process for stand-alone hybrid systems by using SPEA2 is shown in Figure 5.1. The calculation example in further details is as follows:

1. Some examples of input data is shown in Table E.1. The load demand profile was detailed in Section 5.4.1.1 and Appendix D. For 30 kW at peak load, load power per unit was multiplied by 30. Hourly wind speeds and solar radiation data were referred from [53] and [54] and their details were described in Appendix D.

Table E.1 Input data

Time	Load power (pu)	Wind speed (m/s)	Hourly global radiation (kWh/m^2)
12 AM, 1-Jan	0.4563	4.53	0
01 AM, 1-Jan	0.4212	5.13	0
……..	……..	……..	……..
……..	……..	……..	……..
10 PM, 31-Dec	0.460013	3.45	0
11 PM, 31-Dec	0.428288	3.45	0

2. All optimization problems in this study used the SPEA2, run with 150 populations, 70 archives and 100 generations. Mutation and crossover probabilities were set to be 0.001 and

0.8 respectively. The simulation time is every hour of a whole year (8,760 hours). The total evaluation time of each case is approximately 20 minutes.

3. Power output of a WT at time *t* can be calculated from Equation 2.2, with conditions explained in Section 2.3.1:

$$P_{wt}(t) = \begin{cases} 0, & 0 \le U(t) < 3m/s \\ 0.5\rho_a C_p A U^3(t), & 3m/s \le U(t) \le U_r \\ P_{wt,r}, & U_r < U(t) \end{cases}$$

WT configurations and costs were described in Section 5.4.1.2 and Appendix B, respectively. Some results are shown in Table E.2.

4. Power output of a PV at time *t* can be calculated from Equation 2.1. The global radiation on an inclined surface was computed from equations in Chapter 13 of [69]. The PV system efficiency was calculated from [81]. Some results are shown in Table E.2.

Table E.2 Power output of a WT and a PV module

Time	**WT power output (kW)**	**PV power output (kW)**
12 AM, 1-Jan	0.5566	0
01 AM, 1-Jan	0.8084	0
……..	……..	……..
……..	……..	……..
10 PM, 31-Dec	0.2459	0
11 PM, 31-Dec	0.2459	0

5. Initial populations of the number of WTs, PV modules and batteries were calculated from equations in Section 5.2.1, Section C.1 and Section C.2, respectively. The maximum and minimum numbers of system components are shown in Table E.3.

Table E.3 The number of WTs, PV modules and batteries for boundaries of random initial populations

WTs		**PV modules**		**Batteries**	
Min	Max	Min	Max	Min	Max
0	91	0	1,365	576	3,000

6. The operation process of stand-alone hybrid wind-solar systems was described in Section 5.3. It runs in series, 8,760 hours, with 150 populations, 70 archives and 100 generations, by

using SPEA2. The final solutions, in Table E.4, show objectives (LPSP and LCOE) and chromosomes (the number of WTs, PV modules and batteries).

Table E.4 Results of stand-alone hybrid WT-PV-Battery systems, 3 battery groups with the minimum SOC of 0.25 and 0.5

Archive no.	LPSP	LCOE	PVs	WTs	Batteries
1	0.0000	0.3633	1,020	3	720
2	0.0001	0.3613	1,005	3	720
……..	……..	……..	……..	……..	……..
……..	……..	……..	……..	……..	……..
69	0.0634	0.2221	750	1	288
70	0.0705	0.2144	525	4	288

7. The appropriated solution was selected. This study focuses the system reliability so LPSP equal to be zero was chosen as shown in Table E.5.

Table E.5 Comparisons of stand-alone hybrid systems between using battery management and DSG support

Particular	WT-Battery	WT-PV-Battery	WT-PV-DSG-Battery	PV-Battery	DSG only
Number of battery groups	3	3	1	3	-
Minimum state of charge, SOC_{min}	0.5 and 0.25*	0.5 and 0.25*	0.5	0.5 and 0.25*	-
Number of WTs	40	3	1	-	-
Number of PV modules	-	1,020	1,215	915	-
Number of Batteries	2,880	720	1,320	1,008	-
DSG capacity (kW)	-	-	20	-	30
Annual WT energy (MWh/year)	624.40	46.83	15.61	-	-
Annual PV energy (MWh/year)	-	197.07	234.74	176.78	-
Annual DSG energy (MWh/year)	-	-	21.45	-	161.37
Annual battery discharging energy (MWh/year)	37.74	59.38	74.72	87.22	-
Annual total useful energy (MWh/year)	273.87	192.41	221.34	202.22	-
Annual total waste energy (MWh/year)	336.60	108.90	87.61	61.78	-
Fuel consumption (litres/year)	-	-	7,709.90	-	61,811.51
Total initial capital cost of system (k£)	1,830	667.29	879.30	631	12.00
Expected annual O&M (k£)	29.16	10.58	16.79	12.192	1.50
Levelized annual capital cost (£/kWh)	0.459	0.238	0.249	0.214	0.005
Levelized annual O&M cost (£/kWh)	0.142	0.073	0.092	0.080	0.012
Levelized replacement cost (£/kWh)	0.146	0.052	0.077	0.069	0.024
Levelized annual fuel cost (£/kWh)	-	-	0.290	-	0.309
LCOE (£/kWh)	0.746	0.363	0.707	0.369	0.350
CO_2 (Ton/year)	-	-	14.99	-	112.80
Lifetime of a DSG (years)	-	-	18	-	3

8. The results were verified about the charging and discharging battery processes as demonstrated in Figure E.1 and E.2. These are examples of the stand-alone WT-Battery system and stand-alone PV-Battery system, using three battery groups, setting the two minimum SOC levels, respectively.

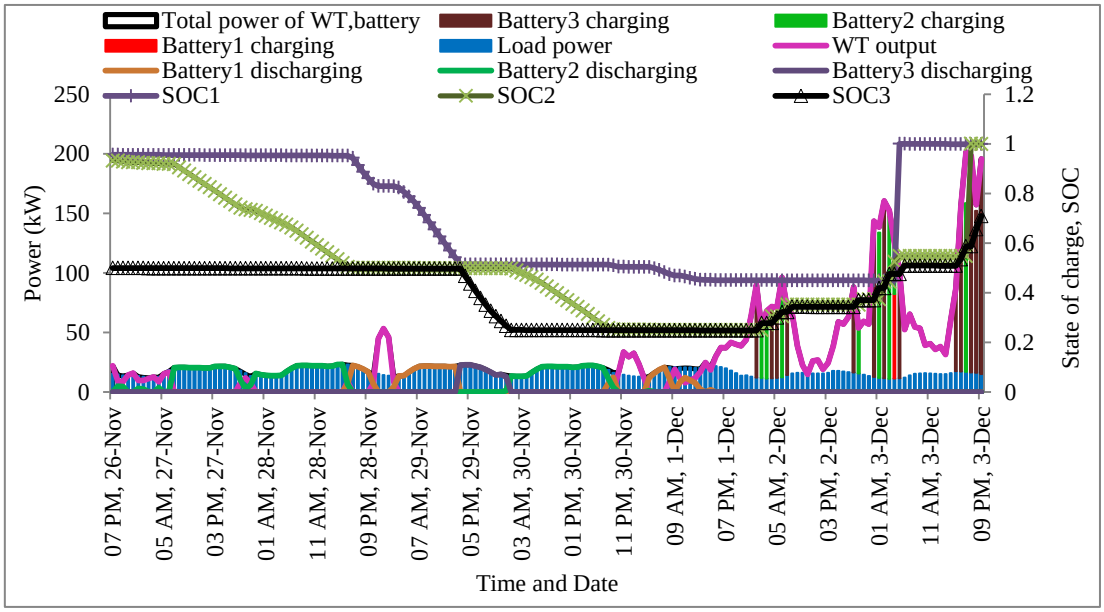

Figure E.1 The SOC and power supplies for load demand, of the stand-alone WT-Battery system using three battery groups, setting the two minimum SOC levels

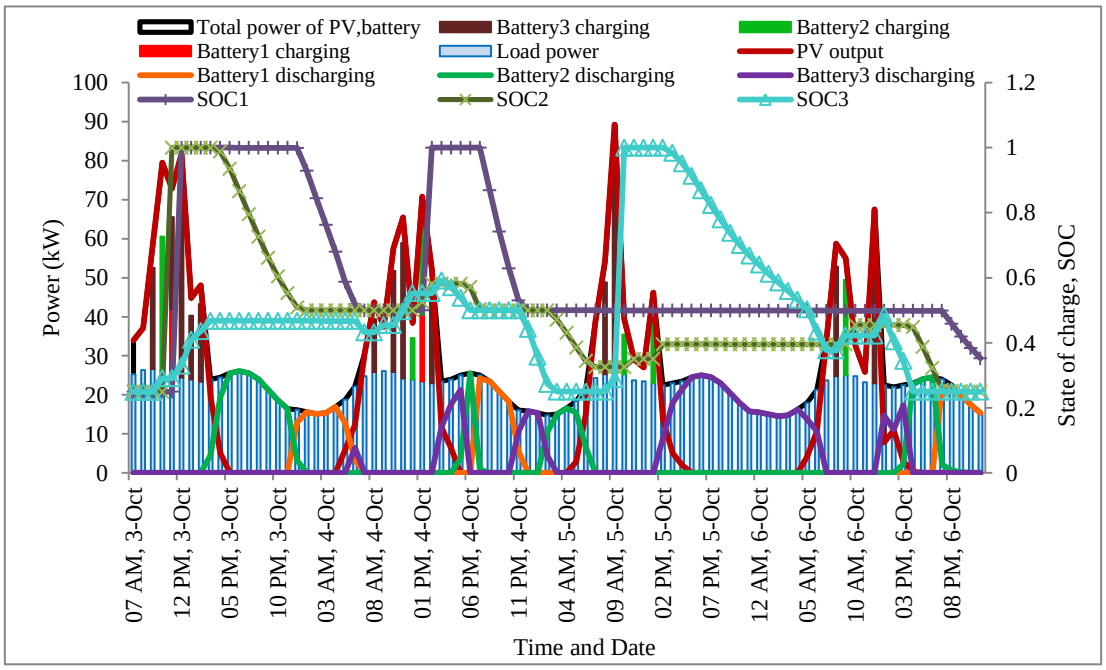

Figure E.2 The SOC and power supplies for load demand, of the stand-alone PV-Battery system using three battery groups, setting the two minimum SOC levels

E.2.2 Case study II: Economic feasibility of stand-alone hybrid systems using LWSTs and HWSTs

This case study also applies the optimization process for stand-alone hybrid systems by using SPEA2 is shown in Figure 5.1. The calculation is the same as Case study I.

1. Input data: the system load peak is assumed to be 1 MW and the system configurations was described in Section 5.4.2.2.

2. The Sum-component cost model, proposed in Chapter 4, was utilized for calculating the ICC of WTs in the objective evaluation process as explained in Section 5.3.4. The results of LWSTs having rated wind speeds of 8 and 9 m/s are shown in Table E.6.

Table E.6 Results of stand-alone WT-Battery systems, by using LWSTs having rated wind speeds of 8 and 9 m/s

Archive no.	Rated wind speeds of 8 m/s				Rated wind speeds of 9 m/s			
	LPSP	LCOE	WTs	Batteries	LPSP	LCOE	WTs	Batteries
1	0.0000	0.2307	5	5,200	0.0000	0.3032	6	5,800
2	0.0034	0.2001	4	4,800	0.0002	0.2855	6	5,200
……..	……..	……..	……..	……..	……..	……..	……..	……..
……..	……..	……..	……..	……..	……..	……..	……..	……..
69	0.0450	0.1299	3	2,400	0.0648	0.1278	4	1,200
70	0.0687	0.1246	3	2,000	0.0790	0.1201	4	1,000

3. A Net Present Value (NPV), an Internal Rate of Return (IRR), a Payback Period (PBP) and a Profitability Index (PI) calculated following methods in [75], [136] were used to the economic feasibility of the hybrid systems. The profitability criteria for decision making are shown in Table 2.4. The results of this case study presented in Figure 5.17 and 5.18 and Table E.7 and E.8 were discussed in Section 5.4.2.3.

Table E.7 LCOE and economic feasibility of stand-alone WT-PV-Battery systems in different rated wind speeds, for the adder of £0.07/kWh

Rated wind speeds (m/s)	Number of WTs	Number of Batteries	LCOE (£/kWh)	NPV (k£)	IRR	Payback (years)	Profit index
8	6	16,200	0.305874	-2.36E+06	0.0559	>25	-0.1265
9	6	17,400	0.303223	-1.83E+06	0.0588	>25	-0.1032
10.7	9	18,000	0.323415	-3.74E+06	0.0469	>25	-0.1930
11.54	11	18,000	0.333186	-4.76E+06	0.0414	>25	-0.2335
13	13	24,600	0.393003	-1.14E+07	0.0042	>25	-0.4657

Table E.8 LCOE and economic feasibility of stand-alone WT-PV-Battery systems in different rated wind speeds, for the adder of £0.16/kWh

Rated wind speeds (m/s)	Number of WTs	Number of Batteries	LCOE (£/kWh)	NPV (k£)	IRR	Payback (years)	Profit index
8	6	16,200	0.305874	3.18E+06	0.0922	18.21	-0.1265
9	6	17,400	0.303223	3.71E+06	0.0969	13.04	-0.1032
10.7	9	18,000	0.323415	1.80E+06	0.0832	20.74	-0.193
11.54	11	18,000	0.333186	7.80E+05	0.0767	23.00	-0.2335
13	13	24,600	0.393003	-5.91E+06	0.0400	>25	-0.4657

E.3 Chapter 6

The optimization process for hybrid wind-solar systems using batteries for peak demand in remote area power systems, by applying SPEA2 is shown in Figure 6.3. The calculation example in further details is as follows:

1. Some input data are shown in Table E.1. The load demand profile was detailed in Section 6.6.3 and Appendix D. Hourly wind speeds and solar radiation data were referred from [53] and [54] and their details were described in Appendix D.

2. All optimization problems in this study used the SPEA2, run with 150 populations, 70 archives and 100 generations. Mutation and crossover probabilities were set to be 0.001 and 0.8 respectively. The simulation time is every hour of a whole year (8,760 hours). The total evaluation time of each case is approximately 20 minutes.

3. WT and PV power output can be calculated as same as Step 3 and 4 in Section E.2.1, by using the configurations described in Section 6.6.2.

4. Initial populations of WT and PV systems are determined by considering the voltage rise issue as explained in Section 6.5.1. Therefore, WTs, PV modules and batteries were calculated as explained in Section 5.2.1, by considering load energy at peak demand. However, the capacity of WT and PV systems is limited with the possible maximum power generation ($P_{G,max}$), estimated by using Equation 6.9 and data of the grid hybrid systems in Table D.1. The possible maximum power generations of System A, B and C are 6.28 MW, 5.58 MW and 5.58 MW, respectively.

5. The minimum capacitive power compensation can be estimated by using Equation 6.11.

$$Q_{c,min} = Q_{L,max} - \left(\frac{\Delta V_{max} V_{2,min} - R P_{L,max}}{X}\right)$$

$$Q_{c,min} = 2.25 - \left(\frac{2.2 * 20.9 - 12.3144 * 3}{9.5859}\right)$$

$$Q_{c,min} = 1{,}307 \text{ kVAr}$$

6. The Sum-component cost model, proposed in Chapter 4, was utilized for calculating the ICC of WTs in the objective evaluation process as explained in Section 6.5.2. The results are shown in Figure 6.12 and the results of LWSTs having rated wind speeds of 8 and 9 m/s are shown in Table E.9.

Table E.9 Results of WT-Battery systems, by using LWSTs having rated wind speeds of 8 and 9 m/s

Archive no.	Rated wind speeds of 8 m/s					Rated wind speeds of 9 m/s				
	LBP	LCOE	WOE	WTs	Batteries	LBP	LCOE	WOE	WTs	Batteries
1	0.0000	0.0215	0.0000	6	5,400	0.0000	0.0251	0.0000	6	5,800
2	0.0005	0.0194	0.0000	5	4,800	0.0003	0.0236	0.0000	6	5,200
……..	……..	……..	……..	……..	……..	……..	……..	……..	……..	……..
……..	……..	……..	……..	……..	……..	……..	……..	……..	……..	……..
69	0.0468	0.0093	0.0000	4	1,000	0.0385	0.0130	0.0000	5	1,600
70	0.0700	0.0080	0.0000	3	1,000	0.0790	0.0099	0.0000	4	1,000

7. NPV, IRR, PBP and PI calculated following methods in [75], [136] were used to the economic feasibility of the hybrid systems. The profitability criteria for decision making are shown in Table 2.4. The results of this case study presented in Figure 6.11 and 6.13 and Table E.10 to E.16 were discussed in Section 5.4.2.3.

Table E.10 LCOE and economic feasibility of the stand-alone PV-Battery systems in different PV prices

% of current PV module price	PV module prices (£/W)	LCOE (£/kWh)	NPV (k£)	IRR	Payback (years)	Profit index
25%	0.74	0.0658	1.65E+07	0.1821	6.01	1.0292
50%	1.47	0.1050	2.21E+05	0.1311	16.50	0.1261
75%	2.21	0.1439	-2.33E+05	0.0416	>25	-0.2407
100%	2.95	0.1830	-5.38E+03	0.0120	>25	-0.4404
125%	3.68	0.2220	-9.45E+05	-0.0151	>25	-0.5657
150%	4.42	0.2612	-1.21E+06	-0.0452	>25	-0.652

Table E.11 LCOE and economic feasibility of the stand-alone WT-Battery systems in different WT prices

% of current WT price	WT prices (£/W)	LCOE (£/kWh)	NPV (k£)	IRR	Payback (years)	Profit index
25%	0.15	0.0357	1.29E+07	0.4943	2.24	3.2356
50%	0.30	0.0407	1.18E+07	0.3804	2.93	2.3089
75%	0.45	0.0457	1.07E+07	0.3055	3.67	1.7150
100%	0.60	0.0507	9.56E+06	0.2522	4.44	1.3018
125%	0.75	0.0557	8.44E+06	0.2120	5.24	0.9978
150%	0.89	0.0607	7.32E+06	0.1806	6.10	0.7647

Table E.12 LCOE and economic feasibility of stand-alone WT-PV-Battery systems in different WT prices

% of current WT price	WT prices (£/W)	LCOE (£/kWh)	NPV (k£)	IRR	Payback (years)	Profit index
25%	0.15	0.0283	1.56E+07	0.4313	2.5896	2.8834
50%	0.30	0.0327	1.45E+07	0.353	3.1819	2.2191
75%	0.45	0.0372	1.34E+07	0.2967	3.8038	1.7488
100%	0.60	0.0416	1.23E+07	0.254	4.4563	1.3984
125%	0.75	0.0460	1.11E+07	0.2205	5.1318	1.1273
150%	0.89	0.0505	1.00E+07	0.1933	5.8464	0.9112

Table E.13 LCOE and economic feasibility of the stand-alone WT-PV-Battery systems in different PV module prices

% of current PV module price	PV module prices (£/W)	LCOE (£/kWh)	NPV (k£)	IRR	Payback (years)	Profit index
25%	0.74	0.0277	1.58E+07	0.3994	2.8019	2.6252
50%	1.47	0.0327	1.46E+07	0.3338	3.3754	2.0648
75%	2.21	0.0371	1.33E+07	0.2905	3.8859	1.6999
100%	2.95	0.0416	1.23E+07	0.254	4.4563	1.3984
125%	3.68	0.046	1.12E+07	0.2242	5.0424	1.1553
150%	4.42	0.0505	1.02E+07	0.1992	5.6726	0.9551

Table E.14 LCOE and economic feasibility of the stand-alone WT-Battery systems in different battery prices

% of current Battery price	Battery prices (£/Ah)	LCOE (£/kWh)	NPV (k£)	IRR	Payback (years)	Profit index
25%	0.1141045	0.0301	1.30E+07	0.3785	2.96	2.4499
50%	0.2282091	0.037	1.19E+07	0.3281	3.43	1.9805
75%	0.3423136	0.0439	1.07E+07	0.2868	3.91	1.6067
100%	0.4564182	0.0507	9.56E+06	0.2522	4.44	1.3018
125%	0.5705227	0.0576	8.41E+06	0.2223	4.97	1.0485
150%	0.6846273	0.0645	7.56E+06	0.1961	5.56	0.8346

Table E.15 LCOE and economic feasibility of the stand-alone PV-Battery systems in different battery prices

% of current Battery price	Battery prices (£/Ah)	LCOE (£/kWh)	NPV (k£)	IRR	Payback (years)	Profit index
25%	0.74	0.1746	-4.85E+05	0.0186	>25	-0.407
50%	1.47	0.1774	-5.01E+05	0.0157	>25	-0.4184
75%	2.21	0.1802	-5.16E+05	0.0134	>25	-0.4295
100%	2.95	0.183	-5.35E+05	0.0120	>25	-0.4404
125%	3.68	0.1858	-5.47E+05	0.0105	>25	-0.4511
150%	4.42	0.1887	-5.56E+05	0.0091	>25	-0.4620

Table E.16 LCOE and economic feasibility of the stand-alone WT-PV-Battery systems in different battery prices

% of current Battery price	Battery prices (£/Ah)	LCOE (£/kWh)	NPV (k£)	IRR	Payback (years)	Profit index
25%	0.74	0.0363	1.26E+07	0.3018	3.74	1.7956
50%	1.47	0.0403	1.21E+07	0.2740	4.12	1.5533
75%	2.21	0.0409	1.18E+07	0.2570	4.41	1.4253
100%	2.95	0.0416	1.16E+07	0.2552	4.45	1.3984
125%	3.68	0.0427	1.14E+07	0.2511	4.51	1.3721
150%	4.42	0.043	1.10E+07	0.2483	4.56	1.3462

References

[1] A. Niez, "Comparative Study on Rural Electrification Policies in Emerging Economies: Keys to successful policies," *International Energy Agency*, 2010.

[2] D. Barnes and G. Foley, "Rural Electrification in the Developing World: A Summary of Lessons from Successful Program," *Joint UNDP/World Bank Energy Sector Management Assistance Programme (ESMAP) World Bank, Washington DC*, 2004.

[3] S. Jonas, F. Tor Martin, and G. Shirish, "Assessing Technology Options for Rural Electrification: Guidelines for Project Development," 2009.

[4] J. Saghir, "Operational Guidance for World Bank Group Staff Designing Sustainable Off-Grid Rural Electrification Projects: Principles and Practices," *The World Bank and The Energy Mining Sector Board*, 2008.

[5] R. Simon, "Rural Electrification with Renewable Energy Technologies, quality standards," *Alliance for Rural Electrification*, 2011.

[6] R. Jean-François, "Rural Energy and Development for Two Billion People," *Meeting the Challenge for Rural Energy and Development, The World Bank*, 1997.

[7] A. R. Inversin and V. Arlington, "Reducing the Cost of Grid Extension for Rural Electrification," *NRECA International, Ltd.*, 2000.

[8] H. White, N. Blöndal, M. Rota, A. Vajja, R. Banerjee, M. Fair, T. Lonnberg, A. Waxman, and A. Barbu, "The Welfare Impact of Rural Electrification: A Reassessment of the Costs and Benefits," *The Independent Evaluation Group (IEG), The World Bank*, 2008.

[9] R. A. Butler, "Crude oil, avg, spot price chart, 2000-2011," *11/01/2012*. [Online]. Available: www.mongabay.com. [Accessed: 12-Jan-2012].

[10] "Petroleum Retail Price Differences between Bangkok and Upcountry by Amphoe," *Energy Policy and Planning Office,17/07/2006*. [Online]. Available: www.eppo.go.th. [Accessed: 20-Nov-2011].

[11] "Currency Exchange Rate." [Online]. Available: www.exchangerates.org.uk. [Accessed: 10-Nov-2011].

[12] "Wave Power," *Pelamis Wave Power Ltd.* [Online]. Available: http://www.pelamiswave.com/wave-power. [Accessed: 10-Nov-2012].

[13] Department of Alternative Energy Development and Efficiency, "Thailand Alternative Energy Situation 2010," 2010.

[14] N. Watjanatepin, C. Boonmee, P. Unaalekhaka, W. Srisongkram, T. Kruehong, and C. Wannasut, "Evaluation of Electrical Service Acceleration Project by Solar Home System: SHS," in *4th Conference on Energy Network of Thailand*, 2008, p. 7.

[15] "Market Report 2011," *The European Photovoltaic Industry Association (EPIA)*, 2011.

[16] "Module Pricing," *Solarbuzz, an NPD Group company, 01/2012*. [Online]. Available: www.solarbuzz.com. [Accessed: 20-Jan-2012].

[17] "Solar Generation 6: Solar Photovoltaic Electricity Empowering the World," *The European Photovoltaic Industry Association (EPIA) and Greenpeace International*, 2011.

[18] "World Market recovers and sets a new record: 42 GW of new capacity in 2011, total at 239 GW," *World Wind Energy Association (WWEA)*. [Online]. Available: www.wwindea.org. [Accessed: 21-Feb-2012].

[19] "World Wind Energy Report 2010," *World Wind Energy Association (WWEA)*, 2011.

[20] "Global Wind Report: Annual market update 2010," *Global Wind Energy Council (GWEC)*, 2011.

[21] C. L. Archer and M. Z. Jacob, "Evaluation of Global Wind Power," *Journal of Geophysical Research*, vol. 110, pp. 1–20, 2005.

[22] "The wind classes and power density," *Energy Information Administration, Official Energy Statistics from the U.S. Government*. [Online]. Available: http://www.eia.doe.gov/cneaf/solar.renewables/page/wind/wind.html. [Accessed: 22-Nov-2008].

[23] "WT Technology status," *European Wind Energy Association (EWEA)*. [Online]. Available: www.wind-energy-the-facts.org. [Accessed: 20-Feb-2012].

[24] D. A. BODE, B. ANTHONY, and J. CLOUD, "Oklahoma Wind Power Assessment Committee Interim Report," *The Oklahoma State Legislature*, no. 1, 2005.

[25] "Wind Power Today 2010," *The National Renewable Energy Laboratory (NREL)*, 2010.

[26] "2010 Small Wind Turbine Global Market Study," *America Wind Energy Association (AWEA)*, 2009.

[27] N. Tanaka, "Technology Roadmap: Wind Energy," *The International Energy Agency (IEA)*, 2009.

[28] N. Brown, "Upwind study: 20 MW Wind Turbines are on the Horizon," 2011. [Online]. Available: http://cleantechnica.com/2011/12/09/upwind-study-20-mw-wind-turbines-are-on-the-horizon/. [Accessed: 20-Dec-2011].

[29] P. Hearps and D. Mcconnell, “Renewable Energy Technology Cost Review,” *Melbourne Energy Institute*, 2011.

[30] M. Bolinger and R. Wiser, “Understanding Trends in Wind Turbine Prices Over the Past Decade,” *Lawrence Berkeley National Laboratory, Environmental Energy Technologies Division*, 2011.

[31] W. Zhou, C. Lou, Z. Li, L. Lu, and H. Yang, “Current status of research on optimum sizing of stand-alone hybrid solar–wind power generation systems,” *Applied Energy*, vol. 87, no. 2, pp. 380–389, Feb. 2010.

[32] R. Baños, F. Manzano-Agugliaro, F. G. Montoya, C. Gil, A. Alcayde, and J. Gómez, “Optimization methods applied to renewable and sustainable energy: A review,” *Renewable and Sustainable Energy Reviews*, vol. 15, no. 4, pp. 1753–1766, 2011.

[33] G. Coppez, S. Chowdhury, and S. P. Chowdhury, “Review of Battery Storage Optimisation in Distributed Generation,” *Power Electronics, Drives and Energy Systems (PEDES) & 2010 Power India, 2010 Joint International Conference on*, 2010.

[34] C. A. C. Coello, “20 Years of Evolutionary Multi-Objective Optimization : What Has Been Done and What Remains To Be Done,” pp. 1–34, 2006.

[35] E. Zitzler, M. Laumanns, and L. Thiele, “SPEA2: Improving the strength pareto evolutionary algorithm.” Eidgenössische Technische Hochschule Zürich (ETH), Institut für Technische Informatik und Kommunikationsnetze (TIK), 2001.

[36] R. Dufo-López and J. L. Bernal-Agustín, “HOGA Version 1.96 User Manual,” *Electrical Engineering Department, University of Saragossa (Spain)*, 2011.

[37] A. D. Alarcón-rodríguez, “A Multi-objective Planning Framework for Analysing the Integration of Distributed Energy Resources,” *Doctoral Dissertation, Institute for Energy and Envi-ronment, Department of Electronic and Electrical Engineering, University of Strathclyde*, 2009.

[38] V. Gevorgian, D. A. Corbus, S. Drouilhet, R. Holz, and K. E. Thomas, “Modeling , Testing and Economic Analysis of a Wind-Electric Battery Charging Station,” *National Renewable Energy Laboratory*, 1998.

[39] R. Kaiser, “Optimized battery-management system to improve storage lifetime in renewable energy systems,” *Journal of Power Sources*, vol. 168, no. 1, pp. 58–65, May 2007.

[40] M. I. Desconzi, R. C. Beltrame, C. Rech, L. Schuch, and H. L. Hey, “Photovoltaic Stand-Alone Power Generation System with Multilevel Inverter Key words,” *International Conference on Renewable Energies and Power Quality (ICREPQ’11) Las Palmas de Gran Canaria (Spain)*, 2010.

[41] “Electrification Development Projects during the National Plan of Thailand Issue Number 10, โครงการตามแผนพัฒนาระบบไฟฟ้าในช่วงแผนพัฒนาแห่งชาติฉบับที่ 10,” *Provincial Electricity Authority (PEA)*, 2007.

[42] “Royal Project Foundation.” [Online]. Available: www.royalprojectthailand.com. [Accessed: 20-Jan-2012].

[43] “Office of the Royal Development Projects Board.” [Online]. Available: http://www.rdpb.go.th/RDPB/front/king.aspx?p=1. [Accessed: 20-Jan-2012].

[44] “IEA database.” [Online]. Available: www.iea.org/weo/databas_electricity/electricity_access_database.htm. [Accessed: 20-Jan-2012].

[45] P. Reduction, E. Management, S. Unit, and P. Region, “Thailand Investment Climate Assessment Update,” *Thailand’s Ministry of Industry (MOI), Office of the National Economic and Social Development Board (NESDB), Foundation for Thailand Productivity Institute (FTPI), and the World Bank*, no. 44248, 2008.

[46] “Wind Energy Report,” *Wind Energy Group, Department of Alternative Energy Development and Efficiency (DADE)*.

[47] “Wind Energy Resource ATLAS of Southeast Asia.” TrueWind Solutions, LLC, The World Bank Asia Alternative Energy Program.

[48] “Wind Resource Assessment of Thailand,” *Fellow Engineers Consultants Co., Ltd. supported by Department of Energy Development and Promotion, Thailand*, 2001.

[49] “แผนพัฒนาพลังงานทดแทน 15 ปี (2551-2565), Renewable Energy Development Plan 15 years (2008-2022),” *Ministry of Energy*.

[50] J. Weawsak, M. Mani, N. Nankongnab, S. Tirawanichkul, T. Theppaya, and N. Matan, “Assessment of Micrositing Wind Energy Potential along the Coasts of Sothern Thailand,” *Taksin University, Songkranarin University and Walailuk University*, 2008.

[51] U. Sangpanich, G. A. Ault, and K. L. Lo, “Economic feasibility of wind farm using low wind speed turbine,” in *Universities Power Engineering Conference (UPEC), 2009 Proceedings of the 44th International*, 2009, pp. 1–5.

[52] “Photovoltaics for Electrification in Thailand,” *National Energy Policy Office, Thailand*, 1998.

[53] “Wind Speeds at Lam Takhong Dam, Nakorn Ratchasima Province in Thailand.” Electricity Generating Authority (EGAT), Thailand, 2006.

[54] S. Janjai and K. Sricharoen, “Solar radiation data in Thailand.” Sinlapakorn University, Thailand, 2006.

[55] T. Sutabutr, A. Choosuk, and P. Siriput, “Thailand Renewable Energy Policies and Wind Development Potentials,” *Department of Alternative Energy Development and Efficiency (DEDE), Ministry of Energy, Thailand*, 2010.

[56] “โครงการตามแผนพัฒนาระบบไฟฟ้าในช่วงแผนพัฒนาแห่งชาติฉบับที่ 10, Electrification Development Projects during the National Plan of Thailand Issue Number 10,” *Provincial Electricity Authority (PEA)*, 2007.

[57] “The Electricity Access Database.” [Online]. Available: http://www.iea.org/weo/database_electricity/electricity_access_database.htm. [Accessed: 22-Jan-2012].

[58] B. Stuart, “7.5 MW PV plant in Thailand online,” *PV magazine: Photovoltaic markets and technology*. [Online]. Available: www.pv_magazine.com. [Accessed: 15-Mar-2012].

[59] N. Tanpipat, A. Limmanee, and S. Sucontanikorn, “Thailand PV Status Report 2011,” *The Solar Club, Thailand*, p. 24, 2011.

[60] “มติคณะกรรมการนโยบายพลังงานแห่งชาติ, The National Energy Policy Council No. 6/2011 (No. 139),” *Energy Policy and Planning Office*, 2011.

[61] K. Kirtikara, “Lessons Learnt from Using PV Stand – Alone Systems to Provide a Better Quality of Life for Rural People,” in *Technical Digest of the 14th International PVSEC, Bangkok, Thailand*, 2004, pp. 3–6.

[62] G. Baldwin, B. Childs, C. Hunter, and V. Urrea, “Developing a Strategy to Improve Solar Home System Sustainability in Rural Thailand,” 2007.

[63] “Promoting Renewable Energy in Mae Hong Son Province,” *UNDP Project Document, Government of Thailand, United Nations Development Programme*, 2004.

[64] N. Dabbaransi, “EGAT Clean Development Mechanism (CDM) Wind and Solar project development experience,” 2010, April, pp. 1–11.

[65] M. K. Das and T. Leephakpreeda, “A Review Study on Trends to Wind Energy in a Global and Thailand Context,” *Suranaree Journal Science Technology*, vol. 18, no. 1, pp. 1–13, 2011.

[66] “งานพัฒนาพลังงานลมเพื่อผลิตไฟฟ้า, Project Development of Wind Energy for Electricity Generation,” *Renewable Energy Development Department, Electricity Generating Authority of Thailand (EGAT)*. [Online]. Available: www.egat.co.th/re. [Accessed: 18-Mar-2012].

[67] S. Sikkhabandit, “Economic Evaluation of Wind Project & Cost Trend,” *Electricity Generating Authority of Thailand (EGAT)*.

[68] T. Suwannakum, S. Pengma, and D. Pongchawee, “Four Year ’ s Experience on Mini-Grid System for Rural Electrification in Thailand,” in *World Renewable Energy Congress 2009 - Asia, The 3rd International Conference on “Sustainable Energy and Environment (SEE 2009)”*, 2009, May, pp. 657–662.

[69] M. A. Green, *Solar Cells: Operating Principles, Technology and System Applications*. Prentice-Hall, Inc., Englewood Cliffs, N.J., 1982, p. 274.

[70] A. D. Hansen, P. Sorensen, L. H. Hansen, and H. Bindner, "Models for a Stand-Alone PV System," *Riso National Laboratory, Roskilde*, 2000.

[71] B. Engel and M. Meinhard, "State of the Art and Future Trends of PV-System-Technology," *SMA Technologie AG, Germany*, 2006.

[72] K. Ali Kashefi, B. Hamid Reza, and R. Gholam Hossein, "Optimal Sizing of a Stand-alone Wind/Photovoltaic Generation Unit using Particle Swarm Optimization," *SIMULATION*, vol. 85, no. 2, pp. 89–99.

[73] H. Yang, W. Zhou, L. Lu, and Z. Fang, "Optimal sizing method for stand-alone hybrid solar-wind system with LPSP technology by using genetic algorithm," *Solar Energy*, vol. 82, no. 4, pp. 354–367, 2008.

[74] D. Xu, L. Kang, and L. Chang, "Optimal sizing of standalone hybrid wind/PV power systems using genetic algorithms," in *Electrical and Computer Engineering, Canadian Conference*, 2005.

[75] G. M. Masters, *Renewable and Efficient Electric Power Systems*. New Jersey: John Wiley and Sons, Inc., 2004.

[76] F. O. Hocaoğlu, Ö. N. Gerek, and M. Kurban, "A novel hybrid (wind–photovoltaic) system sizing procedure," *Solar Energy*, vol. 83, no. 11, pp. 2019–2028, 2009.

[77] I. B. Askari and M. Ameri, "Optimal sizing of photovoltaic–battery power systems in a remote region in Kerman, Iran," *Proceedings of the Institution of Mechanical Engineers Part A Journal of Power and Energy*, vol. 223, no. 5, pp. 563–570, 2009.

[78] T. Senjyu, D. Hayashi, A. Yona, N. Urasaki, and T. Funabashi, "Optimal configuration of power generating systems in isolated island with renewable energy," *Renewable Energy*, vol. 32, no. 11, pp. 1917–1933, 2007.

[79] H. Suryoatmojo, T. Hiyama, A. A. Elbaset, and M. Ashari, "Optimal Design of Wind-PV-Diesel-Battery System using Genetic Algorithm," *The Institute of Electrical Engineers of Japan, IEEJ Trans. PE*, vol. 129, No.3, no. 3, pp. 413–420, 2009.

[80] D. B. Nelson, M. H. Nehrir, and C. Wang, "Unit sizing and cost analysis of stand-alone hybrid wind/PV/fuel cell power generation systems," *Renewable Energy*, vol. 31, no. 10, pp. 1641–1656, 2006.

[81] D. L. Evans, "Simplified method for predicting photovoltaic array output," *Solar Energy*, vol. 27, no. 6, pp. 555–560, 1981.

[82] M. A. Habib, S. A. M. Said, M. A. El-Hadidy, and I. Al-Zaharna, "Optimization procedure of a hybrid photovoltaic wind energy system," *Energy*, vol. 24, no. 11, pp. 919–929, 1999.

[83] M. K. Deshmukh and S. S. Deshmukh, "Modeling of hybrid renewable energy systems," *Renewable and Sustainable Energy Reviews*, vol. 12, no. 1, pp. 235–249, 2008.

[84] S. Diaf, D. Diaf, M. Belhamel, M. Haddadi, and A. Louche, "A methodology for optimal sizing of autonomous hybrid PV/wind system," *Energy Policy*, vol. 35, no. 11, pp. 5708–5718, 2007.

[85] M. Tao, "Inorganic Photovoltaic Solar Cells: Silicon and Beyond," *The Electrochemical Society Interface*, 2008.

[86] T. Burton, D. Sharpe, N. Jenkin, and E. Bossanyi, *Wind Energy Hand Book*. England: John Wiley & Sons, Ltd., 2001.

[87] E. Hau, *Wind Turbines: Fundamentals, Technologies, Application and Economics (2nd Edition)*. Springer Berlin Heidelberg New York, 2006.

[88] E. Muljadi and C. P. Butterfield, "Pitch-controlled variable-speed wind turbine generation," *IEEE Transactions on Industry Applications*, vol. 37, no. 1, pp. 240–246, 2001.

[89] A. W. Dahmouni, M. Ben Salah, F. Askri, C. Kerkeni, and S. Ben Nasrallah, "Assessment of wind energy potential and optimal electricity generation in Borj-Cedria, Tunisia," *Renewable and Sustainable Energy Reviews*, vol. 15, no. 1, pp. 815–820, Jan. 2011.

[90] G. M. Joselin Herbert, S. Iniyan, E. Sreevalsan, and S. Rajapandian, "A review of wind energy technologies," *Renewable and Sustainable Energy Reviews*, vol. 11, no. 6, pp. 1117–1145, 2007.

[91] Shikha, T. S. Bhatt, and D. P. Kothari, "The Evolution of Wind Power Technology-a Review," *IE(I) Journal-ID*, vol. 84, p. 6, 2003.

[92] L. El Chaar, L. A. Lamont, and N. Elzein, "Wind Energy Technology – Industrial Update," pp. 1–5, 2011.

[93] H. Riegler, "HAWT versus VAWT," *Refocus*, August, pp. 44–46, 2003.

[94] "Components of a Wind Turbine," *Encyclopædia Britannica, Inc.*, 2009. [Online]. Available: www.britannica.com. [Accessed: 15-Mar-2012].

[95] T. Jimenez, "Wind Energy: Technology & Applications," no. February, 2009.

[96] L. F. Hansen, P. Jamieson, C. Morgan, and F. Rasmussen, "Wind Energy: The Facts, Part I Technology," *The European Wind Energy Association (EWEA)*, 2009.

[97] Y. Duan and R. G. Harley, "Present and future trends in wind turbine generator designs," *Computer Engineering*, no. 11, pp. 1–6, 2009.

[98] S. Muller, M. Deicke, and W. De Doncker, Rik, “Doubly Fed Induction Generator Systems for Wind Turbines,” *IEEE Industry Applications Magazine*, pp. 26–33, 2002.

[99] H. Choi, J. Kim, J. Cho, and Y. Nam, “Active Yaw Control of MW class Wind Turbine,” in *International Conference on Control, Automation and Systems*, 2010, pp. 1075–1078.

[100] B. Bradley, “An International Wind Turbine Gearbox Standard,” *Gear Technology*, July, pp. 36–39, 2009.

[101] A. Binder and T. Schneider, “Permanent magnet synchronous generators for regenerative energy conversion-a survey,” in *Power Electronics and Applications, 2005 European Conference*, 2005, p. 10.

[102] H. Polinder, D.-J. Ban, H. Li, and Z. Chen, “Concept Report on Generator Topologies, Mechanical & Electromagnetic Optimization,” p. 79, 2007.

[103] M. R. Patel, *Wind and Solar Power Systems: Design, Analysis and Operation*, 2nd ed. Taylor & Francis Group, LLC, 2006, p. 473.

[104] D. Weisser and R. Garcia, “Instantaneous wind energy penetration in isolated electricity grids: concepts and review,” *Renewable Energy*, vol. 30, no. 8, pp. 1299–1308, 2005.

[105] W. Cui, X. Liu, F. Yu, and J. Whitty, *Analysis of the passive yaw mechanism of small horizontal-axis wind turbines*. IEEE, 2009, pp. 1–5.

[106] Z. Wu and H. Wang, “Research on Active Yaw Mechanism of Small Wind Turbines,” *Energy Procedia*, vol. 16, pp. 53–57, 2012.

[107] W. Musial, S. Butterfield, and B. McNiff, “Improving Wind Turbine Gearbox Reliability,” in *the 2007 European Wind Energy Conference*, 2007.

[108] A. Ragheb and M. Ragheb, “Wind turbine gearbox technologies,” *2010 1st International Nuclear Renewable Energy Conference INREC*, pp. 1–8, 2010.

[109] J. Rizk and M. Nagrial, “Design of permanent-magnet generators for wind turbines,” *Proceedings IPEMC 2000. Third International Power Electronics and Motion Control Conference (IEEE Cat. No.00EX435)*, vol. 1, pp. 208–212, 2000.

[110] H. Piggott and S. Khennas, “PMG construction manual,” pp. 1–49, 2001.

[111] E. Muljadi and J. Green, “Cogging Torque Reduction in a Permanent Magnet Wind Turbine Generator,” *American Society of Mechanical Engineers*, pp. 340–342, 2002.

[112] J. R. Bumby, N. Stannard, and R. Martin, “A Permanent Magnet Generator for Small Scale Wind Turbines,” in *Analysis*, 2006.

[113] G. L. Johnson, “Wind Turbines with Asynchronous Electrical Generators,” in *Wind Energy Systems*, 2001, pp. 1–44.

[114] A. I. Estanqueiro, J. O. Tande, and J. A. P. Lopes, "Assessment of Power Quality Characteristics of Wind Farms," in *2007 IEEE Power Engineering Society General Meeting*, 2007, pp. 1–4.

[115] M. Ragheb, "Structural towers," *University of Illinois at Urbana-Champaign*, 2012.

[116] "Hybrid Mini-Grids for Rural Electrification: Lessons Learned," *Alliance for Rural Electrification (ARE)*, p. 67, 2011.

[117] T. Ackermann, *Wind Power in Power Systems*. John Wiley & Sons, Ltd., 2005, p. 745.

[118] "Technical and Economic Assessment of Off-Grid , Mini-Grid and Grid Electrification Technologies Annexes," *The World Bank group, Energy Unit, Energy, Transport and Water Department*, p. 155, 2006.

[119] T. Ackermann, "Embedded wind generation in weak grids—economic optimisation and power quality simulation," *Renewable Energy*, vol. 18, no. 2, pp. 205–221, 1999.

[120] N. Rugthaicharoencheep and S. Auchariyamet, "Technical and Economic Impacts of Distributed Generation on Distribution System," *World Academy of Science, Engineering and Technology*, pp. 288–292, 2012.

[121] I. Waseem, S. Member, M. Pipattanasomporn, and S. Rahman, "Reliability Benefits of Distributed Generation as a Backup Source," *Power, Energy, & Industry Applications, Power & Energy Society General Meeting, IEEE*, pp. 1–8, 2009.

[122] P. Fuangfoo, "The Impact of Distributed Generation on the Thailand's Electric Power System," *Doctoral Dissertation, Institute for the Faculty of the Graduate School of the University of Taxas at Arlington*, 2006.

[123] W. Limpananwadi and W. Tayati, "Impacts of Multiple Distributed Generations on a Weak Distribution Network - A Case Study," *International Journal of Emerging Electric Power Systems*, vol. 7, no. 2, 2006.

[124] I. P. Gyuk and S. Eckroad, "Energy Storage for Grid Connected Wind Generation Applications: EPRI-DOE Handbook Supplement," p. 144, 2004.

[125] A. Mohd, E. Ortjohann, A. Schmelter, N. Hamsic, and D. Morton, "Challenges in integrating distributed Energy storage systems into future smart grid," *Energy*, pp. 1627–1632, 2008.

[126] K. C. Divya and J. Østergaard, "Battery energy storage technology for power systems—An overview," *Electric Power Systems Research*, vol. 79, no. 4, pp. 511–520, 2009.

[127] "Energy storage technologies for wind power integration," *Service BEAMS groupe Energie, Université Libre de Bruxelles*, no. March, 2010.

[128] P. D. Lund and J. V Paatero, "Energy storage options for improving wind power quality," in *Nordic Wind Power Conference*, 2006, vol. 1000, no. 2000, pp. 22–23.

[129] M. Ibrahim, A. Khairy, H. Hagras, M. Zaher, A. El Shafei, A. Shaltout, and N. A. Rehim, "Studying the Effect of Decentralized Battery Storage to Smooth the Generated Power of a Grid Integrated Wind Energy Conversion System.," *Proceedings of the 14th International Middle East Power Systems Conference (MEPCON'10)*, pp. 641–645, 2010.

[130] B. Nyamdash, E. Denny, and M. O'Malley, "The viability of balancing wind generation with large scale energy storage," *Energy Policy*, vol. 38, no. 11, pp. 7200–7208, 2010.

[131] P. Pinson, G. Papaefthymiou, B. Klockl, and J. Verboomen, "Dynamic sizing of energy storage for hedging wind power forecast uncertainty," *2009 IEEE Power Energy Society General Meeting*, pp. 1–8, 2009.

[132] H. Bludszuweit, J. A. Domínguez, and J. L. Bernal, "Pre-feasibility study of a grid connected wind-PV hybrid system with energy storage and power prediction," in *Iinternational Conference on Renewable Energies and Power Quality (ICREPQ'06)*, 2006.

[133] Y. Riffonneau, S. Bacha, F. Barruel, and S. Ploix, "Optimal Power Flow Management for Grid Connected PV Systems With Batteries," *IEEE Transactions on Sustainable Energy*, vol. 2, no. 3, pp. 309–320, 2011.

[134] P. Arun, R. Banerjee, and S. Bandyopadhyay, "Optimum sizing of battery-integrated diesel generator for remote electrification through design-space approach," *Energy*, vol. 33, no. 7, pp. 1155–1168, 2008.

[135] J. F. Manwell, "Hybrid Energy Systems," *Encyclopedia of Energy*, vol. 3, pp. 215–229, 2004.

[136] R. Tiffin, *Practical Techniques for effective project investment appraisal*. London: Thorogood; Spi edition, 1999.

[137] R. Luna-Rubio, M. Trejo-Perea, D. Vargas-Vázquez, and G. J. Ríos-Moreno, "Optimal sizing of renewable hybrids energy systems: A review of methodologies," *Solar Energy*, vol. 86, pp. 1077–1088, Dec. 2011.

[138] P. Nema, R. K. Nema, and S. Rangnekar, "A current and future state of art development of hybrid energy system using wind and PV-solar: A review," *Renewable and Sustainable Energy Reviews*, vol. 13, no. 8, pp. 2096–2103, 2009.

[139] J. L. Bernal-Agustín and R. Dufo-López, "Simulation and optimization of stand-alone hybrid renewable energy systems," *Renewable and Sustainable Energy Reviews*, vol. 13, no. 8, pp. 2111–2118, Oct. 2009.

[140] T. Markvart, "Sizing of hybrid photovoltaic-wind energy systems," *Solar Energy*, vol. 57, no. 4, pp. 277–281, 1996.

[141] B. S. Borowy and Z. M. Salameh, “Methodology for Optimally Sizing the Combination of a Battery Bank and PV Array in a Wind/PV Hybrid System,” vol. 11, no. 2, 1996.

[142] B. Ai, H. Yang, H. Shen, and X. Liao, “Computer-aided design of PV/wind hybrid system,” *Renewable Energy*, vol. 28, no. 10, pp. 1491–1512, Aug. 2003.

[143] C. Protogeropoulos, B. J. Brinkworth, and R. H. Marshall, “Sizing and Techno-Economical Optimization for Hybrid Solar Photovoltaic/Wind Power Systems with Battery Storage,” *International Journal of Energy Research*, vol. 21, no. 6, pp. 465–479, 1997.

[144] A. N. Celik, “Techno-economic analysis of autonomous PV-wind hybrid energy systems using different sizing methods,” *Energy Conversion and Management*, vol. 44, no. 12, pp. 1951–1968, 2003.

[145] A. C. Bakirtzis, “A probabilistic method for the evaluation of the reliability of stand alone,” *IEEE Transactions on Energy Conversion*, vol. 7, no. 1, 1992.

[146] S. H. Karaki, R. B. Chedid, and R. Ramadan, “Probabilistic Performance Assessment of Autonomous Solar-Wind Energy Conversion Systems,” vol. 14, no. 3, 1999.

[147] S. Conti, G. Tina, and U. Vagliasindi, “A NEW METHOD FOR ESTIMATING THE LONG-TERM AVERAGE PERFORMANCE OF HYBRID WIND / PV SYSTEMS,” in *Proceedings of Eurosun, Copenhagen, Denmark*, 2000.

[148] G. Tina, S. Gagliano, and S. Raiti, “Hybrid solar/wind power system probabilistic modelling for long-term performance assessment,” *Solar Energy*, vol. 80, no. 5, pp. 578–588, May 2006.

[149] G. La Terra, G. Salvina, and T. G. Marco, “Optimal Sizing Procedure for Hybrid Solar Wind Power Systems by Fuzzy Logic,” *MELECON 2006, IEEE Mediterranean Electrotechnical Conference*, pp. 865–868, 2006.

[150] W. D. Kellogg, M. H. Nehrir, G. Venkataramanan, and V. Gerez, “Generation Unit Sizing and Cost Analysis for Stand-Alone Wind, Photovoltaic and Hybrid Wind PV Systems,” *IEEE Transactions on Energy Conversion*, vol. 13, no. 1, pp. 70–75, 1998.

[151] H. X. Yang, L. Lu, and J. Burnett, “Weather data and probability analysis of hybrid photovoltaic–wind power generation systems in Hong Kong,” *Renewable Energy*, vol. 28, no. 11, pp. 1813–1824, Sep. 2003.

[152] H. Yang, L. Lu, and W. Zhou, “A novel optimization sizing model for hybrid solar-wind power generation system,” *Solar Energy*, vol. 81, no. 1, pp. 76–84, Jan. 2007.

[153] A. Kaabeche, M. Belhamel, and R. Ibtiouen, “Sizing optimization of grid-independent hybrid photovoltaic/wind power generation system,” *Energy*, vol. 36, no. 2, pp. 1214–1222, 2011.

[154] M. Fadaee and M. A. M. Radzi, “Multi-objective optimization of a stand-alone hybrid renewable energy system by using evolutionary algorithms: A review,” *Renewable and Sustainable Energy Reviews*, vol. 16, no. 5, pp. 3364–3369, 2012.

[155] A. Alarcon-Rodriguez, S. Galloway, and G. W. Ault, “Multi-objective planning of distributed energy resources: A review of the state-of-the-art,” *Renewable and Sustainable Energy Reviews*, vol. 14, no. 5, pp. 1353–1366, 2010.

[156] J.-H. Shi, X.-J. Zhu, and G.-Y. Cao, “Design and techno-economical optimization for stand-alone hybrid power systems with multi-objective evolutionary algorithms,” *International Journal of Energy Research*, vol. 31, no. 3, pp. 315–328, 2007.

[157] H. Yang, Z. Wei, and L. Chengzhi, “Optimal design and techno-economic analysis of a hybrid solar–wind power generation system,” *Applied Energy*, vol. 86, no. 2, pp. 163–169, 2009.

[158] E. Zitzler and L. Thiele, “Multiobjective evolutionary algorithms: a comparative case study and the strength Pareto approach,” *IEEE Transactions on Evolutionary Computation*, vol. 3, no. 4, pp. 257–271, 1999.

[159] J. L. Bernal-Agustín, R. Dufo-López, and D. M. Rivas-Ascaso, “Design of isolated hybrid systems minimizing costs and pollutant emissions,” *Renewable Energy*, vol. 31, no. 14, pp. 2227–2244, 2006.

[160] R. Dufo-López and J. L. Bernal-Agustín, “Multi-objective design of PV-wind-diesel-hydrogen-battery systems,” *Renewable Energy*, vol. 33, no. 12, pp. 2559–2572, 2008.

[161] “HOMER Software.” [Online]. Available: www.homerenergy.com. [Accessed: 05-May-2012].

[162] J. F. Manwell and J. G. McGowan, “Lead acid battery storage model for hybrid energy systems,” *Solar Energy*, vol. 50, no. 5, pp. 399–405, May 1993.

[163] R. Dufo-López and J. L. Bernal-Agustín, “Design and control strategies of PV-Diesel systems using genetic algorithms,” *Solar Energy*, vol. 79, no. 1, pp. 33–46, Jul. 2005.

[164] R. Dufo-López, J. L. Bernal-Agustín, and J. Contreras, “Optimization of control strategies for stand-alone renewable energy systems with hydrogen storage,” *Renewable Energy*, vol. 32, no. 7, pp. 1102–1126, Jun. 2007.

[165] M. Wetter, “Generic Optimization Program User Manual, Version 3.0.0,” 2009.

[166] Ø. Ulleberg and R. Glöckner, “HYDROGEMS: Hydrogen Energy Models,” *Institute for Energy Technology*, 2001.

[167] “TRNSYS: Transient System Simulation Tool.” [Online]. Available: http://www.trnsys.com/. [Accessed: 20-May-2012].

[168] “Hybrid2 software.” [Online]. Available: http://www.ceere.org/rerl/projects/software/hybrid2/. [Accessed: 20-May-2012].

[169] “INSEL software.” [Online]. Available: http://www.insel.eu. [Accessed: 20-May-2012].

[170] “Power Supply Simulator (RAPSIM).” [Online]. Available: http://wwwcomm.murdoch.edu.au/synergy/9803/rapsim.html. [Accessed: 20-May-2012].

[171] “Simulation and Optimization Model for Renewable Energy Systems (SOMES) version 3.2.” [Online]. Available: http://nws.chem.uu.nl/publica/Publicaties 1997/97020.htm. [Accessed: 20-May-2012].

[172] S. Boyd and L. Vandenberghe, *Convex Optimization*. Cambridge University Press, 2004.

[173] K. Deb, *Multi-Objective Optimization Using Evolutionary Algorithms*. John Wiley and Sons, Inc., 2001.

[174] Y. Song and M. R. Irving, “Optimization Techniques for Electrical Power Systems: Part 2, Heuristic Optimization Methods,” *Power Engineering Journal*, vol. 15, no. 3, pp. 151–160, 2001.

[175] R. Bellman, *Mathematical optimization techniques*. University of California Press; First Edition, 1963.

[176] K. Y. Lee and M. A. El-Sharkawi, *Modern Heuristic Optimization Techniques*. John Wiley and Sons, Inc., 2008.

[177] K. Miettinen, *Nonlinear Multiobjective Optimization*. 1989.

[178] T. Weise, *Global Optimization Algorithms – Theory and Application –*, 2nd ed. 2009.

[179] M. Gen, R. Cheng, and L. Lin, *Decision Engineering Series: Network Models and Optimization: Multiobjective Genetic Algorithm Approach*. Springer-Verlag London limited, 2008.

[180] D. Beasley, D. R. Bull, and R. Martin, “An Overview of Genetic Algorithms: Part 1 , Fundamentals,” *University Computing*, pp. 1–16, 1993.

[181] A. Abraham, L. Jain, and R. Goldberg, *Evolutionary Multiobjective Optimization: Theoretical Advances and Applications*. Springer-Verlag London limited, 2004.

[182] C. A. C. Coello, “Twenty Years of Evolutionary Multi-Objective Optimization: A Historical View of the Field,” *IEEE Computational Intelligence Magazine*, vol. 1, no. 1, pp. 28–36, 2006.

[183] K. Deb, M. Mohan, and S. Mishra, “A Fast Mult-Objective Evolutionary Algorithm for Finding Well-Spread Pareto-Optimal Solutions,” *KanGAL Report Number 2003002*.

[184] E. Zitzler and L. Thiele, “An Evolutionary Algorithm for Multiobjective Optimization: The Strength Pareto Approach,” *TIK-Report*, no. 43, 1998.

[185] L. Fingersh, M. Hand, and A. Laxson, “Wind Turbine Design Cost and Scaling Model,” *Technical Report NREL/TP-500-40566*, no. December, 2006.

[186] D. Bradley, “General Electric’s New Low Wind Speed Turbine,” *Wind Action Group*, 2011. [Online]. Available: http://wagengineering.blogspot.co.uk/2011/06/general-electrics-new-low-wind-speed.html. [Accessed: 21-Jul-2012].

[187] E. de Vries, “Blades of the future,” *Wind Power monthly*, 2012. [Online]. Available: http://www.windpowermonthly.com. [Accessed: 28-Jul-2012].

[188] J. Quilter, “Gamesa launches low wind speed turbine,” *Wind Power monthly*, 2012. [Online]. Available: http://www.windpowermonthly.com/. [Accessed: 28-Jul-2012].

[189] R. Davidson, “Good year for GE but future lies outside US,” *Wind Power monthly*, 2012. [Online]. Available: http://www.windpowermonthly.com. [Accessed: 28-Jul-2012].

[190] J. Quilter, “Vestas wins 139MW First Wind deal,” *Wind Power monthly*, 2011. [Online]. Available: http://windpowermonthly.com. [Accessed: 28-Jul-2012].

[191] J. Quilter, “Vestas wins low wind order for Mexico,” *Wind Power monthly*, 2012. [Online]. Available: http://www.windpowermonthly.com. [Accessed: 28-Jul-2012].

[192] W. Qi, “Chinese low-wind developments,” *Wind Power monthly*, 2012. [Online]. Available: http://www.windpowermonthly.com/. [Accessed: 27-Jul-2012].

[193] “Siemens: Swt - 2.3 - 113,” in *Siemens Wind Power A/S*, 2011.

[194] R. Davidson, “Low wind projects and technology flourish,” *Wind Power monthly*, 2011. [Online]. Available: http://windpowermonthly.com. [Accessed: 28-Jul-2012].

[195] R. Poore and C. Walford, “Development of an Operations and Maintenance Cost Model to Identify Cost of Energy Savings for Low Wind Speed Turbines,” *Subcontract Report NREL/SR-500-40581*, January, 2008.

[196] D. J. Malcolm and A. C. Hansen, “WindPACT Turbine Rotor Design Study,” in *Subcontract Report NREL/SR-500-32495, Revised April 2006*, 2006.

[197] “Currency Exchange Rates.” [Online]. Available: www.exchangerates.org.uk. [Accessed: 10-Nov-2011].

[198] “Inflation rate, Bank of Thailand.” [Online]. Available: www.bot.or.th. [Accessed: 11-Nov-2011].

[199] R. L. Haupt and S. E. Haupt, *Practical Genetic Algorithms*. John Wiley and Sons, Inc., 2004.

[200] D. A. Coley, *An Introduction to Genetic Algorithms for Scientists and Engineers*. World Scientific, 1997.

[201] K. Deb, A. Pratap, S. Agarwal, and T. Meyarivan, "A Fast and Elitist Multiobjective Genetic Algorithm:," *IEEE Transactions on Evolutionary Computation*, vol. 6, no. 2, pp. 182–197, 2002.

[202] J. P. Dunlop, "Batteries and Charge Control in Stand-Alone Photovoltaic Systems," *Florida Solar Energy Center*, 1997.

[203] B. Espinar and D. Mayer, "The Role of Energy Storage for Mini-Grid Stabilization," *Iea-pvps, Report*, 2011.

[204] "Charging Lead Acid," *Battery University*. [Online]. Available: http://batteryuniversity.com/learn/article/charging_the_lead_acid_battery. [Accessed: 22-Aug-2011].

[205] I. Buchmann, "How to charge - when to charge table," 2005. [Online]. Available: http://batteryuniversity.com/partone-23.htm. [Accessed: 04-Sep-2012].

[206] "Temperature data in Thailand." Thai Meteorological Department , Bangkok, Thailand, 2008.

[207] C. Grigg, P. Wong, P. Albrecht, R. Allan, M. Bhavaraju, R. Billinton, Q. Chen, C. Fong, S. Haddad, S. Kuruganty, W. Li, R. Mukerji, D. Patton, N. Rau, D. Reppen, A. Schneider, M. Shahidehpour, and C. Singh, "The IEEE Reliability Test System-1996. A report prepared by the Reliability Test System Task Force of the Application of Probability Methods Subcommittee," *Power Systems, IEEE Transactions on*, vol. 14, no. 3, pp. 1010–1020, 1999.

[208] "Climate of Thailand." [Online]. Available: http://www.tmd.go.th/en/archive/season.php. [Accessed: 20-May-2010].

[209] "10 kW Wind Turbine," *The Home of Green Energy Products in the UK*, 2010. [Online]. Available: http://www.windpoweruk.com. [Accessed: 05-May-2010].

[210] "100 W Mono-crystalline solar panel." [Online]. Available: www.esolarsystems.co.uk. [Accessed: 05-Jun-2010].

[211] "SB Retail Pricing," *Solarbuzz, an NPD Group company, 01/2012*. [Online]. Available: www.solarbuzz.com. [Accessed: 10-Nov-2011].

[212] N. Phuangpornpitak and S. Kumar, "PV hybrid systems for rural electrification in Thailand," *Renewable and Sustainable Energy Reviews*, vol. 11, no. 7, pp. 1530–1543, Sep. 2007.

[213] I. Muhammad, *An introduction to solar radiation*. Toronto London Academic, 1983, p. 390.

[214] “Sealed lead-acid SLA UXL550-1100.” [Online]. Available: www.batterymasters.co.uk. [Accessed: 12-Nov-2011].

[215] “Retail oil price in Thailand,” *Eenergy Policy and Planning Office (EPPO), Ministry of Energy, Thailand*. [Online]. Available: www.eppo.go.th. [Accessed: 11-Nov-2011].

[216] A. Chowdhury and D. Koval, *Power Distribution System Reliability:Practical Methods and Applications*, 2nd ed. Wiley-IEEE Press, 2009.

[217] F. Viawan, “Voltage Control and Voltage Stability of Power Distribution Systems in the Presence of Distributed Generation,” *Doctoral Dissertation, Department of Energy and Environment, Chalmers University of Technology*, 2008.

[218] J. Isles, “Still a role for synchronous condensers,” *The Energy Industry Times*, vol. Febuary, 2009.

[219] M. Raap, P. Raesaar, and E. Tiigimägi, “Reactive Power Pricing in Distribution Networks,” *Oil Shale*, vol. 28, no. 1S, p. 223, 2011.

[220] S. Kumar, “Applications of Power Capacitors in Electrical Distribution Systems (Part-I),” *Electrical Engineering, National Institute of Technology Calicut, India*, 2004.

[221] J. Dixon, L. Morán, J. Rodríguez, and R. Domke, “Reactive Power Compensation Technologies , State- of-the-Art Review,” *Proceedings of the IEEE*, vol. 93, no. 12, pp. 2144 – 2164, 2005.

[222] O. S. Ogidi, L. Yanli, and S. Hui, “Application of Switched Capacitor banks for Power Factor Improvement and Harmonics Reduction on the Nigerian Distribution Electric Network,” *International Journal of Electrical & Computer Sciences IJECS-IJENS*, December, pp. 58–68, 2011.

[223] M. Braun, “Reactive Power Supplied by Wind Energy Converters – Cost-Benefit-Analysis,” *Europe’s premier wind energy event, Brussels*, 2008.

[224] A. Ellis, R. Nelson, E. Von Engeln, R. Walling, J. Mcdowell, L. Casey, E. Seymour, W. Peter, C. Barker, and B. Kirby, “Reactive Power Interconnection Requirements for PV and Wind Plants – Recommendations to NERC,” *Sandia report, Sandia National Laboratories, California*, February, 2012.

[225] T. A. Short, *Electric Power distribution handbook*, CRC Press LLC, 2004.

[226] “Steps and Stage Size considerations,” *Northeast Power Systems, Inc.*, 2009. [Online]. Available: www.nepsi.com. [Accessed: 20-Sep-2011].

[227] T. M. Blooming and D. J. Carnovale, “Capacitor Application Issues,” *IEEE Transactions on Industry Applications*, vol. 44, no. 4, pp. 1013 – 1026, 2008.

[228] R. D. Zimmerman, *Matpower 4.05b User’s Manual*. Power Systems Engineering Research Center (PSERC), 2010.

[229] J. J. Grainger and W. D. Stevenson, *Power System Analysis*. McGraw-Hill, Inc., 1994.

[230] A. J. Wood and B. F. Wollenberg, *Power Generation Operation and Control*, 2nd ed. John Wiley and Sons, Inc., 1996.

[231] S. J. Haig, R. M. Tumilty, G. M. Burt, and J. R. McDonald, "Analysing the Technology Needs of Future Distribution Networks," *Proceedings of the 41st International Universities Power Engineering Conference*, pp. 217–221, Sep. 2006.

[232] J. a. P. Lopes, N. Hatziargyriou, J. Mutale, P. Djapic, and N. Jenkins, "Integrating distributed generation into electric power systems: A review of drivers, challenges and opportunities," *Electric Power Systems Research*, vol. 77, no. 9, pp. 1189–1203, Jul. 2007.

[233] C. L. Masters, "Voltage rise: the big issue when connecting embedded generation to long 11 kV overhead lines," *Power Engineering Journal*, vol. 16, no. 1, pp. 5–12, 2002.

[234] "Power System Planning Criteria," *Provincial Electricity Authority (PEA), Thailand*, 2010.

[235] C. Turchi, "Solar Power and the Electric Grid," *National Renewable Energy Laboratory*, 2010.

[236] M. Nicolosi, "Wind Power Integration , Negative Prices and Power System Flexibility - An Empirical Analysis of Extreme Events in Germany by Wind Power Integration" no. 10, 2010.

[237] I. Ziari, "Planning of Distribution Networks for Medium Voltage and Low Voltage," *Doctoral Dissertation, Faculty of Built Environment and Engineering, Quensland Unversity of Technology, Australia*, August, 2011.

[238] "Very Small Power Producer (VSPP) rate," *Provincial Electricity Authority (PEA)*, 2011.

[239] "คู่มือค่าพารามิเตอร์สายระบบจำหน่ายแรงสูง 22/33 เควี, ระบบจำหน่ายแรงต่ำ 380/220 โวลท์และระบบสายส่ง 115 เควี, A Manual of line Parameters in 22/33 kV and 380/220 V Distribution Systems and 115 kV in Transmission Systems," *Power System Planning Department, Provincial Electricity Authority (PEA)*, 2005.

[240] "Cost and Quality of Fuels for Electric Plants." U.S. Energy Information Administration, www.eia.doe.gov/cneaf/electricity/cq/cq_sum.html.